UNIVERSITY OF GHANA

COLLEGE OF BASIC AND APPLIED SCIENCES,

SCHOOL OF BIOLOGICAL SCIENCES

HUMAN LEUKOCYTE ANTIGEN (HLA) CLASS I ASSEMBLY AND TRAFFICKING IN TRANSPORTER ASSOCIATED WITH ANTIGEN PROCESSING (TAP)-DEFICIENT CELLS

BY

OLOCHE OWOICHO

(10804038)

THIS THESIS IS SUBMITTED TO THE UNIVERSITY OF GHANA, LEGON, IN PARTIAL FULFILMENT OF THE REQUIREMENT FOR THE AWARD OF A DOCTOR OF PHILOSOPHY DEGREE IN MOLECULAR CELL BIOLOGY OF INFECTIOUS DISEASES

DEPARTMENT OF BIOCHEMISTRY, CELL, AND MOLECULAR BIOLOGY

NOVEMBER 2024

DECLARATION

I, Oloche Owoicho, of the Department of Biochemistry, Cell and Molecular Biology at the University of Ghana, declare that this thesis is a study conducted by me at the Department of Microbiology and Immunology, Michigan Medicine, University of Michigan, Ann Arbor, United States of America. This thesis was supervised by Prof. Malini Raghavan (University of Michigan), Prof. Osbourne Quaye (University of Ghana), and Prof. Emmanuel Ayitey Tagoe (University of Ghana). I declare that this work, in whole or in part, has not been and is not being submitted for another degree at the University of Ghana or elsewhere. I also declare that this thesis represents my original research, except where acknowledgments indicate otherwise.

…… 08-27-2025 ……..

Oloche Owoicho (Candidate)

…… 29/08/2025 ……..

Prof. Osbourne Quaye (Supervisor)

…… 9/2/2025 ……

Prof. Malini Raghavan (Supervisor)

…… 01/09/2025 ……

Prof. Emmanuel Ayitey Tagoe (Co-supervisor)

ABSTRACT

Human leukocyte antigen (HLA) class I molecules play a crucial role in immunity against infectious pathogens and cancers by presenting antigens to cytotoxic T lymphocytes (CTLs) and regulating natural killer (NK) cell activities. HLA class I assembly largely depends on peptide availability via the transporter associated with antigen processing (TAP). Viral infections and cancers often inhibit TAP to evade immune responses. While TAP deficiency typically leads to HLA class I degradation, some TAP-deficient cells maintain low but detectable surface HLA class I expression through poorly understood mechanisms. This thesis investigated the assembly and trafficking of HLA class I molecules under TAP-deficient conditions. TAP deficiency induces increased high mannose, Endoglycosidase H (Endo-H)-sensitive glycans on HLA class I molecules, but without activating canonical ER stress mediators. Factors implicated in unconventional glycoprotein trafficking do not selectively affect surface HLA class I expression in TAP-deficient cells. Instead, HLA class I surface expression in these cells is brefeldin A sensitive, suggesting the involvement of the conventional Golgi-dependent secretory route. TAP deficiency does not significantly alter ER and Golgi alpha-1,2 mannosidase levels, and other conditions that compromise HLA class I assembly, such as tapasin deficiency, also induce increased high mannose HLA class I surface glycans. Notably, TAP-deficient cells share over 80% of HLA class I-eluted peptides with wild-type cells, and the surface HLA class I expression in both cell types is sensitive to pH gradient-dependent assembly in endocytic compartments. Based on these findings, we propose a model where saturated recognition mechanisms for misfolded HLA class I molecules result in their partial Golgi-dependent secretory trafficking, accounting for impaired glycan maturation. This Golgi-mediated export of HLA class I with high mannose glycans may represent a homeostatic response to misfolded HLA class I accumulation in the

ER. These results also highlight the relevance of supplemental HLA class I assembly in endocytic compartments. Together, these findings provide new insights into HLA class I assembly and trafficking in TAP-deficient cells and could inform the development of novel immunotherapies against infectious pathogens and cancers that inhibit TAP.

DEDICATION

This work is dedicated to my wife, Debbie, for her patience and understanding through thick and thin of my Ph.D. journey, and to Peter and Paul, for enduring my absence during this research.

ACKNOWLEDGEMENTS

I extend my sincere gratitude to my thesis committee members: Prof. Malini Raghavan (University of Michigan), Prof. Osbourne Quaye (University of Ghana), Prof. Alice Telesnitsky (University of Michigan), and Prof. Emmanuel Ayitey Tagoe (University of Ghana), for their invaluable guidance and support throughout this research. I am grateful to the West African Centre for Cell Biology of Infectious Pathogens (WACCBIP), University of Ghana, and the National Institutes of Health for funding this research. Special thanks to Prof. Gordon Awandare, the WACCBIP team, and Prof. Raghavan for their efforts in securing the funding. Again, I thank Prof. Telesnitsky and Prof. Quaye for forging the collaboration between WACCBIP and the Department of Microbiology and Immunology, University of Michigan, and I am grateful to Prof. Raghavan for accepting me into her lab. I appreciate the contributions of past and present members of the Raghavan Lab. Many thanks to Jie Geng for preparing Figure 3.7C, and to Amanpreet Kaur, Avrokin Surnilla, and Prof. Raghavan for the data analysis in Figure 5.3. I also acknowledge Avrokin Surnilla for generating Figure 5.4. I thank the Department of Microbiology and Immunology, Michigan Medicine, University of Michigan, for providing an environment that was conducive to my research. I am grateful to Venkatesha Basrur and Kevin Conlon of the Proteomics Resource Facility, Department of Pathology, University of Michigan, for their technical support with mass spectrometry experiments. The Microscopy Core of the Biomedical Research Core Facility, University of Michigan, provided valuable assistance with the colocalization experiment. Finally, I extend my appreciation to my family, friends, and classmates across Nigeria, Ghana, and the United States for their unwavering support throughout this journey.

TABLE OF CONTENTS

LIST OF FIGURES

LIST OF TABLES

LIST OF ABBREVIATIONS

ABC	ATP-Binding Cassette
ADP	Adenosine Diphosphate
Arf6	ADP-Ribosylation Factor 6
ATCC:	American Type Culture Collection
ATP	Adenosine Triphosphate
BSA	Bovine Serum Albumin
Cas9	CRISPR-Associated Protein 9
CD	Cluster of Differentiation 8
CD4	Cluster of Differentiation 4
CRISPR	Clustered Regularly Interspaced Short Palindromic Repeats
DMEM	Dulbecco's Modified Eagle Medium
DTT	Dithiothreitol
ECL	Enhanced Chemiluminescence
EDEM1	Endoplasmic Reticulum Degradation-Enhancing α-Mannosidase-Like Protein 1
EDEM2	Endoplasmic Reticulum Degradation-Enhancing α-Mannosidase-Like Protein 2

EDEM3	Endoplasmic Reticulum Degradation-Enhancing α-Mannosidase-Like Protein 3
EE	Early Endosome
ER	Endoplasmic Reticulum
ERAD	Endoplasmic Reticulum-Associated Degradation (ERAD)
ERp57	Endoplasmic Reticulum (ER)–Resident Protein 57
FBS	Fetal Bovine Serum
FDR	False Discovery Rate
FITC	Fluorescein Isothiocyanate Fluorescence
HLA	Human Leukocyte Antigen
KD	Knockdown
KO	Knockout
LE	Late Endosome
MAN1A1	Mannosyl-Oligosaccharide 1,2-Alpha-Mannosidase IA
MAN1B1	Mannosyl-Oligosaccharide 1,2-Alpha-Mannosidase IB
MAN1C1	Mannosidase Alpha Class 1C Member 1
MFI	Mean Fluorescent Intensity
MHC	Major Histocompatibility Complex

NK	Natural Killer
OST	Oligosaccharyltransferase
PLC	Peptide-Loading Complex
RPMI	Roswell Park Memorial Institute
SDS-PAGE	Sodium Dodecyl Sulfate Polyacrylamide Gel Electrophoresis
Sec22B	SEC22 Homolog B
SV40	Simian Virus 40
TAP	Transporter Associated with Antigen Processing
TAPBP	TAP-Binding Protein
TBST	Tris-Buffered Saline with Tween 20
TMT	Tandem Mass Tag
WACCBIP	West African Centre for Cell Biology of Infectious Pathogens
WT	Wild-type

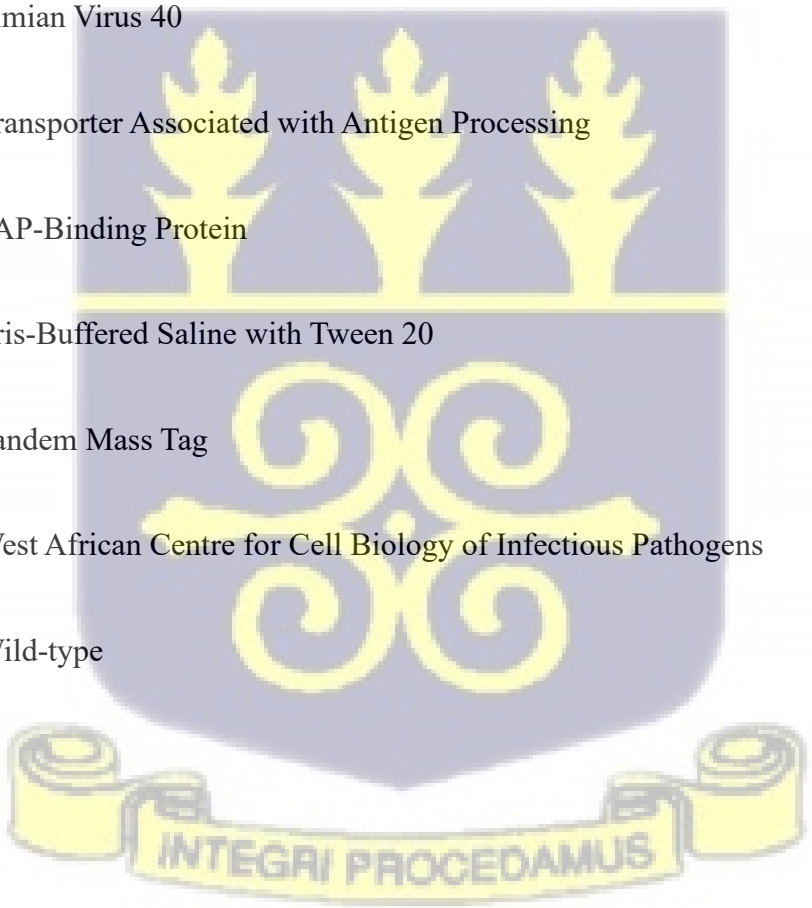

CHAPTER ONE

INTRODUCTION

1.1 Background

The major histocompatibility complex (MHC) class I, also known as human leukocyte antigen (HLA) class I in humans, is a glycoprotein that mediates immune response by presenting antigens to cytotoxic lymphocytes (CTLs) and regulating the activities of natural killer (NK) cells. The conventional (canonical) pathway for endogenous antigen presentation involves the transport of cytosolic peptides into the endoplasmic reticulum (ER) through the transporter associated with antigen processing (TAP) and the subsequent assembly of peptides with HLA class I heavy and light chains in the ER. This process is facilitated by generic and HLA class I-specific chaperones, including calreticulin, calnexin, tapasin, and the ER oxidoreductase ERp57 (Blum et al., 2013; Zaitoua et al., 2020). Upon assembly with peptides, HLA class I molecules exit the ER and transit through the Golgi to the plasma membrane, where they are surveyed by effector cells (Blum et al., 2013).

The conventional pathway largely depends on TAP, a peptide source for HLA class I assembly. Given this crucial function of TAP, many viruses and cancers target TAP to subvert antigen presentation and evade immune responses (Mantel et al., 2022). TAP dysfunction generally deprives HLA class I molecules of peptides, retains empty HLA class I in the ER, and reduces the stability of HLA class I expressed on the cell surface (de la Salle et al., 1999; Ljunggren et al., 1990; Raposo et al., 1995). However, HLA class I allotypes exhibit reduced TAP dependence, and can be expressed at measurable levels on the cell surface under TAP-deficient conditions (Geng et

al., 2018; Henderson et al., 1992; Lampen et al., 2010; Wei & Cresswell, 1992). The molecular mechanism(s) underlying this TAP-independent antigen presentation is poorly understood.

A previous study also observed an altered glycosylation profile of HLA class I molecules expressed on the plasma membrane of TAP-deficient cells (Geng et al., 2018). Specifically, Geng et al (2018) noted that surface HLA class I molecules express endoglycosidase (Endo)-H sensitive glycans under TAP deficiency. These Endo-H sensitive glycoforms on secreted glycoproteins are largely attributed to ER stress-induced unfolded protein response and unconventional protein secretion bypassing the canonical ER-trans-Golgi pathway (Grieve & Rabouille, 2011; Nickel & Seedorf, 2008). ER stress is a dysregulated cellular state induced by an accumulation of unfolded or misfolded proteins beyond the ER's homeostatic capacity (Haeri & Knox, 2012; Oslowski & Urano, 2011). Under TAP deficiency, the burden of unfolded or misfolded empty HLA class I molecules in the ER increases (de la Salle et al., 1994; Raposo et al., 1995). However, whether TAP deficiency induces ER stress is understudied (Sabapathy & Nam, 2008), and whether TAP-independent HLA class I proteins utilize unconventional secretory pathways is unknown.

Additionally, studies have shown that dysfunction of key chaperones, such as tapasin, increases the amount of empty HLA class I in the ER, reducing overall cell surface HLA class I expression (Grandea et al., 2000; Ortmann et al., 1997; Yabe et al., 2002). However, it has not been investigated whether the altered HLA class I glycosylation profile induced by TAP deficiency is TAP-specific or applies to the deficiency of chaperones required for efficient HLA class I assembly and trafficking.

HLA class I molecules have a highly conserved asparagine residue (Asn86) to which a high mannose precursor N-glycan, Glc3Man9GluAc2, is appended early in the ER (Ryan & Cobb,

2012). Generally, as glycoproteins traffic from the ER to the plasma membrane, the precursor glycan is modified by glycan-processing enzymes, including mannosidases, in a manner that dictates the fate of the proteins (Aebi, 2013; Bieberich, 2014). Generic ER and Golgi mannosidases for glycoprotein processing include ER degradation-enhancing alpha-mannosidase-like 1 proteins (EDEM1, EDEM2, and EDEM3) and 1,2-alpha-mannosidases (Bieberich, 2014). While previous studies have implicated EDEM1 and EDEM2 as regulators of HLA class I expression, targeting misfolded HLA class I for degradation via ER-associated degradation (Burr et al., 2013; Timms et al., 2016), the role of the other ER and Golgi 1,2-alpha-mannosidases in the regulation and trafficking of HLA class I molecules has not been reported. The influence of TAP deficiency on ER and Golgi-glycan processing enzymes has also not been reported.

Trafficking of MHC class I proteins via the endocytic recycling pathways is relevant to TAP-independent MHC class I cross-presentation (of exogenous antigens) (Barbet et al., 2021; Colbert et al., 2020; Sengupta et al., 2024). In these pathways, MHC class I molecules in endocytic compartments, such as phagosomes or endosomes, acquire exogenous peptides that they present to $CD8^+$ T cells. Recently, the involvement of the endocytic pathway in endogenous antigen presentation has been observed in primary professional antigen-presenting cells, with functional TAP (Olson et al., 2023). While there is evidence for MHC class I exogenous antigen presentation under TAP deficiency (Barbet et al., 2021; Sengupta et al., 2024) and endogenous antigen presentation under functional TAP (Olson et al., 2023; Olson & Raghavan, 2023), whether bulk HLA class I molecules utilize the endocytic pathways or not for surface expression and endogenous antigen presentation under TAP-deficient conditions has not been addressed.

The nature of peptides presented under TAP-deficient conditions and their source proteins could offer relevant insights into the mechanisms governing TAP-independent HLA class I trafficking.

Previous efforts, though using mass spectrometric analysis, have so far identified a relatively small number of TAP-independent peptides (Marijt et al., 2018; Wei & Cresswell, 1992; Weinzierl et al., 2008). These peptides are mostly restricted to HLA-A*02 allotype (Marijt et al., 2018; Wei & Cresswell, 1992). Hence, more informative quantitative mass spectrometric analyses are needed to increase the repertoire of peptides presented by HLA class I allotypes independent of TAP (Mamrosh et al., 2023).

Understanding the pathways and mechanisms underlying bulk HLA class I trafficking and the nature of peptides presented by HLA class I under TAP-deficient conditions could inform the development of novel immunotherapeutics against infectious pathogens and cancers that evade immune surveillance by inhibiting TAP. Thus, this study focuses on elucidating HLA class I trafficking pathways in TAP-deficient cells, the influence of ER and Golgi mannosidases on HLA class I regulation, and understanding the nature of peptides presented under TAP-deficient conditions.

1.2 Statement of Problem

Many cancers and pathogenic viruses inhibit TAP, downregulating surface HLA class I and subverting immune surveillance (Mantel et al., 2022). Some HLA class I allotypes can present antigens even when TAP is inhibited (Geng et al., 2018; Henderson et al., 1992; Lampen et al., 2010; Wei & Cresswell, 1992). However, the pathways through which this presentation occurs have not been elucidated, and the nature of the peptides presented is poorly understood, making it difficult to exploit TAP-independent antigens for immunotherapies.

1.3 Research Questions

1) What trafficking pathways do HLA class I proteins follow in cells deficient in TAP?
2) How do various ER and Golgi mannosidases influence HLA class I trafficking?
3) What is the nature of peptides presented by HLA class I proteins under TAP deficiency and what is the relevance of endolyosomal pathways for HLA class I assembly?

1.4 Study Hypotheses

1) TAP deficiency induces canonical unfolded protein response, resulting in unconventional (ER-trans-Golgi independent) HLA class I trafficking.
2) Supplemental HLA class I assembly and antigen presentation occur in endocytic compartments of TAP-deficient cells in a pH gradient-dependent manner.

1.5.0 Aim of the Study

To elucidate HLA class I secretory pathways under TAP deficiency.

1.5.1 Specific Objectives

1. To determine HLA class I trafficking route(s) in TAP-deficient cells.

    i. To assess the human monocyte THP-1 cells for induction of canonical unfolded protein response markers – spliced X-box binding protein 1 (XBP1s), binding immunoglobulin protein (BiP), CCAAT-enhancer-binding proteins (C/EBP) homologous protein (CHOP), and activating transcription factor 4 (ATF4) by reverse transcriptase quantitative polymerase chain reaction RT-qPCR under TAP deficiency.

ii. To assess the influence of the Golgi reassembly-stacking protein of 55 kDa (GRASP55), a key mediator of unconventional protein secretion, and the vesicle-trafficking protein SEC22 homolog B (Sec22B) on HLA class I trafficking in TAP-deficient THP-1 cells.

iii. To assess the influence of impaired conventional protein secretory pathway on HLA class I trafficking in TAP-deficient THP-1 cells.

2. To assess the influence of ER and Golgi mannosidases on HLA class I trafficking.

i. To assess the influence of ER degradation-enhancing alpha-mannosidase-like 1 proteins (EDEM1, EDEM2, and EDEM3) on HLA class I trafficking in THP-1 cells.

ii. To determine the influence of mannosyl-oligosaccharide 1,2-alpha-mannosidase IA (MAN1A1), mannosyl-oligosaccharide 1,2-alpha-mannosidase IB (MAN1A2), endoplasmic reticulum mannosyl-oligosaccharide 1,2-alpha-mannosidase (MAN1B1), and mannosyl-oligosaccharide 1,2-alpha-mannosidase IC (MAN1C1) on HLA class I trafficking in THP-1 cells.

iii. To assess the influence of TAP deficiency on the expression of EDEM1, EDEM2, and EDEM3, as well as MAN1A1, MAN1A2, MAN1B1, and MAN1C1 in THP-1 cells.

3. To assess the contribution of endocytic compartments to HLA class I assembly and trafficking in TAP-deficient THP-1 cells.

i. To determine HLA class I immunopeptidome and identify TAP-independent peptides in THP-1 cells.

ii. To assess the influence of pH-dependent endocytic organelles on HLA class I trafficking in TAP-deficient THP-1 cells.

iii. To assess the influence of RAB11A small GTPase on HLA class I trafficking in TAP-deficient THP-1 cells.

iv. To assess the influence of HLA class II invariant chain (Ii or CD74) on HLA class I assembly and trafficking in TAP-deficient THP-1 cells.

1.6 Significance of the Study

Several cancers and viruses disrupt the peptide transport function of TAP to downregulate the HLA class I antigen presentation pathway (Mantel et al., 2022), evading their detection and elimination by CTLs. With limited therapeutic options, the burden of cancers and the threat of pathogenic viruses are a growing concern globally (Graham & Sullivan, 2018; Sung et al., 2021). Elucidating HLA class I secretory pathways and understanding the nature of peptides presented by HLA class I molecules under TAP-dysfunctional conditions could inform new therapeutic approaches for malignant and viral diseases.

CHAPTER TWO

LITERATURE REVIEW

2.1.0 The human leukocyte antigen class I

Cells are constantly faced with assaults from pathogenic microorganisms or malignant conditions that pose threats to their survival. To survive these threats, the immune system must distinguish between normal cells and invading microorganisms or malignant conditions and mount an appropriate response to eliminate or resist these pathogens. Central to the recognition of pathogens and activation of the immune system is antigen presentation, a process through which proteins from infectious pathogens or cancerous cells are processed into peptides and displayed on the cell surface by two groups of proteins known as the major histocompatibility complex (MHC) class I and class II. MHC class I proteins display peptides on all nucleated cells and activate cytotoxic T lymphocytes (CTLs) or clusters of differentiation (CD)8^+ T cells (Raskov *et al.*, 2021). However, MHC class II displays peptides on specialized antigen-presenting cells (APCs), such as dendritic cells, macrophages, and B cells, and activates $CD4^+$ T cells (Roche and Furuta, 2015). Upon activation, CTLs induce apoptosis of the infected or malignant cells and secrete cytokines that enhance immune response (Raskov *et al.*, 2021). Similarly, activated $CD4^+$ T cells secrete cytokines that modulate immune response but promote antibody production by B cells. By presenting antigens to CTLs or $CD4^+$ T cells, MHC proteins play a crucial role in the adaptive immune response (Roche and Furuta, 2015).

The human leukocyte antigen (HLA) class I (the MHC class I in humans) is a glycoprotein expressed in all nucleated cells. Functionally, HLA class I presents peptides to $CD8^+$ T cells and

regulates natural killer (NK) cells. These peptides may be derived from the cell under physiological conditions (self-peptides) or from infectious agents (non-self-peptides) invading the cells, or from host proteins under malignant conditions (tumour antigens) (Li et al., 2023; Yewdell, 2022; Yewdell et al., 1996; Yewdell & Nicchitta, 2006). The tumour antigens may be referred to as self-peptides if they are derived from non-mutated proteins, or as non-self-peptides when they are derived from mutated proteins. By presenting peptides to $CD8^+$ T cells and regulating NK cells' activities, HLA class I mediates the surveillance and cytotoxic functions of the cells (Neefjes et al., 2011; Zaitoua et al., 2020).

Structurally, HLA class I is a heterotrimeric protein comprising a heavy chain (α chain), a light chain (β_2 microglobulin (β_2m)), and a short peptide (Figure 2.1). The α chain consists of three domains: α1, α2, and α3, with the first two domains forming the membrane-distal, peptide-binding site, and the membrane-proximal α3 domain, as also the β_2m, adopting immunoglobulin (Ig)-like folds (Bjorkman et al., 1987).

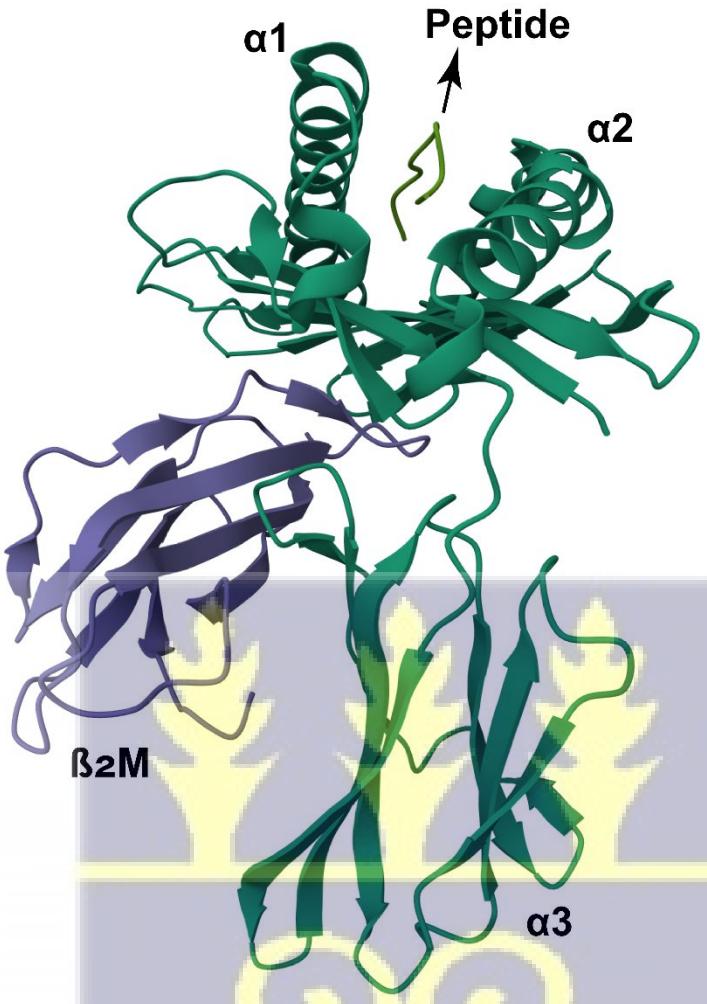

Figure 2.1: Crystal structure of HLA class I-peptide complex. The structure depicts HLA-A2 (PDB ID: 1HHI) at 2.50 Å resolution (Madden et al., 1993). The heavy α chain (green) and the light β2-microglobulin chain (purple) in complex with a peptide are shown. The structure was obtained from the RCSB Protein Data Bank (https://www.rcsb.org/structure/1HHI).

2.1.1 Genetic diversity of HLA class I

To date, three classical HLA class I proteins have been described: HLA class 1 A (HLA-A), HLA-B, and HLA-C. These proteins are encoded by three classical HLA class I genes: *HLA-A, HLA-B*, and *HLA-C*, respectively (Zaitoua et al., 2020). The classical HLA class I genes are located within the class I region of the MHC loci on the short arm of chromosome 6 (6p21.3). Additionally, *HLA-E, HLA-F,* and *HLA-G,* encoding their respective non-classical HLA class I proteins on the MHC region have been reported. Notably, the MHC region is the most polymorphic loci of the human genome, encoding more than 140 protein-coding genes and accounting for about 0.75% of all protein-coding genes on the human chromosome (Kulski et al., 2022; Wassenaar et al., 2024). As of September 2024, the Immuno Polymorphism Database - International ImMunoGeneTics Information System / Human Leukocyte Antigen (IPD-IMGT/HLA) Database (https://www.ebi.ac.uk/ipd/imgt/hla/) has recorded more than 26,000 combined confidential alleles for *HLA-A, -B,* and *-C*, encoding more than 15 000 distinct HLA class I allotypes (Figure 2). This polymorphism is considered to have evolved as a survival mechanism, enabling HLA-expressing cells to cope with the constant assaults from a wide range of rapidly evolving pathogenic conditions.

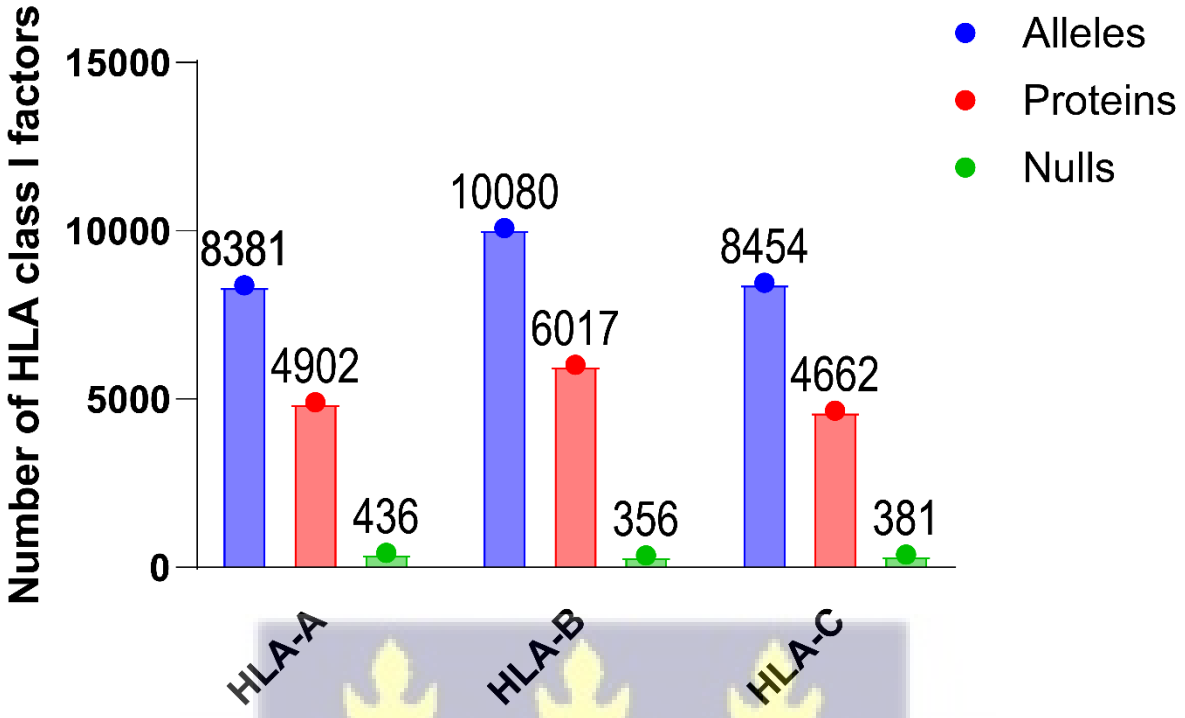

Figure 2.2: Classical HLA class I factors. Classical HLA class I alleles (blue bars), the proteins they encode (red), and HLA class I alleles encoding no known proteins (green bars) are presented. Data was retrieved from IPD-IMGT/HLA Database https://www.ebi.ac.uk/ipd/imgt/hla/about/statistics/ on September 28, 2024.

2.1.2.0 HLA class I antigen presentation

Classically, HLA class I proteins present endogenous peptides, which are peptides generated from within the cell. These peptides are displayed on the plasma membrane through a series of molecular processes involving the conventional (Golgi-dependent) protein secretory pathway (Figure 2.3). In the classical HLA class I antigen presentation pathway, proteins in the cells are degraded by the proteasome, generating antigenic peptides that are then transported into the endoplasmic ER through the TAP (Blum et al., 2013; Lehnert & Tampe, 2017). In the ER, the peptides are trimmed

by ER aminopeptidase associated with antigen processing and assembled with HLA class I proteins. The peptide-assembled HLA class I molecules then exit the ER and translocate to the plasma membrane, passing through the ER-Golgi intermediate compartment (ERGIC) and the Golgi apparatus (Figure 2.3). Peptide assembly with HLA class I is facilitated by many ER chaperones, including the TAP-binding protein (TAPBP or tapasin), the protein disulfide isomerase (ERp57), and two glycan-binding lectins – calreticulin and calnexin (Blum et al., 2013; Neefjes et al., 2011; Zaitoua et al., 2020).

The peptides displayed by HLA class I on the cell surface are surveyed by $CD8^+$ T cells through their T cell receptors (TCRs) (Figure 2.4). Upon encountering non-self (foreign) antigenic peptides, $CD8^+$ T cells are activated through a cascade of reactions mediated by signaling factors. Activated $CD8^+$ T cells undergo clonal expansion and exert many effector functions, including the production of interferon-γ (IFN-γ, a pro-inflammatory cytokine), the release of perforin and granzymes (cytotoxic granules), and apoptosis-inducing Fas ligand (FasL) interaction with Fas receptors on target cells. Collectively, these effector functions promote the elimination of infected or malignant cells (Zhang & Bevan, 2011).

Surface HLA class proteins are also surveyed by NK cells. Through their inhibitory receptors, such as the killer immunoglobulin-like receptors (KIRs) (Figure 2.4), NK cell's cytotoxic activation is inhibited by self-HLA class I molecules expressed on the surface of healthy cells. In pathological conditions, such as viral infections or malignancies that downmodulate surface HLA class I, the inhibitory receptors are inhibited, resulting in the activation of NK cells (Greppi et al., 2024; Yokoyama et al., 2010). HLA class I molecules can also interact with activating receptors on NK cells. For example, the interaction of some HLA-C allotypes with the activating receptors, killer immunoglobulin-like receptor two Ig domains and short cytoplasmic tail 1 (KIR2DS1), KIR2DS2,

and KIR2DS4 has been reported. Additionally, the NK cell receptor G2-C (NKG2C) in dimer with CD94 has been reported to be activated by the non-classical HLA-E (Della Chiesa et al., 2015; Greppi et al., 2024). By regulating NK cell activation/inhibition, HLA class I molecules modulate immune response.

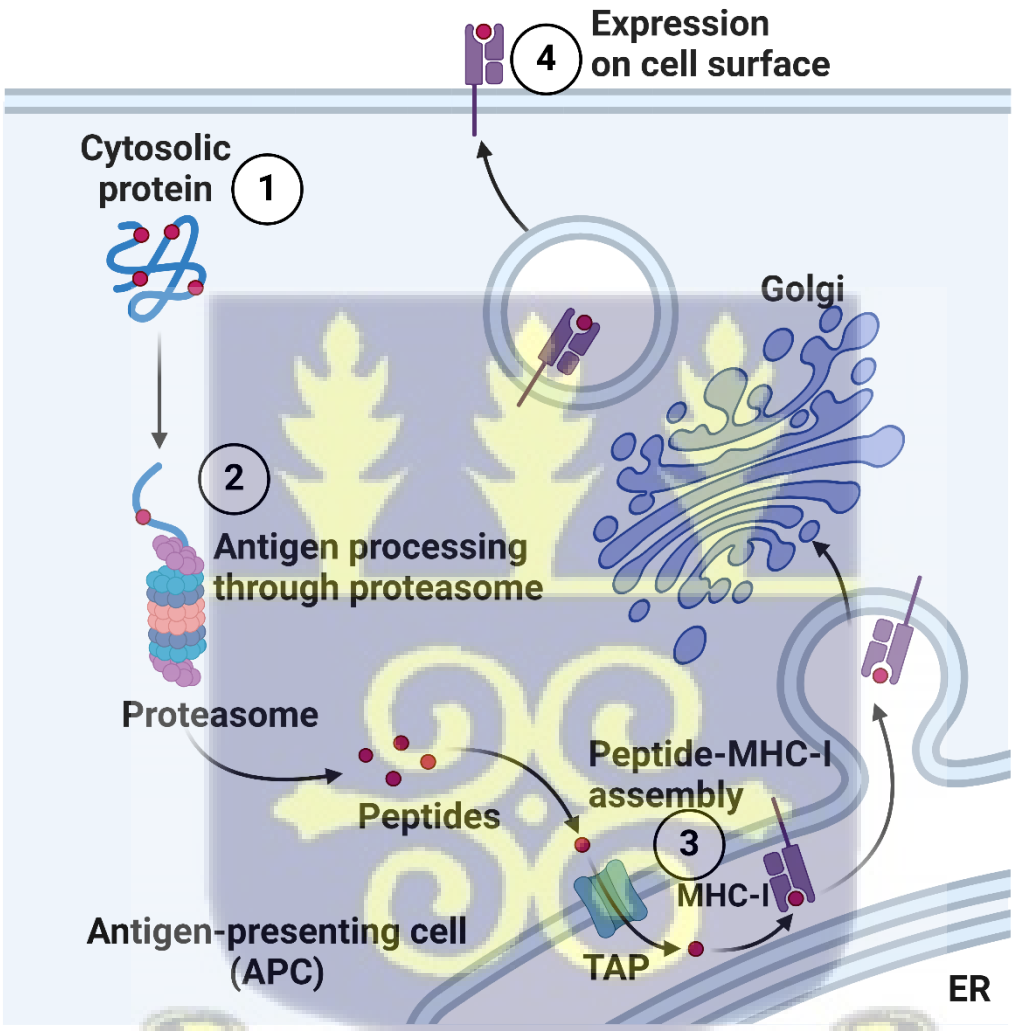

Figure 2.3: The HLA class I conventional trafficking pathway. Proteins in the cytosol (1) are degraded in the proteasome (2) to generate antigenic peptides, which are funneled into the ER. In the ER, the peptides are loaded onto the peptide-binding pocket of MHC class I (3). The peptide-

MHC class I complex exits the ER and transits to the plasma membrane, traversing the Golgi apparatus. Image created using Biorender.com.

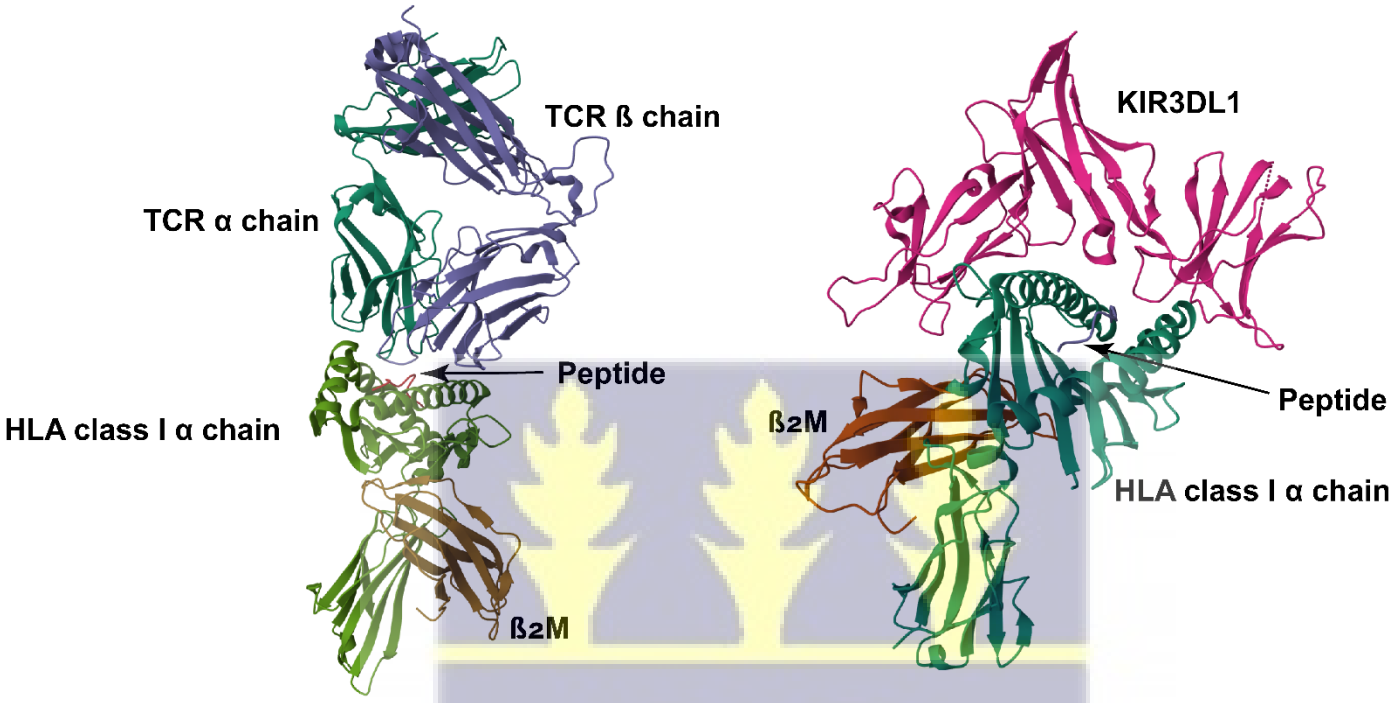

Figure 2.4: HLA class I interaction with cytotoxic T cell receptor (TCR) and NK cell KIR3DL1. The left panel depicts a complex between HLA-*02 in complex with a peptide and TCR (PDB ID: 5D2N) at 2.10 Å resolution (Yang et al., 2015). The structure was obtained from the RCSB Protein Data Bank https://www.rcsb.org/structure/5D2N). The right panel depicts HLA-A*57:01 in complex with a peptide and NK cell KIR3DL1 (PDB ID: 3WUW) at 2.00 Å resolution (O'Connor et al., 2014). The structure was obtained from the RCSB Protein Data Bank (https://www.rcsb.org/structure/3WUW).

2.1.2.1 HLA class I antigen cross-presentation

In addition to endogenous antigens, HLA class I presents exogenous peptides, which are peptides derived from proteins or pathogens internalized from the extracellular compartment. The presentation of exogenous antigens by HLA class I is referred to as cross-presentation. By presenting exogenous antigens, HLA class I functions like HLA class II but presents its antigens to $CD8^+$ T cells instead of $CD4^+$ T cells, the effector cells of HLA class II (Figure 2.4) (Gutierrez-Martinez et al., 2015; van Endert, 2016).

Endocytic organelles, such as phagosomes and endolysosomal compartments, have been implicated in cross-presentation (Adiko et al., 2015; Blander, 2016, 2018). Endocytic compartments could acquire HLA class I from the plasma membrane through constitutive internalization via an adenosine diphosphate (ADP)-ribosylation factor 6 (Arf6)-dependent clathrin-independent pathway (Blander, 2016; Naslavsky et al., 2004; van Endert, 2016) and, possibly, clathrin-dependent endocytosis (Lizee et al., 2003; Montealegre & van Endert, 2018; Munz, 2018). A fraction of HLA class I from the ER can also be transported into endolysosomes, escorted by the HLA class II invariant chain (Ii, CD74) (Figure 2.5).

The rate and extent of this internalization vary depending on the conformational status of the HLA class I molecules and the type of cells involved (van Endert, 2016). When internalized, HLA class I molecules enter early endosomes and are sorted into the fast or slow recycling pathway or targeted for lysosomal degradation (Figure 2.6). In the fast-recycling route, HLA class I proteins are rapidly returned to the plasma membrane, predominantly regulated by Rab4 and Rab35 small GTPases. The slow recycling pathway, on the other hand, directs HLA class I molecules to endocytic recycling compartments (ERC) and is regulated by many proteins, including Rab11,

Arf6, and Rab22 professional antigen-presenting cells (APC) (Blander, 2016; Grant & Donaldson, 2009; Montealegre & van Endert, 2018; van Endert, 2016).

Although endocytic recycling of MHC class I molecules is mostly associated with cross-presentation, the involvement of endolysosomal assembly of MHC class I for endogenous antigens presentation is an emerging concept in the field, with strong evidence that HLA class I allotypes indeed assemble in endolysosomes, but to different degrees (Olson et al., 2023; Olson & Raghavan, 2023).

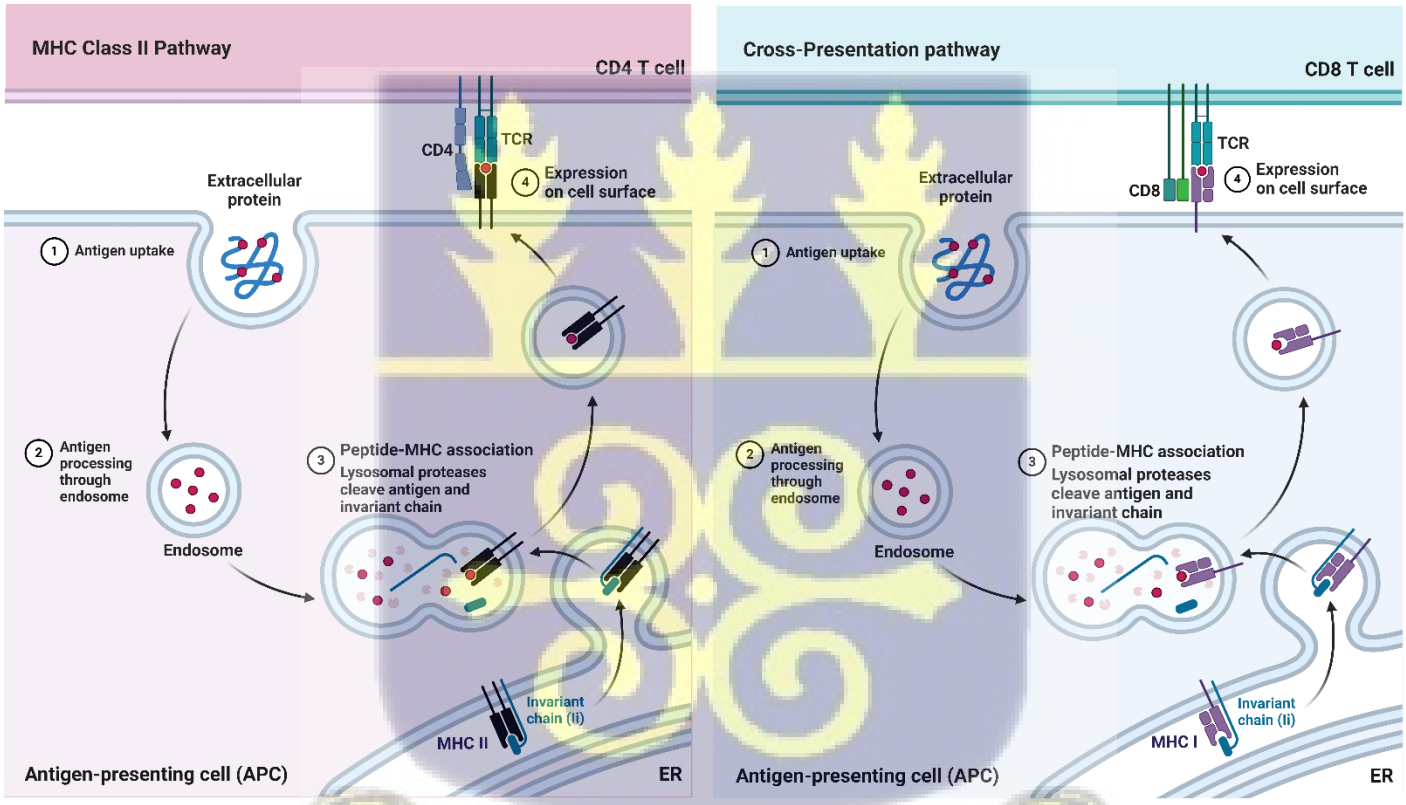

Figure 2.5: Similar role of invariant chain in HLA class II antigen presentation and HLA class I cross-presentation. The involvement of invariant chain (Ii, or CD74) in HLA class II antigen presentation (left) and HLA class I cross-presentation (right) of exogenous antigens is

shown. Antigens are internalized (1) into an endosome (2), which fuses with the lysosome to form an endolysosomal compartment (3). HLA class II (MHC II) or HLA class I (MHC I) associates with CD74 in the endoplasmic reticulum (ER) and is directed to the endolysosomal compartment through the interaction of the two dileucine-based sorting signals in the cytosolic domain region of CD74. Antigens processed by lysosomal enzymes are assembled on the HLA proteins, which then traffic to the plasma membrane (4). HLA class II is surveyed by $CD4^+$ T cells and HLA class I by $CD8^+$ T cells. Image created using BioRender.com.

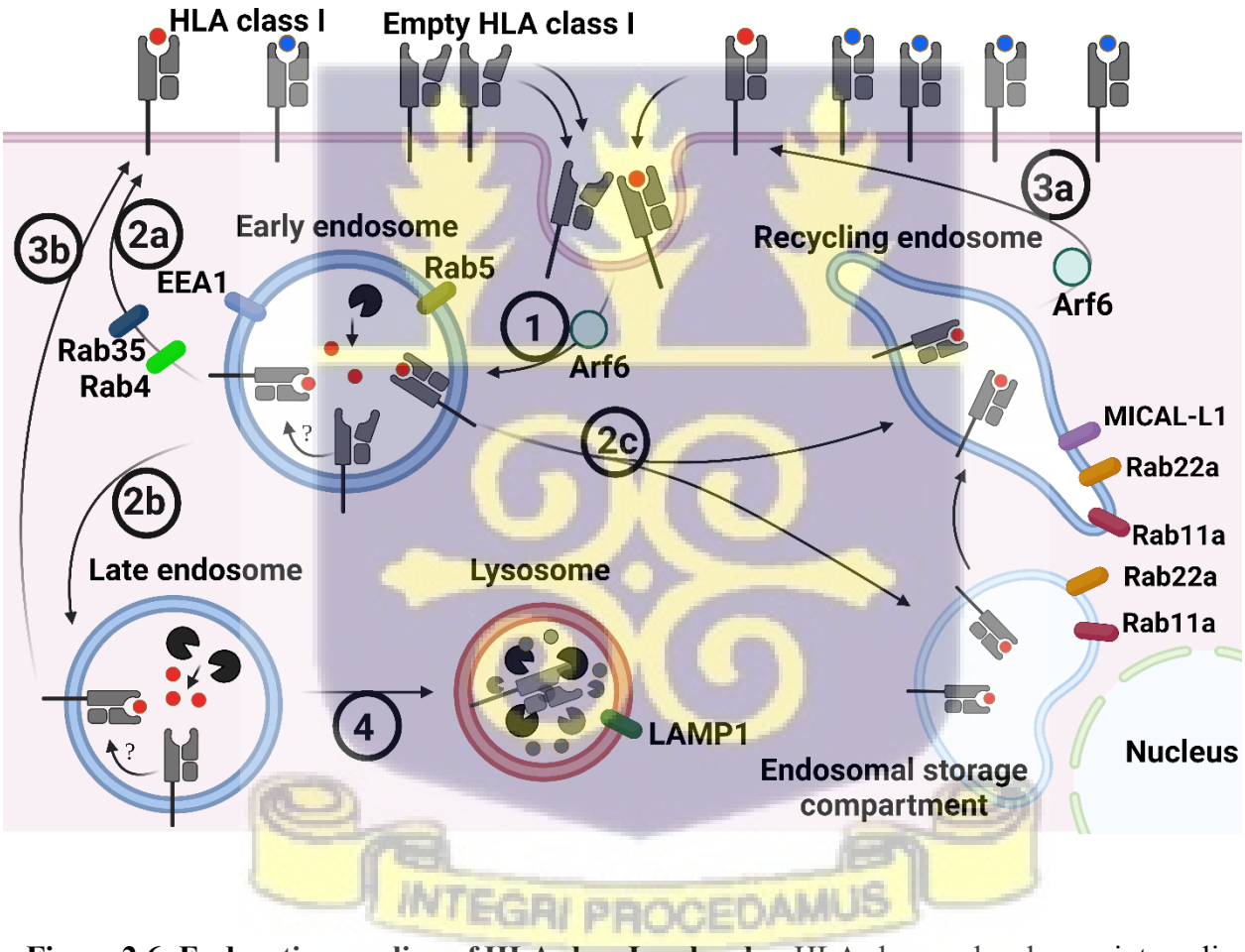

Figure 2.6: Endocytic recycling of HLA class I molecules. HLA class molecules are internalized into early endosomes (EE) marked by early endosomal antigen (EEA) and Rab5 small GTPase. This internalization occurs through clathrin-independent endocytosis (CIE) mediated by adenosine

diphosphate ribosylation factor 6 (Arf6) (1). A possible clathrin-dependent internalization of HLA class I molecules (not shown) has also been described (Lizee et al., 2003; Montealegre & van Endert, 2018; Munz, 2018). HLA class I molecules in EE may rapidly recycle to the plasma membrane through the fast-recycling pathway facilitated by the small GTPases Rab4 and Rab35 (2a) or proceed to the late endosome (2b), which then fuses with the lysosome. The fate of HLA class I molecules in LE may be largely degradative after lysosomal fusion; however, a possible assembly with peptides in this compartment and the EE has been proposed (Olson & Raghavan, 2023), enabling recycling to the plasma membrane (3b). HLA class I molecules from the EE could also proceed to a perinuclear endocytic recycling compartment (ERC, also called endosomal storage compartment) or tubular recycling endosomes (2c). Both ERC and the tubular recycling endosomes are collectively called recycling endosomes, marked by Rab11a and Rab22a. In addition, tubular recycling endosomes are marked by molecules interacting with CasL-like protein 1 (MICAL-L1). HLA class I proteins from recycling endosomes are transported to the plasma membrane through the slow recycling route, also facilitated by Arf6 (van Endert, 2016). This figure was adapted from (Olson & Raghavan, 2023) and slightly modified using BioRender.com.

2.1.3.0 HLA class I glycosylation and quality control

As glycoproteins, HLA class I molecules undergo glycosylation, a posttranslational modification, and quality control from the ER to the Golgi before arriving at the plasma membrane. Generally, upon arriving in the ER, nascent proteins destined to be glycoproteins are labeled with a precursor glycan. This glycan is then sequentially modified by diverse glycan-processing enzymes during the proteins' ER-trans-Golgi odyssey. The covalent attachment of glycans to would-be glycoproteins (such as HLA class I) or lipids is termed "glycosylation" (Aebi, 2013; Bieberich, 2014).

Many types of glycosylation have been reported, but to date, the *O*- and *N*-glycosylation are the two major types well-described (He et al., 2024). The *O*-glycosylation occurs primarily in the Golgi and involves the covalent attachment of glycans to the oxygen atom of serine (Ser) or threonine (Thr) residues. *N*-glycosylation is the most common type of glycosylation. It involves the attachment of glycans to specific asparagine residues within three amino acid sequence: Asn-X-Ser/Thr, where Asn, X, Ser, and Thr are asparagine, any amino acid, serine, and threonine residues respectively. This tripartite amino acid sequence is referred to as "sequon" (Bieberich, 2014; He et al., 2024; Stanley et al., 2022).

HLA class I molecules could undergo *O*-glycosylation (Yoneyama et al., 2017) and N-glycosylation (Barber et al., 1996). The *O*-glycosylation has been observed at least on the allotype HLA-A*24, where *N*-acetylgalactosamine (GalNAc) transferase covalently links a precursor GalNac to the threonine 187 (Thr187) residue of α2 domain below the peptide-binding cleft (Figure 2.7A). The GalNac could be further modified into glycoforms that affect HLA class I functionally (Yoneyama et al., 2017). For N-glycosylation, a high-mannose precursor Glucose3-Mannose9-N-acetylglucosamine2 (Glc3Man9GlcNAc2) is transferred from the lipid carrier, dolichol phosphate, to the asparagine 86 residue (Asn86) on α3 domain of nascent HLA class I heavy chain in the ER (Barber et al., 1996) (Figure 2.7B). The Glc3Man9GlcNAc2 is modified into high mannose (Figure 2.7C), hybrid (Figure 2.7D), or complex N-glycans (Figure 2.7E) through concerted activities of N-glycan processing enzymes in the ER and the Golgi.

Among the three broad classes of N-glycans, high mannose glycans can be differentiated from complex glycans by their sensitivity to enzymatic cleavage by Endoglycosidase H (Endo-H) (Bieberich, 2014). Unlike complex glycans, high mannose glycans possess two free terminal mannose residues (black ring in Figure 2.7), accommodated by Endo-H, conferring the sensitivity

(Du et al., 2020). Upon encountering the mannose residues, the Endo-H enzyme cleaves the internal glycosidic bond between the two N-acetylglucosamine (GlcNAc) residues in the chitobiose core of high mannose glycans (marked by * in Figure 2.7), leaving one GlcNAc attached to the asparagine residue on the protein (Du et al., 2020). Like high mannose glycans, some hybrid glycans that possess the two free terminal mannose residues are sensitive to Endo-H cleavage (Williams et al., 2022). By discriminating complex glycans from high mannose glycans, the Endo-H enzyme has become a crucial biochemical tool for studying protein glycosylation and trafficking (Cleyrat et al., 2014; Du et al., 2020; Geng et al., 2018; Williams et al., 2022).

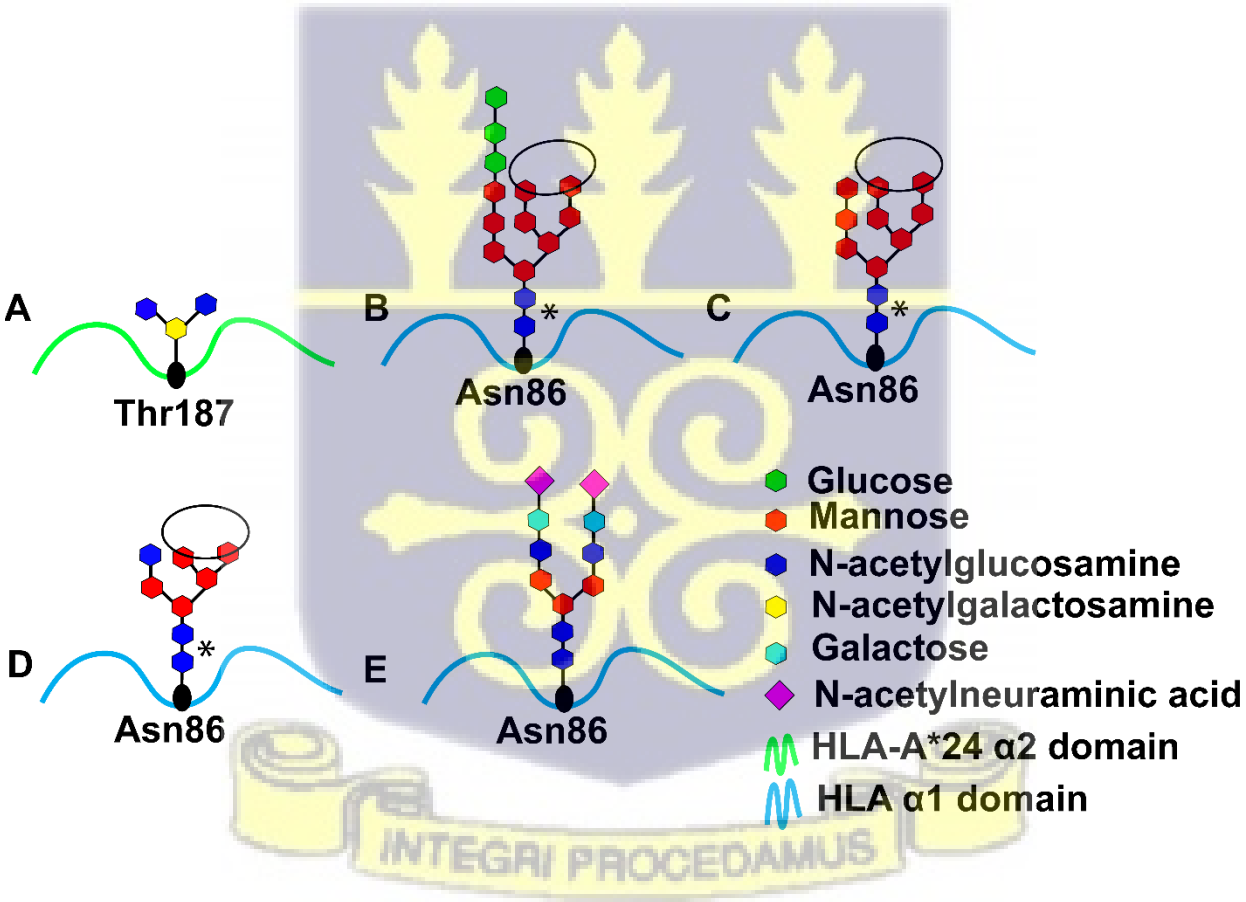

Figure 2.7: Types of HLA class I glycosylation and broad classification of N-glycans. A) *O*-glycans on 187 threonine residue of α2 domain observed on HLA-A*24 (Yoneyama et al., 2017). B) Precursor *N*-glycan (Glc3Man9GlcNAc2) on asparagine 86 of α1 domain. This precursor

glycan is transferred from the lipid carrier, dolichol phosphate, to HLA class I molecules early in the ER. Asn 86 is conserved in all HLA class I molecules enabling their *N*-glycosylation on the residue. C) High mannose *N*-glycan derived from Glc3Man9GlcNAc2 through hydrolytic cleavage of the 3 glucose residues by glucosidase I and II. D) A hybrid glycan possessing a third *N*-acetylglucosamine apart from the two in the chitobiose core. E) A complex glycan. The precursor *N*-glycan (B), high mannose glycan (C), and hybrid glycan (D) have two free terminal mannose residues and are sensitive to Endo-H. The enzyme cleavage site on these glycans is marked with *. The complex glycan has no free terminal mannose residues and is not sensitive to Endo-H enzyme. Image created using Adobe Illustrator.

2.1.3.1 N-glycans processing enzymes

Many enzymes are involved in processing the precursor N-glycans from the ER to the Golgi, transitioning high mannose (immature) N-glycans in the ER to complex (mature) N-glycans in the Golgi (Figure 2.8). This processing includes the sequential trimming of glucose and mannose residues by ER glucosidases and ER and Golgi mannosidases (Bieberich, 2014; Stanley et al., 2022). Two glucosidases involved in N-glycan glucose trimming have been reported to date: Glucosidase I (Glu I) which catalyzes the hydrolytic cleavage of the terminal (first) glucose residue from Glc3Man9GlcNAc2, generating Glc2Man9GlcNAc2, and Glucosidase II (Glu II) which cleaves the second and third glucose residues from Glc2Man9GlcNAc2, converting the glycan into the deglucosylated intermediate, Man9GlcNAc2 (Aebi, 2013; Bieberich, 2014; Stanley et al., 2022).

The trimming of mannosidases depends on the folding state, dictates the fate of the glycoprotein, and is performed by ER degradation-enhancing alpha-mannosidase-like 1 proteins (EDEMs) and

1,2-alpha-mannosidases. EDEM1, EDEM2, and EDEM3 activities mark unfolded proteins for degradation through endoplasmic reticulum-associated degradation (ERAD) (Bieberich, 2014). The ER 1,2-alpha-mannosidase (Mannosidase alpha class IB member 1, MAN1B1) cleaves a mannose residue from the middle branch of the Man9GlcNAc2, promoting anterograde transport to the Golgi (Sakhi et al., 2021). MAN1B1 has also been implicated in the retrograde transport of unfolded glycoproteins from the Golgi back to the ER for refolding or degradation through ERAD (Iannotti et al., 2014; Pan et al., 2013). In addition to this quality control measure, unfolded deglucosylated proteins are reglucosylated by uridine diphosphate-glucose: glycoprotein glucosyltransferase 1 (UGGT1) into monoglucosylated glycoforms, which are refolded by calreticulin/calnexin activities (Adams et al., 2021). Other mannosidases trim more mannose residues in the Golgi, resulting in the glycoform Man3GlcNAc2, which is modified into a complex glycan before the protein exits the Golgi (Bieberich, 2014).

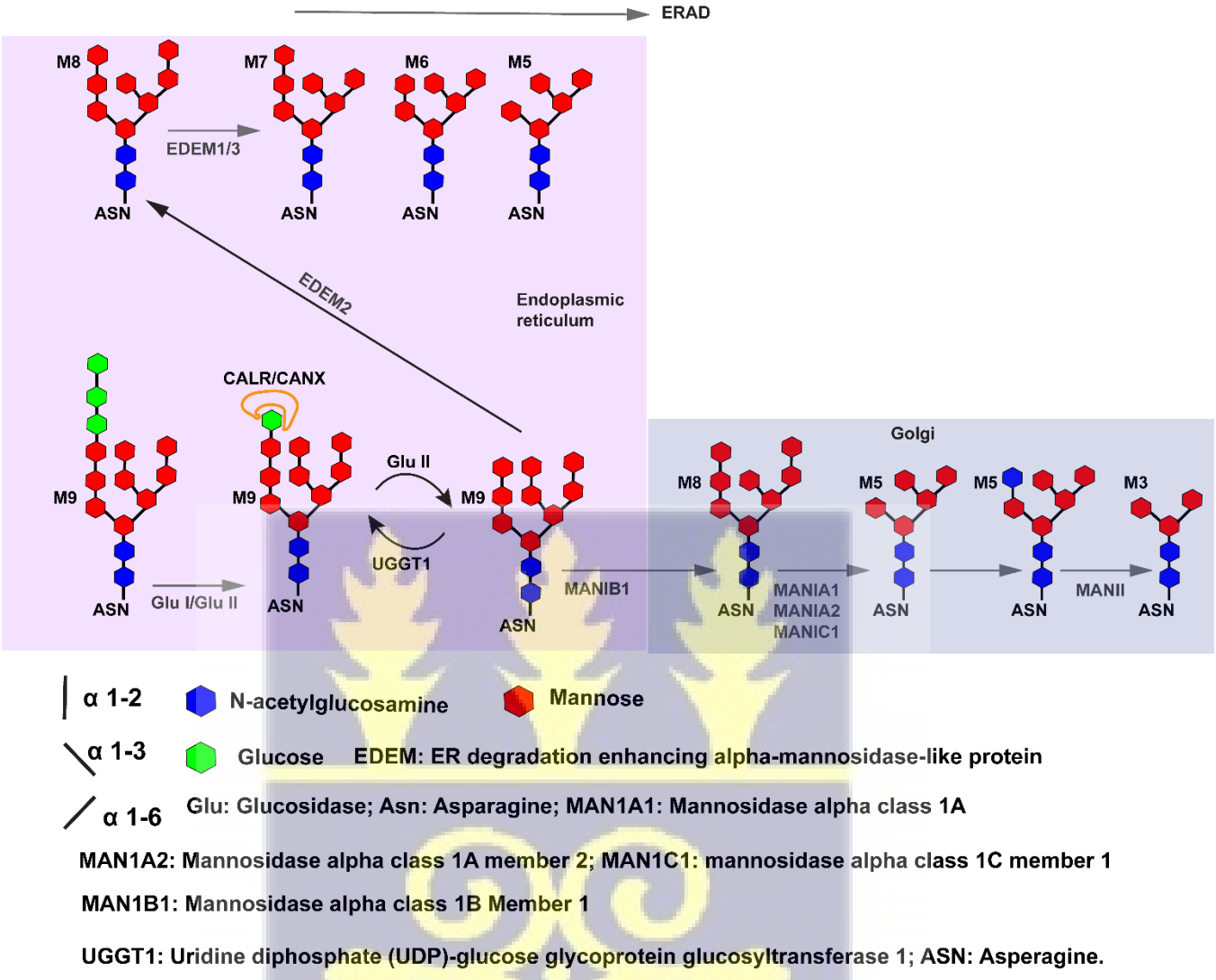

Figure 2.8 N-glycans processing by ER and Golgi exomannosidases. The precursor N-glycan (Glc3Man9GlcNAc2) appended on the nascent glycoprotein is trimmed by glucosidases and mannosidases. Glu I cleaves one glucose molecule from the precursor glycan and Glu II cleaves the second and third glucose residues to generate deglucosylated glycan, Man9GlcNAc2. If the protein is not in its native state, Man9GlcNAc2 is reglucosylated by UGGT1 to the monoglucosylated form, Glu1Man9GlcNAc2. Glu1Man9GlcNAc2-labelled glycoproteins are

refolded by the ER chaperons, calreticulin/calnexin. Man9GlcNAc2 on proteins that failed multiple rounds of refolding by calreticulin/calnexin is trimmed by EDEM2, EDEM1, and EDEM3 and proceeds to ERAD-mediated degradation. Man9GlcNAc2 on native proteins is sequentially trimmed by mannosidases to form Man3GluNAc2, a glycoform that could be modified into complex glycans. This figure was created with Adobe Illustrator.

2.2 The transporter associated with antigen processing (TAP)

TAP is a heterodimeric transmembrane protein and a member of the adenosine triphosphate (ATP) binding cassette (ABC) family. TAP consists of two subunits, TAP-1 and TAP-2 (Figure 2.9), both required for its peptide transport function (Lehnert & Tampe, 2017). The chronological events building up to the discovery and functional and structural elucidation of TAP have been well-documented (Mantel et al., 2022). Briefly, Alain Townsend proposed about 35 years ago that a protein could transport peptides across cellular membranes. Since then, concerted efforts by different research groups have uncovered the structural composition and many additional details about TAP (Lehnert & Tampe, 2017; Mantel et al., 2022).

Structurally, each TAP subunit consists of the transmembrane domain (TMD) and the nucleotide-binding domain (NBD). The TMD forms the peptide binding site and the peptide translocation pathway from the cytosol into the ER lumen. The NBD forms the ATP-binding and hydrolysis site. The exact mechanism underlying peptide transport by TAP is not completely understood; however, it is believed that the binding of the peptide to the TMD initiates the hydrolysis of ATP bound to the NBD, resulting in a conformational change that translocates the peptide into the ER lumen (Lehnert & Tampe, 2017). This model is supported by a recent structural analysis using cryo-electron microscopy (Lee et al., 2024). The study revealed that a bridge-like occupation of peptides

in the peptide-binding pockets of the transmembrane domain approximates the two TAP subunits, priming TAP isomerization and ATP hydrolysis (Lee et al., 2024). Although TAP can transport up to 40 amino acids long peptides, it binds peptides of 8-16 amino acids more efficiently and mostly transports 8-12 amino acids long (Abele & Tampe, 2004). The two TAP subunits provide architecture for calreticulin, calnexin, and the oxidoreductase ERp57 interaction in the peptide-loading complex (PLC) (Abele & Tampe, 2004; Lehnert & Tampe, 2017). Hence, TAP is a central component of the PLC and the HLA class I antigen presentation pathway.

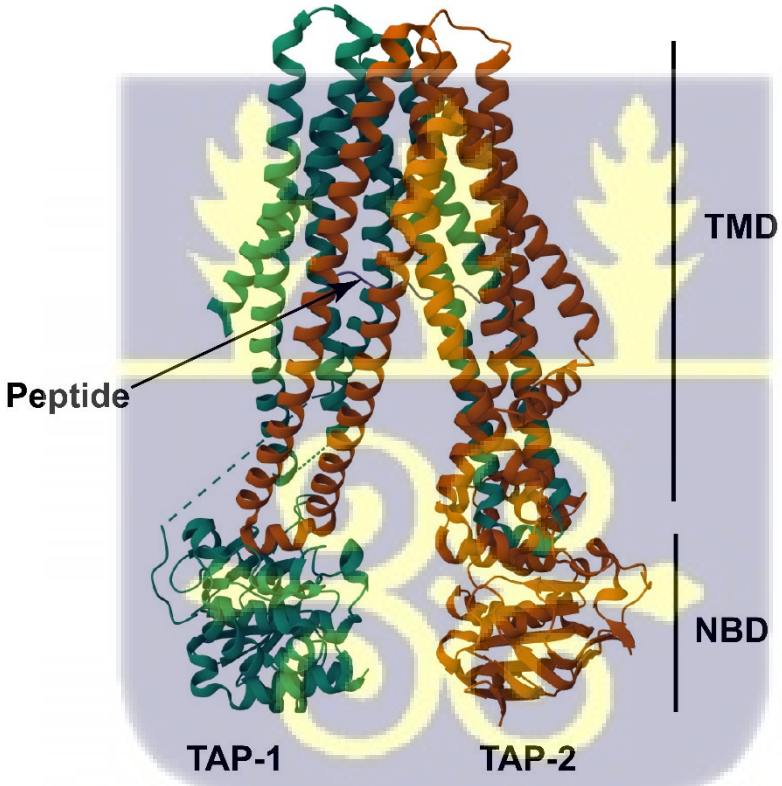

Figure 2.9: A crystal structure of TAP in complex with a peptide. The structure depicts TAP-1 and TAP-2 subunits in complex with a peptide at 3.50 Å (PDB ID: 8T4G). The nucleotide-

binding domain (NBD) and transmembrane domain (TMD) are shown. The structure was obtained from the RCSB Protein Data Bank (https://www.rcsb.org/structure/8T4G).

2.3 The role of tapasin in HLA class I antigen presentation

Tapasin is a transmembrane glycoprotein that is crucial to the PLC architecture in the ER. Tapasin is covalently linked to ERp57 through a disulfide bond (Dick et al., 2002; Dong et al., 2009; Peaper & Cresswell, 2008) and this heterodimer recruits HLA class I (Muller et al., 2022; Rizvi & Raghavan, 2010; Tan et al., 2002; Wearsch & Cresswell, 2007) (Figure 2.10) and calreticulin (Del Cid et al., 2010; Rizvi et al., 2011; Rizvi & Raghavan, 2010) to the PLC. Tapasin interacts with and stabilizes TAP, hence contributing to the architectural frame of the PLC (Bangia et al., 1999; Ortmann et al., 1997; Raghuraman et al., 2002). Tapasin also interacts with nascent (empty) HLA class I, tethering the empty HLA class I to TAP and facilitating peptide loading (Ortmann et al., 1997; Sadasivan et al., 1996). Another key function of tapasin is peptide editing, an iterative process through which low-affinity peptides on HLA class I peptide-binding grooves are displaced and replaced with high-affinity ones (Chen & Bouvier, 2007; Howarth et al., 2004; Praveen et al., 2010; Williams et al., 2002). Due to these relevant functions, tapasin depletion reduces the expression of HLA class I on the plasma membrane (Garbi et al., 2000; Greenwood et al., 1994). However, the influence of tapasin on peptide loading and surface expression varies among HLA class I alleles, with some less tapasin-dependent alleles able to maintain surface expression and

antigen presentation under tapasin-deficient conditions (Bashirova et al., 2020; Peh et al., 1998; Rizvi et al., 2014).

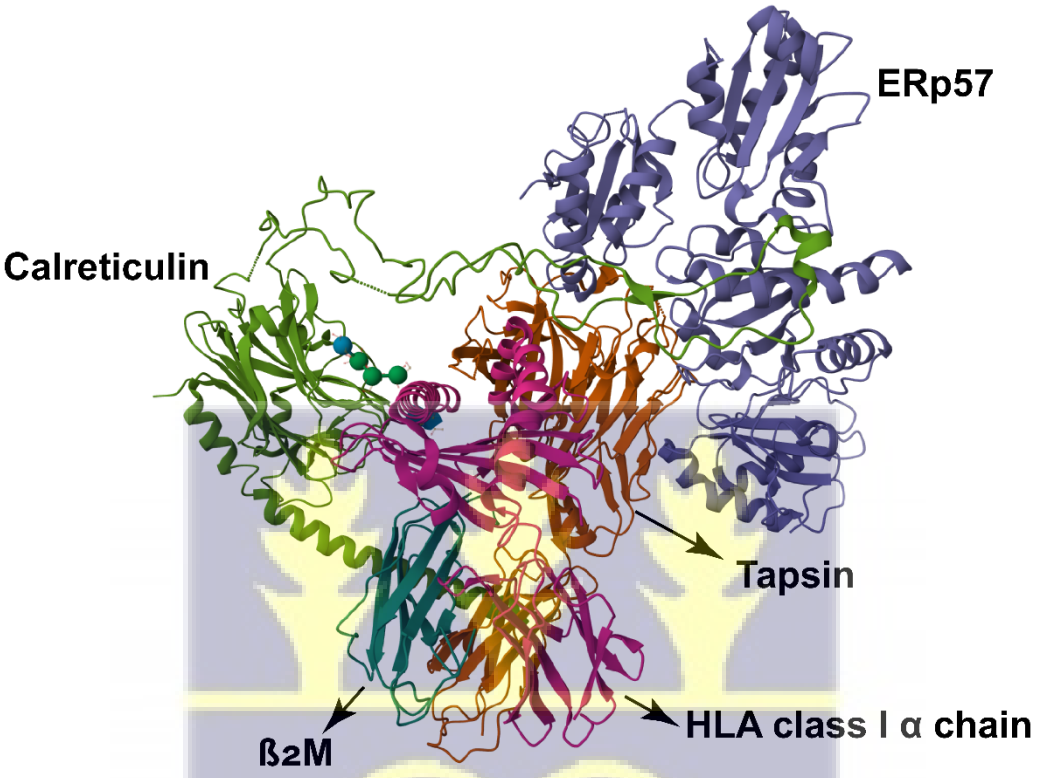

Figure 2.10: The structure of the peptide-loading complex. The structure depicts HLA class I-tapasin-calreticulin-ERP57 complex (PDB ID: 6ENY) at 5.80 Å resolution. Tapasin interacts with HLA class I and ERp57, stabilizing the empty HLA class I. Calreticulin interacts with HLA class I through its glycan-binding domain. The structure was obtained from the RCSB Protein Data Bank (**https://www.rcsb.org/structure/6ENY**).

2.4 The role of calreticulin in HLA class I antigen presentation

Calreticulin is a lectin-like glycan-binding chaperone primarily resident in the ER. The structure of calreticulin consists of a globular N-terminal domain possessing a lectin-like glycan-binding property, a flexible proline-rich P-domain that interacts with polypeptides, and an acidic amino acid-rich C-domain containing the ER-retention sequence (KDEL) and calcium ion (Ca^{2+})-binding region (Desikan et al., 2023). Calreticulin performs many critical functions for HLA class I assembly and trafficking. Notably, its lectin-like N-terminal domain binds monoglycosylated HLA class I, recruiting glycosylated, native HLA class I to the peptide-loading complex (Domnick et al., 2022). In the peptide-loading complex, calreticulin stabilizes peptide-receptive HLA class I proteins, and cells lacking calreticulin mostly have impaired HLA class I antigen presentation (Gao et al., 2002). Calreticulin also contributes to the overall architecture of the peptide-loading complex by facilitating an intricate network of interactions between HLA class I proteins and other components of the peptide-loading complex (Figure 2.10) (Del Cid et al., 2010; Domnick et al., 2022; Wearsch et al., 2011). To achieve this function, the glycan-binding domain of calreticulin binds the HLA class I monoglycosylated glycan, and its polypeptide-binding P-loop interacts with the ER oxidoreductase ERp57, which connects to tapasin (Del Cid et al., 2010; Domnick et al., 2022; Wearsch et al., 2011). Calreticulin also retrieves aberrantly folded HLA class I proteins from post-ER compartments to the ER (Howe et al., 2009; Raghavan et al., 2013). Together, these functions highlight the role of calreticulin in the HLA class I antigen presentation pathway.

2.5 The role of calnexin in HLA class I antigen presentation

Calnexin is a transmembrane ER chaperone with some structural and functional similarities with calreticulin. Like calreticulin, calnexin has an N-terminal domain that performs a lectin-like glycan-binding function. Calnexin also has P- and C-terminal domains, but unlike calreticulin, possesses a transmembrane domain. Calnexin is important in the early stage of HLA class I assembly, protecting nascent HLA class I heavy chains from premature degradation (Rajagopalan & Brenner, 1994). Besides directly interacting with empty HLA class I molecules, calnexin recruits ERp57 to catalyze disulfide bond formation that stabilizes nascent HLA class I heavy chains, prior to their assembly with β2m (Adhikari & Elliott, 2003; Diedrich et al., 2001). Calnexin also facilitates the assembly of β2m with HLA class I heavy chains (Adhikari & Elliott, 2003), and like calreticulin, is involved in the ER-retention of unfolded HLA class I for refolding, including those retrieved from post-ER compartments (Adams et al., 2021).

2.6 ER stress and unconventional protein secretion

Proper protein folding is key to ER homeostasis; however, certain conditions, such as nutrient deprivation, hypoxia, and protein mutations, can increase unfolded or misfolded proteins in a manner that the ER is unable to maintain proper protein folding. The accumulation of unfolded or aberrantly folded proteins in the ER causes an imbalanced homeostatic state referred to as "ER stress" (Braakman & Hebert, 2013; Chen et al., 2023).

The cell has evolved multiple mechanisms, collectively referred to as the unfolded protein response (UPR), to relieve itself of misfolded proteins and counteract ER stress. Three ER transmembrane sensors maintained in their inactive state by the ER chaperone binding immunoglobulin protein (BiP) initiate and regulate the cell's induction of UPR. They are inositol-requiring enzyme 1 (IRE1), protein kinase R-like ER kinase (PERK), and activating transcription factor 6 (ATF6) (Chen et al., 2023) (Figure 2.11). Upon sensing unfolded proteins, these sensors are activated, initiating multiple signaling mechanisms that result in increased synthesis of ER chaperones responsible for protein refolding, enhanced degradation of unfolded or misfolded proteins, and transient inhibition of overall protein synthesis in the cell (Almanza et al., 2019; Chen et al., 2023). Importantly, UPR activation reduces the ER-Golgi-dependent conventional protein secretion but has been observed to increase alternative ER-Golgi-independent protein secretory pathways, collectively known as unconventional protein secretion (trafficking) (Kim et al., 2018; Meyer & Doroudgar, 2020).

By activating unconventional protein trafficking in response to the accumulation of unfolded or misfolded proteins, cells can attenuate ER stress and restore protein homeostasis (proteostasis) when protein folding or the conventional secretory pathway is impaired. One key protein implicated in mediating unconventional trafficking is the Golgi reassembly-stacking protein 2 (GORASP2), also known as the Golgi reassembly and stacking protein of 55 kDa (GRASP55). Under homeostatic conditions, GRASP55 is resident in the Golgi and participates in maintaining the Golgi stacking. However, upon ER stress induction, GRASP55 relocates from the Golgi and mediates unconventional secretion of some transmembrane and soluble proteins, including mutant cystic fibrosis transmembrane conductance regulator (CFTR) (Ahat et al., 2019; Ahat et al., 2022; Chiritoiu et al., 2019).

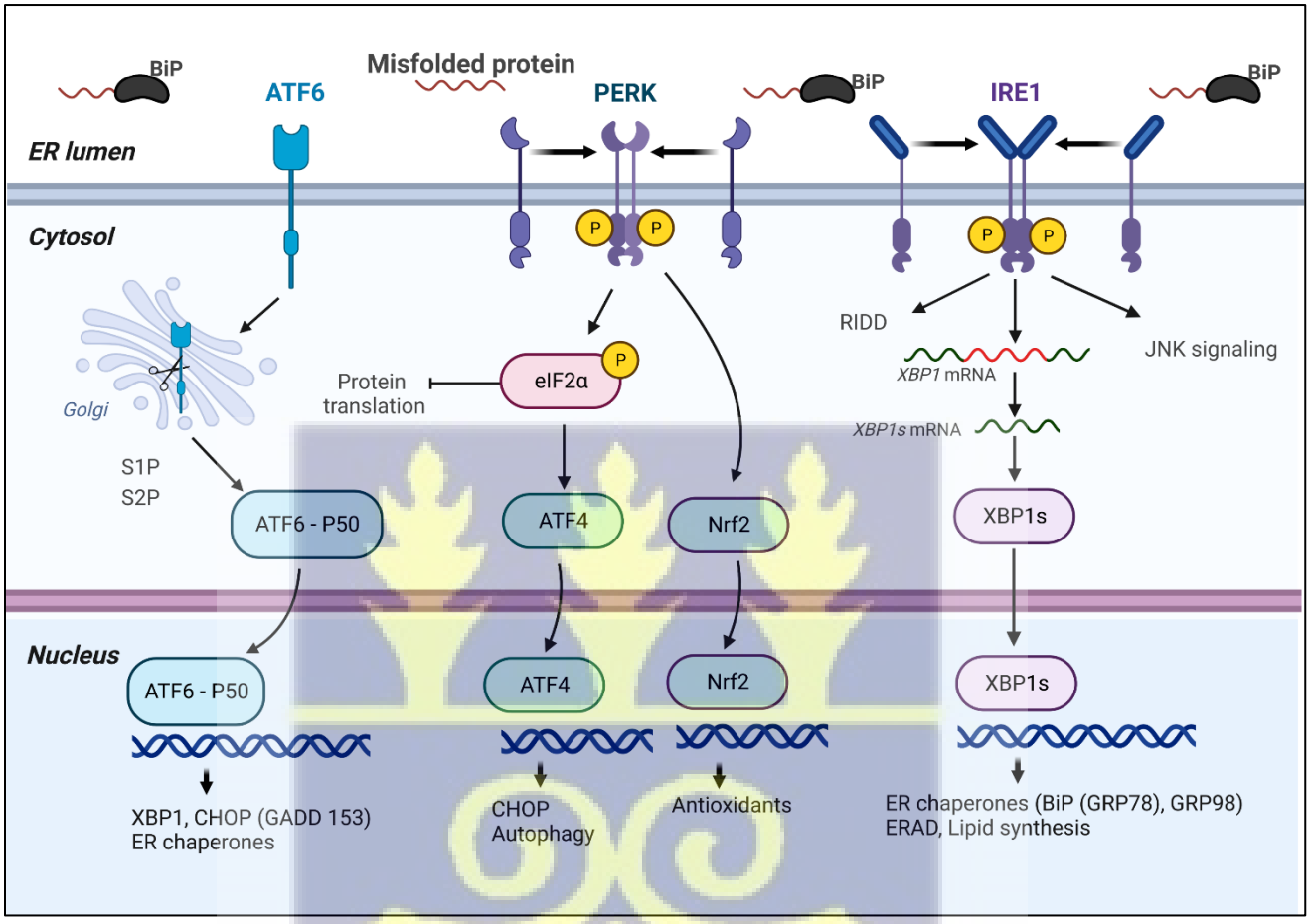

Figure 2.11: Unfolded protein response signaling pathways. BiP dissociates from IRE1, PERK, and ATF6 when unfolded or misfolded proteins accumulate in the ER. IRE1 has endoribonuclease and serine/threonine kinase domains. Upon BiP dissociation, IRE1 dimerizes and is activated through autophosphorylation. Activated IRE1 has endoribonuclease activity, allowing it to unconventionally splice X-box binding protein 1 (XBP1) mRNA, producing spliced XBP1s, an active transcription factor, increasing the transcription of the genes for ER chaperones (such as

BiP), ER-associated degradation (ERAD), and lipid biosynthesis. IRE1 is also involved in the regulated IRE1-dependent decay (RIDD) pathway, which transiently reduces protein synthesis by selectively degrading mRNAs in the ER. Additionally, IRE1 can activate apoptotic signaling pathways through c-Jun N-terminal kinase (JNK) (Siwecka et al., 2021). Like IRE1, protein kinase R-like ER kinase (PERK) oligomerizes and phosphorylates when BiP dissociates from it. Activated PERK phosphorylates the eukaryotic initiation factor-2α (eIF2α) and represses protein synthesis globally. eIF2α, however, selectively promotes the synthesis of activation transcription factor 4 (ATF4), a transcription factor that upregulates the synthesis of CCAAT-enhancer-binding protein (C/EBP) homologous protein (CHOP) and proteins involved in autophagy. Activated PERK also phosphorylates nuclear factor erythroid 2-related factor 2 (Nrf2), causing it to translocate to the nucleus and upregulate the synthesis of antioxidant proteins. When BiP dissociates, ATF6 (a 90 kDa transmembrane protein) relocates from the ER membrane to the Golgi and is cleaved by Site-1 (S1P) and Site-2 (S2P) proteases, releasing a 50 kDa fragment (ATF6-p50), an active transcription factor. ATF6-p50 migrates to the nucleus and promotes the transcription of the genes encoding XBP1, CHOP, and ER chaperones. Additional details about these UPR pathways have been well-reviewed (Almanza et al., 2019; Chen et al., 2023). Image created using BioRender.com.

2.7 HLA class I immunopeptidome

To mediate immune surveillance, HLA class I proteins present antigenic peptides to CTL (Zinkernagel & Doherty, 1974). A collection of the diverse array of peptides presented by HLA class I proteins is referred to as HLA class I immunopeptidome (Istrail et al., 2004; Yewdell, 2022). Beginning from the discovery that HLA class I proteins present short amino acid sequences (peptides) to CTL (Zinkernagel & Doherty, 1974) to the identification of allele-specific peptide

motif (Falk et al., 1991) and the advent of mass spectrometry in the identification of HLA class I-bound peptides (Henderson et al., 1992), HLA class I immunopeptidome analysis has undergone a remarkable refinement that has increased the repertoire of peptides identified so far.

Recent studies assessing pan HLA class I or specific allotypes' immunopeptidome have relied on mass spectrometry to identify eluted peptides (Gravel et al., 2023; Kaur et al., 2023; Mamrosh et al., 2023). In the more distant past, the mass spectrometric approach has enabled the identification of HLA class I presented in the context of specific infectious pathogens, including Epstein-Barr virus (Herr et al., 1999) and measles virus (van Els et al., 2000), placing this approach at the heart of immunopeptidome analyses. Two quantitative mass spectrometry strategies have been reported for HLA class I eluted peptides identification and quantification (Gravel et al., 2023; Kaur et al., 2023; Mamrosh et al., 2023). These are label-free and tandem mass tag (TMT)-mass spectrometry. Some studies have compared the relative performance of these methods, though not in the context of immunopeptidome (Megger et al., 2014; O'Connell et al., 2018). Label-free mass spectrometry, as the name implies, is used to determine the relative amount of proteins in biological samples without subjecting peptides in the samples to chemical labeling. This approach infers peptide abundance from spectral counting or precursor ion signal intensity. For TMT-mass spectrometry, peptides are first labeled with chemicals of the same nominal mass but different isotopic composition (isobaric chemical tags), allowing multiple samples to be analyzed together in a single mass spectrometry run. Although the label-free approach can identify a broader breadth of peptides, the TMT approach has more quantitative accuracy (Megger et al., 2014; O'Connell et al., 2018). Notably, the TMT approach has been used recently to quantify the relative contributions of various peptide sources, including the cytosolic proteasome and lysosome, to HLA class I immunopeptidome (Mamrosh et al., 2023).

2.8 Conclusion

HLA class I molecules play a crucial role in the immune response against infectious pathogens and cancers by presenting antigens to CTLs and regulating NK cell activation and inhibition. Several years of studies have uncovered many details about HLA class I assembly and trafficking, including how peptides are generated in the cytosol, funneled into the ER, and assembled with peptide-receptive HLA class I molecules (Blum et al., 2013; Neefjes et al., 2011; Zaitoua et al., 2020). The cooperative roles of TAP subunits and many chaperones in the ER to achieve a successful peptide assembly with HLA class I in the peptide-loading complex are well-researched (Domnick et al., 2022; Lehnert & Tampe, 2017; Muller et al., 2022). However, the molecular mechanism underlying peptide transport by TAP remains poorly understood. Additionally, TAP inhibition by viruses and cancers as an immune evasion strategy has been studied (Mantel et al., 2022), and persistent antigen presentation by some HLA class I allotypes under TAP-deficient conditions has been observed (Geng et al., 2018; Wei & Cresswell, 1992). Nevertheless, the mechanism driving this peptide presentation is not fully understood. Moreover, more studies are needed to fully understand the glycosylation profile of HLA class I proteins and the regulation of HLA class I secretion by glycan-processing enzymes such as the ER and Golgi mannosidases.

CHAPTER THREE

Manuscript 1: Misfolded HLA Class I Accumulation in the Endoplasmic Reticulum Induces the Cell Surface Expression of High Mannose Glycoforms via a Golgi-Mediated Secretory Route

3.0 Abstract

HLA class I assembly depends largely on peptide availability via the transporter associated with antigen processing (TAP). Many TAP-deficient cells display low but measurable cell surface HLA class I, and increased levels of high mannose Endoglycosidase H (Endo-H)-sensitive cell surface HLA class I glycans. Endoplasmic Reticulum (ER) stress signals and unconventional protein trafficking are frequently implicated in the occurrence of high mannose cell surface glycoprotein glycans. However, TAP deficiency does not induce canonical ER stress mediators and several factors implicated in unconventional glycoprotein trafficking do not selectively affect HLA class I expression in TAP-deficient cells. Rather, HLA class I cell surface expression in TAP-deficient cells is brefeldin A-sensitive, similar to wild-type cells, implicating the conventional Golgi-dependent secretory route. Furthermore, cell surface glycosylation changes in TAP-deficient cells are HLA class I-specific rather than global. Moreover, other conditions that compromise HLA class I assembly, such as tapasin deficiency, also induce high mannose HLA class I cell surface glycans. Thus, Golgi-mediated export of HLA class I with high mannose glycans from the ER appears to reflect a homeostatic response to misfolded HLA class I accumulation in the ER. Overall, these findings suggest a model wherein saturated recognition mechanisms for misfolded HLA class I molecules result in their partial Golgi-dependent secretory trafficking and account for impaired glycan maturation.

3.1 Background

The human leukocyte antigen (HLA) class I molecule (major histocompatibility complex (MHC) class I in humans) is a heterotrimeric protein comprising a heavy chain (α chain), a light chain, β_2 microglobulin (β_2m), and a short peptide. The α chain consists of three domains: α1, α2, and α3, with the first two domains forming the membrane distal peptide binding site and the membrane-proximal α3 domain as also β_2m adopting immunoglobulin (Ig)-like folds (Bjorkman et al., 1987). HLA class I proteins present endogenous peptides to clusters of differentiation 8 ($CD8^+$) T cells and regulate the activities of natural killer (NK) cells. Peptides bound to HLA class I molecules may be derived from endogenous cellular proteins such as defective ribosomal products (DRiPs) (Yewdell et al., 1996; Yewdell & Nicchitta, 2006), mutated proteins in cancers (Li et al., 2023), or foreign proteins from pathogens that infect host cells (Yewdell, 2022). In addition to endogenous peptides, HLA class I molecules can present exogenous (extracellular) peptides to $CD8^+$ T cells through a pathway called cross-presentation, particularly in dendritic cells and other professional antigen-presenting cells (Bevan, 1976; Gutierrez-Martinez et al., 2015). By presenting peptides to effector $CD8^+$ T cells, HLA class I molecules play a crucial role in the adaptive immune response. HLA class I expression is often subverted by pathogens for immune evasion (Petersen et al., 2003; Taylor & Balko, 2022).

The canonical pathway for antigen presentation by HLA class I proteins has been well described (Blum et al., 2013; Raghavan et al., 2008). Briefly, proteins in the cells are degraded predominantly in the proteasome, generating peptides. A fraction of these peptides is translocated into the ER by the transporter associated with antigen processing (TAP), a heterodimeric transmembrane protein and a member of the ATP-binding cassette family. In the ER, the peptides are trimmed by aminopeptidases and assembled with HLA class I in the peptide loading complex (PLC). This

assembly process is assisted by several ER chaperones, including calnexin, calreticulin, tapasin, and ERp57. Peptide-bound HLA class I molecules exit the ER and transit to the plasma membrane through the Golgi-dependent conventional protein secretory pathway. Because TAP is the channel for transporting cytosolic peptides into the ER, many viruses and certain cancers compromise HLA class I antigen presentation by inhibiting TAP (Alimonti et al., 2000; Fruh et al., 1995; Henle et al., 2017; Verweij et al., 2015).

TAP dysfunction results in HLA class I proteins being largely retained in the ER, resulting in an overall downmodulation of surface HLA class I molecules (de la Salle et al., 1994; Raposo et al., 1995). Despite this downmodulation in TAP-dysfunctional cells, HLA class I expression is readily measurable on the plasma membrane and can maintain $CD8^+$ T cell activation (de la Salle et al., 1999; Geng et al., 2018). Furthermore, some professional antigen-presenting cells (APC), particularly dendritic cells (DCs), can cross-present antigens without a functional TAP (Barbet et al., 2021; Sengupta et al., 2019). Moreover, studies on HLA class I presentation by TAP-mutant cell lines revealed the ability of the HLA class I allotype HLA-A*02:01 to present peptides bearing signal sequences independent of TAP (Henderson et al., 1992; Wei & Cresswell, 1992). Collectively, these studies highlight the existence of TAP-independent pathways through which peptides can be assembled, at least with some HLA class I proteins. The molecular mechanisms governing the assembly and trafficking of HLA class I in TAP-deficient cells remain poorly characterized thus far.

Proteins trafficking through the conventional secretory pathway undergo certain post-translational modifications. Particularly, glycoproteins such as HLA class I acquire high mannose Endo-H sensitive N-glycans in the ER. As they traverse the ER and Golgi compartments, the mannose residues are sequentially trimmed and the high mannose glycans are modified into complex Endo-

H-resistant forms (Aebi, 2013; Bieberich, 2014; Stanley et al., 2022). The acquisition of Endo-H-resistant glycans has emerged as a marker for protein trafficking through the canonical Golgi-dependent secretory pathway. However, there are several reported examples of the expression of Endo-H-sensitive glycans on glycoproteins in the plasma membrane (Grieve & Rabouille, 2011; Nickel & Seedorf, 2008). Generally, unconventional Golgi-independent secretory trafficking pathways have been implicated in the cell surface expression of such glycoproteins (Grieve & Rabouille, 2011; Nickel & Seedorf, 2008).

A previous study evaluating TAP-independent HLA-B expression also reported increased levels of Endo-H sensitive glycans on surface HLA class I of TAP-deficient cells (Geng et al., 2018). These findings highlight major gaps in our basic understanding of the trafficking pathway(s) undertaken by HLA class I in TAP-dysfunctional cells. Specifically, whether endogenous HLA class I molecules in TAP-deficient cells traffic through the conventional or non-conventional secretory pathway has not been addressed to date. This study aims to determine the trafficking pathway of endogenous HLA class I proteins in TAP-deficient cells. Elucidating the molecular mechanisms underlying the assembly and trafficking of endogenous HLA class I proteins in TAP-deficient cells could advance the development of novel immunotherapies against TAP-inhibiting infectious pathogens and cancers.

3.2.0 Methods

3.2.1 Cell Culture

THP-1 cells (TIB-202) were purchased from the American Type Culture Collection (ATCC) and maintained in RPMI 1640 (ATCC modification, catalogue number: A1049101) supplemented with 10% (v/v) fetal bovine serum (FBS), 2 mM L-glutamine, and 1X antibiotic/antimycotic. Human embryonic kidney cells expressing the simian virus 40 (SV40) large T antigen (HEK239T) were maintained in Dulbecco's Modified Eagle Medium (DMEM) supplemented with 10% (v/v) FBS and 1X antibiotic/antimycotic. ST-EMO (TAP2-deficient cells expressing HLA-B*35:01 (ST-EMO-B*35:01; a gift from Dr. H. De la Salle) were cultured in RPMI 1640 supplemented with 10% (v/v) fetal bovine serum (FBS) and 1X antibiotic/antimycotic. All the cells were cultured in 5% CO_2 at 37ºC except indicated otherwise.

3.2.2.0 CRISPR-Cas9 Knockout of relevant genes

TAP-1 or other relevant genes (indicated in the results section) were knocked out using a 6-well modified lentiviral vector-based CRISPR-Cas9 genome editing protocol previously described. The single guide RNAs used for genome editing are listed in Table 3.1 (Shalem et al., 2014).

3.2.2.1 Lentivirus preparation

About 0.5 x 10^6 HEK293T cells were seeded into 6-well plates and grown overnight to attain about 70% confluence. Solution A was prepared by adding 1.7 µg psPAX2 (Addgene; 12260), 1.1 µg pMD2.G (Addgene; 12259), and 2.25 µg of pLentiCRISPRv2 or pLentiCRISPRv2 containing the single guide RNA for TAP1 or indicated genes (Table 1) into 130 µL OptiMEM and 5 µL lipofectamine plus reagent. The solution was mixed by vortexing briefly and incubated for 5

minutes at room temperature. Solution B was prepared by adding 130 µL OptiMEM to 15 µL lipofectamine LTX, vortexing briefly, and incubating for 5 minutes. Solution C was prepared by mixing solutions A and B. The medium for HEK293T cells grown overnight was replaced with 2 mL of fresh DMEM containing 10% FBS but without antibiotic/antimycotic. Solution C was added to the cells after incubating for 20 minutes. The plates were gently swirled, and the cells were cultured for 48 hours.

3.2.2.2 Infection of THP-1 cells with lentivirus

The virus (in the culture medium) was harvested from HEK293T cells and filtered through a 0.45 µm syringe filter. The virus was added to 0.5 x 10^6 THP-1 cells in a 24-well plate and incubated for 15 – 20 minutes at room temperature after adding 1X Polybrene (8 µg/mL). The plates were centrifuged at 2500 rpm for 2 hours at room temperature to infect the cells by spinoculation. Two-thirds of the supernatant was replaced with modified RPMI, and the cells were rested overnight. The culture medium was replaced with fresh ATCC-modified RPMI (A1049101), and the cells were again rested overnight.

3.2.2.3 Selection of lentivirus-infected THP-1 cells

Successfully transduced THP-1 cells were selected using appropriate drugs based on the lentiCRISPR vector. Cells transduced with lentiCRISPR vector containing blasticidin or hygromycin B resistance gene were selected using 5 µg/mL blasticidin or 300 µg/mL hygromycin B for 4 – 5 weeks.

Table 3.1: Genes, sgRNA used for CRISRP-Cas9 genome editing, and antibodies used to confirm knockout by immunoblot.

Gene	gRNA (5' - 3')	Immunoblot antibody
TAP-1	F: AGTTCGAAGCTTTGCCAACG R: CGTTGGCAAAGCTTCGAACT	Anti-TAP-1 (Clone 148.3)
CANX	F: TTTAGAAAGCAGTTTCACAT R: ATGTGAAACTGCTTTCTAAAC	
CANX	F: TTGTCTTGTAGGAAAGTGGG R: CCCACTTTCCTACAAGACAAC	
CANX	F: AAATCCTTCACGTGAAATTG R: CAATTTCACGTGAAGGATTTC	
Tapasin	F: AAGCGGCTCATCTCGCAGTG R: CACTGCGAGATGAGCCGCTT	Anti-Tapasin (Clone 7F6)

F: Forward sequence; R: Reverse complement sequence

3.2.3 Small interfering RNA (siRNA)-mediated sec22B depletion

Sec22B was knocked down using the ON-TARGET plus SMARTpool siRNA (Dharmacon, Catalogue number: L-011963-00-0020), adapting a protocol previously described (Troegeler et al., 2014). Briefly, 15 µL of 20 µM sec22B-siRNA or non-targeting siRNA and 15 µL of HiPerFect transfection reagent were placed in 0.5 mL OptiMEM and incubated for 15 minutes at room temperature. The transfection mix was added dropwise to about 0.75 x 10^6 THP-1 or THP-TAP-1-KO cells in 1 mL filtered, antibiotic/antimycotic-free modified RPMI in 6-well plates. The plates were gently swirled, and the cells were incubated at 37ºC for 4 hours in the presence of 5% CO_2. The culture medium was made up to 2 mL, and the cells were cultured for 48 hours.

3.2.4 Confirmation of gene knockout or knockdown by immunoblot

The cells were lysed in ice-cold lysis buffer containing 50 nM TRIS, 1% Triton, 150 nM NaCl, and 5 mM $CaCl_2$ for 1 hour. The lysates were centrifuged at 13,000 rpm for 30 minutes at 4^0C. The supernatant was boiled in 1X SDS and subjected to 4 – 20% (Bio-Rad, catalogue number: 4561096) SDS-PAGE for 120 minutes at 120 V. The proteins were transferred to PVDF membranes, blocked in 5% skimmed milk in 1X TBST for 30 minutes, and blotted with indicated primary antibodies (Table 1), or anti-GAPDH or anti-vinculin antibody as loading controls for 1.5 hours at room temperature or overnight at 4^0C. The membranes were washed in three changes of 1X TBST for 30 minutes and blotted with goat-anti-mouse or goat-anti-rabbit horse radish peroxidase for 30 minutes at room temperature. The membranes were washed in three changes of 1X TBST for 30 minutes and treated with enhanced chemiluminescence (ECL) reagents following the manufacturer's protocol. The membranes were exposed to X-ray film (HyBlot CL, Thomas Scientific) multiple times using an X-ray film processor to detect the chemiluminescent signals from the immunoblot. For TAP-1 knockout confirmation, TAP-1 was immunoprecipitated by incubating the lysates with anti-TAP-1 antibody (148.3) at 4^0C overnight, protein G Sepharose for 2 – 3 hours at 4^0C, followed by washing in three changes of ice-cold lysis buffer at 1000 G for 1 minute and elution into 5X SDS before performing immunoblot.

3.2.5 Endoglycosidase H (Endo-H) sensitivity assay

Proteins on the plasma membrane were biotinylated by incubating the cells with cell-impermeant biotin, EZ-Link NHS-PEG4-Biotin (Thermo Scientific), following the manufacturer's instructions. Briefly, the cells were washed in 1X PBS three times and incubated with 2 mM biotin in 1X PBS for 10 minutes at room temperature, followed by a wash in 0.1 M glycine and 3 changes

of 1X PBS. After washing, the biotinylated cells were lysed in an ice-cold buffer containing 50 nM TRIS, 1% triton, 150 nM NaCl, and 5 mM $CaCl_2$ for 1 hour. The lysates were cleared by centrifuging at 13 000 RPM for 30 minutes and the labeled proteins were incubated with streptavidin agarose beads (Thermo Scientific, Catalouge number: 20) for 2 hours at 4ºC. The beads were washed by centrifuging in 3 changes of lysis buffer at 4000 RPM for 10 mins. Endo-H sensitivity assay was performed using Endo-H_f (New England Biolabs) according to the manufacturer's protocol, with slight modifications. Biotin-labeled surface proteins or unlabeled lysates were boiled in 1X glycoprotein denaturing buffer at 100ºC for 10 minutes. The eluate from the beads and the unlabeled lysates were split into two parts, and one half was treated with 1X Glyco buffer 3 and two-fold dilutions of Endo-H_f for 2 hours at 37°C. Endo-H_f-digested or undigested lysates and proteins were subjected to 8% SDS-PAGE at 120 V for 120 minutes, followed by blotting with HC10 and goat-anti-mouse or anti-vinculin and goat-anti-rabbit.

3.2.6 Purification of W6/32 antibody

Ascites of W6/32, a pan-HLA class I antibody, was obtained from the University of Michigan Hybridoma Core and purified using HiTrap Protein G HP column. The ascites was centrifuged at 13000 rpm for 30 minutes and the supernatant was filtered through a 0.45 µm syringe filter to remove particulate materials. 10 mL of elution buffer (0.1 M glycine-HCl, pH 2.7) was passed through the column, followed by equilibration with 25 mL binding buffer (20 mM sodium phosphate, pH 7.0) at 1 mL/minute. The antibody was loaded into the column and incubated on ice for 30 minutes. The column was washed with 50 mL binding buffer at 1 mL/minute, and the antibody was eluted with 25 mL elution buffer at 1 mL/minute in aliquots of 800 µL into 1.5 mL tubes containing 200 µL of neutralizing buffer (1 M Tris-HCl, pH 9.0). The column was regenerated by washing with 15 mL binding buffer four times and equilibrated with 15 mL 20%

ethanol. The antibody was dialyzed in the binding buffer multiple times until the neutralizing buffer was less than 4.5 x 10^{-3} nM. The purity and integrity of the purified antibody were confirmed by subjecting the antibody to 8% SDS-PAGE, followed by staining with Coomassie brilliant blue for 1 hour. After staining, the gel was destained in several changes of 50% ethanol to visualise the bands corresponding to W6/32 antibody (Supplementary Figure 3.1).

3.2.7 Conjugation of W6/32 with fluorescein isothiocyanate (FITC)

Buffer exchange was performed for purified W6/32 by centrifuging the antibody in ten changes of 100 mM bicarbonate buffer (pH 8.3) containing 500 mM Sodium Chloride at 4000 rpm and 4ºC for 10 – 20 minutes in 3 kDa molecular weight cut-off (MWCO) centricon. 50 µL of 1 mM FITC was placed in ~ 2 mg/mL W6/32 antibody and rocked slowly at room temperature for 1 hour, followed by centrifugation in several changes of bicarbonate buffer in 3 kDa MWCO centricon at 4000 rpm and 4 ºC for 10 – 20 minutes until the flowthrough is visibly clear of unconjugated FITC. The concentrated FITC-conjugated antibody was diluted to 500 µL and stored at 4ºC until further use.

3.2.8 Flow cytometry

Cell surface HLA class I proteins were measured by flow cytometry. Briefly, 50 – 100,00 cells were seeded into 96-well plates and washed with ice-cold 1X PBS at 2500 rpm for 1 minute. The cells were incubated in an Fc receptor (FcR)-blocking buffer (5% normal mouse serum in the staining buffer) for 10 minutes and stained with FITC-conjugated W6/32 (W6/32-FITC) on ice for 30 minutes in a staining buffer containing 2% fetal bovine serum (FBS) in 1X PBS. After staining with W6/32-FITC, the cells were rinsed twice with ice-cold staining buffer and stained for viability using 7-aminoactinomycin D (7-AAD) in the staining buffer. Flow cytometry was performed on a

BD LSRFortessa cell analyzer, and the data (flow cytometry standard files) were exported to FlowJo for analysis. Cells were gated based on forward and side scattering, and viable cells were gated based on negative 7-AAD staining (Supplementary Figure 3.2). The mean fluorescence intensity (MFI) values of W6/32-FITC were chosen to represent surface HLA class I expression on the cells.

3.2.9 Reverse transcriptase quantitative polymerase chain reaction (RT-qPCR)

RT-qPCR was used to quantify messenger ribonucleic acid (mRNA) levels in THP-1 or THP-1-TAP-1-KO cells. Total RNA was isolated from THP-1 or THP1-1-TAP-1-KO cells using RNeasy kit (Qiagen), following the manufacturer's instructions. RNA concentration and purity were assessed using a NanoDrop spectrophotometer (Thermo Fisher Scientific). Complementary DNA (cDNA) was synthesized from total RNA using the SuperScript III First-Strand Synthesis kit (Invitrogen), following the manufacturer's instructions. Briefly, 2µg of the total RNA was combined with 1 µL of oligo dT primers and 10 mM dNTPs, and made up to 10 µL with nuclease-free water to constitute solution A. This solution was incubated at 65^{o}C for 5 minutes and chilled on ice for 1 minute. Solution B was prepared by combining 2 µL of 10X RT buffer with 25 mM $MgCl_2$ (4 µL), 0.1 M DTT (2 µL), RNAse Out (1 µL), and SS III enzyme (1 µL). 10 µL each of solutions A and B were mixed and incubated in a thermocycler at 50^{o}C for 50 minutes, 85^{0}C for 5 minutes and chilled on ice for 1 minute. The cDNA was treated with RNaseH (1 µL) and incubated at 37^{o}C for 20 minutes. The cDNA was stored at -80^{0}C until further use. The qPCR was performed using ABI 7500 Fast real-time PCR machine and Applied Biosystems SYBR Green Master Mix (4309155), following the manufacturers' instructions. 1 µL each of 5 µM forward primer, 5 µM reverse primer, and the cDNA were placed in 5 µL of 2X Master Mix and made up to 10 µL with nuclease-free water. The reaction mix was placed in the qPCR machine, and a standard 2-hour run

was performed using delta CT mode. *GAPDH*, *HPRT1*, and *ACTB* were used as housekeeping genes. The genes assessed and the primers used are listed in Table 3.2

Table 3.2: The primers used for ER stress assessment by RT-qPCR

Gene	Primers (5'- 3')
ATF4	FP: CAGCAAGGAGGATGCCTTCT RP: CCAACAGGGCATCCAAGTC
BiP	FP: GATGAAGCTCTCCCTGGTGG RP: TAGGTGGTCCCCAAGTCGAT
CHOP	FP: TAAAGATGAGCGGGTGGCAG RP: TCTGCTTTCAGGTGTGGTGA
Spliced XBP1	FP: TTACGAGAGAAAACTCATGGC RP: GGGTCCAAGTTGTCCAGAATGC
GAPDH	FP: GAGTCAACGGATTTGGTCGT RP: TTGATTTTGGAGGGATCTCG
ACTB (β-Actin)	FP: GGACTTCGAGCAAGAGATGG RP: AGCACTGTGTTGGCGTACAG

FP: Forward primer; RP: Reverse primer.

3.2.10 Acid stripping and brefeldin A treatment

Cells were stripped of antigenic HLA class I proteins using a well-known acid treatment protocol, described more than three decades ago (Sugawara et al., 1987). Briefly, the cells were washed in ice-cold 1X PBS twice, treated with 500 mL ice-cold phosphate citrate buffer (pH 3) for 2 minutes, and neutralized with 30 mL cold, antibiotic/antimycotic-free modified RPMI medium. The buffer was prepared from an equal volume of citric acid (263 mM) and disodium hydrogen phosphate

(123 mM). The cells were washed in three changes of ice-cold medium, and surface HLA class I was assessed by flow cytometry as previously described. Acid-stripped or unstripped cells were cultured in a suitable medium containing 10 µg/mL brefeldin A (B7651, Sigma Alderich) for 1, 2, 3, or 4 hours. Surface HLA class I on the cells was assessed by flow cytometry.

3.2.11 Mass spectrometry (MS)

Three biological MS replicates were conducted for THP-1 and THP-1-TAP-1-KO cells. The cells were biotinylated, lysed, and incubated with streptavidin agarose beads as described in section 3.2.4. The beads were washed in 1X PBS thrice and used for mass spectrometry at the Proteomics Core of the Department of Pathology, University of Michigan. The beads were resuspended in 50 µL of 0.1 M ammonium bicarbonate buffer (pH 8) and incubated at 45 °C for 30 minutes after adding 50 µL of 10 mM DTT. The beads were further incubated with 65 mM 2-chloroacetamide at room temperature for 30 minutes in the dark and digested with 1 µg modified trypsin at 37 °C overnight. The digestion was performed on a thermomixer to ensure constant shaking. The reaction mixture was acidified to stop the digestion, followed by desalting using SepPak C18 cartridges and complete desiccation in a vacufuge. The peptides were then reconstituted in 8 µL solution containing 0.1% formic acid and 2% acetonitrile. A one-quarter aliquot of the reconstituted peptides was resolved on a nano-capillary reverse phase column (Acclaim PepMap C18, 2 µm, 50 cm Thermo Fisher Scientific) using 0.1% formic acid/increasing acetonitrile gradient elution method over three hours at a flow rate of 300 mL/minute. The elution was initiated with 2–25% acetonitrile for 105 minutes, followed by 25–40% for 20 minutes, 90% for 10 minutes, and re-equilibration of the column with 2% for 30 minutes. The eluted peptides were directly injected into a Q Exactive HF mass spectrometer via an EasySpray source. Using 120 000 resolution, with automatic gain control (AGC) target set at 1×10^6 and maximum injection time (IT) at 50

milliseconds, MS1 scans (measuring the mass-to-charge ratio (m/z) of intact peptides) were acquired, followed by TopSpeed (3 seconds) acquisition of data-dependent collision-induced dissociation MS/MS spectra after every MSI scan normalized collision energy (28 – 32 %), AGC target (1×10^5), and max IT (45 milliseconds).

To identify the proteins, the MS/MS data were searched against the Homo sapiens UniProt database using Proteome Discoverer software and search parameters including specific mass tolerances, allowed missed cleavages, and considerations for various modifications. To increase the reliability of the results, all proteins and peptides with a false discovery rate (FDR) > 0.01 were excluded and those ≤ 0.01 were retained for further analysis. Furthermore, proteins with peptide spectrum match (PSM) values < 3 in all three biological MS replicates of THP-1 and THP-1-TAP-1-KO cells were excluded and only those with ≥ 3 PSM values in at least two of the three THP-1 or THP-1-TAP-1-KO replicates were considered for further analysis. PSM values were used as surrogates for protein abundance.

Abundance ratio was calculated for each protein by dividing the PSM value of the protein in THP-1-TAP-1-KO by the value in THP-1 cells. The abundance ratio was further normalized to control for batch differences between experiments (Total PSM values of THP-1-KO/Total PSM values of THP-1). Statistical analysis was then performed using paired two-tailed t-tests, with p-values ≤ 0.05 considered statistically significant. Results were visualized using volcano plots. Calnexin was selected for further studies because of its relevance to HLA class I protein assembly and trafficking (Neefjes et al., 2011).

3.2.12 Immunofluorescence microscopy

Coverslips were coated with an excess of poly-L-lysine (0.01% solution, Sigma; catalogue number: P4707) for 1 hour at room temperature. The poly-L-lysine solution was aspirated, and the coverslips were allowed to dry completely. 1 x 10^6 THP-1 or THP-1-TAP-1-KO cells in 500 µL modified RPMI 640 were added to the coverslip and incubated at 37ºC for 2 hours. The medium was aspirated, and the cells were rinsed twice in 1X PBS. The cells were fixed with 4% paraformaldehyde (PFA) in 1X PBS and rinsed three times in 1X PBS. The cells were then permeabilized in 0.2% saponin for 10 minutes and stained overnight at 4ºC with anti-GM130 (Cell Signaling) and W6/32 in 0.2% saponin containing 5% normal goat serum. The cells were further stained for 30 minutes on ice with goat-anti-rabbit Alexa Fluor 647 and goat-anti-mouse Alexa Fluor 488 in 0.2% saponin containing 5% normal goat serum. The cells were rinsed three times in 1X PBS, stained with Hoechst for 10 minutes, and rinsed in 1X PBS three times. The coverslips were mounted on glass slides containing 10 µl ProLong Diamond mountant. A fiber-free paper was used to wipe off excess mountant, and the coverslips were air-dried in the dark overnight. The images were acquired as z-stacks on Leica Stellaris 5 confocal microscope and analysed using the Fiji ImageJ software.

3.2.13 Statistical analysis

Unless stated otherwise, data analysis in this study was performed using GraphPad Prism version 10.0.0 for Windows, GraphPad Software, Boston, Massachusetts, USA, www.graphpad.com. The data were subjected to Shapiro-Wilk normality test. This normality test was chosen because of the small sample size of the data. The data were found to be normally distributed; hence, a paired *t*-

test was used to compare HLA class I expression or other measured biomolecules between two conditions.

3.3.0 Results

3.3.1 Cell surface HLA class I is readily measurable in a TAP-1-deficient version of the human monocyte cell line THP-1 and has Endo-H sensitive glycans

To investigate HLA class I assembly and trafficking in TAP-deficient conditions, we used the human monocyte cell line, THP-1, obtained from ATCC, as an antigen-presenting cell model. The cells were maintained in RPMI 1640 (ATCC modified) as described in the methods. THP-1 cells from ATCC have 3 HLA class I alleles: HLA-A*02:01, HLA-B*15:11, and HLA-C*03:03 (McMurtrey et al., 2016; Nyambura et al., 2018). We confirmed this genotype as HLA-A*02:01, HLA-B*15:11, and HLA-C*03:03 by genotyping at HLA A, B, and C as previously described (Yarzabek et al., 2018).

TAP is a heterodimer consisting of TAP-1 and TAP-2 subunits. These two subunits are both required for the peptide transport function (Lehnert & Tampe, 2017).To generate a TAP-deficient antigen presenting cell model, we transduced THP-1 cells with an empty lentivirus Clustered Regularly Interspaced Short Palindromic Repeats (CRISPR)-CRISPR-associated protein (Cas9) vector (EV) or a lentivirus CRISPR-Cas9 vector expressing TAP-1 single guide RNA (TAP-1-sgRNA). TAP knockout was confirmed in TAP-1-sgRNA-transduced cells by immunoblot (Supplementary Figure 1) and immunoblot after immunoprecipitating TAP from the cell lysates with anti-TAP-1 (148.3) (Figure 3.1A). We quantified the total HLA class I expression on the surface of the THP-1 or THP-1-TAP-1-KO cells by flow cytometry after staining the cells with W6/32, an antibody that detects all HLA class I allotypes in their peptide-loaded forms (Barnstable et al., 1978). As expected, a significant downmodulation of surface HLA class I expression was observed on THP-1-TAP-1-KO cells relative to THP-1 cells (Figure 3.1B). However, despite this

down-modulation, a fraction of HLA class I molecules was still measurable on the surface of TAP-deficient cells (Figure 3.1B), highlighting the role of one or more TAP-independent mechanisms for the assembly and trafficking of these HLA class I molecules in the TAP-deficient cells.

The canonical HLA class I assembly and trafficking model involves the secretion of HLA class I proteins through the ER-Golgi-dependent pathway (Neefjes et al., 2011). Generally, proteins trafficking through this pathway are subject to post-translational modifications, beginning from their arrival in the ER and through their trans-Golgi transit (Lee et al., 2023). Via aspargine-linked (N-linked) glycosylation, the oligosaccharide structure (N-glycan), Glc3Man9GlcNAc2, assembled on dolichylpyrophosphate, a lipid carrier, is transferred and appended to asparagine residues that are part of Asn-X-Ser/Thr motif, where Asn, X, Ser and Thr are asparagine, any amino acid, serine, and threonine residues, respectively (Aebi, 2013; Bieberich, 2014; Stanley et al., 2022). Upon their addition to nascent proteins, N-glycans are trimmed and modified by a gamut of enzymes, thereby transitioning from a high mannose, Endo-H sensitive, immature glycans in the ER into complex Endo-H resistant mature glycans as the proteins traverse the Golgi (Aebi, 2013; Stanley et al., 2022). Accordingly, the nature of glycans borne by secreted proteins and proteins resident on the plasma membrane could offer insight into their trafficking route. For instance, plasma membrane proteins bearing complex (Endoglycosidase (Endo)-H resistant) glycans are generally considered to have arrived at the plasma membrane via an ER-Golgi-dependent conventional secretory pathway (Freeze & Kranz, 2010).

To compare the HLA class I trafficking pathways in wild-type THP-1 and TAP-deficient THP-1, we assessed the Endo-H sensitivity of HLA class I in the lysates or surface proteins from the cells, using an established method (Figure 3.1C) (Freeze & Kranz, 2010; Geng et al., 2018). The cells were treated (or untreated) with EZ-Link™ NHS-PEG4-Biotin (ThermoFisher Scientific), a

membrane-impermeable biotin, and lysates prepared from the cells were incubated with streptavidin agarose beads. The surface proteins eluted from the beads or lysates were digested with Endo-H enzyme (NEB) or left untreated and then subjected to SDS-PAGE and immunoblot (Figure 3.1C). HLA class I molecules contain a highly conserved Asn86 in the α1 domain of the heavy chain that is their sole glycosylation site. In the ER, immature forms of this glycan are sensitive to Endo-H, which specifically cleaves the β-1,4-glycosidic bond between the two GlcNAc residues in the diacetylchitobiose core of high mannose glycans (Glc3Man5-9GlcNAc2) (Freeze & Kranz, 2010). However, as the protein traffics from the ER to the Golgi, the mannose residues are sequentially trimmed and modified, acquiring resistance to Endo-H cleavage. The Endo-H sensitivity assay revealed a highly significant ($p < 0.001$) enrichment of Endo-H-sensitive glycans on HLA class I expressed on the plasma membrane of TAP-deficient cells relative to the wild-type (Figures 3.1D and 3.1E), as previously noted in other TAP-deficient cells (Geng et al., 2018).

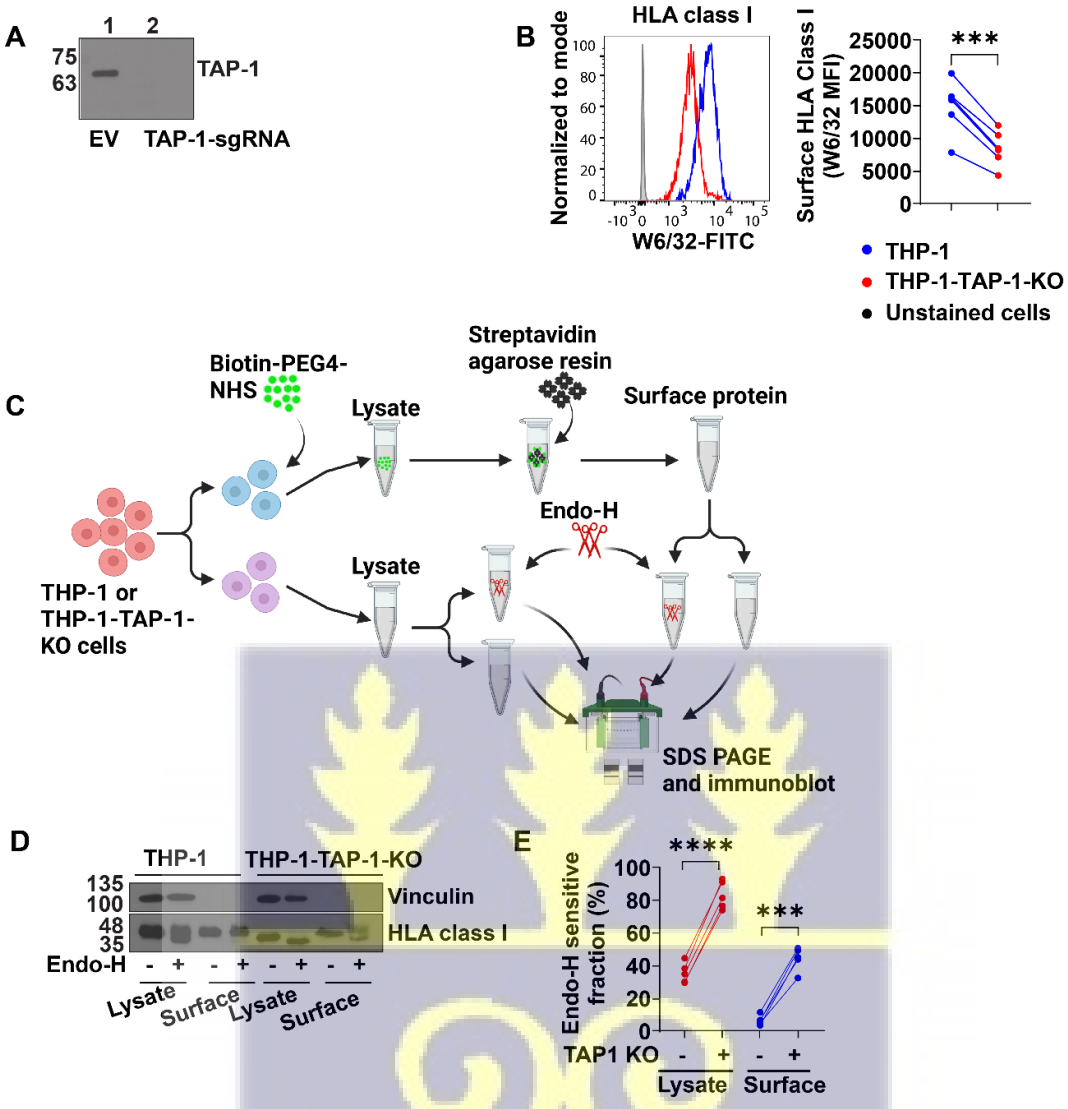

Figure 3.1: Cell surface HLA class I is readily measurable in a TAP-1-deficient version of the human monocyte cell line THP-1 with Endo-H sensitive glycans. A) Immunoblot of empty vector (EV) or TAP-1-gRNA-transduced THP-1 cells obtained after immunoprecipitation from cell lysates with anti-TAP-1 (148.3). B) Flow cytometric measurements of total HLA class I (n = 6) on THP-1 or THP-1-TAP-1-KO cells after staining the cells with the W6/32 antibody that measures all HLA class I allotypes (Barnstable et al., 1978). Representative histograms are shown on the left and averaged data across experiments are on the right. C) Protocol for HLA class I Endo-H sensitivity assay. Cells were treated with membrane-impermeable biotin and lysates prepared from the cells were incubated with streptavidin agarose beads. Proteins eluted from the

beads were treated with the Endo-H enzyme or buffer and subjected to SDS PAGE and immunoblots. D) Endo-H sensitivity of HLA class I proteins isolated from the plasma membrane of THP-1 or THP-1-TAP-1-KO cells. E) Averaged data from D across 5 experiments. Paired *t*-test was used in B and E for pair-wise comparisons. *** = p value < 0.001, **** = p value < 0.0001.

3.3.2 TAP deficiency does not induce the canonical unfolded protein response (UPR) mediators

These findings of Figure 3.1 suggested a possible Golgi-independent route for HLA class I cell surface expression or a Golgi-dependent trafficking pathway accompanied by impaired glycan processing in TAP-deficient cells. We first assessed the possible involvement of non-conventional secretory pathways in the trafficking of HLA class I in TAP-deficient conditions. Various non-conventional pathways have been implicated in the secretion of misfolded integral proteins, including mutant cystic fibrosis transmembrane conductance regulator (CFTR)(Gee et al., 2011), pendrin (Jung et al., 2016), proton-pump ATPase PmaA and PalI pH-sensing component (Dimou et al., 2022), and the thrombopoietin receptor, also known as myeloproliferative leukemia virus oncogene (Mpl) (Cleyrat et al., 2014), especially in the context of ER stress. Generally, the accumulation of misfolded proteins in the ER is known to induce the unfolded protein response (UPR) pathway, evidenced in the upregulation of key UPR mediators such as binding immunoglobulin protein (BiP) (Kozutsumi et al., 1988), spliced X-box binding protein 1 (XBP1) (Yoshida et al., 2001), CCAAT-enhancer-binding proteins (C/EBP) homologous protein (CHOP) (Wang et al., 1996), and activating transcription factor 4 (ATF4) (Harding et al., 2000). Peptide-deficient, suboptimally assembled, or misfolded HLA class I proteins are known to accumulate in the ER/ERGIC in TAP dysfunctional states (de la Salle et al., 1999; Raposo et al., 1995). We

therefore performed reverse transcriptase-quantitative polymerase chain reaction (RT-qPCR) to assess the transcript levels of spliced XBP1, BiP, CHOP, and ATF4 (Figures 3.2A, 3.2B, C, and 3.2D, respectively). We validated this assay by including cells treated with 0.5 µM thapsigargin (TG) as positive controls. TG inhibits the sarco/endoplasmic reticulum $Ca2^{+}$-ATPase (SERCA), causing ER $Ca2^{+}$ depletion and ER stress (Thastrup et al., 1990). As shown in Figure 3.2, XBP1, BiP, CHOP, and ATF4 are significantly induced by TG treatment in THP-1 and THP-1-TAP-1-KO cells but are equivalently expressed in the absence of the treatment. These findings indicate that TAP deficiency does not induce canonical UPR markers.

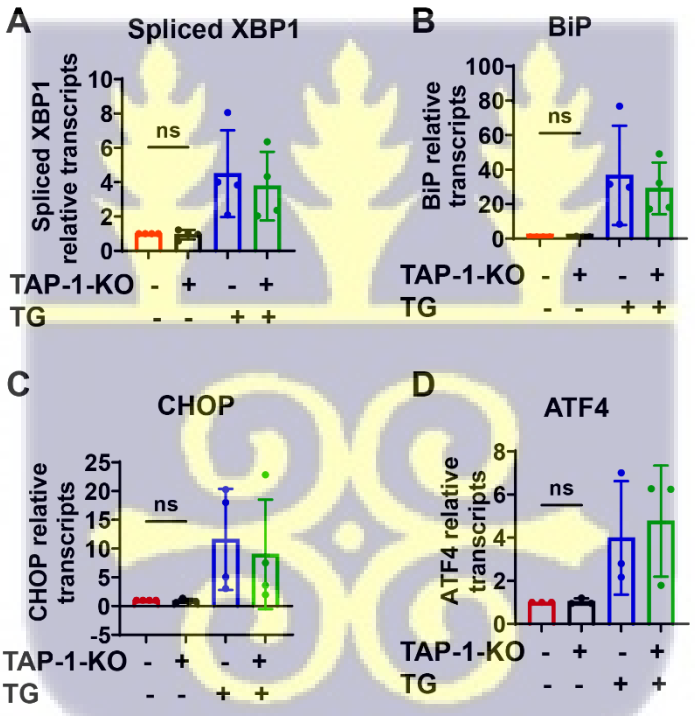

Figure 3.2: TAP deficiency does not induce canonical unfolded protein response (UPR) mediators. Relative transcript levels of indicated ER stress mediators. A) Spliced X-box binding protein 1 (XBP1), B) Binding immunoglobulin protein (BiP), C) CCAAT-enhancer-binding proteins (C/EBP) homologous protein (CHOP), and D) Activating transcription factor 4 (ATF4) measured by RT-qPCR (n=3-4, as indicated in the plots). The transcripts were normalized using glyceraldehyde-3-phosphate dehydrogenase (GAPDH), β-actin (ACTB), and Hypoxanthine-

guanine phosphoribosyl transferase (HGPRT1). Cells treated with 0.5 µM thapsigargin (TG), a known ER stress-inducing drug (Thastrup et al., 1990), for 6.5 h were used as positive controls. Paired *t*-tests were used to compare the relative transcript levels of the indicated UPR mediators in THP-1 and THP-1-TAP-1-KO cells. ns = p value > 0.05.

3.3.3 Depletion of GRASP55 and Sec22b does not selectively reduce surface HLA class I on TAP-deficient cells

The Golgi reassembly-stacking protein of 55 kDa (GRASP55) (also called Golgi reassembly-stacking protein 2 [GORASP2]) is primarily associated with the medial and trans cisternae of the Golgi (Shorter et al., 1999). GRASP55, together with its homologue, GRASP65, is functionally involved in Golgi stacking formation (Xiang & Wang, 2010). However, besides maintaining the Golgi structure, recent studies have implicated GRASP55 in the non-conventional transport of soluble and integral proteins, including mutant CFTR (Gee et al., 2011), interleukin (IL)-1β (Dupont et al., 2011), Mpl (Cleyrat et al., 2014), and, more recently, mutant huntingtin (Ahat et al., 2022). Given this emerging function of GRASP55 in unconventional protein trafficking, we assessed the role of GRASP55 in the trafficking of HLA class I in TAP-deficient THP-1 cells. We depleted GRASP55 in THP-1 and THP-1-TAP-1-KO cells using a lentivirus CRISPR-Cas9 vector expressing GRASP55 sgRNA (Figure 3.3A). We then assessed HLA class I expression on the plasma membrane of the cells by flow cytometry after staining the cells with W6/32-FITC on ice for 30 minutes (Figure 3B). Although GRASP55 depletion down-modulates surface HLA class I on TAP-deficient THP-1 cells significantly ($p < 0.01$), suggesting a possible involvement of GRASP55-dependent unconventional trafficking, HLA class I was equally reduced on the surface

of wildtype THP-1 cells (Figure 3.3B), demonstrating that the influence of GRASP55 is not specific to TAP-deficient THP-1 cells.

Next, we assessed the role of vesicle-trafficking protein SEC22 homolog B (Sec22B) in HLA class I trafficking in THP-1-TAP-1-KO cells. Sec22B is a member of soluble *N*-ethylmaleimide-sensitive factor attachment protein receptors (SNAREs), which are a family of cytosolic and membrane proteins that mediate membrane fusion of intracellular vesicles with organelles (Hay et al., 1997). The structure and function of Sec22B in physiological and pathological contexts have been extensively reviewed (Jahn et al., 2024; W. Sun et al., 2020). Briefly, sec22B resides in the ER-Golgi intermediate compartment (ERGIC) and promotes the trafficking of vesicles from the ER to the Golgi apparatus (anterograde transport) and from the Golgi apparatus to the ER (retrograde transport). Sec22B performs this function by serving as one of the SNARE components of coat protein complex II (COPII) and coat protein complex I (COPI) vesicles, respectively. Sec22B is also suggested to promote cargo delivery from the ERGIC to the phagosome. To achieve this function, sec22B is suggested to form complexes with syntaxin 4, a t-SNARE in the phagosome, enabling sec22B-positive compartments budding from the ERGIC to fuse with and deliver their protein cargoes to the phagosome. By regulating phagosomal maturation, sec22B is also suggested to regulate the cross-presentation of exogenous antigens by MHC class I (Cebrian et al., 2011), although these effects of sec22b remain controversial (Wu et al., 2017). Recent studies have also highlighted the role of sec22B in antigen cross-presentation in TAP-deficient dendritic cells (Barbet et al., 2021; Blander, 2023; Blander et al., 2023; Yee Mon & Blander, 2023). Briefly, during conventional cross-presentation, MHC class I proteins in endocytic recycling compartments (ERCs) are suggested to be delivered through toll-like receptor (TLR)-mediated signaling to antigen-bearing phagosomes, where the antigens are assembled with MHC class I

molecules and presented for $CD8^+$ T cells priming. In TAP-dysfunctional states, ERCs are depleted of MHC class I and are suggested to no longer be delivered to phagosomes through the TLR-dependent pathway. Rather, MHC class I proteins accumulate in the ERGIC and are delivered to antigen-positive phagosomes through sec22B-positive compartments (Barbet et al., 2021). However, whether bulk MHC class I proteins utilize a sec22B-dependent pathway for presenting endogenous antigens in TAP-deficient cells has not been addressed. We therefore investigated the role of sec22B in HLA class I trafficking in THP-1-TAP-1-KO cells. Sec22B was depleted from wild-type THP-1 and THP-1-TAP-1-KO cells using sec22B SMARTpool® siRNA (Dharmacon, catalogue no: L-011963-00-0020) (Figure 3.3C). We measured the surface HLA class I expression on the cells by flow cytometry after staining with W6/32-FITC on ice for 30 minutes. The results reveal that sec22B neither influences bulk HLA class I trafficking in wild-type nor TAP-deficient THP-1 cells (Figure 3.3D).

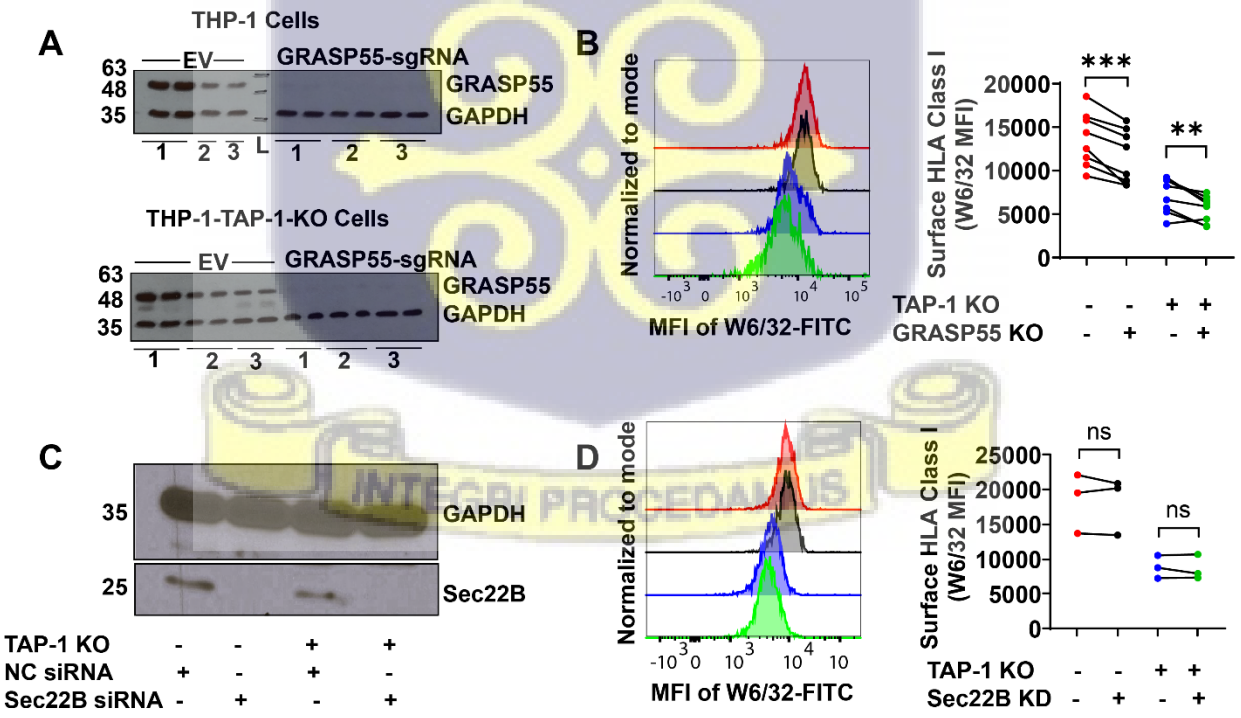

Figure 3.3: Depletion of GRASP55 or Sec22b does not selectively reduce surface HLA class I on TAP-deficient cells. A and C) Representative immunoblots of CRISPR-Cas9-mediated GRASP55 knockout and sec22B knockdown by siRNA as indicated in THP-1 and THP-1-TAP-1-KO cells. B and D) Surface HLA class I on THP-1 and THP-1-TAP-1-KO cells with or without GRASP55 knockout or sec22B knockdown, respectively, measured by flow cytometry after staining with W6/32-FITC. Representative histograms are shown on the left and compiled data across 3-7 experiments are on the right. Paired *t*-tests were used for the indicated pair-wise comparisons. ns = $p > 0.05$, ** = p value < 0.01, *** = p value < 0.001.

3.3.4 HLA class I trafficking in TAP-deficient cells is sensitive to brefeldin A (BFA)

Our survey of key unconventional secretory pathway components in Figure 3.3 and additional components (our unpublished results) did not define a specific unconventional mode of HLA class I trafficking in THP-1-TAP-1-KO cells. Hence, we assessed the conventional secretory pathway for its possible involvement in HLA class I trafficking in TAP-deficient cells. Although there is a consensus that HLA class I trafficking is governed by the conventional secretory pathway in a TAP-dependent manner, whether the conventional secretory pathway also influences HLA class I trafficking in TAP-deficient cells has not been addressed. To study the involvement of this pathway, we treated THP-1 and THP-1-TAP-1-KO cells with BFA for 4 hours and measured the surface HLA class I by flow cytometry after staining with W6/32-FITC. BFA is a fungal antibiotic that blocks the transport of proteins between the ER and the Golgi (Chardin & McCormick, 1999; Fujiwara et al., 1988) and has been widely used to study the conventional secretory pathway (Hong et al., 2019; Lamoreaux et al., 2006; Natsume et al., 2024; van Raam et al., 2017). Upon treatment, BFA inhibited HLA class I trafficking in wild-type THP-1 cells, evidenced by surface HLA class I downmodulation, which was expected (Figure 3.4A). However, we also observed a highly

significant ($p < 0.001$) down-modulation of surface HLA class I in BFA-treated THP-1-TAP-1-KO cells (Figure 3.4A), suggesting the involvement of the conventional secretory pathway in these cells.

BFA blocks the trafficking of nascent proteins, including HLA class I (Figure 3.4A), between the ER and the Golgi (Chardin & McCormick, 1999; Fujiwara et al., 1988). However, HLA class I molecules stably expressed on the plasma membrane of THP-1 or THP-1-TAP-1-KO cells prior to BFA treatment could confound the results in Figure 3.4A. To address this limitation, we stripped THP-1 and THP-1-TAP-1-KO cells of peptide-assembled surface HLA class I detectable by W6/32 (Figure 3.4B) by treating the cells with a citric acid solution (pH 3), as described by (Sugawara et al., 1987). BFA treatment of the acid-stripped cells for 4 hours disrupted HLA class I trafficking in wild-type and TAP-deficient THP-1 cells, relative to acid-stripped but BFA-untreated cells (Figure 3.4C), and validating our observations in Figure 3.4A. Additionally, to assess HLA class I trafficking in another TAP-deficient cell line, we treated ST-EMO, a TAP-2-deficient cell line (de la Salle et al., 1994), transduced with HLA-B*35:01 (ST-EMO-B*35:01) with BFA to assess the role of the conventional pathway in HLA class I trafficking. Like THP-1-TAP-1-KO cells, BFA blocked HLA class I trafficking (Figure 3.4D) in ST-EMO-B*35:01. Taken together, these assays highlight the involvement of the ER-Golgi conventional secretory pathway in HLA class I trafficking in TAP-deficient cells, despite the enrichment of Endo-H sensitive glycans on surface HLA class I of TAP-deficient cells (Figures 3.1D and 3.1E).

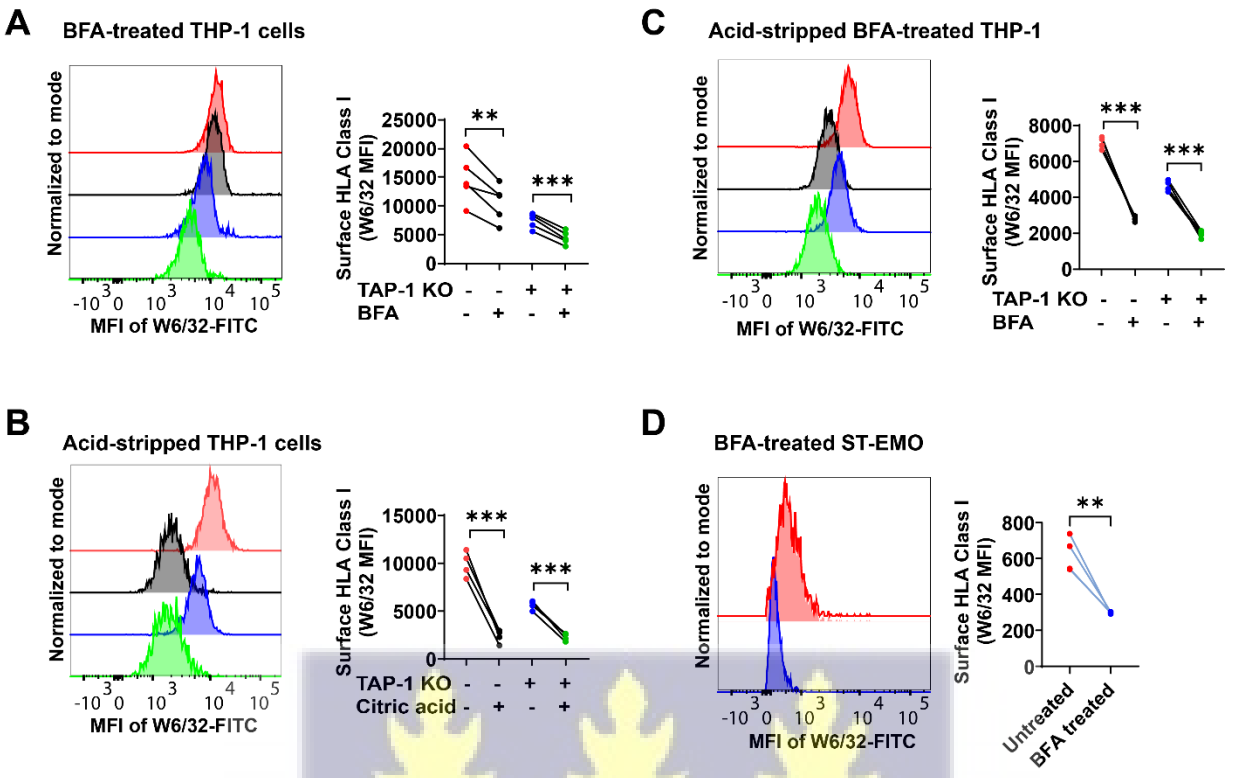

Figure 3.4: HLA class I trafficking in TAP-deficient cells is sensitive to brefeldin A (BFA).

Surface HLA class I of BFA-treated (A), acid-stripped (B), and acid-stripped BFA-treated (C) THP-1 and THP-1-TAP-1-KO cells measured by flow cytometry after staining with W6/32-FITC. D) Surface HLA class of BFA-treated ST-EMO-B*35:01, a TAP-2-deficient cell line (de la Salle et al., 1994). The cells were treated with 10 µg/mL BFA for 4 h before staining. Acid stripping was performed by treating the cells with citric acid (pH 3.0) for 2 minutes (Sugawara et al., 1987). Representative histograms are shown on the left, and compiled data across 3 – 5 experiments are on the right. Paired *t*-tests were used for the indicated pair-wise comparisons. ** = p value < 0.01, *** = p value < 0.001.

3.3.5 Peptide-assembled HLA class I proteins colocalize with cis-Golgi network in THP-1-TAP-1-KO cells

To further assess the trafficking of HLA class I proteins through the conventional pathway in TAP-deficient cells, we performed immunofluorescence staining for colocalization of HLA class I in the cis-Golgi of TAP-deficient cells. THP-1 or THP-1-TAP-1-KO cells were fixed and stained for HLA class I and a cis-Golgi network marker (GM130) and examined under Leica Stellaris 5 confocal microscope. The microscopy revealed a degree of W6/32 colocalization with anti-GM130 in THP-1 and THP-1-TAP-1-KO cells, suggesting the same trafficking pathway for HLA class I wild-type and TAP-deficient THP-1 cells.

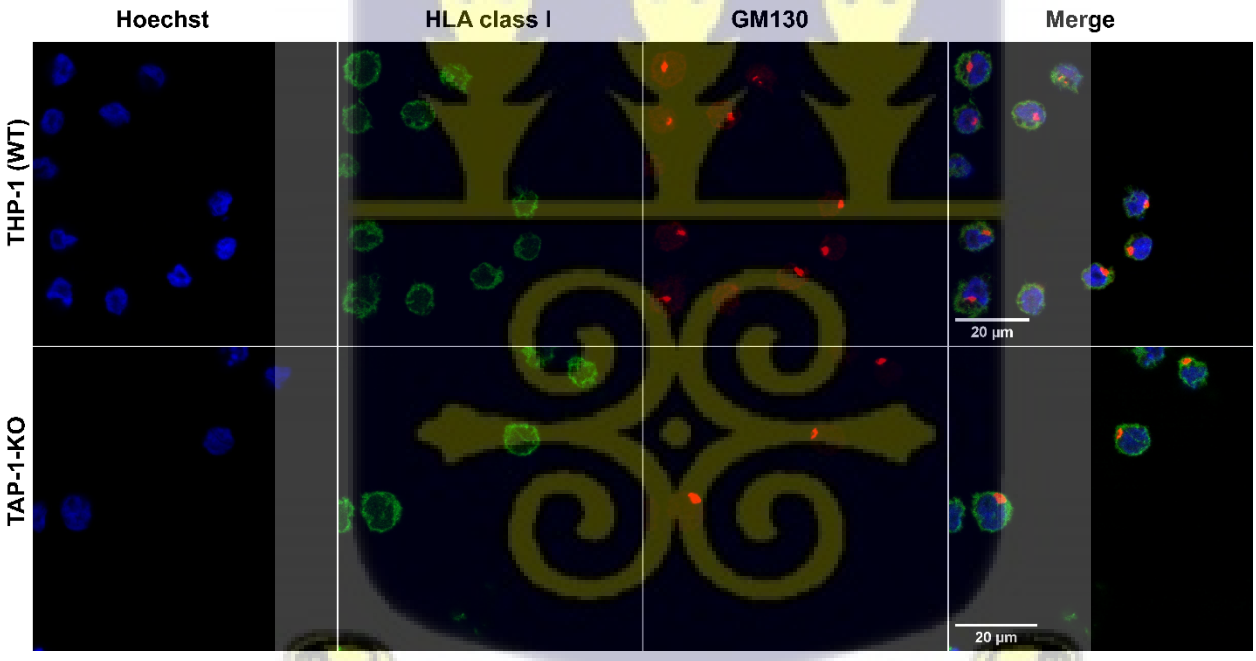

Figure 3.5: Immunofluorescence of THP-1 and THP-1-TAP-1-KO cells stained with Hoechst, W6/32, and anti-GM130 antibodies. THP-1 or THP-1-TAP-1-KO cells were fixed and stained for HLA class (W6/32-FITC, green) and a cis-Golgi network marker (GM130-Alexa fluor 647,

red). The nucleus was stained with Hoechst.3.3.6 Calnexin is induced on the surface of TAP-deficient THP-1 cells, but calnexin knockdown maintains high mannose cell surface HLA class I glycosylation

Since TAP deficiency maintains Golgi-dependent secretory trafficking of HLA class I, we considered that specific MHC class I-associated factors might associate with MHC class I molecules in the vicinity of their glycan and thus impair MHC class I glycan maturation in the Golgi of TAP-deficient cells. For global assessment of such factors in TAP-deficient cells, we surveyed the surface proteome of THP-1 and THP-1-TAP-1-KO cells for proteins differentially expressed on THP-1-TAP-1-KO cells. The cells were treated with membrane-impermeable biotin, and the surface protein was pulled down using streptavidin beads. The beads were trypsinized, and the eluted peptides were subjected to liquid chromatography/mass spectrometry (LC/MS) (Figure 3.6A). The peptide-spectrum match (PSM) values were set at ≥ 3 PSM in at least two of three THP-1 or THP-1-TAP-1-KO replicates. The PSM values of proteins in THP-1-TAP-1-KO cells were normalized to THP-1 cells (PSM values in TAP-1-KO/PSM values in THP-1) and further normalized for batch difference (Total PSM values of THP-1-KO/Total PSM values of THP-1) between experiments. Comparing THP-1-TAP-1-KO cells with THP-1 cells, calnexin (CANX) was significantly overexpressed and, as expected, HLA class I alleles were downregulated on the surface of THP-1-TAP-1-KO cells (Figure 3.6B). Calnexin is a transmembrane lectin in the ER and is among the chaperones that play a crucial role in glycoprotein folding and ER quality control (Adams et al., 2021). Structurally, calnexin is similar to calreticulin, a component of the MHC class I peptide loading complex, but calnexin is thought to interact with MHC class I heavy chains prior to their binding β2m and prior to their incorporation into the PLC (Adhikari & Elliott, 2003). Both calreticulin and calnexin have lectin domains that interact with monoglycosylated glycans on

nascent glycoproteins, including HLA class I (Figure 3.6C), to promote their native folding (Adams et al., 2021; Adhikari & Elliott, 2003). In the ER, monoglucosylated glycans can be generated via the activity of glucosidase II on the initial glycan, Glc3Man9GlcNAc2, that is added to N-linked glycoprotein. Glucosidase II can also remove the terminal glucose residue. Non-native proteins can be re-glucosylated by UDP-glucose:glycoprotein glucosyltransferase 1 (UGGT1) to enable multiple rounds of calnexin/calreticulin-mediated folding (Ferris et al., 2014; Sousa & Parodi, 1995; Trombetta & Parodi, 1992). The overexpression of calnexin in the surface proteome of TAP-deficient THP-1 cells (Figure 3.6B) suggested a possible co-trafficking with HLA class I proteins. We hypothesized that calnexin might bind to monoglucosylated HLA class I glycans (illustrated in Figure 3.6C) in TAP-deficient cells and co-traffic through the Golgi, preventing access by glycan-modifying enzymes. Based on this hypothesis, calnexin depletion is expected to reduce the enrichment of Endo-H sensitive glycans on surface HLA class I of TAP-deficient cells.

To test this hypothesis, calnexin was depleted in THP-1 and THP-1-TAP-1-KO cells using the CRISPR-Cas9 approach (Figure 3.6D). Surface HLA class I on the cells was measured by flow cytometry, and Endo-H sensitivity assay was performed using the surface biotinylation approach described in Figure 3.1C. Calnexin depletion significantly decreases HLA class I on wild-type but increases HLA class I on TAP-deficient THP-1 cells, although non-significant (Figure 3.6E). Calnexin depletion also maintains the Endo-H sensitive fraction on THP-1 and THP-1-TAP-1-KO cells (Figure 3.6F and G). These results suggest that calnexin plays an important role in the ER retention of HLA class I proteins in TAP-deficient THP-1 cells, but calnexin-HLA class I interaction does not account for the impairment in N-glycan processing in TAP-deficient THP-1 cells

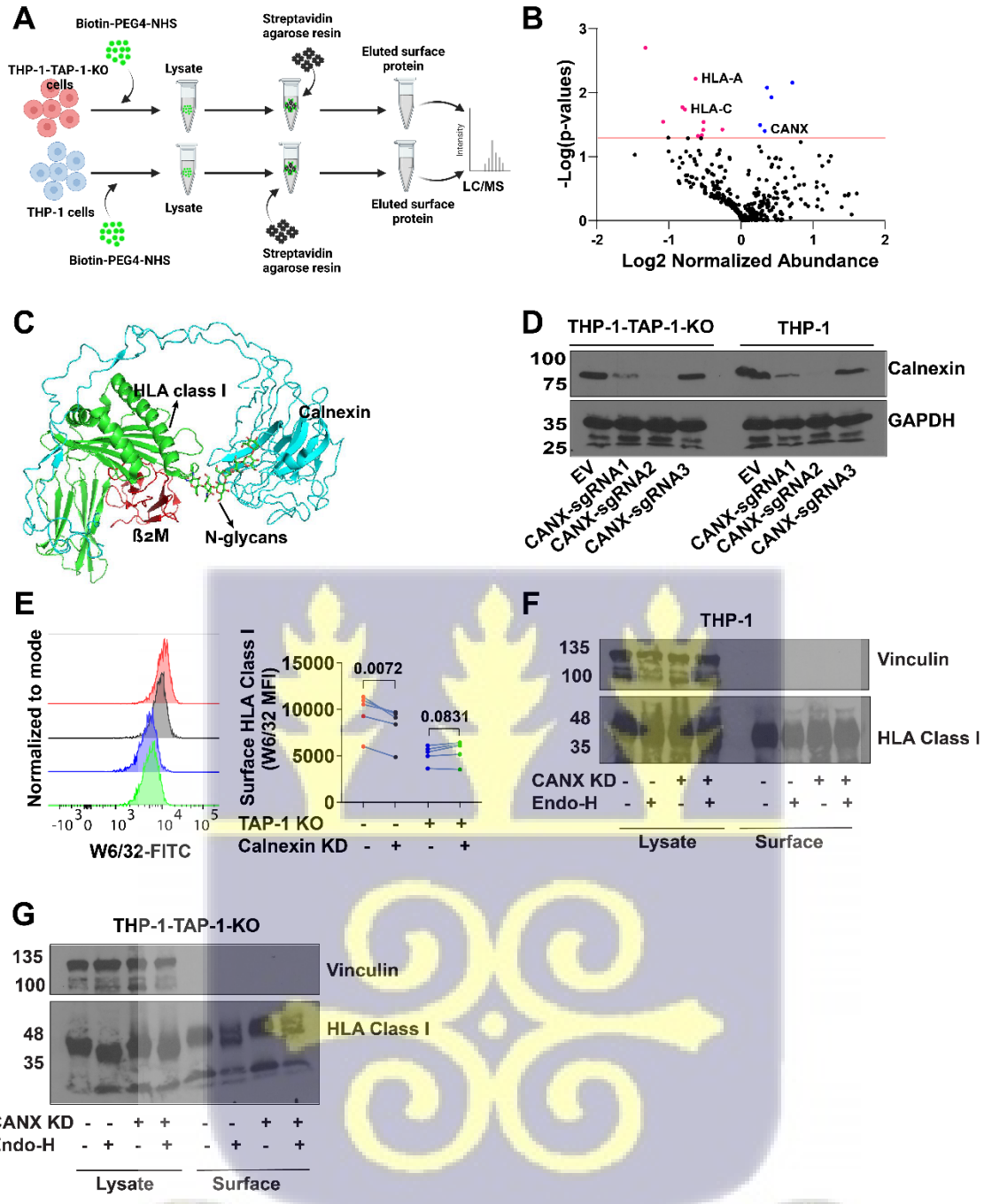

Figure 3.6 Calnexin is induced on the surface of TAP-deficient THP-1 cells, but calnexin knockdown maintains high mannose cell surface HLA class I glycosylation. A) Protocol for identification of THP-1 and THP-1-TAP-1-KO cells' surface proteome by mass spectrometry. B) A volcano plot showing not significantly changed (black), downregulated (red), and overexpressed (blue) proteins in THP-1-TAP-1-KO cells' surface proteome. C) A cartoon structure of calnexin (cyan) interacting with N-glycan on HLA class I protein (green). D) An immunoblot showing

calnexin depletion in THP-1 or THP-1-TAP-1-KO cells. Cells were transduced with an empty vector (EV) or a vector with one of calnexin (CANX)-sgRNA1, 2, or 3. CANX-sgRNA2 was most effective; hence, cells transduced with it were used for further experiments. E) Surface HLA class I measurements of THP-1 and THP-1-TAP-1-KO cells with/without calnexin depletion measured using flow cytometry. Representative histograms (left) and compiled data across 5 experiments (right) are shown. Paired *t*-tests were used for pair-wise comparisons across 5 experiments in (E). F and G) Immunoblots of the Endo-H sensitivity of THP-1 (F) or THP-1-TAP-1-KO (G) with/without calnexin depletion.

3.3.7 TAP deficiency induces Endo-H sensitive HLA class I glycans, but the induction is HLA class I-specific rather than global

The increased Endo-H sensitive glycans on surface HLA class I and the involvement of the conventional pathway in HLA class I trafficking in TAP-deficient cells raise two possibilities as to why the glycans are not modified into complex forms before HLA class I molecules are expressed on the cell surface. One possibility is that TAP deficiency impairs the cellular activities of the glycan processing enzymes, altering the glycosylation profile of all secreted glycoproteins, including HLA class I, in THP-1-TAP-1-KO cells. In this scenario, the enrichment of Endo-H sensitive glycans on surface HLA class I proteins on THP-1-TAP-1-KO cells is not HLA-class I specific but instead affects all other surface glycoproteins. The second possibility is that the altered glycosylation is HLA class I-specific.

We explored the first possibility by quantifying the total high mannose (Endo-H sensitive) or complex (Endo-H resistant) glycans on the surface of THP-1 and THP-1-TAP-1-KO cells using concanavalin-A (ConA) and Phytohemagglutinin-L (PHA-L) lectins, respectively. ConA and PHA-L are lectins that bind high mannose and complex glycans, respectively (Cummings & Etzler, 2009). To impair glycosylation and induce Endo-H sensitive glycans on glycoproteins globally,

THP-1 or THP-1-TAP-1-KO cells were also treated with 10 nM kifunensine (KIF), a potent alkaloid that broadly inhibits mannosidases (Almahayni et al., 2022; Elbein et al., 1990), for 48 hours. Assessment of cell surface HLA class I expression on THP-1 cells by flow cytometry indicates that KIF treatment increases HLA class I cell surface expression (Figure 3.7A). In addition, KIF treatment phenocopies the Endo-H sensitive glycans enrichment on surface HLA class I observed in TAP-deficient THP-1 cells (Figure 3.7E). Furthermore, flow cytometric assessment comparing high mannose glycans on THP-1 and THP-1-TAP-1-KO cells after staining with ConA-FITC revealed no significant difference (Figure 3.7B). In contrast, high mannose glycans are overexpressed on KIF-treated THP-1 (Figure 3.7C) and THP-1-TAP1-KO cells (Figure 3.7D). Whereas PHA-L-FITC staining did not reveal a significant difference in surface complex glycans between THP-1 and THP-1-TAP-1-KO cells (Figure 3.7F), complex glycans are significantly decreased on KIF-treated THP-1 ($p \leq 0.05$) and KIF-treated THP-1-TAP-1-KO cells ($p < 0,01$). Together, these results suggest that altered glycosylation in TAP-deficient THP-1 cells is specific to HLA class I proteins.

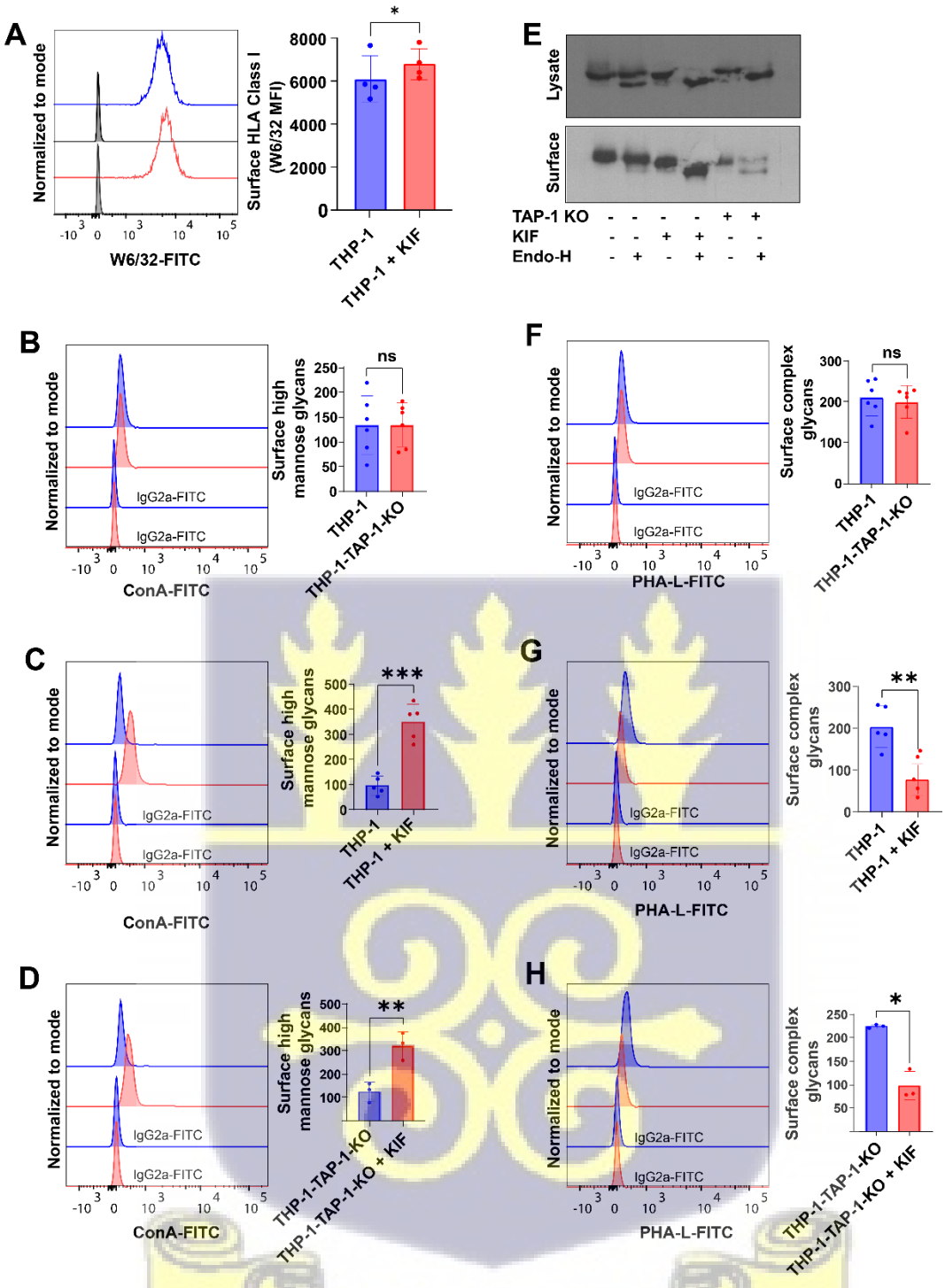

Figure 3.7 TAP deficiency induces high mannose HLA class I glycans, but the induction is HLA class I-specific rather than global. A) Surface HLA class I on Kifunensine (KIF)-treated THP-1 cells measured by flow cytometry. Cells were treated with 10 nM KIF, and flow cytometry was performed 48 h after treatment. B-D) High mannose glycans on the surface of parental THP-

1 and THP-1-TAP-1-KO (B) Kifunensine (KIF)-treated parental THP-1 (C) and KIF-treated THP-1-TAP-1-KO cells (D) measured by flow cytometry after staining the cells with Concanavalin A-FITC. E) Endo-H sensitivity assay of HLA class I in the lysate or surface protein of THP-1 cells treated with KIF. Kifunensine treatment of wildtype cells phenocopies altered HLA class I glycosylation observed in TAP-deficient cells. F-H) Complex glycans on the surface of parental THP-1 and THP-1-TAP-1-KO (F), Kifunensine (KIF)-treated parental THP-1 (G), and KIF-treated THP-1-TAP-1-KO cells (H) measured by flow cytometry after staining the cells with Phytohemagglutinin-L (PHA-L)-FITC. Paired *t*-tests were used for pair-wise comparisons (n = 3-6 across different comparisons). ns = $p > 0.05$, * = p value ≤ 0.05, ** = p value < 0.01, *** = p value < 0.001.

3.3.8 High mannose cell surface HLA class I glycans are not specific to TAP-deficiency

To further examine whether altered N-glycan processing is specific to TAP deficiency or also induced by other conditions that interfere with MHC class I assembly, we examined HLA class I surface glycosylated in cells lacking tapasin, an important component of the PLC (Blum et al., 2013), and assessed the expression and Endo-H sensitivity of surface HLA class I. Notably, tapasin depletion in THP-1 cells by CRISPR-Cas9 (Figure 3.8A) decreases surface HLA class I (Figure 3.8B) and, similar to TAP knockout, enriches Endo-H sensitive N-glycans on surface HLA class I (Figures 3.8C and D). Together, these results suggest that multiple conditions that compromise peptide assembly cause the release of HLA class I with high mannose glycans to the plasma membrane.

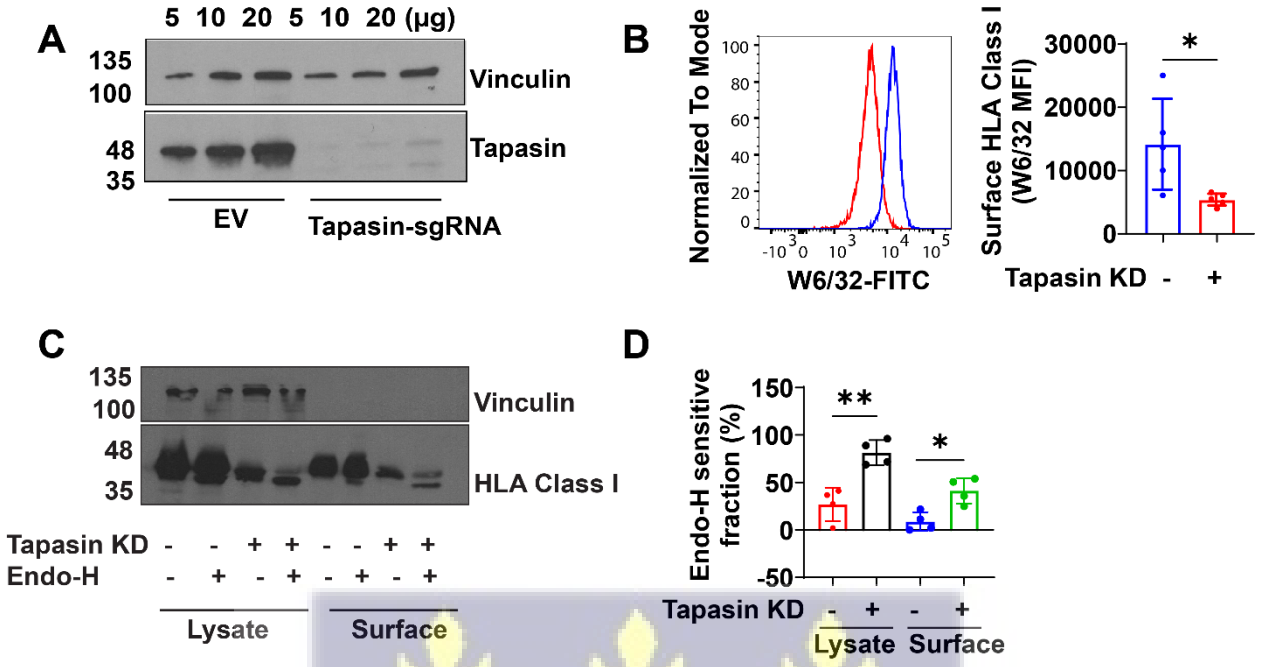

Figure 3.8 Tapasin deficiencies also enrich for high mannose cell surface HLA class I glycans. A) Representative immunoblots showing tapasin knockout by CRISPR-Cas9 in THP-1 cells. The cells were transduced with empty vector (EV), or a vector with tapasin-sgRNA. B) Total surface HLA class I of THP-1 and THP-1-tapasin-KO cells measured by flow cytometry after staining the cells with W6/32-FITC. Representative histograms (left) and compiled data across 4 experiments (right) are shown. C) HLA class I Endo-H sensitivity in the lysates or surface protein of THP-1 or THP-1-tapasin-KO cells. Representative immunoblots are shown in the left panels and compiled data across 3 replicates are shown in the right panels. Paired *t*-tests were used for pair-wise comparisons. * = *p* value ≤ 0.05.

3.4 Discussion

Antigen presentation by HLA class I proteins is a key component of the adaptive immune system. Subverting HLA class I functions, for example, by inhibiting TAP, could compromise immune defense against infectious pathogens and cancers (Alimonti et al., 2000; Fruhet al., 1995; Henle et

al., 2017; Verweij et al., 2015). However, the substantial expression of HLA class I on the plasma membrane of TAP-deficient cells (Figure 3.1B) indicates that HLA class I dependence on peptide supply by the ER TAP is not absolute. Relative dependence of HLA class I alleles on TAP has indeed been reported (Geng et al., 2018), as well as the ability of HLA class I to access signal sequence-derived peptides independently of TAP (Henderson et al., 1992; Wei & Cresswell, 1992). The ability to present such peptides ensures that antigen presentation is maintained to some degree even when the cells are infected by TAP-inhibiting viruses or cancers that downregulate TAP.

Glycosylation is a crucial post-translational modification that governs the ER/Golgi quality control of glycoproteins, such as HLA class I, as they traverse the secretory pathway (Aebi, 2013; Bieberich, 2014; Stanley et al., 2022). Although the enrichment of Endo-H sensitive glycans has been observed previously in TAP-deficient cells (Geng et al., 2018), how Endo-H sensitive glycans persist on surface HLA class I and the mechanisms driving their impaired processing into complex (Endo-H resistant glycans) have not been elucidated. Expression of Endo-H-resistant glycans on secreted glycoproteins generally marks their Golgi-dependent secretory trafficking (Bieberich, 2014). However, there is uncertainty about the trafficking pathway when Endo-H-sensitive glycans are maintained on glycoproteins expressed on the plasma membrane. The enrichment of Endo-H sensitive glycans on surface HLA class I observed (Figures 3.1D and E and Geng et al., 2018) raises the possibility for conventional (Golgi-dependent) or unconventional (Golgi-independent) secretory pathways.

Unconventional protein secretion (UPS) pathways have emerged as important cellular response mechanisms against protein misfolding and ER stress (Kim et al., 2018; Maricchiolo et al., 2022; Rabouille, 2017). UPS bypasses the classical ER-Golgi route, has been observed for several transmembrane and leaderless cargo proteins, and is often triggered by the accumulation of

unfolded proteins or other ER stress-inducing conditions (Kim et al., 2018; Maricchiolo et al., 2022; Rabouille, 2017). Although misfolded or suboptimally assembled HLA class I proteins are prevalent and retained in the ER in TAP-deficient cells, the findings in this study indicate that TAP deficiency does not induce the UPR (Figure 3.2A-D). Notably, this absence of evidence for classical UPR induction suggests that the export of HLA class I with Endo-H sensitive glycans from the ER is another layer of homeostatic response to unfolded HLA class I accumulation in TAP-deficient cells.

GRASP55 depletion does not specifically reduce surface HLA class I in TAP-deficient cells, as surface HLA class I was also reduced on the plasma membrane of GRAP55-depleted wild-type cells (Figures 3.3A and B). Under physiological conditions, GRASP55 resides in the Golgi and promotes stacking formation (Ahat et al., 2019; Kim et al., 2018; Maricchiolo et al., 2022; Rabouille, 2017). Previous studies have reported the influences of GRASP55 on the trafficking of cargo proteins that pass through the Golgi. GRASP55 depletion decreases the secretion of many proteins, including huntingtin (Ahat et al., 2022), Interleukin-1β (Chiritoiu et al., 2019), matrix metallopeptidase 2 (Nuchel et al., 2021), and mutant CFTR (Gee et al., 2011). The decrease in surface HLA class I observed in wild-type or TAP-deficient cells suggests that normal Golgi structure is required for optimal HLA class I trafficking, and structural perturbations of the Golgi (such as decreased cisterna stacking) induced by GRASP55 knockdown (Zhang & Wang, 2020), could compromise HLA class I surface expression, making GRASP55 a potential target of viruses or cancers that evade immune response by downmodulating HLA class I.

Although TAP-independent cross-presentation in DCs is suggested to rely on a sec22B-dependent pathway (Barbet et al., 2021; Blander, 2023; Blander et al., 2023), our results (Figures 3.3C and D) suggest that sec22B does not influence the constitutive bulk trafficking of HLA class I proteins

in wild-type or TAP-deficient THP-1 cells. Other studies have reported the significant role of sec22B in cross-presentation by DCs (Alloatti et al., 2017; Biscari et al., 2023; Cebrian et al., 2011), although the role remains controversial (Wu et al., 2017).

The decrease in surface HLA class I of BFA-treated THP-1, THP-1-TAP-1-KO, and ST-EMO cells (Figures 3.4A, C, and D) suggests that HLA class I traffics through the Golgi-dependent secretory pathway. Additionally, peptide-assembled HLA class I proteins colocalize with the cis-Golgi network marker GM130 to some extent (Figure 3.5), reinforcing the point that not all surface glycoproteins bearing Endo-H sensitive glycans have taken a Golgi-independent route. The Endo-H sensitive glycan enrichment of surface HLA class I proteins observed in this study seems specific to HLA class I since there was no significant difference in the overall amounts of high mannose or complex cell surface glycans between wild-type and TAP-deficient cells (Figures 3.6B and F). In contrast, there is a global induction of high mannose glycans (up to 3.5-fold) and a simultaneous reduction of complex glycans on KIF-treated THP-1 and THP-1-TAP-1-KO cells (Figures 3.6C, D, G, and H). Notably, KIF treatment increased HLA class I trafficking and Endo-H sensitive glycans on surface HLA class I, suggesting that some N-glycans processing enzymes inhibited by KIF divert a subset of HLA class I for degradation, possibly through ERAD. Hence, further studies of the effects of KIF or its analogs could offer insights into developing suitable pharmacological agents for rescuing antigen presentation to $CD8^+$ T cells in pathological conditions that downmodulate HLA class I.

Although our mass spectrometric analysis indicates overexpression of calnexin in TAP-deficient THP-1 cells' surface proteome (Figure 3.6B), the enrichment of Endo-H sensitive glycans on surface HLA class I is not explained by co-trafficking with calnexin since calnexin depletion did not influence the Endo-H sensitivity. Besides calnexin, other proteins were overexpressed in the

surface proteome of THP-1-TAP-1-KO cells. However, this study did not evaluate their involvement in the Endo-H sensitive glycan enrichment of surface HLA class I, since there is no prior information on their HLA class I associations

Our assessment of surface HLA class I glycosylation also shows that Endo-H-sensitive glycans enrichment is not specific to TAP deficiency, as tapasin depletion also induces enrichment (Figures 3.8A, C, and D). Thus, factors common to TAP and tapasin deficiency drive the increase in Endo-H sensitive glycans on surface HLA class I in TAP or tapasin-dysfunctional cells. Although Endo-H sensitive glycans enrichment on surface HLA class I of TAP-deficient cells has been previously observed (Geng et al., 2018), the observation that tapasin deficiency also induces Endo-H sensitive glycans on surface HLA class I has never been reported. Like TAP, tapasin is an important component of the PLC and is required for optimal HLA class I assembly with peptides (Neefjes et al., 2011). Tapasin deficiency increases misfolded HLA class I and down-modulates surface HLA class I expression, features also observed in TAP-deficient cells (de la Salle et al., 1994; de la Salle et al., 1999; Yabe et al., 2002). Together, these results suggest that conditions, such as TAP or tapasin deficiency, that compromise HLA class I-peptide assembly and promote HLA class I misfolding also induce surface HLA class I with Endo-H-sensitive glycans on the cell surface.

In a physiological state, ER/Golgi quality control mechanisms ensure that only properly folded glycoproteins proceed from the ER to the Golgi (Adams et al., 2021; Anelli & Sitia, 2008; Ferris et al., 2014). The current generic model for N-glycan processing and maturation on glycoproteins (Aebi, 2013; Bieberich, 2014) indicates that Glu3Man9GlcNac2 is transferred “en bloc” from dolichol phosphate to a nascent protein in a reaction catalyzed by oligosaccharyltransferase (OST). The terminal glucose residue of Glu3Man9GlcNac2 is trimmed by glucosidase I (Gluc I), and the second by Glu II, yielding a monoglucosylated glycan (GluMan9GlcNac2). Proteins bearing

monoglucosylated glycans are bound by calnexin/calreticulin to enable their proper folding. When released, the remaining glucose residue is also trimmed by Glu II. The protein proceeds through the Golgi, where specific Golgi mannosidases trim the mannose residues before the high mannose glycans are modified into complex glycans (Bieberich, 2014) (Figure 3.9). Proteins that are not properly folded are reglucosylated by UGGT, rebound by calnexin/calreticulin, and kept in this cycle until they assume their native state or are disposed of to the proteasome through ERAD (Adams et al., 2021; Anelli & Sitia, 2008; Luo et al., 2023). The first step of ERAD is thought to involve the processing of the middle branch of the Man9GlcNac2 structure by EDEM2 (George et al., 2020), followed by the trimming of additional terminal mannose residues by EDEM1 and EDEM2 (Figure 3.9) (George et al., 2021). These steps generate a Man5-7GlcNac2 glycan structure recognized by the lectin OS9 or its functional homologs to direct glycoproteins for ERAD. It is possible that saturation of one or more of the factors relevant to HLA class I ERAD impedes subsequent glycan processing in the ER, allowing the escape of misfolded molecules via the secretory pathway.

In the HLA class I assembly pathway, calreticulin is a component of the peptide loading complex, which includes tapasin, ERp57, and TAP. (Blees et al., 2017; Ortmann et al., 1997) Tapasin preferentially binds the peptide-free conformation of HLA class I molecules (Jiang et al., 2022; Muller et al., 2022; Rizvi & Raghavan, 2006). The calreticulin/calnexin cycle is suggested to ensure the proper folding of HLA class I proteins by retrieving unfolded HLA class I from the ERGIC to the ER (Howe et al., 2009). The retrieval mechanism is thought to be facilitated by UGGT1, which reglucosylates the improperly folded HLA class I (Wearsch et al., 2011; Zhang et al., 2011). Recent studies also indicate a role for TAPBPR in UGGT1 activity towards HLA class I reglucosylation (Sagert et al., 2023). Like tapasin, TAPBPR prefers peptide-free conformers of

HLA class I molecules (Jiang et al., 2017; Muller et al., 2022). Thus, multiple specific and generic players can function alone and in combination in the retention and/or retrieval of peptide-deficient HLA class I proteins.

HLA class I assembly impairments due to the absence of peptide (TAP deficiency) or the inability to efficiently capture peptides (tapasin deficiency) are expected to cause misfolded HLA class I molecules to accumulate in the ER. Under these conditions, components of the PLC, the PLC as a whole, or factors such as TAPBPR and UGGT1, or components of the ERAD machinery, may become overwhelmed, enabling the partial escape of non-native HLA class I molecules to the Golgi, in the absence of the normal sequence of glycan processing events that precede such trafficking. In turn, this would impair the normal pathway of glycan maturation in the Golgi, resulting in the production of HLA class I molecules bearing incompletely processed glycans. Glycomic analyses by mass spectrometry of cell surface HLA class I glycans in TAP and tapasin-deficient cells are expected to provide further insights into the nature of the glycan maturation defects driving the expression of high mannose glycans on surface HLA class I molecules under these conditions.

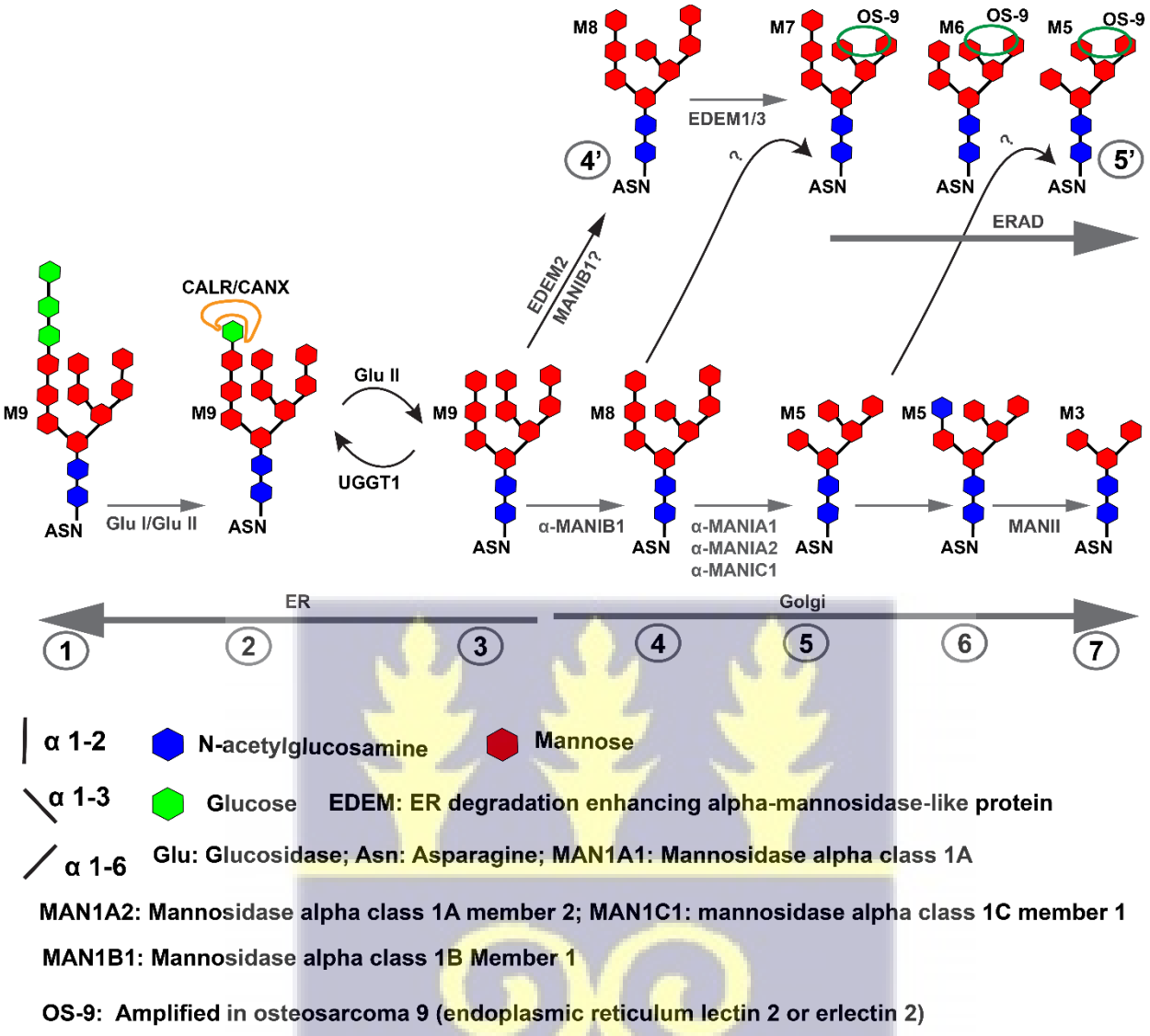

Figure 3.9 Model: Saturated quality control and canonical secretory trafficking underlie HLA class I cell surface expression and aberrant glycosylation in TAP-deficient cells. In normal conditions, an efficient ER/Golgi quality control mechanism ensures the proper folding and maturation of N-glycans on HLA class I exported to the plasma membrane. 1) Precursor N-glycan (Glc3Man9GlcNAc2) is appended on Asn86 (ASN) on nascent HLA class I protein (not shown). 2) Glucosidase I cleaves one glucose molecule from the precursor glycan, generating Glu2Man9GlcNAc2 (not shown). Glu2Man9GlcNAc2 is converted to Gluc1Man9NAc2, a monoglucosylated glycan, through hydrolytic cleavage of the second glucose residue by glucosidase II. Calreticulin (CALR)) binds the monoglucosylated HLA class I as a component of a complex with tapasin and ERp57 and TAP (the peptide loading complex (PLC) not shown) to

promote HLA class I folding and peptide loading. 3) Peptide binding induces deglucosylation of the glycan by glucosidase II. 4-7) Well-folded, deglucosylated HLA class I molecules undergo sequential mannose trimming by Golgi mannosidases to form Man3GluNAc2 (7), which are further modified into complex glycans and exported to the plasma membrane. Various intermediate glycans with 3-7 mannose residues are shown. Alternatively, UGGT1 reglucosylates HLA class I molecules that are not in their native form. This process is facilitated by tapasin-related binding protein TAPBPR (not shown). The HLA class I can undergo multiple rounds of folding by the calreticulin cycle, deglucosylation by glucosidase II, and reglucosylation by UGGT-1. 4) 4' and 5') After many rounds of CALR binding and folding attempts, deglucosylated HLA class I that remain non-native are disposed of in the cytosol through the endoplasmic reticulum-associated degradation (ERAD). Based on current models, EDEM2 trims unfolded deglucosylated Man9GluNAc2 into Man8GluNAc2, which EDEM1 and EDEM3 further convert into glycoforms that can be bound by OS-9 and degraded through ERAD. Under TAP or tapasin deficiency, an essential component of this unfolded HLA class I quality control mechanism is expected to become saturated, resulting in the accumulation of HLA class I with immature, Endo-H sensitive glycans in the ER. To maintain ER homeostasis, these HLA class I molecules escape the ER, transit to the Golgi, and are exported to the plasma membrane. This figure was created with Adobe Illustrator.

3.5 Supplementary figures

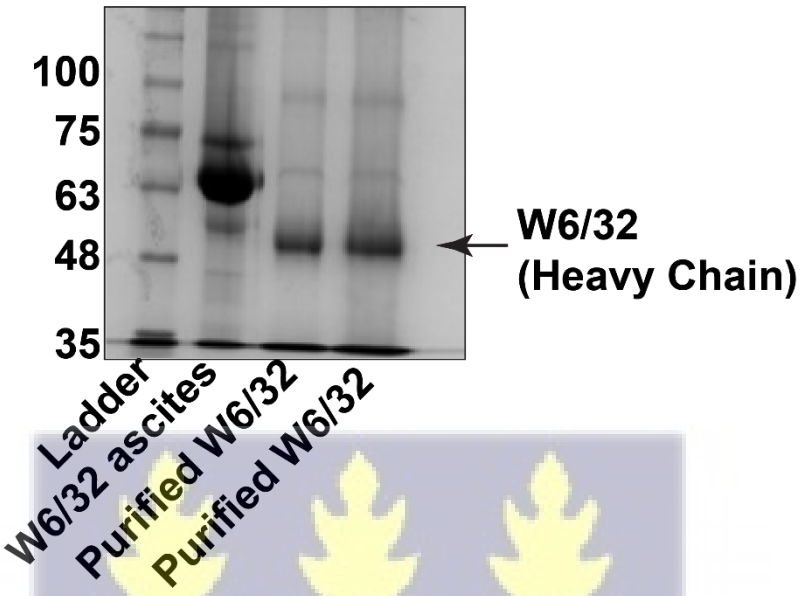

Supplementary Figure 3.1: Confirmation of purified W6/32 purity and integrity by Coomassie brilliant blue stained SDS-PAGE gel.

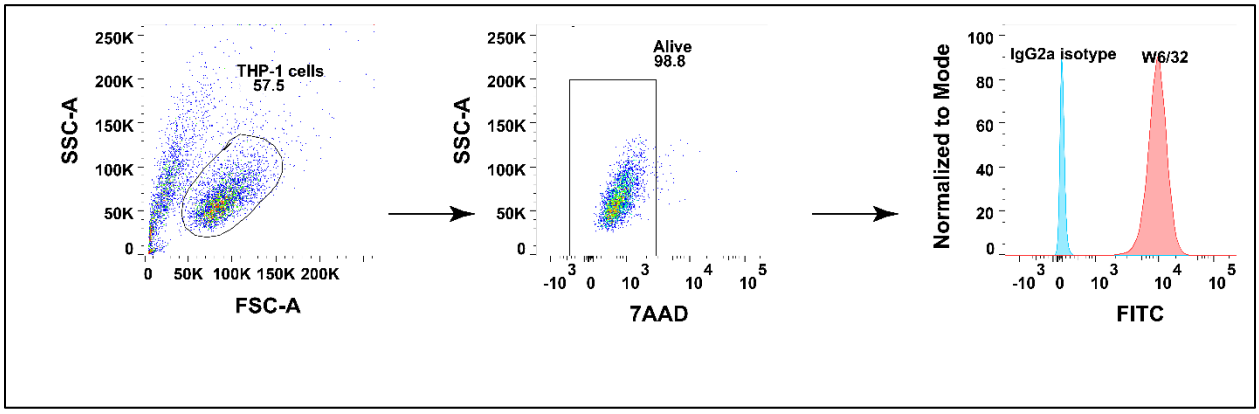

Supplementary Figure 3.2: Flow cytometric gating strategy for measuring surface HLA class I. Cells were gated based on their forward (FSC) and side (SSC) scattering. 7-AAD-negative cells were gated as viable (live) cells. W6/32-FITC mean fluorescent intensity of viable cells represents surface HLA class I expression.

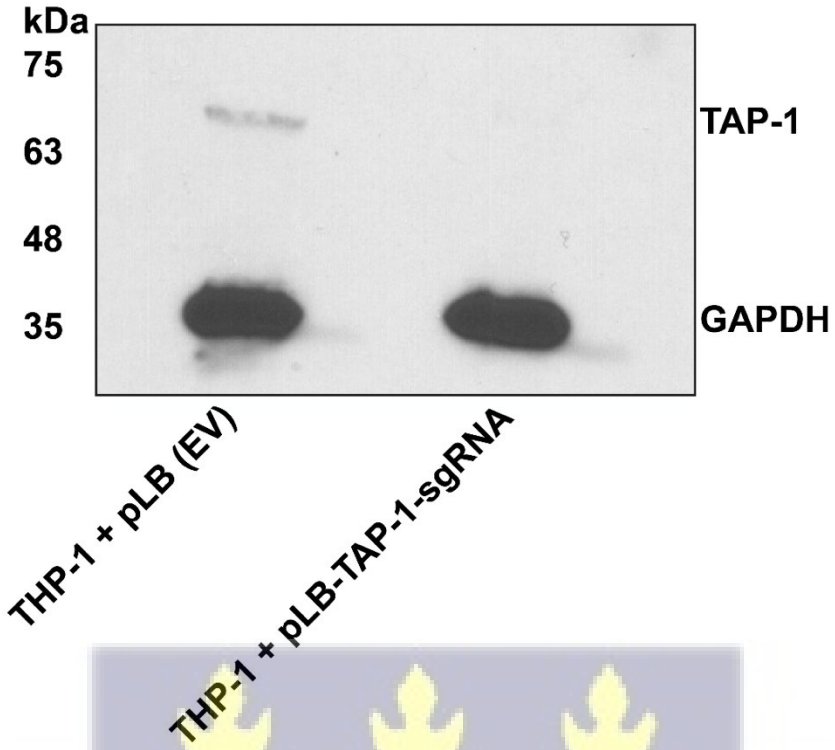

Supplementary Figure 3.3: Immunoblot showing TAP-1 knockout in THP-1 cells. THP-1 cells were transduced with an empty lentivirus CRISPR vector expressing blasticidin resistance (pLB) or a lentivirus CRISPR vector with TAP-1 sgRNA (pLB-TAP-1-sgRNA). The cells were cultured in RPMI (ATCC modified) supplemented with blasticidin (5µg/mL) for 30 days to select successfully transduced cells. Lysates were prepared from the cells and subjected to SDS PAGE and immunoblot with anti-TAP-1 (148.3) and anti-GAPDH antibodies.

CHAPTER FOUR

Manuscript 2: Multiple Alpha-1,2 Mannosidases Regulate HLA Class I Cell Surface Expression

4.0 Abstract

Human leukocyte antigen (HLA) class I molecules mediate immunity against infections and cancers by presenting antigens to cytotoxic T lymphocytes (CTLs) and regulating the activities of natural killer (NK) cells. Many pathogens and cancers exploit pathways that induce HLA class I degradation to evade CTL and NK cell responses. Mannose trimming during ER-Golgi trafficking of glycoproteins is a key step for targeting misfolded proteins for degradation via ER-associated degradation (ERAD). Several ER and Golgi alpha-1,2 mannosidases participate in glycoprotein mannose trimming via specific and redundant pathways. Roles for endoplasmic reticulum degradation-enhancing α-mannosidase-like protein 1 and EDEM2 in HLA class I ERAD-mediated degradation have been described previously, but the roles of other alpha-1,2 mannosidases in HLA class I expression regulation have not been defined. Using a CRISPR-Cas9-based approach in the monocyte cell line THP-1, we show that the depletion of not only EDEM1 and EDEM3 but also mannosyl-oligosaccharide 1,2-alpha-mannosidase IA (MAN1A1) and MAN1B1 increases the surface expression of HLA class I. In contrast, EDEM2 depletion reduces the HLA class I surface expression. A deficiency in the transporter associated with antigen processing (TAP), a key HLA class I assembly factor, does not induce the expression of any alpha-1,2 mannosidase. However, the mannosidases are differentially expressed in many tumors in The Cancer Genomic Atlas (TCGA) and are significantly associated with survival outcomes. Taken together, the findings of this study indicate that multiple alpha-1,2 mannosidase activities regulate the cell surface

expression of HLA class I and that mannosidase expression is potentially exploited by cancers for immune evasion.

4.1 Background

Glycosylation is a post-translational protein modification that plays a crucial role in the quality control, trafficking, and functions of glycoproteins (Adams et al., 2021; Aebi, 2013; Bieberich, 2014; Stanley et al., 2022). N-glycosylation, the addition of glycans to specific asparagine residues in the recipient protein, begins in the endoplasmic reticulum (ER) with an *en bloc* transfer of the precursor glycan (Glu3Man9GluNac2) from dolichol pyrophosphate, a lipid anchor, to nascent proteins destined to be glycoproteins (Stanley et al., 2022). This initial step of the N-glycosylation process is catalyzed by oligosaccharyltransferase (OST) and the precursor glycan is specifically transferred to an asparagine residue within a specific tripartite amino acid sequence, Asn-X-Ser/Thr (referred to as "sequon"), in the nascent protein, where Asn, X, Ser and Thr are asparagine, any amino acid, serine, and threonine residues respectively (Bieberich, 2014; Stanley et al., 2022). Upon the linkage of the precursor glycans to the sequons, the glycans are sequentially trimmed by glucosidases and ER/Golgi mannosidases, resulting in transient high mannose glycoproteins that are sensitive to digestion by Endoglycosidase H (Endo-H). Subsequently, the glycans are further modified into complex Endo-H-resistant glycans (Bieberich, 2014; Stanley et al., 2022).

The glycoprofiles of glycoproteins dictate their fate in the ER and the Golgi compartments, as glycans serve as folding sensors, promoting either the anterograde transport of well-folded proteins from the ER to the Golgi (Bieberich, 2014) or the degradation of unfolded proteins through the ER-associated degradation (ERAD) pathway (Roth & Zuber, 2017). Recent studies have demonstrated that glycans also influence the functional states of glycoproteins, including

antibodies (Cobb, 2020; Gaifem et al., 2024; Haslund-Gourley et al., 2024; Plomp et al., 2017; Trzos et al., 2023), highlighting the emerging significance of the glycosylation status of glycoproteins in immune response pathways.

The major histocompatibility complex (MHC) class I protein, also known as human leukocyte antigen (HLA) class I in humans, is a glycoprotein that plays a crucial role in the adaptive immune system by presenting antigens to cytotoxic T lymphocytes (CTL) and regulating the activities of natural killer (NK) cells. Structurally, HLA class I is a heterotrimer comprised of a heavy chain (α chain), a light chain (β_2 microglobulin [β_2M]), and a short peptide. The heavy chain consists of three distinct domains referred to as α1, α2, and α3. Together, the α1 and α2 domains form a groove that accommodates the short peptide (Bjorkman et al., 1987). Notably, the α1 domain contains a highly conserved N-glycan binding motif at the 86th asparagine amino acid residue (N86), where a precursor high mannose N-glycan, Glu3Man9GluNAc2, is appended in the endoplasmic reticulum (ER). Like other N-glycan-bearing glycoproteins (Bieberich, 2014; Stanley et al., 2022), high mannose N-glycan on HLA class I is trimmed by exomannosidases in the ER and the Golgi, and modified into complex glycans by additional enzymes before HLA class I is transported to the plasma membrane. Because HLA class I molecules play a crucial role in the immune system, it is often downregulated from the cell surface by cancers and infectious pathogens (Petersen et al., 2003; Taylor & Balko, 2022).

Global pharmacological inhibition of ER and Golgi mannosidases by the drug kifunensine which is an inhibitor of 1,2-alpha-mannosidase activity (Elbein et al., 1990) increases surface HLA class I expression and phenocopies the endoglycosidase-sensitive glycan profile on surface HLA class I of cells deficient in key assembly factors such as TAP or tapasin. (Chapter 3 of this thesis). These findings reinforce the involvement of 1,2-alpha-mannosidases in the quality control of HLA class

I trafficking and the acquisition of mature glycans by HLA class I molecules. A previous study has implicated ER degradation-enhancing alpha-mannosidase-like 1 proteins (EDEM1 and EDEM2) in targeting misfolded HLA class I for degradation via ERAD (Burr et al., 2013; Timms et al., 2016). However, the specific roles of the other ER and Golgi 1,2-alpha-mannosidases, including EDEM3, and MAN1B1, mannosyl-oligosaccharide 1,2-alpha-mannosidase IA (MAN1A1), mannosyl-oligosaccharide 1,2-alpha-mannosidase IA member 2 (MAN1A2), and mannosidase alpha class 1C member 1 (MAN1C1) in HLA class I assembly or quality control have not been elucidated thus far. Understanding the role of these enzymes in the quality control of HLA class I trafficking could provide new insights into the regulation of antigen-bearing HLA class I proteins on the cell surface and inform novel immunotherapeutics against cancers and infectious diseases.

HLA class I molecules generally use the conventional ER-Golgi secretory route to the cell surface and bear complex (mature) Endoglycosidase H-resistant glycans on the plasma membrane. However, under certain pathological conditions, such as those that induce deficiencies in TAP or tapasin ((Geng et al., 2018) and Chapter 3 of this thesis), which are key assembly factors for HLA class I molecules, glycan processing becomes impaired and HLA class I molecules become expressed on the cell surface with Endoglycosidase H-sensitive glycans, despite trafficking via the Golgi (Chapter 3 of this thesis). These findings point to important connections between HLA class I misfolding and cell surface glycan signatures that involve altered mannose processing. Further elucidation of the specific 1,2-alpha-mannosidase activities that are relevant to HLA class I assembly is thus also important towards a better understanding of how glycosylation becomes altered under conditions that induce protein misfolding. While some of the 1,2-alpha-mannosidases have redundant roles in glycan processing, there are known specificities at the substrate level (Tu et al., 2017; Wei et al., 2023). Elucidating such specificities in the HLA class I

assembly/degradation context is significant. Since many pathogens and cancers exploit constitutive pathways for enhancing the degradation of HLA class I, further elucidating such specificities in the HLA class I assembly/degradation context is significant

4.2.0 Methods

4.2.1 Cell culture

THP-1 cells (TIB-202) were purchased from the American Type Culture Collection (ATCC) and maintained in RPMI 1640 (ATCC modification, catalog number: A1049101) supplemented with 10% (v/v) fetal bovine serum (FBS), 2 mM L-glutamine, and 1X antibiotic/antimycotic. Modified human embryonic kidney cells expressing the simian virus 40 (SV40) large T antigen (HEK239T) were maintained in Dulbecco's Modified Eagle Medium (DMEM). The DMEM was supplemented with 10% (v/v) FBS and 1X antibiotic/antimycotic. The cells were cultured in 5% CO_2 at 37ºC.

4.2.2.0 CRISPR-Cas9-mediated gene editing

4.2.2.1 Single RNA cloning into lentiCRISPR-Cas9 vector

CRISPR-Cas9 single guide RNA (sgRNA) for EDEM1, EDEM2, EDEM3, MAN1A1, MAN1B1, and MAN1C1 were identified using the open-source sgRNA design tool CHOCHOP (https://chopchop.cbu.uib.no/) (black ink nucleotides in Table 1). The sgRNA were selected based on high efficiency, absence of mismatch (theoretically zero off-target effect), and self-complementarity. The sgRNAs were modified (red ink nucleotides in Table 1), purchased from Integrated DNA Technology (IDT), and separately cloned into *BsmBI* site in the lentiCRISPRv2 vector (Addgene, 52961). Briefly, 1 µL each of the 100 µM forward and reverse oligonucleotides (oligos) were mixed with 6.5 µL nuclease-free water, 1 µL 10X T4 ligation buffer (NEB) and 0.5

µL T4 polynucleotide kinase (NEB). The oligos were phosphorylated and denatured at 37 ºC for 30 minutes and 95 °C for 5 minutes, respectively, and allowed to cool on ice water for 1 minute. 4 µL of the oligo mix was diluted to 1 mL (1:250) with nuclease-free water. 100 ng lentiCRISPRv2 was combined with 2 µL diluted oligos, 2 µL 10X FastDigest buffer (Thermo Fisher Scientific), 1 mM DTT, 1 mM ATP, 1 µL FastDigest *BsmBI*, 0.5 µL T4 ligase and made up to 20 µL with nuclease-free water. The digestion-ligation step was performed using six incubation cycles at 37 °C for 5 minutes and 23 °C for 5 minutes in a thermocycler (Agilent Technologies SureCycler 8800). The ligation mix was held at 4 °C until further use.

For transformation, 50 µL STBL3 competent cells pre-chilled on ice were incubated with 1 – 2 µL of the ligation mix on ice for 30 minutes. The cells were transferred to a water bath at 42 ºC for 45 seconds and placed on ice for 2 minutes. To recover from the heat shock, 0.5 mL of super optimal broth was added to the cells, and they were incubated at 37 ºC for 1 hour, with constant agitation. After this, the cells were spun at 5,000 rpm for 2 minutes, and about 80% of the supernatant was removed. The cells were resuspended in the remaining media and plated on Luria Bertani (LB) agar supplemented with ampicillin (100 µg/mL) and grown overnight at 37ºC. Using a sterile plastic loop, a discrete colony was selected and grown in ampicillin-supplemented LB broth overnight. The plasmid was isolated using the Promega Wizard® *Plus* SV Minipreps DNA Purification kits and assessed for purity and concentration using NanoDrop spectrophotometer (Thermo Fisher Scientific).

To determine whether the cloning was successful, the plasmids were subjected to Sanger sequencing using the human U6 forward primer (5'-GAGGGCCTATTTCCCATGATT-3'). LentiCRISPRv2 vectors with successfully cloned sgRNAs are presented in Supplementary Figure 4.1.

Table 4.1: Single guide RNAs (sgRNAs) used for CRISPR-Cas9-based gene editing for ER and Golgi mannosidases.

Gene	sgRNA sequence (5'- 3')
EDEM1	F: CACCGGAGTACGAGAAGCGCTACAG R: AAACCTGTAGCGCTTCTCGTACTCC
EDEM2	F: CACCGTGACCCGGTGTTCGAAGATG R: AAACCATCTTCGAACACCGGGTCAC
EDEM3	F: CACCGTCATCAACGTCACCGCGACT R: AAACAGTCGCGGTGACGTTGATGAC
MAN1A1	F: CACCGTTAGTCCGCTGCTAGACTTG R: AAACCAAGTCTAGCAGCGGACTAAC
MAN1B1	F: CACCGCGTCGATCAGTGTGAGACCG R: AAACCGGTCTCACACTGATCGACGC

F: Forward sequence; R: Complementary reverse sequence.

Nucleotides in red are BsmBI/Esp3I restriction site overhang

4.2.2.2 Preparation of lentivirus and infection of THP-1 cells

HEK293T (0.5 x 10^6 cells) were seeded into 6-well plates a day before transfections to achieve about 70% confluency. For transfections, solution A with 1.7 µg, 1.1 µg, and 2.25 µg of psPAX2 (Addgene; 12260), pMD2.G (Addgene; 12259), and transfer plasmid (pLentiCRISPRv2 empty vector or pLentiCRISPRv2 containing appropriate sgRNA), respectively, in 130 µL OptiMEM and 5µl lipofectamine plus reagent (Invitrogen). The solution was mixed and incubated undisturbed

for 5 minutes at room temperature (RT). Solution B was prepared by diluting 15 µL lipofectamine LTX (Invitrogen) in 130 µL OptiMEM for each transfection and incubating for 5 minutes. Solutions A and B were combined, incubated for 20 minutes at RT, and added dropwise to HEK293T cells in a 2 mL fresh antibiotic/antimycotic-free DMEM containing 10% FBS. The plates were gently swirled, and the cells were cultured for 48 hours at 37ºC.

After 48 hours, the virus released into the culture medium was harvested, filtered through a 0.45 µm syringe filter, and used to infect THP-1 cells. About 0.5 x 10^6 THP-1 cells were infected with ~2 mL viral supernatant collected from one well of HEK293T cells. Infection was done in 24-well plates, and an uninfected control consisting of THP-1 cells incubated with an equivalent volume of culture media instead of viral supernatant was included. Cells were incubated with virus for 15 – 20 minutes at RT after adding 1X Polybrene (8 µg/mL from a 1000X stock) and spinfected at 2500 rpm for 2 hours at RT. After the centrifugation, about 600 µL of the viral supernatant was replaced with fresh culture medium, and the cells were incubated for 24 hours, following which the virus-containing medium was completely replaced with fresh medium. Cells were rested for 24 h before selecting the transduced cells using 300 µg/mL of hygromycin B for 4-5 weeks.

4.2.3 Reverse transcriptase quantitative polymerase chain reaction (RT-qPCR)

Total RNA was isolated from wild-type THP-1 or THP-1 cells transduced with TAP-1, EDEM1, EDEM2, EDEM3, MAN1A1, or MAN1B1 sgRNA using RNeasy kit (Qiagen), following the manufacturer's instructions. The concentration and purity of the RNA were assessed using a NanoDrop spectrophotometer (Thermo Fisher Scientific). RNA with an A260/A230 ratio between 2.0 and 2.2 was considered pure. Complementary DNA was synthesized from the RNA using the SuperScript III First-Strand Synthesis kit (Invitrogen), following the manufacturer's instructions.

A standard 2-hour qPCR was performed using ABI 7500 Fast real-time PCR machine and Applied Biosystems SYBR Green Master Mix (Catalogue number: 4309155; Invitrogen), following the manufacturers' instructions. *GAPDH*, *HPRT1*, and *ACTB* were included as housekeeping genes, and the ΔΔCT mode was used to determine relative fold change in the expression of genes being assessed. The qPCR primers used to quantify EDEM1, EDEM2, and EDEM3, as well as MAN1A1 and MAN1B1 transcripts (Table 4.2), have been previously reported (Jin et al., 2018; Tang et al., 2014).

Table 4.2: qPCR primers used for inferring ER and Golgi mannosidases' genes knockdown.

Gene	qPCR primers (5'- 3')
EDEM1	FP: AAACGATATGGTGCCCTCCCTG
	RP: CGTGATGCAGCGTGGCGTAC
EDEM2	FP: CTGGACACCTTGCTGATTTTGG
	RP: TACTTCCACCCCAGCCTTCTTG
EDEM3	FP: AGTGGAGTTGGAGCAGGGATTG
	RP: GCATTCAGCATTGGTTTGTGGA
MAN1A1	FP: GCAGTGGAACTTGGGGTAAA
	RP: TTCAGCAAAGATGGGGTTTC
MAN1B1	FP: GCCTTTCTGCTTTTCTGTGG
	RP: GACTGTCCTCTGCGGATCTC

FP: Forward primer. RP: Reverse primer.

4.2.4 Flow cytometry

To measure HLA class I molecules on the plasma membrane, 50,000 – 100,000 THP-1 cells were seeded in a 96-well plate and washed twice with ice-cold 1X PBS at 2500 rpm for 1 minute. Staining solution was prepared by diluting fluorescein isothiocyanate (FITC)-conjugated W6/32 antibody (a pan HLA class I antibody, W6/32-FITC) in a staining buffer containing 2% fetal bovine serum (FBS) in 1X phosphate buffer saline (PBS). Staining was performed on ice for 30 minutes and the cells were washed twice with ice-cold staining buffer by centrifugation at 2500 rpm for 1 minute. The cells were then resuspended in a staining buffer containing 7-aminoactinomycin D (7-AAD) before performing the flow cytometry on a BD LSRFortessa cell analyzer. The flow cytometry standard files (FCS) were exported to and analyzed using FlowJo.

4.3.0 Results

4.3.1 EDEM1, EDEM2, and EDEM3 play differential roles in the quality control of HLA class I in THP-1 cells

EDEMs have been implicated in extracting misfolded proteins from the ER for degradation through ERAD (Olivari & Molinari, 2007). EDEM1 and EDEM2 interact with hydrophobic regions on aberrantly folded proteins, directing the proteins to ERAD (Shenkman et al., 2018; Sokolowska et al., 2015). Mannosidase functions of specific EDEMs have also been described (George et al., 2021; George et al., 2020; Shenkman et al., 2018; Ninagawa et al., 2014), with EDEM2 performing the hydrolytic cleavage of a terminal mannose from Man9GlcNAc2 to generate Man8GlcNAc2, which serves as a substrate for other mannosidases acting downstream (George et al., 2020; Ninagawa et al., 2014). EDEM2 activity depends on its covalent interaction with thioredoxin domain-containing protein 11 (TXNDC11) in the ER (George et al., 2020). In HLA class I-specific context, EDEM1 and EDEM2 have been reported to regulate the surface expression (Burr et al., 2013; Timms et al., 2016); however, the role of EDEM3 has not been defined.

To investigate the possible role of EDEMs in the quality control of HLA class I, we performed a CRISPR-Cas9-mediated knockdown of *EDEM1, EDEM2,* and *EDEM3*. Specific guide RNA for each gene was cloned into a lentivirus CRISPR-Cas9 vector, as described in the methods. After confirming the cloning by Sanger sequencing (Supplementary Figure 4.1), THP-1 cells were transduced with the vectors to achieve knockdown. *EDEM1, EDEM2*, or *EDEM3* transcript depletion was deduced by RT-qPCR (Figures 4.1A, C, and E), and HLA class I expression on the plasma membrane was measured by flow cytometry to gain insight into the influence of each

EDEM on HLA class I trafficking. We observed an increase in the surface expression of HLA class I in EDEM1 (Figure 4.1B) and EDEM3 (Figure 4.1F)-depleted THP-1 cells relative to the wild-type. In contrast, depletion of EDEM2 downmodulates surface HLA class I expression (Figure 4.1D), suggesting that rather than extracting HLA class I from the ER for degradation, EDEM2 may be involved in promoting the secretory trafficking of HLA class I. Although the increase in HLA class I surface expression driven by EDEM1 depletion did not attain a statistically significant level, these results support a model that EDEM1 and 3 extract misfolded HLA class I for degradation but EDEM2 promotes productive trafficking of these proteins.

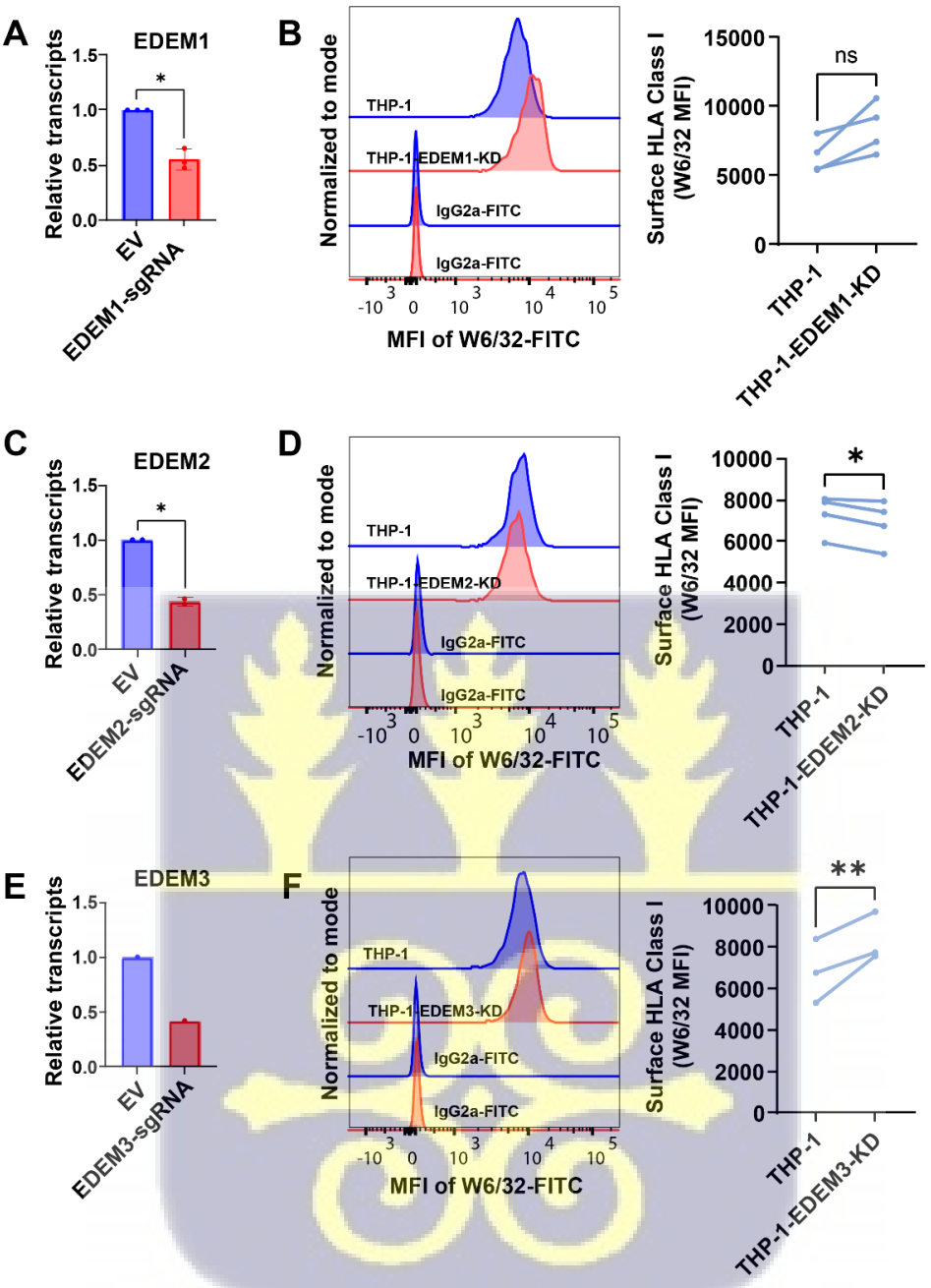

Figure 4.1. Role for ER Mannosidases in HLA class I quality control. A, C, and E) Confirmation of EDEM1 (A), EDEM2 (C), and EDEM3 (E) depletion by RT-qPCR. Relative expression was normalized to GAPDH, HPRT1, and beta-actin. B, D, and F) Surface HLA class I

levels of EDEM1-, EDEM2-, or EDEM3-depleted THP-1 cells measured by flow cytometry after staining the cells with W6/32-FITC. Representative histograms (left) and averaged data across 3-4 experiments (right) are shown. Paired *t*-test was used for pair-wise comparisons. ns = p value > 0.05, * = p value ≤ 0.05, ** = p value < 0.01.

4.3.2 MAN1A1 or MAN1B1 knockdown increases HLA class I cell surface expression

MAN1B1 localizes to the ER and the Golgi and performs a quality control function on misfolded proteins (Iannotti et al., 2014). MAN1B1 in the ER marks misfolded glycoproteins for ERAD-dependent degradation by catalyzing the hydrolytic cleavage of the terminal mannose residue on the middle branch of the high mannose N-glycan (Man9GlcNAc2) on the proteins (Rymen et al., 2013; Sakhi et al., 2021). In the Golgi, MAN1B1 associates with the gamma subunit of coat protein complex I (COPI) and helps in retrieving back to the ER aberrantly folded glycoproteins that had escaped ER quality control mechanisms (Pan et al., 2013). The retrieved glycoproteins are channeled for degradation through ERAD. This retrograde quality control by MAN1B1 is functionally independent of its mannosidase or catalytic activities (A. H. Sun et al., 2020). MAN1A1 is a Golgi exomannosidase that participates in trimming mannose residues from high mannose N-glycans, providing intermediate glycoforms for conversion to complex glycans in the Golgi (Oliveira-Ferrer et al., 2017).

To evaluate the involvement of MAN1A1 and MAN1B1 in the quality control and trafficking of HLA class I proteins, *MAN1A1* or *MAN1B1*was genetically knocked down by CRISPR-Cas9 approach using specific single guide RNA (Supplementary Figure 4.1). MAN1A1 and MAN1B1 depletion were inferred by RT-qPCR (Figures 4.2A and C), and surface HLA class I expression on

the cells was measured by flow cytometry (Figures 4.2B and D). We observed an increase in HLA class I on the plasma membrane of THP-1 cells with MAN1A1 knockdown compared to the wild-type (Figure 4.2B). Similarly, MAN1B1 depletion increased the surface HLA class on THP-1 cells (Figure 4.2D), indicating that MAN1A1 and MAN1B1 are involved in the quality control of HLA class I trafficking. Our attempts to knock down MAN1A2 and MAN1C1 were not successful, so we were unable to assess their influence on HLA class I quality control and trafficking.

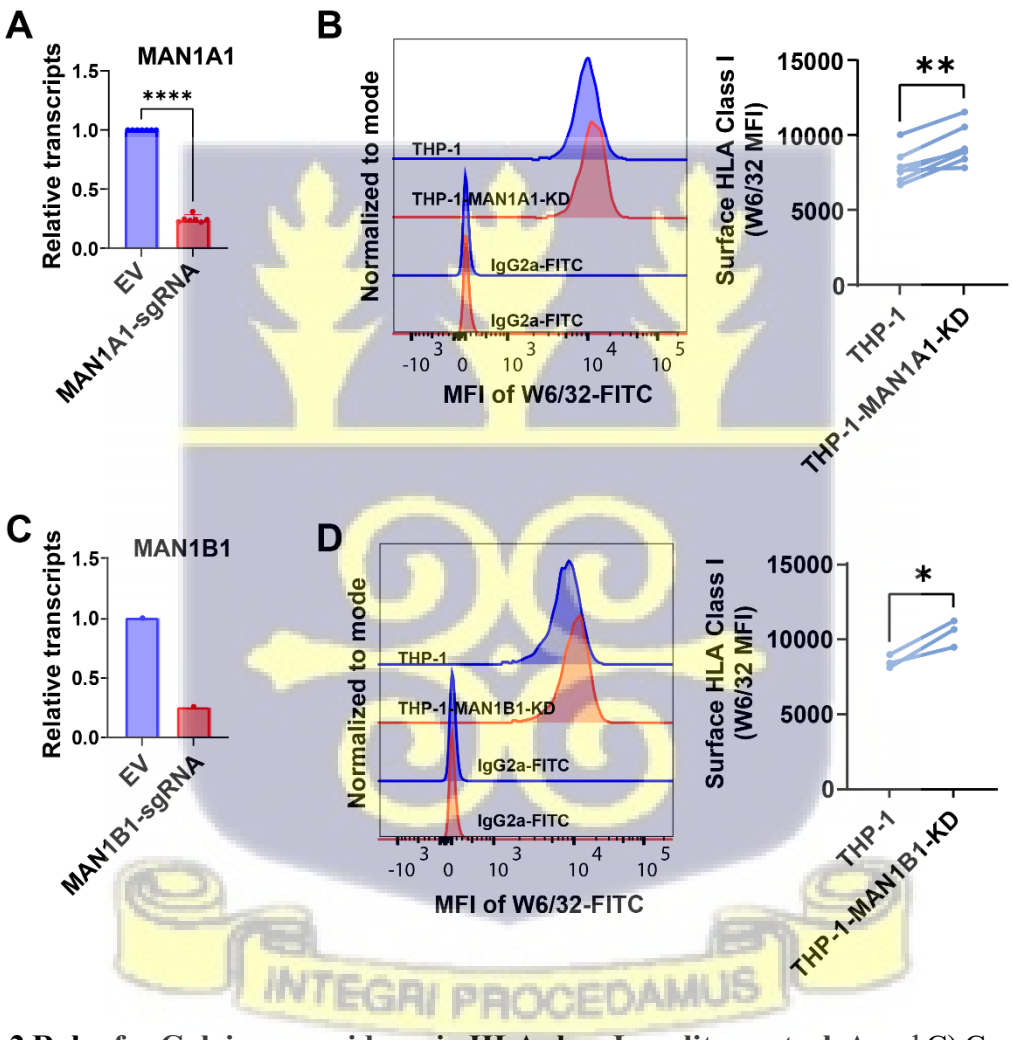

Figure 4.2 Roles for Golgi mannosidases in HLA class I quality control. A and C) Confirmation of MAN1A1 (A) and MAN1B1 (C) depletion by RT-qPCR. Relative expression was normalized to *GAPDH*, *HPRT1*, and *ACTB* (*beta-actin)*. B and D) Surface HLA class I of MAN1A1 (B)- or

MAN1B1 (D)-depleted THP-1 cells measured by flow cytometry after staining the cells with W6/32-FITC. Representative histograms (left) and averaged data from 3-7 experiments (right) are shown. Paired *t*-test was used for pair-wise comparisons. * = p value ≤ 0.05, ** = p value < 0.01.

4.3.3 Expression of mannosidases is not significantly altered in TAP-1-KO cells

We next assessed the expression levels of the genes encoding mannosidase enzymes in wild-type and TAP-deficient human monocyte cell line, THP-1, using RT-qPCR. TAP is a transmembrane protein and a member of the ATP-binding cassette (Deverson et al., 1990). TAP transports peptides from the cytosol to the ER where the peptides are assembled on HLA class I molecules (Lehnert & Tampe, 2017). TAP deficiency deprives the ER of peptides, compromises the optimal assembly of HLA class I with peptides, promotes misfolding and retention of HLA class I in the ER, and reduces HLA class I cell surface expression (de la Salle et al., 1999; Ljunggren et al., 1990; Mantel et al., 2022; Raposo et al., 1995). Hence, TAP-deficient THP-1 cells provide a suitable model for assessing possible changes in the expression profiles of mannosidases under conditions that increase the burden of misfolded HLA class I in the ER. Bulk RNA was isolated from THP-1 and THP-1-TAP-1-KO cells and complementary DNA (cDNA) was synthesized from the RNA. RT-qPCR was performed on the cDNA using specific primers for mannosidase genes and the relative fold change of mRNA transcripts was normalized to GAPDH, HPRT1, and ACTB (β-actin). We did not observe any significant changes in the expression of MAN1A1, MAN1A2, MAN1B1, and MAN1C1 in THP-1-TAP-1-KO cells relative to the wild-type cells (Figures 4.3A-D). Although EDEM1, EDEM2, and EDEM3 show trends of increased expression in the THP-1-TAP-1-KO condition, the differences were not statistically significant (Figures 4.3E-G), indicating that

overall, the expression profile of mannosidases is not altered in TAP-1-KO cells even though TAP deficiency induces misfolded HLA class I proteins.

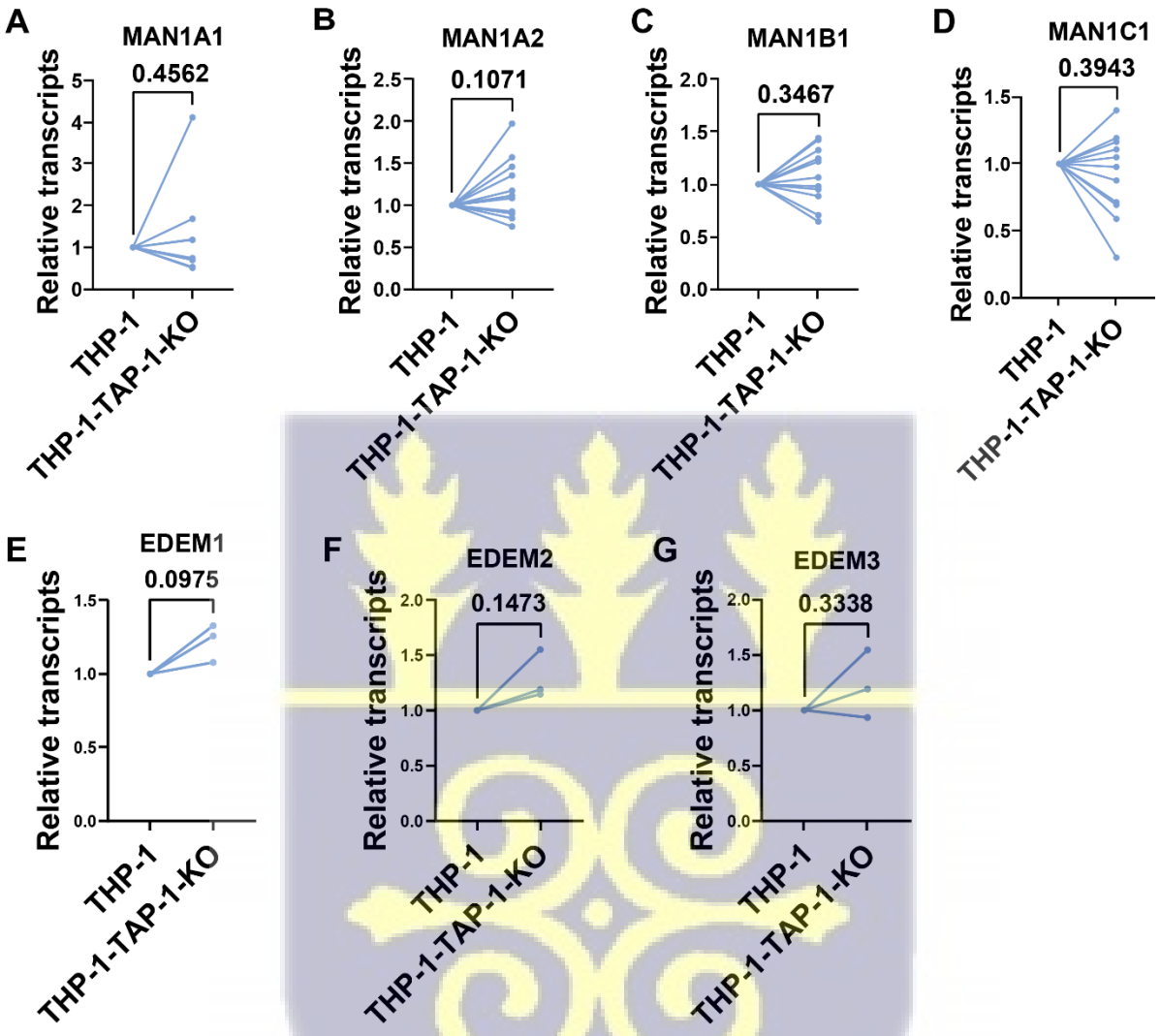

Figure 4.3. Expression of mannosidases is not significantly altered in TAP-1-KO cells. A-D) Relative transcripts of A) MAN1A1, B) MAN1A2, C) MAN1B1, and D) MAN1C1 expression measured by RT-qPCR. Gene expression was normalized to the expression of reference genes: Hypoxanthine phosphoribosyltransferase 1 (HPRT1), Glyceraldehyde 3-phosphate dehydrogenase

(GAPDH) and β-actin, and plotted as fold change relative to the gene expression in THP-1 cells. E-G). Relative expression of EDEM1 (E), EDEM2 (F), and EDEM3 (G), normalized to β-actin.

4.3.4 EDEM1, EDEM2, and EDEM3 are upregulated in most human tumors

To gain further insights into the pathological consequences of alterations in the cellular levels of EDEM1, EDEM2, and EDEM3, we surveyed all human tumors in The Cancer Genome Atlas (TCGA) comparing the expression levels of EDEM1, EDEM2, or EDEM3 in the tumors tissues with paired surrounding normal tissues using the differential gene expression module of the open-source Tumor Immune Estimation Resource (TIMER2.0; http://timer.cistrome.org/) (Li et al., 2020). The differential gene expression module of TIMER2.0 enables users to compare gene expressions between tumors and their adjacent normal tissues across all TCGA tumors (Li et al., 2020). The analysis using TIMER2.0 indicates differential expression of EDEM1, EDEM2, or EDEM3 in many cancer tumors (Figure 4.4), suggesting that many cancers could exploit cellular pathways involving these proteins for survival. EDEM1 is significantly overexpressed in bladder urothelial carcinoma (BLCA), breast invasive carcinoma (BRCA), esophageal carcinoma (ESCA), head and neck squamous cell carcinoma (HNSC), HNSC (human papillomavirus [HPV]positive), kidney renal cell carcinoma (KIRC), skin cutaneous melanoma (SKCM) (metastatic), stomach adenocarcinoma (STAD), and thyroid carcinoma (THCA). However, it is significantly (only mention those significant) downregulated in colon adenocarcinoma (COAD), kidney renal papillary cell carcinoma (KIRP), lung adenocarcinoma (LUAD), lung squamous cell carcinoma (LUSC), rectum adenocarcinoma (READ), and uterine corpus endometrial carcinoma (UCEC) (Figure 4.4A). The expression profile of EDEM2 revealed a significant upregulation in BLCA, BRCA, cervical squamous cell carcinoma (CESC), cholangiocarcinoma (CHOL), COAD, ESCA, Glioblastoma multiforme (GBM), HNSC (HPV positive), KIRP, Liver hepatocellular carcinoma

(LIHC), LUAD, prostate adenocarcinoma (PRAD), READ, SKCM (metastatic), STAD, THCA, and UCEC, but significant downregulation in kidney chromophobe (KICH), LUSC, and pheochromocytoma and paraganglioma (PCPG) (Figure 4.4B). EDEM3 is significantly upregulated in eight tumors, including BRCA, CHOL, HNSC, LIHC, LUAD, PRAD, SKCM (metastatic), and STAD, but significantly downregulated in COAD, KIRP, READ, and THCA (Figure 4.4C).

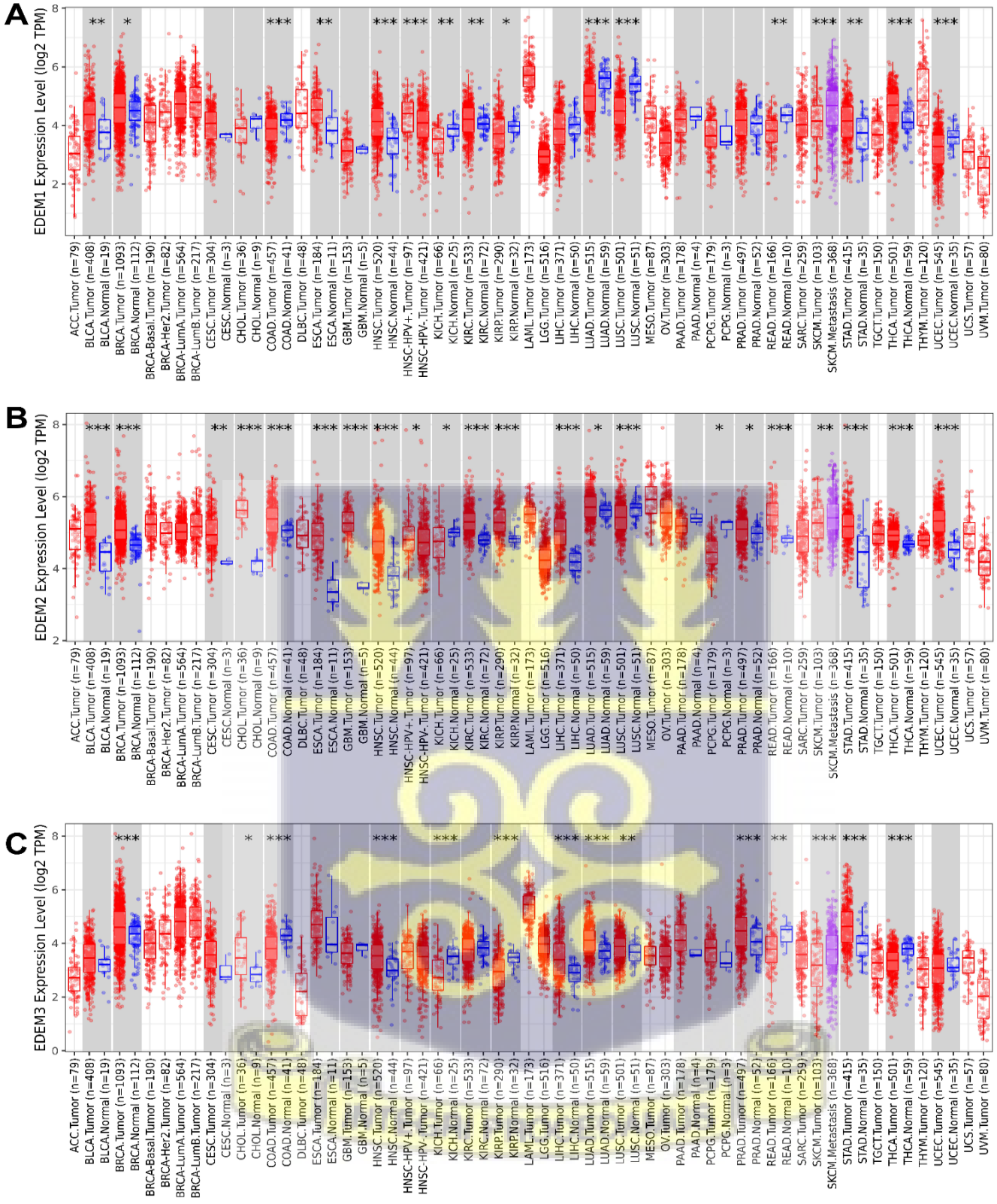

Figure 4.4. Expression of ER mannosidases in cancer. A-C) Differential expression of EDEM1,

EDEM2, and EDEM3 between tumor and adjacent normal tissues across all TCGA tumors using the Gene_DE module of TIMER2.0, an open-source online server. TIMER2.0 computes the statistical significance of gene expression by Wilcoxon test (*: p-value < 0.05; **: p-value <0.01; ***: p-value <0.001).

4.3.5 EDEM1, EDEM2, or EDEM3 differential expression influences the overall survival in some cancers

Next, we evaluated the clinical significance of EDEM1, EDEM2, and EDEM3 by assessing their influence on the overall survival of cancer patients across all tumors in TCGA using Cox proportional hazard model, implemented in the "Gene_Outcome" module of TIMER2.0 (http://timer.cistrome.org/)(Li et al., 2020). The overall survival was adjusted by age, gender, race, clinical stage, and tumor purity, and is displayed as a heatmap (Figure 4.5A). Kaplan Meier (KM) plots for tumors for which the Z scores were statistically significant ($p < 0.05$) were plotted to assess further the clinical relevance of the differential expressions (Figure 4.5B). The KM analysis revealed statistically significant hazard ratios (HR) of 1.57 and 1.47 for higher EDEM1 expression in patients with KIRP and low-grade glioma (LGG) respectively, indicating that EDEM1 overexpression is associated with increased chances of death in these patients by 57 and 47% respectively. Additionally, for patients with KICH and LGG, EDEM2 overexpression is associated with increased fatality risk by 139% and 56% respectively, while in patients with KIRP, higher EDEM3 expression is associated with increased chances of death 63%. Overall, these results suggest that the differential expression of EDEMs, particularly their upregulation, could have clinical relevance in certain cancers.

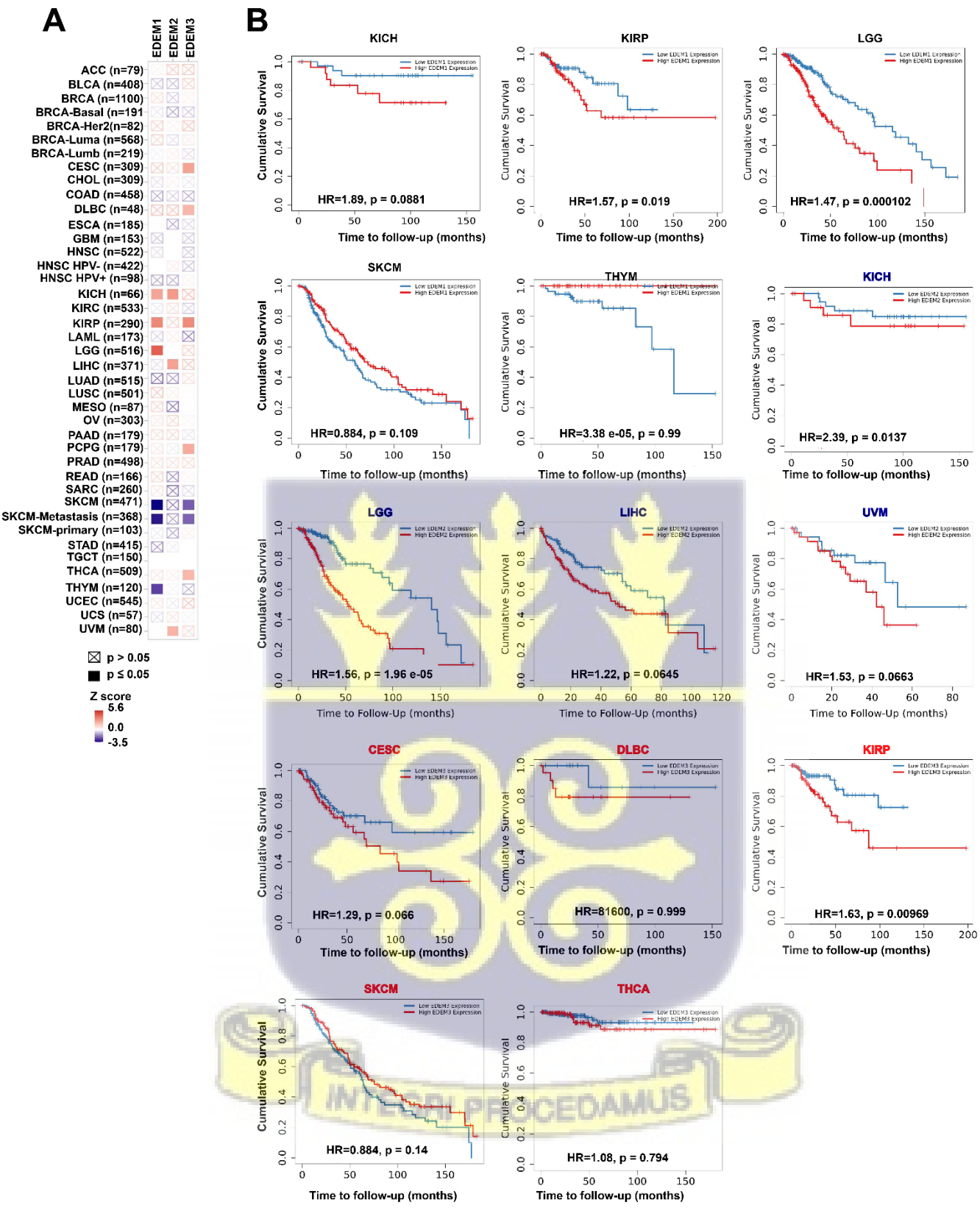

Figure 4.5 Overall survival in some cancers is influenced by differential expression of EDEM1, EDEM2, or EDEM3. A) A heatmap of the clinical relevance of EDEM1, EDEM2, or EDEM3 expression across all cancer tumors in TCGA, adjusted by age, gender, race, clinical stage, and tumor purity. B) Kaplan-Meier curves comparing the survival rates of patients with differential expression of EDEM1 (black titles), EDEM2 (blue titles), and EDEM3 (red titles) in cancers that have significant Z scores (A). For (A) the red block represents increased risk ($p < 0.05$, $z > 0$), the blue block represents decreased risk ($p < 0.05$, $z < 0$), and the grey block represents no significant change in the risk ($p > 0.05$).

4.3.6 MAN1A1 and MAN1B1 are differentially expressed in many cancer tumors relative to normal adjacent tissues

Given the influence of MAN1A1 or MAN1B1 depletion on surface HLA class I proteins, the expression levels of both genes were assessed in cancer tumors in TCGA relative to their adjacent normal tissues using the differential gene expression module of TIMER2.0 (http://timer.cistrome.org/)(Li et al., 2020) (Figure 4.6). Surprisingly, based on their similar effects upon HLA class I expression, MAN1A1 and MAN1B1 have contrasting expression profiles across many cancers, with MAN1A1 frequently downregulated and MAN1B1 upregulated in many tumors (Figures 4.6A and B). MAN1A1 is significantly downregulated in BLCA, BRCA, CHOL, COAD, GBM, KICH, KIRC, KIRP, LIHC, LUAD, LUSC, PCPG, PRAD, READ, THCA, and UVEC, but upregulated in HNSC (HPV positive), SKCM (metastatic), and THYM (Figure 4.6A). Unlike MAN1A1, MAN1B1 is significantly overexpressed in BLCA, BRCA, CHOL, LOAD, ESCA, KIRC, KIRP, LIHC, LUAD, LUSC, PCPG, PRAD, READ, STAD, THCA, and UCEC but

downregulated only in KICH, suggesting that many human tumors may benefit from MAN1B1-dependent HLA class I degradation (Figure 4.6B).

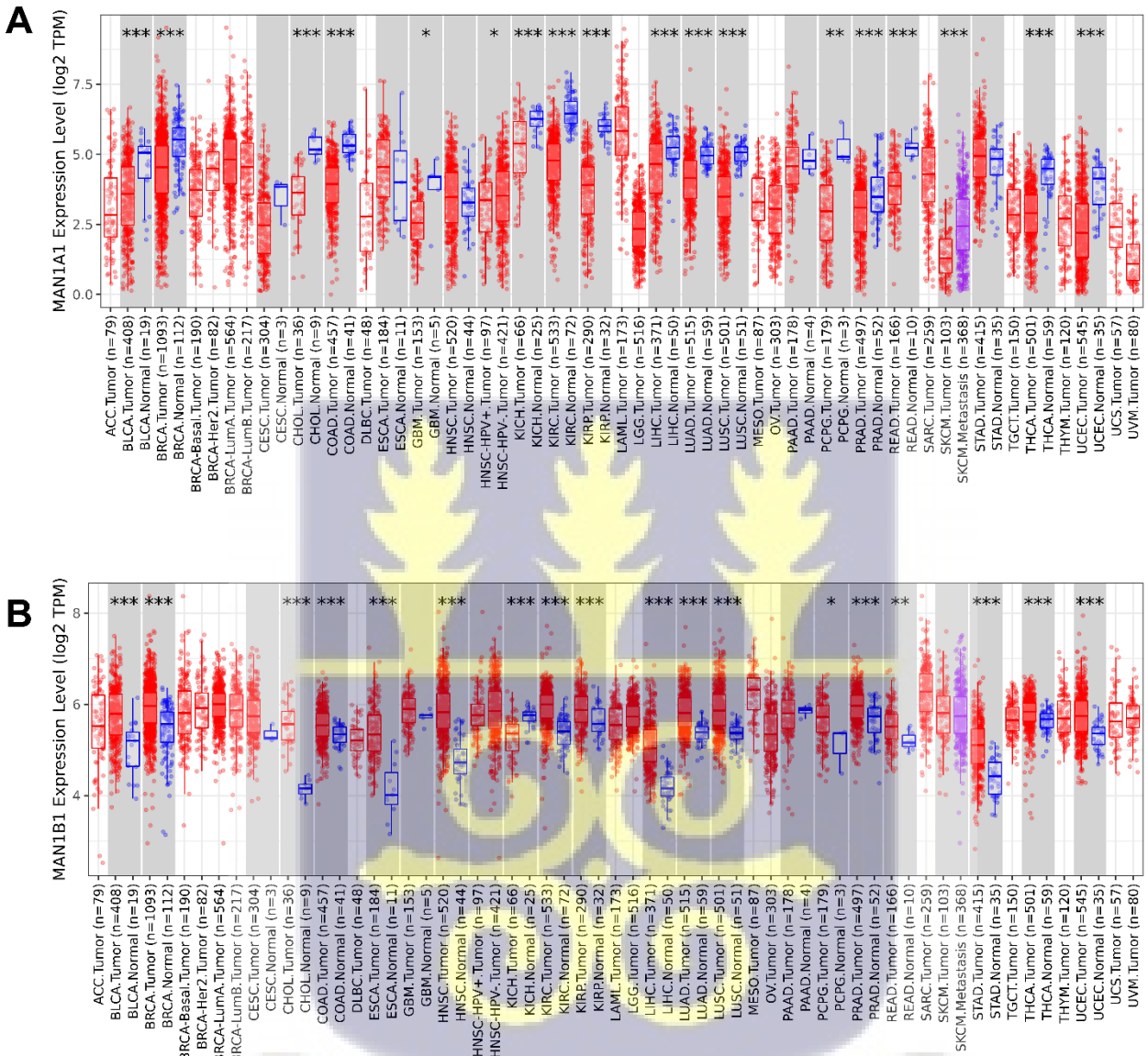

Figure 4.6 Expression of MAN1A1 and MAN1B1 in cancer. A and B) Differential expression of MAN1A1 (A) and MAN1B1 (B) between tumor and adjacent normal tissues across all TCGA

tumors using the Gene_DE module of TIMER2.0. TIMER2.0 computes the statistical significance of gene expression by Wilcoxon test (*: p-value < 0.05; **: p-value <0.01; ***: p-value <0.001).

4.3.7 MAN1A1 or MAN1B1 differential expression influences the overall survival in some cancers.

Given the striking differential expression profiles of MAN1A1 and MAN1B1 in cancer tumors, the influence of both genes on the overall survival of cancer patients across all tumors in TCGA were assessed using the "Gene_Outcome" module of TIMER2.0 (http://timer.cistrome.org/)(Li et al., 2020), adjusted by age, gender, race, clinical stage, and tumor purity (Figure 4.7A). For tumors for which the Z scores were statistically significant ($p < 0.05$), the HR of the differential expression was assessed using KM survival analysis (Figure 4.7B). Consistent with the downregulation of MAN1A1 observed in many tumors, higher MAN1A1 expression is associated with reduced risk of death in KIRC (HR: 0.833) and SCKM (HR: 0.833). Although overexpression of MAN1A1 is associated with a higher risk of death in LGG (HR: 1.13) and UVM (HR: 1.55), these associations were not statistically significant. On the other hand, higher MAN1B1 expression is significantly associated with a higher risk of death in ACC and BRCA, with an HR of 1.87 and 1.65, respectively. Additionally, higher MAN1B1 expression is associated, nearly significantly (p = 0.0644), with a higher risk of mortality in patients with SARC (HR: 1.24). Together, these results suggest that the involvement of MAN1A1 and MAN1B1 in the quality control of HLA class I expression could have significant immunological consequences that influence patients' survival in some cancers.

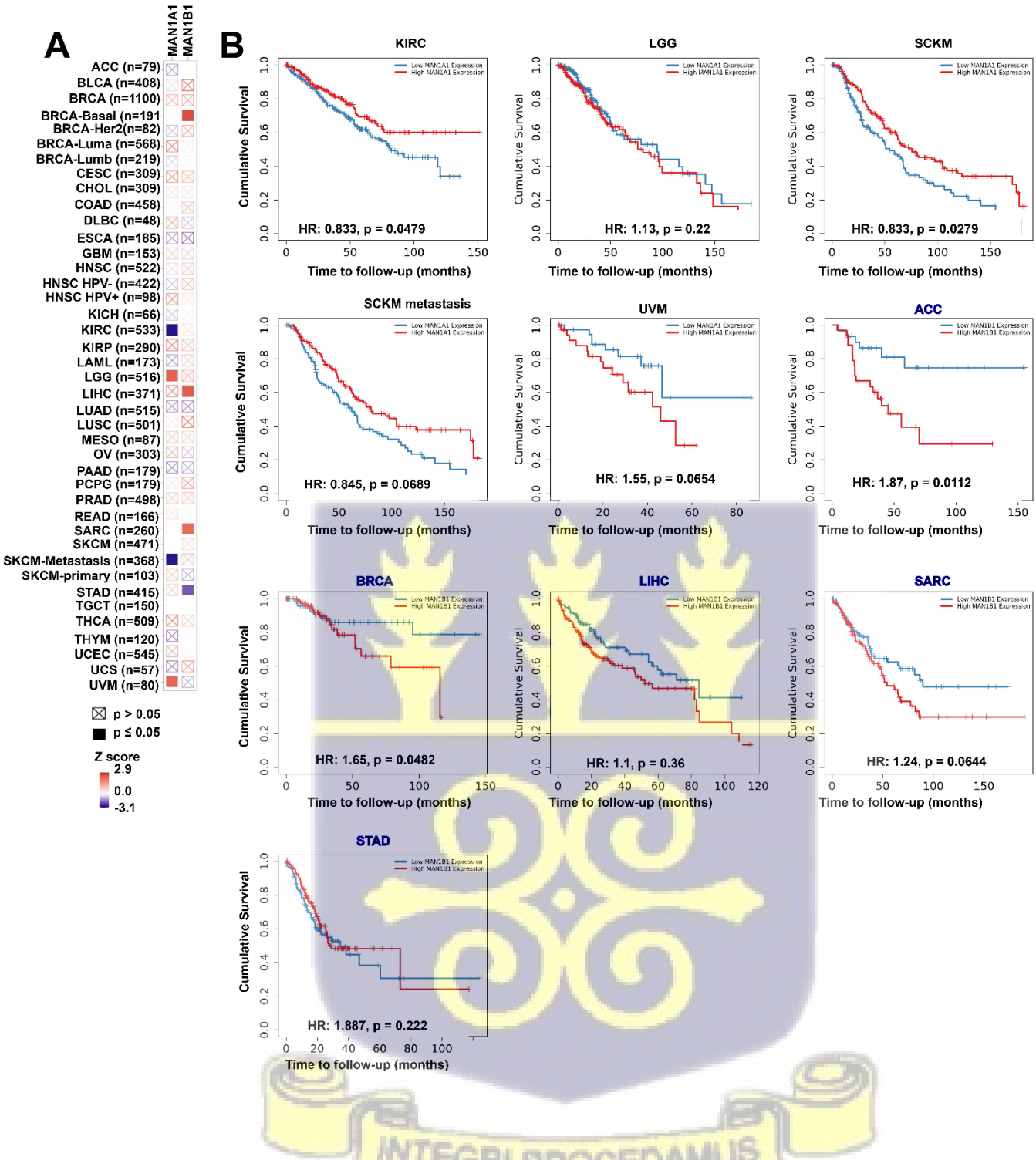

Figure 4.7 Overall survival in some cancers is influenced by differential expression of MAN1A1 or MAN1B1. A) A heatmap of the clinical relevance of MAN1A1 or MAN1B1 expression across all cancer tumors in TCGA, adjusted by age, gender, race, clinical stage, and

tumor purity. B) Kaplan-Meier curves comparing the survival rates of patients with differential expression of MAN1A1 (black titles) and MAN1B1 (blue titles) in cancers that have significant Z scores (A). For (A) the red block represents increased risk ($p < 0.05$, $z > 0$), the blue block represents decreased risk ($p < 0.05$, $z < 0$), and the grey block represents no significant change in the risk ($p > 0.05$).

4.4 Discussion

Antigen presentation by HLA class I constitutes a crucial arm of adaptive immunity against infections and cancers. Viruses and cancers could subvert antigen presentation by targeting relevant proteins such as TAP, depriving HLA class I of peptides, and promoting the accumulation of misfolded forms of HLA class I proteins (Alimonti et al., 2000; Fruh et al., 1995; Henle et al., 2017; Verweij et al., 2015). The role of exomannosidases in trimming mannose residues from deglucosylated glycans on glycoproteins, labeling the proteins with glycoforms that dictate degradation or trafficking, has been reported in previous studies (Bieberich, 2014; Roth & Zuber, 2017). Altered glycoprofile of surface HLA class I proteins, suggesting impaired mannose trimming and quality control, has also been observed (Chapter 3 and Geng et al., 2018). However, studies have not specifically addressed the role of many ER and Golgi mannosidases in the quality control and trafficking of HLA class I. Our finding that the expression levels of ER and Golgi 1,2-alpha-mannosidases are not significantly altered in TAP-deficient cells relative to wild-type cells suggests that the altered glycoprofile of HLA class I proteins, favoring high mannose glycoforms, previously observed in TAP-deficient cells, is likely not driven by a lower abundance of 1,2-alpha-mannosidases, although changes to protein expression and localization were not investigated.

Our results reveal that EDEM1 depletion increases surface HLA class I (Figures 4.1A and B), consistent with previous reports that it is involved in the degradation of HLA class I through ERAD (Burr et al., 2013; Timms et al., 2016). Additionally, a CRISPR screen identified both EDEM1 and EDEM2 as contributing to MHC class I degradation (Timms et al., 2016). In contrast to Timms et al. (2016), we observed that genetic knockdown of EDEM2 decreases surface HLA class I (Figures 4.1C and D), suggesting a role in productive HLA class I trafficking rather than degradation. This discrepancy may stem from differences in experimental design. Whereas they expressed a mutant HLA-A*02 tagged with a green fluorescent protein to study MHC class I ERAD, we assessed endogenous HLA class I proteins existing in their natural cellular state. By promoting HLA class I trafficking, EDEM2 may be targeted by pathogens to downregulate HLA class I and evade immunity. However, EDEM2 is upregulated in many cancers (Figure 4.4B), suggesting it likely regulates other factors more critical to tumour survival than HLA class I downmodulation.

We also observed that EDEM3 knockdown increases surface HLA class I expression (Figures 4.1E and F). These results indicate that EDEM1 and EDEM3 target HLA class I for degradation, and depleting either one could rescue antigen presentation, opening new frontiers for potential therapeutic interventions against pathogens and cancers that downmodulate HLA class I proteins. Whether these phenotypes are also observed in other cells remains to be established. Indeed, we observed an upregulation of EDEM1 or EDEM3 in most tumors in TCGA relative to the adjacent normal tissues (Figures 4.4A and C). Furthermore, we observed that higher EDEM1 or EDEM3 expression levels are associated with a higher risk of death in some cancers. However, further studies are needed to assess the influence of EDEM1 and EDEM3 on HLA class I antigen presentation and the HLA class I-dependent immune responses in cancers and other diseases.

Like EDEM1 and EDEM3, the increase in surface HLA class I observed in MAN1A1 or MAN1B1 depleted cells highlights their roles in the quality control of HLA class I proteins. Notably, the overexpression of MAN1B1 in many cancer tumors suggests that it may potentially promote the degradation of HLA class I in these tumors, thereby enhancing their immune evasion capacity. Unlike MAN1B1, MAN1A1 is downregulated in many cancers, despite the two proteins exerting a similar influence on surface HLA class I expression. This discrepancy suggests that MAN1A1 also regulates other factors more relevant to cancer tumours than HLA class I downregulation. Although MAN1A1 or MAN1B1-reduced expression impairs glycosylation and has been associated with disease progression and death in some cancers (Chatterjee et al., 2021; Hamester et al., 2019; Tu et al., 2017; Wang et al., 2022), our findings suggest that MAN1A1 or MAN1B1 downregulation could promote $CD8^+$ T cell response against many cancer tumors since the number of peptide-assembled HLA class I expressed on the plasma membrane increases in MAN1A1 or MAN1B1-depleted cells.

4.5 Conclusion

In THP-1 cells, depletion of EDEM1, EDEM3, MAN1A1, or MAN1B1 increases surface HLA class I expression, while depletion of EDEM2 decreases it. These findings potentially open new frontiers for immunotherapy against infectious diseases and malignancies and should be verified in cancer cell lines and in vivo models.

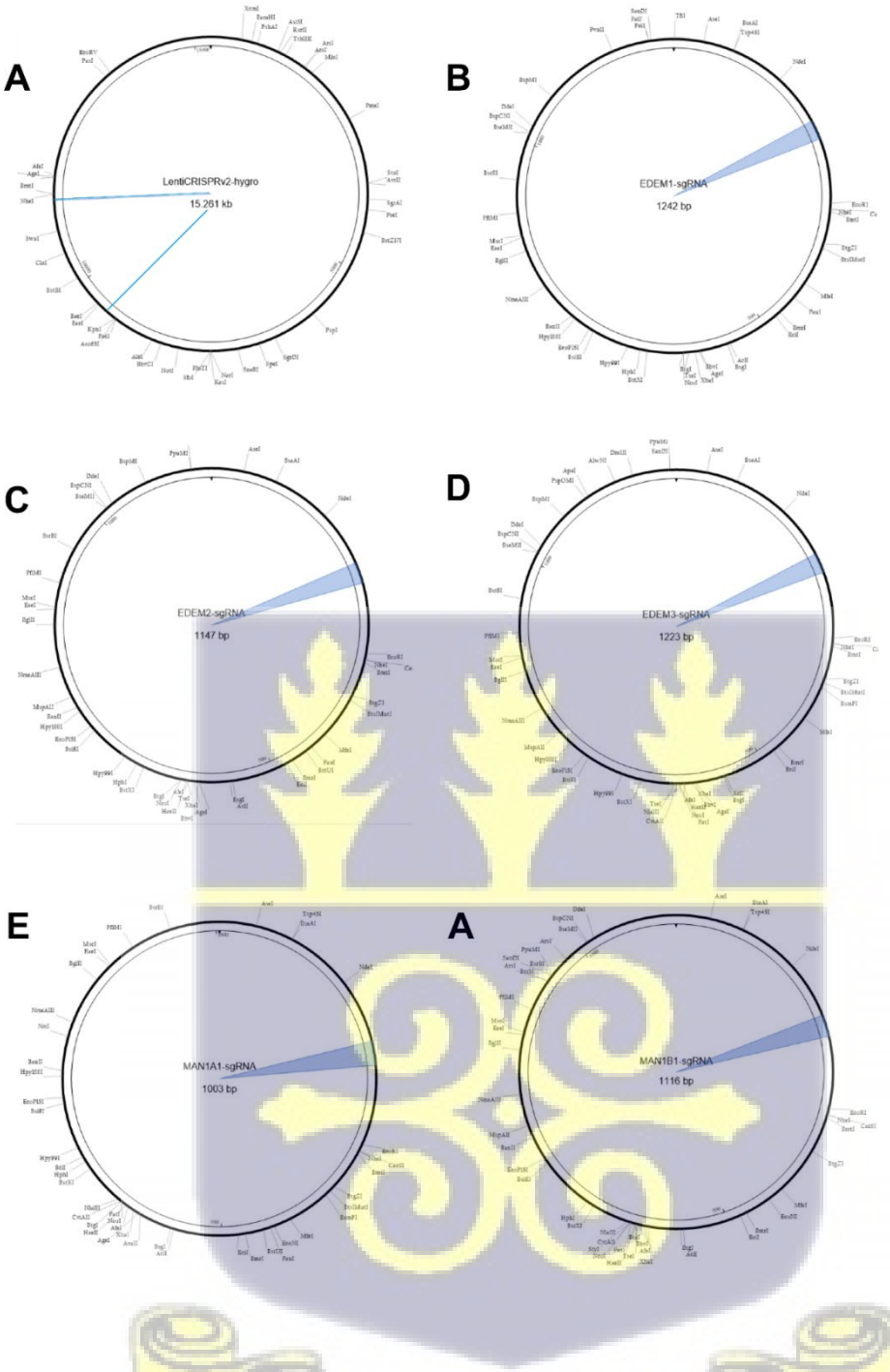

Supplementary Figure 4.1: ER and Golgi mannosidases sgRNA constructs. Plasmid maps of LentiCRISPRv2-Hygromycin (A), with EDEM1 (B), EDEM2 (C), EDEM3 (D), MAN1A1 (E), and MAN1B1 (F) single guide RNA (sgRNA).

CHAPTER FIVE

Manuscript 3: Shared HLA Class I-Associated Peptides of Wild Type and TAP-Deficient Cells and Evidence for Endosomal Assembly

5.0 Abstract

Human leukocyte antigen (HLA) class I molecules present peptide antigens to cytotoxic T-lymphocytes (CTL or $CD8^+$ T cells), playing a critical role in immunity against infectious pathogens and cancers. The transporter associated with antigen processing (TAP) transports peptides from the cytosol into the endoplasmic reticulum (ER) for assembly with HLA class I proteins. TAP is inhibited by many viruses and malignant conditions to evade immune surveillance by CTL. However, many HLA class I allotypes exhibit decreased TAP dependence and can present peptides under TAP-dysfunctional conditions. Understanding the pathways governing TAP-independent peptide presentation could provide insights into the mechanisms underlying HLA class I trafficking in TAP-deficient conditions and advance the design of immunotherapeutics against TAP-inhibiting diseases. Using quantitative mass spectrometry, we analyzed peptides eluted from HLA class I proteins in wild-type and TAP-deficient THP-1 cells. Our analysis identified novel, potentially antigenic peptides unique to TAP-deficient cells. As expected from previous studies, signal sequence-derived peptides are preferentially presented in TAP-deficient cells. Notably, however, ~ 80% of peptides are shared between wild-type and TAP-deficient cells, although peptides from non-canonical protein sources such as the mitochondria, ER, and secreted proteins are enriched in the cells lacking TAP. Treatment with the endosomal acidification inhibitor, bafilomycin, and depletion of Rab11A, a small Rab GTPase that regulates endocytic recycling, reduces HLA class I assembly and surface expression in wild-type and TAP-deficient

cells. Together, these findings support the existence of common endosomal pathways for the constitutive assembly of HLA class I molecules in both wild-type and TAP-deficient cells.

5.1 Background

HLA class I molecules are glycoproteins that facilitate immune surveillance by presenting peptides to CTL and regulating natural killer (NK) cells (Yewdell, 2022). These peptides originate from different subcellular compartments but are largely thought to be generated through proteolytic cleavage by the cytosolic proteasome (Rock et al., 1994; Sijts & Kloetzel, 2011). The diverse collection of HLA class I peptide antigens is collectively termed the "HLA class I immunopeptidome" (Yewdell, 2022).

The classical HLA class I peptide presentation pathway relies on the transporter associated with antigen processing (TAP) (Lehnert & Tampe, 2017). TAP is a heterodimer and transmembrane protein that translocates peptides from the cytosol into the endoplasmic reticulum (ER), specifically, the peptide loading complex (PLC), for assembly with nascent HLA class I molecules (Lehnert & Tampe, 2017). From the PLC, peptide-assembled HLA class I are transported to the plasma membrane, trafficking through the Golgi (Blum et al., 2013; Neefjes et al., 2011). By transporting peptides into the PLC, TAP is a crucial component of the HLA class I antigen presentation pathway and is often inhibited by some malignant conditions and viruses. TAP inhibition significantly downmodulates the surface expression of HLA class I on the plasma membrane (Alimonti et al., 2000; Fruhet al., 1995; Geng et al., 2018; Verweij et al., 2015), promoting immune evasion. However, a subset of HLA class I molecules can still be expressed on the plasma membrane of TAP-deficient cells, presenting antigens capable of activating CTL (de la Salle et al., 2002; Geng et al., 2018). These confirm the existence of TAP-independent pathways through which HLA class I molecules could acquire intracellular peptides for CTL priming. However, these pathways are poorly understood.

Studies using mass spectrometry and computational approaches to explore HLA class I peptide repertoire in TAP-deficient cells have identified some TAP-independent peptides (Henderson et al., 1992; Lorente et al., 2013; Martin-Galiano & Lopez, 2019; Wei & Cresswell, 1992; Weinzierl et al., 2008). TAP-independent peptides have also been identified in peripheral blood mononuclear cells obtained from healthy donors lacking any known TAP-deficient conditions (de Waard et al., 2021). Notably, these peptides are often derived from or contain their parent proteins' ER localizing signal sequences (Henderson et al., 1992; Wei & Cresswell, 1992), suggesting a signal sequence-dependent but TAP-independent transport into the ER. However, the peptides identified to date are relatively few and mostly restricted to the HLA class I allele–HLA-A*02:01, limiting the potential to harness TAP-independent pathway(s) for immunotherapeutic interventions.

In the signal sequence-dependent model for TAP-independent peptide presentation by HLA class I molecules, the peptides are imported into the ER before their assembly and trafficking through the canonical ER-Golgi-dependent secretory pathway (Henderson et al., 1992; Wei & Cresswell, 1992). However, endolysosomal assembly of endogenous peptides with HLA class I proteins has been described in professional antigen-presenting cells obtained from healthy donors (Olson et al., 2023). Additionally, endolysosomal assembly of exogenous peptides with HLA class I for cross-presentation to CTL has been reported (Cruz et al., 2023; Embgenbroich & Burgdorf, 2018). Together, these findings highlight the existence of ER-independent and signal sequence-independent TAP-independent acquisition of endogenous peptides by HLA class I molecules. However, the mechanisms governing the acquisition of these peptides have not been completely elucidated.

Using mass spectrometric analysis of tandem mass tag (TMT)-labeled peptides, we have uncovered peptides presented by HLA-A, -B, and -C alleles in TAP-deficient human monocyte

antigen-presenting cell THP-1. Our data sheds light on the shared peptidomes of wild-type and TAP-deficient cells and identifies a potential pathway for their presentation.

5.2.0 Methods

5.2.1 Cells and cell culture

TAP-deficient THP-1 cells generated from the parental THP-1 cells (TIB-202) purchased from the American Type Culture Collection (ATCC) as described in Chapter 3 of this thesis were used for these experiments. Briefly, TAP deficiency was created in the cells by knocking out the TAP-1 subunit using clustered regularly interspaced short palindromic repeats (CRISPR)/CRISPR-associated protein 9 (Cas9). The forward and reverse single guide RNA (sgRNA) to achieve the knockout were 5'-AGTTCGAAGCTTTGCCAACG-3' and 5'-CGTTGGCAAAGCTTCGAACT-3', respectively. Except indicated otherwise, the cells were cultured in RPMI 1640 (ATCC modification, catalog number: A1049101) supplemented with 10% (v/v) fetal bovine serum (FBS), 2 mM L-glutamine, and 1X antibiotic/antimycotic.

5.2.2 Sodium dodecyl polyacrylamide gel electrophoresis (SDS-PAGE) and immunoblot

To confirm TAP knockout, wild-type or TAP-KO THP-1 cells were incubated in a lysis buffer (50 nM TRIS, 1% Triton, 150 nM NaCl, and 5 mM $CaCl_2$) at 4°C for 1 hour. The lysates were cleared by centrifuging them at 13,000 RPM for 30 minutes at 4°C. After centrifugation, the supernatant was incubated with TAP-1 antibody (148.3) at 4°C overnight to precipitate TAP-1 through immunoaffinity. The lysates were further incubated with protein G Sepharose for 2 – 3 hours at 4°C and washed three times in the lysis buffer at 1000 G for 1 minute. The beads were boiled in 5X SDS for 5 minutes to elute bound proteins. The eluates were subjected to 8% SDS-PAGE at

120 V for 120 minutes, and the proteins were transferred to polyvinylidene fluoride (PVDF) membranes at 100 V for 100 minutes. The membranes were incubated in a blocking buffer (5% skimmed milk in 1X TBST) at room temperature on a shaker for 30 minutes and blotted with mouse anti-TAP-1 (148.3) or rabbit anti-GAPDH antibody at 4ºC overnight. The membranes were washed three times (10 minutes each) with 1X TBST and blotted with goat-anti-mouse or goat-anti-rabbit horse radish peroxidase at room temperature on a shaker for 30 minutes. The membranes were again washed three times in 1X TBST and then treated with equal volumes of enhanced chemiluminescence (ECL) reagents, following the manufacturer's instructions. The membranes were exposed to X-ray film in an X-ray film processor to detect protein bands.

5.2.3 Flow cytometry

About 50,000 – 100,000 THP-1 or THP-1-TAP-1-KO were placed in 96-well plates and rinsed with ice-cold 1X PBS at 2500 rpm for 1 minute. The cells were stained with the indicated antibodies in a staining buffer (2% fetal bovine serum (FBS) in 1X PBS) on ice for 30 minutes. After staining, the cells were rinsed twice with the buffer and resuspended in 7-aminoactinomycin D (7-AAD) (1:1000) in the buffer. Flow cytometry was performed on a BD LSRFortessa cell analyzer, and the data were analyzed in FlowJo and Prism (GraphPad). The mean fluorescence intensity (MFI) values of the indicated fluorophore-conjugated antibodies were chosen to represent surface HLA class I expression on the cells.

5.2.4 W6/32 antibody purification, conjugation to beads, and HLA class I isolation

The pan HLA class I mouse antibody, W6/32, was purified from ascites using HiTrap Protein G HP column (described in Chapter Three of this thesis). Briefly, ascites was passed through a syringe filter (0.45 µm) after centrifuging at 13000 rpm for 30 minutes at 4ºC. An elution buffer

was prepared by adjusting the pH of 0.1 M glycine to 2.7 using concentrated hydrochloric acid (HCl). In addition, binding (20 mM sodium phosphate, pH 7.0) and neutralizing (1 M Tris-HCl, pH 9.0) buffers were prepared and stored at 4ºC until further use. The HiTrap column was washed with 10 mL elution buffer and equilibrated with 25 mL of the binding buffer. The buffers were passed through the column at 1 mL/minute. Following equilibration, the filtered ascites was carefully loaded into the column and incubated at 4ºC for 30 minutes. The column was rinsed in 50 mL of the binding buffer at a constant flow rate of 1 mL/minute. 200 µL neutralization was aliquoted into 1.5 mL Eppendorf tubes, and the antibody was eluted into the neutralizing buffer using 25 mL elution buffer in an aliquot of 800 µL. The antibody was concentrated and dialyzed in the binding buffer multiple times to reduce the residual neutralizing buffer to values less than 4.5×10^{-3} nM.

The purified antibody was coupled and cross-linked to PureProteome protein A magnetic beads (Millipore Sigma; catalogue number: LSKMAGA10) using a protocol described by Kaur et al. (2023) and Lamoliatte et al. (2017). Briefly, using a magnetic rack, the beads were washed in three changes of 200 mM triethanolamine (pH 8.3) and added to the antibody for 1 hour at 4 °C. 1 mL of bead slurry was added to 2 mg of the antibody. The beads were again washed three times with 200 mM triethanolamine (pH 8.3) and then incubated with 5 mM dimethylpimelimidate (DMP, pH 8.3) (1:10) for 60 minutes at 20 – 25ºC to cross-link W6/32. The reaction was quenched by adding 5% (v/v) 1 M Tris-HCl (pH 8) to the bead slurry (50 uL per 1 mL) and incubating at 20 – 25ºC for 30 minutes. After the cross-linking, the slurry was incubated with the elution buffer to remove unbound or uncross-linked antibodies. Lastly, the beads were washed in three changes of ice-cold 1X PBS, resuspended in 0.01% NaN3 in 1X PBS, and stored at 4 °C until further use. 20

µL aliquots taken from every step of the coupling and cross-linking were subjected to SDS PAGE and Coomassie brilliant blue staining to confirm W6/32 cross-linking with the beads (Figure 5.2B).

For HLA class I immunoaffinity precipitation and HLA class I-associated peptides elution, about 2 x 10^8 THP-1 cells or 5 x 10^8 THP-1-TAP-1-KO cells were lysed in a buffer containing 1X PBS, 1 mM EDTA, 1 mM PMSF, 0.2 mM iodoacetamide, 1% octyl-beta-D-1-thioglucopyranoside, 0.25% sodium deoxycholate, and protease inhibitor (Sigma P8340 Cocktail (1:200)) for 1 hour at 4 °C on a rocker. The lysates were centrifuged at 13,000 rpm for 30 minutes at 4ºC and incubated with unfunctionalized (blank) beads (pre-washed in three changes of 1X PBS) for 30 minutes at 4 °C on a rotary shaker. The blank beads were rinsed in three changes of ice-cold 1X PBS, 1 mL cold water, eluted three times with 0.2 mL of 0.2% trifluoroacetic acid (TFA), and washed again in three changes of 1X PBS before being stored for further use. The lysates were incubated with W6/32-cross-linked beads, and the beads were treated similarly to the blank beads to elute HLA class I proteins.

A reverse phase chromatography was performed using C18 SepPak columns (Waters Corp, Catalogue number: WAT020515) to purify peptides from the eluted HLA class I proteins. The column was activated with 5 mL 80% acetonitrile containing 0.1% TFA and rinsed with 5 mL 0.1% acetonitrile-free TFA. The sample was loaded onto the column and the flow through was passed twice. The column was rinsed with 5 mL 0.1% TFA and the peptides were eluted using 1.5 mL 30% acetonitrile containing 0.1% TFA. Protein was eluted from the column with 1.5 mL 80% containing 0.1% TFA. Saved fractions of various elutions were subjected to SDS PAGE and immunoblot to confirm HLA class I precipitation (Figure 5.2C). The peptides were submitted to the Proteomics Resource Facility at the University of Michigan for processing and mass spectrometry data acquisition.

5.2.5 Mass spectrometry

TMT-mass spectrometry improves both the number and relative quantification of eluted peptides recovered from HLA class I immunopeptidome under various conditions (Mamrosh et al., 2023). Hence, we used a TMT-mass spectrometry approach in this study. The samples were first subjected to dithiothreitol treatment (5 mM) for half an hour at 45ºC (cysteine reduction), followed by cysteine alkylation by treatment with 2-chloroacetamide (15 mM) for another half an hour at 20 – 25ºC. For protein precipitation, the samples were treated with six volumes of acetone, incubated for about 12 hours at -20ºC, and centrifuged to obtain pellets. The samples were labeled with 6-plex tandem mass tag isobaric reagent (Thermo Fisher Scientific) following the manufacturer's instructions. The labeled samples were mixed (~200 µg), dried in a vacufuge, and fractionated to eight using a peptide fractionation kit (Pierce; Cat no: 84868). The fractions were dissolved in 9 µl of 0.1% formic acid/2% acetonitrile after they were air-dried. THP-1 cells replicates 1, 2, and 3 were labeled with TMT channels 126, 127, and 128, while THP-1-TAP-1-KO cells replicates 1, 2, and 3 were labeled with 129, 130, and 131, respectively.

To achieve superior quantitation accuracy during MS analysis, we used the multinotch-MS3 liquid chromatography approach, known to minimize reporter ion ratio distortion caused by co-isolated peptide fragmentation (McAlister et al., 2014). The data was acquired on Orbitrap Ascend Tribrid equipped with a FAIMS source (Thermo Fisher Scientific) coupled to a Vanquish Neo Ultra High-Performance Liquid Chromatography (UHPLC) system. Upon data acquisition, the MS raw files were exported to PEAKS for analysis. We searched the MS/MS spectra against the human protein sequences in the UniProt /Swiss-Prot database downloaded in 2018. We set the mass tolerance for precursor and fragment ions at 10 ppm and 0.02 Da respectively. Isotopic error correction was

enabled. Similarly, methionine oxidation as well as N-terminal acetylation and cysteine carbomidomethylation were allowed. Since the peptides were not digested prior to the MS/MS, "None" was selected for the parameter, "enzyme specificity". We used a false discovery rate of 0.01 to filter peptide-spectra matches. 8–14mer peptides were selected for further analysis. From the three replicates of THP-1 or THP-1-TAP-1-KO samples, peptides present in only one replicate (one out of three) were excluded, and only peptides present in at least two of the three replicates were analyzed to generate the results presented here.

5.2.6 CRISPR-Cas9-mediated gene depletion

Single guide RNAs (sgRNAs) in 5'–3' direction for invariant chain were GCTTGGGAAGCTTCATGCGC and GCGCATGAAGCTTCCCAAGC (forward and reverse, respectively. For RAB11A, the forward sgRNA was TGCGCGGCCGAGGAGCGAAA and the reverse was TTTCGCTCCTCGGCCGCGCAC). The sgRNAs were cloned into lentiCRISPRv2 vector (Addgene, 52961). Briefly, 0.001 mL of 100 µM of each forward and reverse oligonucleotides (oligos) were mixed with 6.5 µL double distilled nuclease-free water, 0.001 mL of 10X T4 ligation buffer and 0.0005 mL T4 polynucleotide kinase (NEB). The oligonucleotides were phosphorylated and denatured at 37°C for half an hour and 95°C for 5 minutes respectively. They were then placed on ice water for 1 minute to cool. 4 µL of the oligo mix was diluted to 1 mL (1:250) with nuclease-free water. 100 ng lentiCRISPRv2 was combined with 2 µL diluted oligos, 2 µL 10X FastDigest buffer (Thermo Fisher Scientific), 1 mM DTT, 1 mM ATP, 1 µL FastDigest *BsmBI*, 0.5 µL T4 ligase and the total volume was brought to 0.02 mL with double distilled nuclease-free water. The digestion-ligation step was performed using six incubation cycles at 37 °C for 5 minutes and 23 °C for 5 minutes in a thermocycler (Agilent Technologies SureCycler 8800). The ligation mix was held at 4 °C until further use.

For plasmid preparation, 0.05 µL STBL3 pre-chilled on ice were incubated with 1 – 2 µL of the ligation mix on ice for half an hour, transferred to a water bath at 42ºC for 45 seconds, and placed on ice for 2 minutes. To recover from the heat shock, 0.5 mL of super optimal broth was added to the cells, and they were cultured at 37ºC for 60 minutes, with constant shaking. After this, the cells were spun at 5,000 rpm for 2 minutes, and about 80% of the medium was removed. The cells were resuspended in the remaining media and cultured on Luria Bertani (LB) agar supplemented with ampicillin (100 µg/mL). The cells were allowed to grow for 16 hours at 37ºC. Using a sterile plastic loop, a discrete colony was selected and grown in ampicillin-supplemented LB broth overnight. The plasmid was isolated using the Promega Wizard® *Plus* SV Minipreps DNA Purification kits and assessed for purity and concentration using NanoDrop spectrophotometer (Thermo Fisher Scientific). The cloning was confirmed using Sanger sequencing with the human U6 forward primer (5'-GAGGGCCTATTTCCCATGATT-3').

5.2.7 RAB11A depletion by siRNA

RAB11A was knocked down using the ON-TARGET plus SMARTpool siRNA (Dharmacon, Catalogue number: J-004726-07). 15 µL of 20 µM the siRNA or non-targeting siRNA (negative control siRNA) and 15 µL of HiPerFect transfection reagent were placed in 0.5 mL OptiMEM, vortexed briefly and left to incubate undisturbed at 20 – 25ºC for 15 minutes. The transfection mix was placed in a 6-well plate and 0.5 x 10^6 THP-1 or THP-1-TAP-1-KO cells in 1 mL filtered, antibiotic/antimycotic-free modified RPMI were added to the plate dropwise. The plate was gently swirled to mix the cells and transfection mix, and the cells were incubated at 37ºC for 4 hours in the presence of 5% CO_2. The culture medium was made up to 2 mL and the cells were cultured for 48 hours.

5.2.8 Immunoblot

Cells were placed in a pre-chilled lysis buffer (50 nM TRIS, 1% triton, 150 nM NaCl, and 5 mM $CaCl_2$ for 1 hour). The lysates were cleared by centrifuging at 13 000 RPM for half an hour at 4°C. The supernatant was collected, boiled in 1X SDS for 5 minutes, and subjected to 4 – 20% (Bio-Rad, catalog number: 4561096) SDS-PAGE at 120V for 120 minutes. The proteins were transferred from the blots to a 0.45 µM pore size polyvinylidene fluoride (PVDF) membrane (Millipore; Catalogue number: IPFL00010). The membrane was blocked in 5% skimmed milk in 1X TBST for 30 minutes and blotted with indicated primary antibodies (Table 6.2) for one and a half hours at 20 – 25ºC or overnight at 4ºC. The membrane was blotted with goat-anti-rabbit secondary antibody for 30 minutes after washing in three changes of 1X TBST for 10 minutes each. The membrane was washed in another three changes of 1X TBST for 100 minutes each and then treated with enhanced chemiluminescence reagents (Invitrogen; Catalogue number: P132106) following the manufacturer's protocol. The membranes were exposed to X-ray film (HyBlot CL, Thomas Scientific) to detect the chemiluminescent signals on the membrane.

Table 5.1: Antibodies used for detecting RAB11A and CD74 expression.

Protein	Antibody (Catalogue number, vendor)
RAB11A	Rab11A-specific antibody (202291-AP, Proteintech)
Vinculin	Vinculin antibody (13901S, Cellsignaling Technology)
CD74	CD74 antibody (PA5-29395, ThermoFisher scientific)

5.3.0 Results

5.3.1 TAP deficiency downmodulates HLA class I allotype to different extents in THP-1 cells

To study the immunopeptidome of HLA class I in a TAP-deficient condition, we genetically knocked out *TAP-1* (the gene encoding the TAP-1 subunit of TAP) in THP-1 cells using a lentiviral CRISPR-Cas9-based targeting vector. The THP-1 cells used (ATCC) are known to have HLA-A*02:01, B*15:11, and C*03:03 alleles (McMurtrey et al., 2016; Nyambura et al., 2018). We confirmed this genotype by genotyping at HLA A, B, and C (Yarzabek et al., 2018). TAP1 knockout in the cells was confirmed by immunoblot after immunoprecipitating TAP1 using an anti-TAP1 antibody (148.3) (Meyer et al., 1994) (Figure 5.1A). Flow cytometric measurements of the HLA class I allotypes expressed on the surface of THP-1 cells show significant reductions in B*15:11 (p-value < 0.01), C*03:03 (p-value < 0.01), and A*02:01 (p-value ≤ 0.05), successively using relevant antibodies (Figure 5.1B). The HLA class I allotypes were assessed using BB.7, anti-Bw6, or DT-9, antibodies. These antibodies specifically measure HLA-A*02 (Parham & Brodsky, 1981), HLA-Bw6 (Lutz et al., 1994; Yarzabek et al., 2018), or HLA-C (Braud et al., 1998) of the classical HLA class I alleles, respectively.

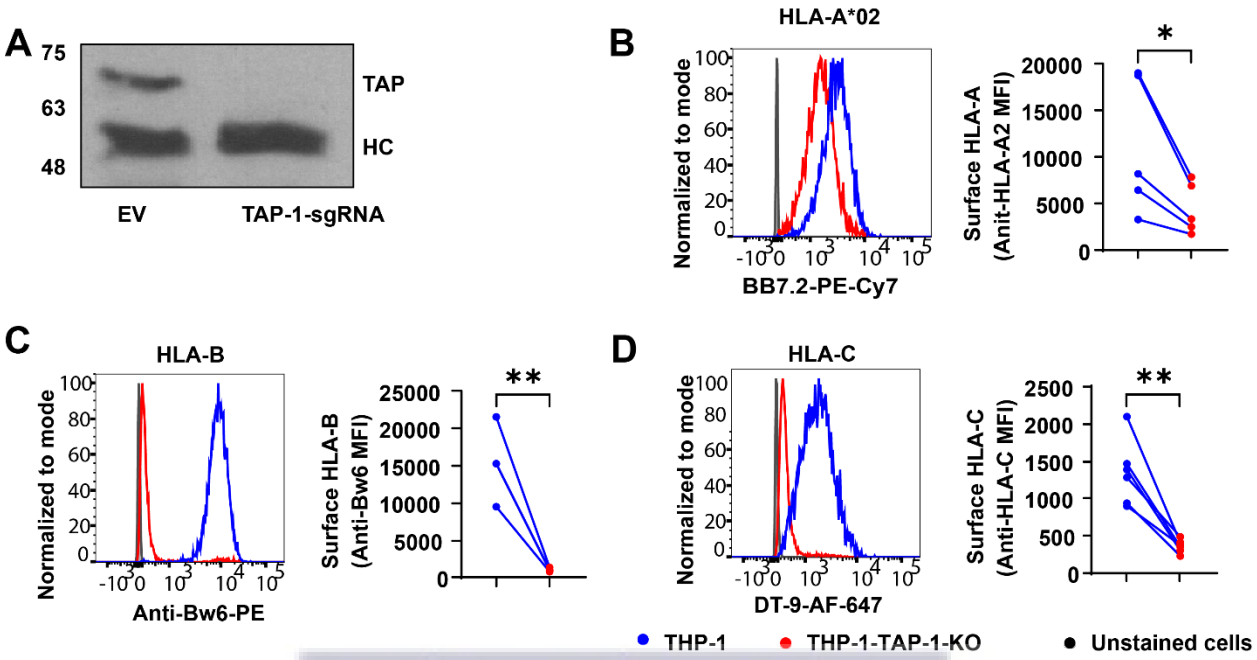

Figure 5.1 Expression of HLA class I allotypes in TAP1-KO cells. A) Immunoblot of empty vector (EV)- or TAP-1-gRNA-transduced THP-1 cells obtained after immunoprecipitation from cell lysates with anti-TAP-1 (148.3). HC: heavy chain of anti-TAP-1 (148.3). B-D) Flow cytometric analyses of cell surface HLA-A2 (B, n = 5), HLA-Bw6 (C; n = 4), and HLA-C (D; n = 6) on THP-1 or THP-1-TAP-1-KO cells measured by flow cytometry after staining the cells with the indicated antibodies. Indicated HLA class I was compared using a paired *t*-test. * (p-value ≤ 0.05), ** (p-value < 0.01).

5.3.2 Isolation of HLA class I associated peptides from wild-type and TAP-deficient cells

The schematic for peptide elution, TMT tags labeling, mass spectrometry, and data analysis is shown in Figure 5.2A. HLA class I proteins bearing peptides interact with W6/32, an antibody that specifically interacts with a conformational epitope formed by the α domains and β_2-microglobulin of HLA class I proteins (Barnstable et al., 1978; Pymm et al., 2024). W6/32 was coupled and cross-linked with proteome A magnetic beads (Figure 5.2B), and the functionalized beads were incubated

with lysates prepared from THP-1 or THP-1-TAP-1-KO cells. The immunoprecipitated peptide-HLA class I complexes were eluted from the beads and further fractionated into peptides and proteins by reverse phase chromatography using C18 SepPak columns (Figure 5.2C). The peptides were subjected to liquid chromatography and mass spectrometry.

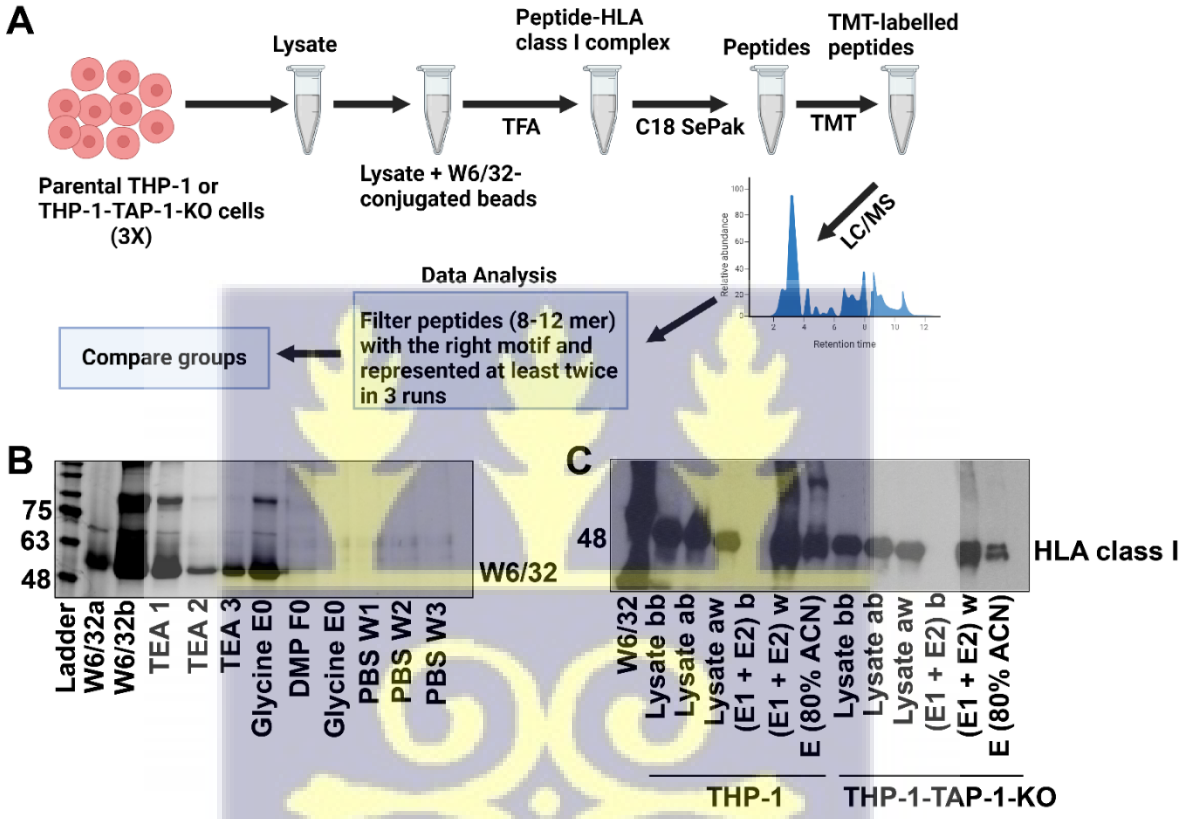

Figure 5.2 Isolation of HLA class I-bound peptides from wild-type and TAP-deficient cells. A) Schematic for immunopeptidome isolation and TMT labeling. B) SDS PAGE of W6/32 monoclonal antibody coupling and cross-linking with proteome A magnetic beads. W6/32a: 5 µL W6/32 antibody, W6/32b: 15 µL of the supernatant after incubating W6/32 with the beads, TEA1-3: 15 µL of Triethanolamine washes, Glycine E0: 10 µL of 0.1 M glycine elution from W6/32-coupled but uncross-linked beads, Glycine F1: 15 µL of supernatant after cross-linking W6/32-beads using dimethylpimelimidate, Glycine E0: 10 µL of 0.1 M glycine elution from beads after cross-linking, PBS1-3: successive 1X PBS washes. C) Immunoblot of HLA class I purified from THP-1 or THP-1-TAP1-KO lysates using the W6/32-cross-linked beads. Lysate bb and ab: 5 µL

lysate before and after incubation with blank (unfunctionalized) beads respectively, Lysate aw: 5 Lysates after incubating with W6/32-cross-linked beads, (E1 + E2) b: Elutions 1 and 2 from blank beads, (E1 + E2) w: Elutions 1 and 2 from W6/32-cross-linked beads, E (80% ACN): 80% acetonitrile elution from C18 chromatography column.

5.3.3 Parental and TAP-1-KO THP-1 cells share a large fraction of their HLA class I peptides

A total of 311 peptides were identified in at least 2 of the 3 THP-1 or THP-1-TAP1-KO replicate samples on which mass spectrometry was performed (Figure 5.3). Of this number, 50 and 6 peptides are unique to wild-type THP-1 and TAP-deficient THP-1 cells, respectively. Notably, more than 80% (255) of the total peptides recovered are presented by both THP-1 and THP-1-TAP-1-KO cells. We refer to these peptides as "shared peptides". More than half (58.04% [148]) of the shared peptides have neither preference for wild-type THP-1 nor THP-1-TAP-1-KO cells. However, 29 and 78 are preferentially presented by TAP-deficient and wild-type THP-1 cells respectively. The peptide preference was determined based on multiple paired t-tests.

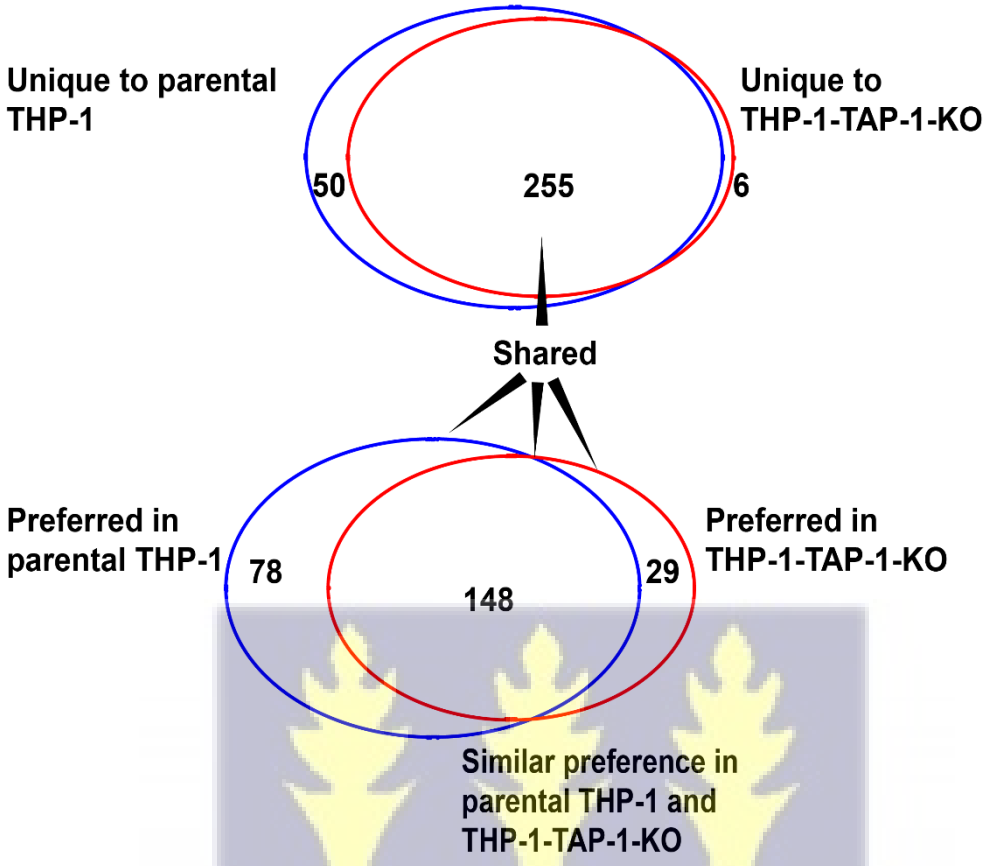

Figure 5.3 Parental and TAP1-KO THP1 cells share a large fraction of their HLA class I peptides. Quantitative Mass spectrometric analyses of peptides from three independent HLA class I peptide elutions of parental and TAP-1-deficient THP-1 cells. Eluted peptides were TMT labeled and subjected to mass spectrometric analyses. Identified peptides were classified as unique to TAP-1-KO or parental cells if detected among peptides unique to one cell line, but absent in all three runs of the second. For shared peptides, a multiple paired t-test analysis was undertaken to identify those preferred in the parental or TAP1-KO cells, or those found to have similar abundance in both. A proportional Venn diagram of HLA class I peptides unique to or shared between THP-1 and THP-1-TAP1-KO cells. Data analyses were performed by Avrokin Surnilla, Amanpreet Kaur, and Malini Raghavan.

5.3.4 THP-1 HLA class I alleles present peptides with unique amino acid motifs.

To understand the nature of peptides presented by each HLA class I allele expressed by the THP-1 cells from ATCC, sequence logos were generated for previously published peptides that were eluted from A*02:01 or C*03:03 and identified using a mass spectrometric approach (Sarkizova et al., 2020). The sequence logos were generated using the Seq2Logo-2.1 (https://services.healthtech.dtu.dk/services/Seq2Logo-2.1/)(Thomsen & Nielsen, 2012). Sequence logos were also generated for B*15:11 peptides retrieved from IEDB (https://www.iedb.org/). The binding motif of HLA-A*02:01 favors leucine or other bulky hydrophobic amino acid residues such as valine and isoleucine at the P_2 and the P_C anchor positions across 9-12mers (Figure 5.4A). HLA-B*15:11 is consistently selective for proline at the P_2 position but prefers tyrosine, phenylalanine, or leucine at the Pc position (Figure 5.4B). C*03:03 strongly prefers phenylalanine and tyrosine, aromatic amino acids with bulky side chains, at the P_1 position. In addition to the P_1, C*03:03 exhibits a degree of flexibility at the P_2 position, binding both hydrophobic (alanine, isoleucine, and valine) and polar uncharged residues (serine) (Figure 5.4C). Furthermore, C*03:03 exhibits flexibility for hydrophobic (leucine) and positively charged (lysine and arginine) residues at the P_C position (Figure 5.4C).

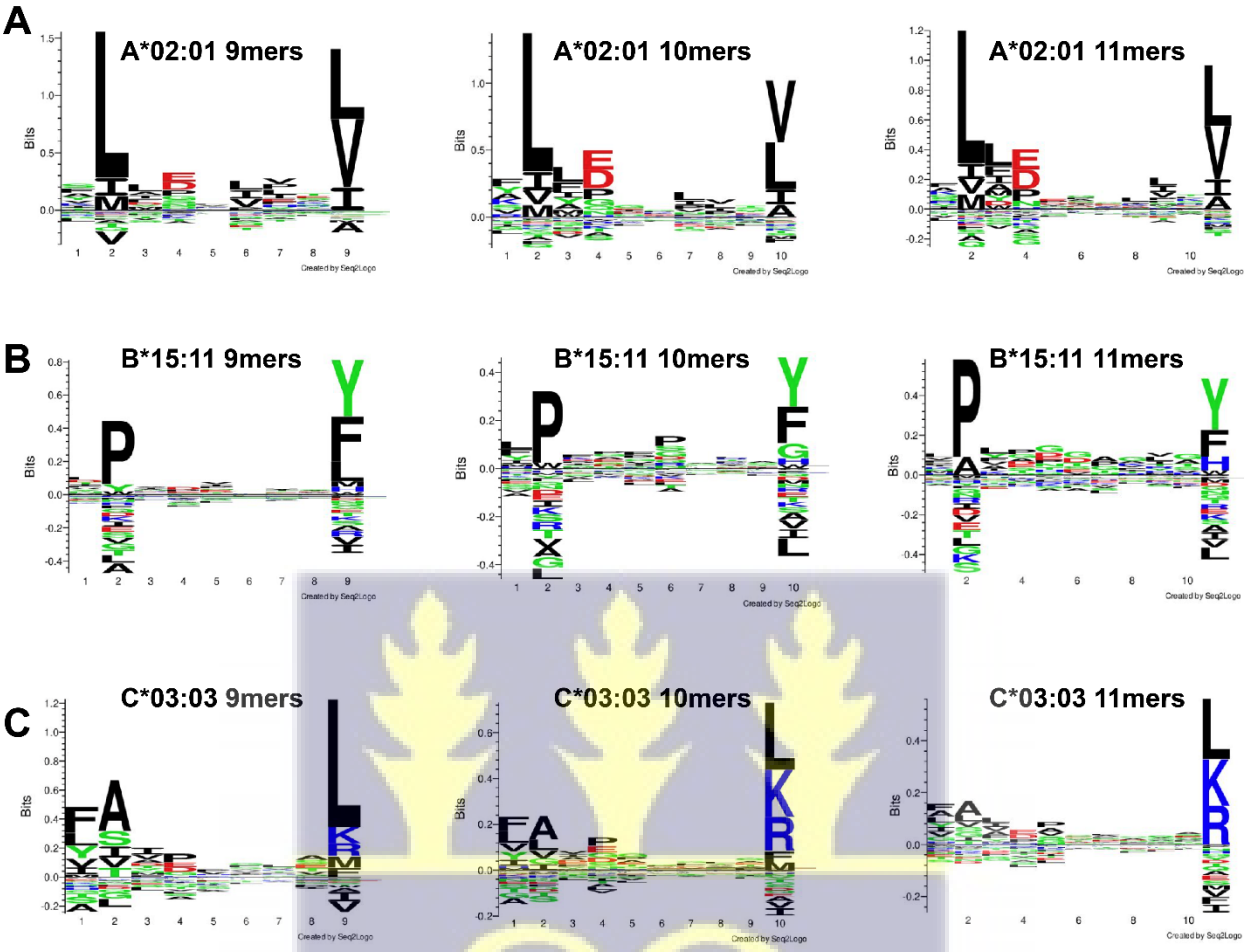

Figure 5.4 Seq to logo plots of HLA-A, -B, and -C alleles in THP-1 cells. The seq to logo plots for HLA-A*02:01 and C*03:03 were plotted using peptides identified by mass spectrometry, previously published by (Sarkizova et al., 2020). For B*15:11, the seq to logo plots were plotted using high-affinity peptides for B*15:11 available in the Immune Epitope Database and Tools (IEDB)(https://www.iedb.org/home_v3.php). These plots were generated by Avrokin Surnilla.

5.3.5 The distribution by length of peptides unique to or preferred by TAP-deficient THP-1 cells varies among HLA class I alleles.

The peptides unique to or preferred by THP-1-TAP-1-KO cells were further assigned to A*02:01, B*15:11, and C*03:03. The peptides were assigned using the percentile rank of the eluted ligand (EL) likelihood scores (% Rank EL) of their binding affinities with HLA class I alleles, computed with NetMHCpan-4.1 (https://services.healthtech.dtu.dk/services/NetMHCpan-4.1/)(Reynisson et al., 2020). The NetMHCpan-4.1 predicts the binding affinity of peptides to HLA class I alleles using artificial neural networks and transforms the predicted binding affinity scores by normalizing them across HLA class I alleles (Reynisson et al., 2020). This transformation accounts for cellular processes that may confound the predicted binding affinity scores and enables comparisons of the binding affinity of different peptides to a given HLA class I allele against the backdrop of some random natural peptides (Reynisson et al., 2020). The threshold for the % Rank EL was < 0.5% for strong binders and ≥ 0. 5% to < 2% for weak binders. The peptides preferred to or unique to TAP1-KO cells (Figure 5.3) were assigned to the HLA class I allotype for which they have the lowest %Rank EL score. Where the %Rank EL scores were high and comparable among the three alleles, peptides were assigned based on their seq-to-logo motif relative to the seq-to-logo motifs of HLA class I-associated peptides (Figure 5.4). Using these criteria, 19, 13, and 2 peptides were assigned to HLA-C*03:03, HLA-A*02:01, and HLA-B*15:11, respectively (Figure 5.5A). These peptide counts are consistent with the findings of a greater loss in HLA-B expression in TAP1-KO cells compared with HLA-A*02:01 or HLA-C*03:03.

Based on the length distribution of the peptides (Figure 5.5B), A*02:01 is mostly restricted to 9mers. Similarly, the 2 peptides presented by B*15:11 are 9mers. In contrast, C*03:03 presents mostly 10mers, followed by 11mers and 12mers, suggesting more length flexibility for this

allotype. The peptides assigned to A*02:01 also generally have high predicted affinities, demonstrated by the closely clustered low % Rank EL values (Figure 5.5C). On the other hand, peptides assigned to C*03:03 have a broader range of % Rank EL (Figure 5.5C). Based on their broad predicted affinity distributions, some peptides assigned to C*03:03 may bind non-classical HLA class I expressed in TAP-deficient cells or are non-specific.

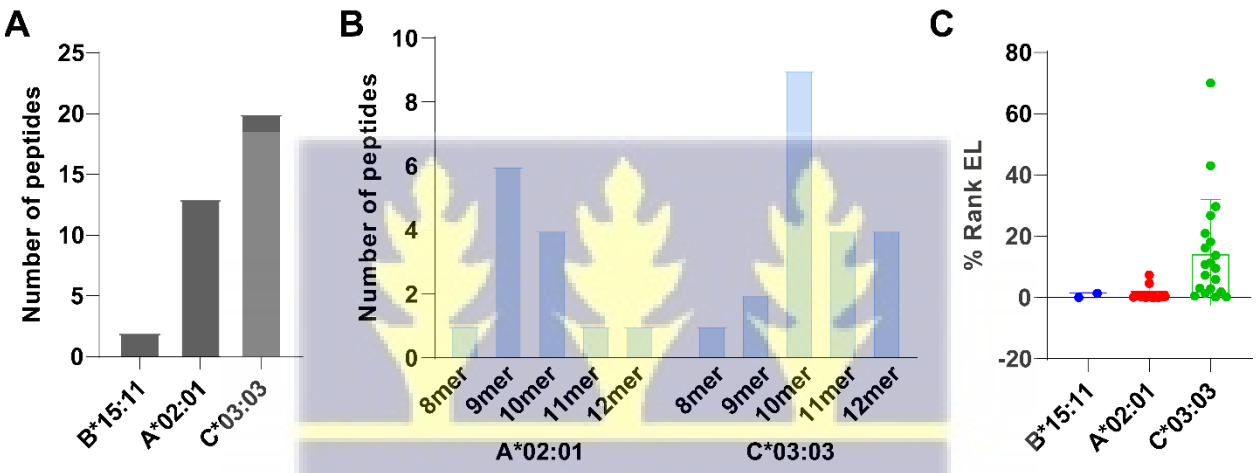

Figure 5.5 Number of peptides, length, and affinity distributions by alleles. A) HLA class I assignments of unique to or preferentially detected in TAP1-deficient THP1 cells. B) Length distribution of peptides assigned to A*02:01 and B*15:11. C) Distribution of percentile rank of the eluted ligand (EL) likelihood scores (% Rank EL) of peptides assigned to HLA class I alleles. The % Rank EL was computed from NetMHCpan-4.1 (https://services.healthtech.dtu.dk/services/NetMHCpan-4.1/). It is predicted binding affinity scores normalized across random natural peptides of HLA alleles to account for cellular processes that may confound the predicted binding affinity scores (Reynisson et al., 2020).

5.3.6 Subcellular distributions of source proteins from TAP-deficient THP-1 cells indicate non-canonical peptide sources for HLA class I assembly.

In the canonical HLA class I antigen presentation pathway, peptides are predominantly generated from cytosolic proteins and translocated into the ER where they are loaded onto HLA class I proteins. To identify the source protein of peptides presented by HLA class I, the peptides were mapped to all human proteins in the UniProt database (https://www.uniprot.org/id-mapping) and information about the subcellular localization of their source proteins were retrieved. As presented in Figure 5.5A, peptides unique to or preferred by wild-type THP-1 cells are mostly derived from proteins in the cytoplasm and the nucleus. In contrast, mitochondrial, ER, and secreted proteins are more frequent source proteins for peptides unique to or preferred by THP-1-TAP-1-KO cells. Additionally, and consistent with previous reports (Marijt et al., 2018; Wei & Cresswell, 1992), peptides derived from the ER-localization signal sequence are enriched in TAP-deficient THP-1 cells relative to the wild-type (Figure 5.5B). This differential protein source landscape suggests that when peptide transport by TAP is impaired, peptides may be derived from non-canonical sources such as the endosomes (for secreted proteins), ER, and mitochondria to sustain antigen presentation.

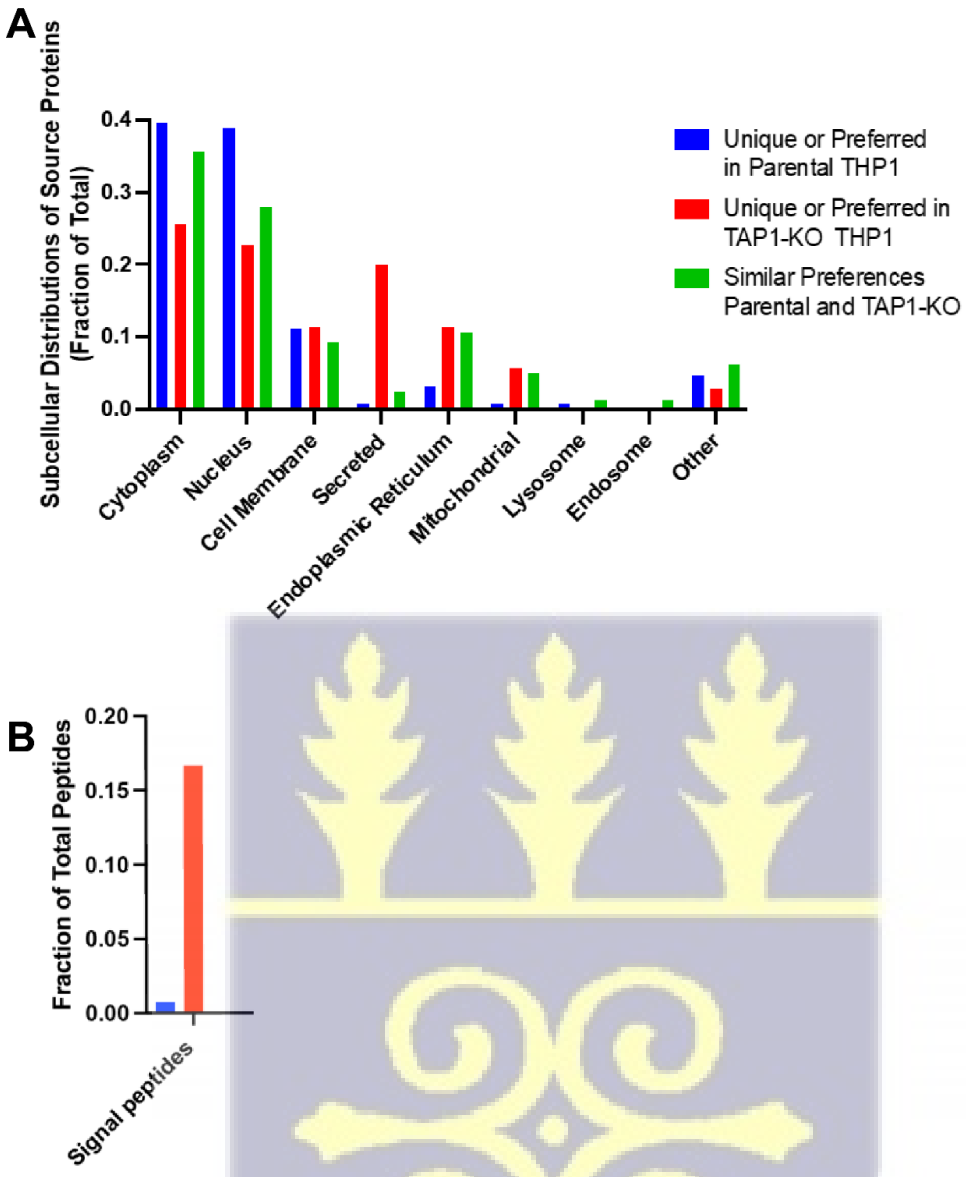

Figure 5.6: TAP-KO unique or preferred peptides' protein source. Mitochondrial, secreted, and ER proteins (A), in addition to signal peptides (B), are more frequent source proteins for peptides bound to HLA class I in TAP-deficient cells. These analyses were performed by Avrokin Surnilla.

5.3.7 Bafilomycin treatment compromises HLA class I surface expression on wild-type and TAP-deficient cells

The presentation of peptides from non-canonical sources in TAP-deficient cells (Figure 5.6A) suggests possible processing and assembly of endogenous peptides beyond the ER. Endocytic organelles have been implicated as providing a suitable compartment for the assembly of antigenic exogenous peptides with HLA class I proteins and their cross-presentation under TAP-deficient conditions (Barbet et al., 2021; Sengupta et al., 2024). Another recent study has also implicated endocytic organelles, particularly the endolysosomes, in the assembly and presentation of endogenous peptides by some HLA class I allotypes in professional antigen-presenting primary cells, with normal TAP functioning (Olson et al., 2023). Against this backdrop, we hypothesize that endocytic organelles are involved, at least, in a supplemental assembly of endogenous peptides with HLA class I proteins under TAP-deficient conditions.

To test this hypothesis, we evaluated the contribution of endolysosomes, which are gradient pH-dependent compartments, to HLA class I surface expression in TAP-deficient THP-1 cells. THP-1 and THP-1-TAP-1-KO cells were treated with 200 nM bafilomycin (BafA1) for 1-4 hours, and the surface HLA class I expression was measured using the pan-HLA class I antibody, W6/32, at the time points. Bafilomycin A1 (BafA1) disrupts pH-dependent endocytic processes by inhibiting the acidification inhibiting V-ATPases and the transport of hydrogen ions (H^+, proton) into the organelles. BafA1 is specific for V-ATPases and over the years, has become a formidable pharmacological agent for studying endocytic recycling of proteins, including HLA class I molecules (Johnson et al., 1993; Olson et al., 2023; Presley et al., 1997; Roeth et al., 2004). The flow cytometric analysis shows that relative to untreated cells, the pan surface HLA class I expression in both wild-type and TAP-deficient THP-1 cells is consistently reduced by BafA1

treatment. Notably, THP-1-TAP-1-KO cells showed greater susceptibility to BafA1, with a statistically significant difference ($p \leq 0.05$) observed four hours post-treatment. This result suggests a constitutive use of the pH-dependent endolysosomal pathway for HLA class I recycling in wild-type and TAP-deficient cells. Wild-type cells lose HLA class I expression more significantly in response to bafilomycin treatment compared with TAP1-KO cells, which is likely due to the expected faster degradation (vs. recycling) rates of HLA class I in the TAP-deficient cells.

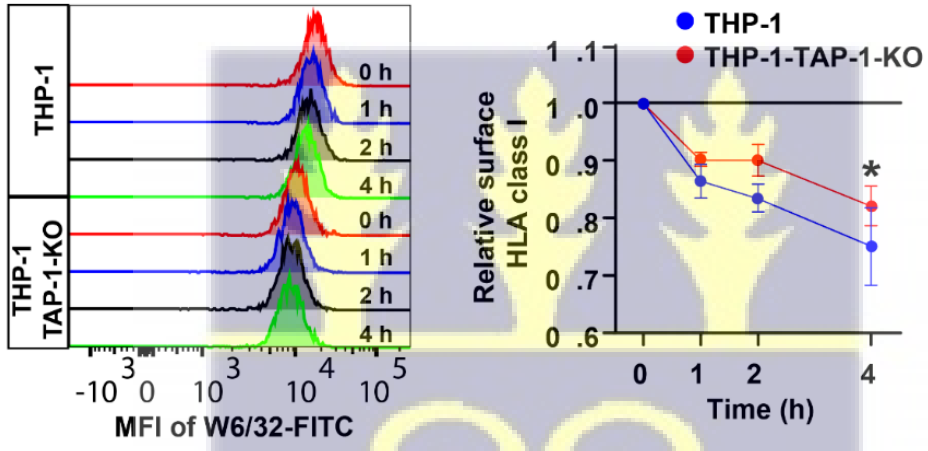

Figure 5.7: Bafilomycin treatment compromises HLA class I surface expression on wild-type and TAP-deficient THP-1cells. The cells were treated with 200 nM BafA1 or dimethyl sulfoxide at the indicated time, and flow cytometry was performed to assess surface HLA class I after staining with W6/32-FITC on ice for 30 minutes. Representative histograms (left) and averaged data across 5 experiments (right) are shown. Surface HLA class I in THP-1 and THP-1-TAP-1-KO cells were compared by a paired *t*-test. * = *p* value ≤ 0.05.

5.3.8. RAB11A depletion decreases surface HLA class I on wild-type and TAP-1-deficient THP-1 cells

RAB11 proteins are members of the RAB family of small GTPases that play significant roles in recycling membrane proteins from endocytic compartments to the plasma membrane. RAB11-dependent recycling contributes to HLA class I assembly with peptides, especially during cross-presentation (Adiko et al., 2015; Nair-Gupta et al., 2014). To further examine the involvement of endocytic recycling in constitutive HLA class I assembly under wild and TAP-deficient conditions, we depleted RAB11A in wild-type THP-1 and THP-1-TAP-1-KO cells using RAB11A SMARTpool ON-TARGET plus siRNA (L-004726-00-0010, Dharmacon), adapting a protocol previously described (Troegeler et al., 2014). RAB11A depletion was confirmed by immunoblot (Figure 5.8A) and surface HLA class I expression was measured by flow cytometry (Figure 5.8B). The analyses revealed that RAB11A depletion reduces surface HLA class I on the plasma membrane of both THP-1 and THP-1-TAP-1-KO cells. In addition to the siRNA-based approach, we depleted RAB11A in THP-1 cells using the CRISPR-Cas9 method (Figure 5.8C) and measured the surface HLA class I (Figure 5.8D). Consistent with our initial observation, CRISPR-Cas9-mediated depletion of RAB11A significantly reduces surface HLA class I on THP-1 cells. These findings support the model that RAB11A contributes to the constitutive recycling of HLA class I not only in TAP-deficient THP-1 cells but also in wild type cells.

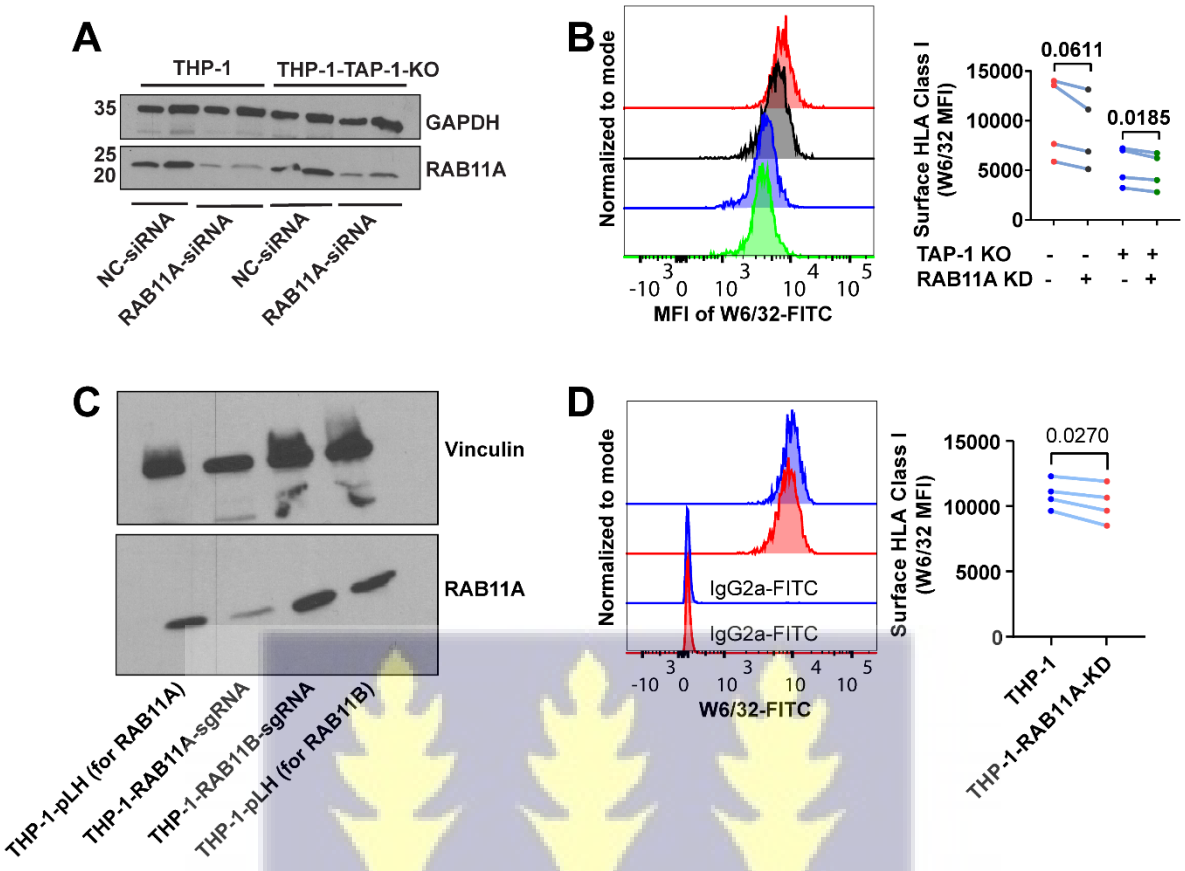

Figure 5.8: RAB11A depletion decreases surface HLA class I on wild-type and TAP-deficient THP-1 cells. A) Immunoblot showing RAB11A knockdown in THP-1 and THP-1-TAP-1-KO cells by siRNA. B) Surface HLA class I on THP-1 and THP-1-TAP-1-KO cells with or without RAB11A knockdown, measured by flow cytometry after staining with W6/32-FITC. Representative histograms (left) and averaged data across 4 experiments (right) are shown. C) Immunoblot showing RAB11A knockdown in THP-1 cells by CRISPR-Cas9. D) Surface HLA class I on THP-1 cells with or without CRSISPR-Cas9-mediated RAB11 depletion, measured by flow cytometry after staining with W6/32-FITC. Representative histograms (left) and averaged data across 4 experiments (right) are shown.

5.3.9 Invariant chain depletion increases surface HLA class I expression on TAP-deficient THP-1 cells

Next, we investigated whether the invariant chain (Ii or CD74), a multifunctional glycoprotein that plays a crucial role in the biosynthesis of HLA class II and antigen presentation to $CD4^+$ T cells (Jones et al., 1979; Schroder, 2016), might also play a role in the trafficking of HLA class I to endosomal compartments. CD74 has been suggested to mediate endosomal trafficking of MHC class I during cross-presentation (Basha et al., 2012; Sugita & Brenner, 1995). CD74 interacts with MHC class I proteins in the ER and facilitates their trafficking to endolysosomal compartments (Sugita & Brenner, 1995). Given these prior findings related to CD74, we investigated whether and how CD74 influences endosomal assembly and trafficking of HLA class I in parental or TAP-deficient THP-1 cells. CD74 was depleted in THP-1 or THP-1-TAP-1-KO cells using the CRISPR-Cas9 approach and stained with W6/32-FITC to measure the surface HLA class I expression by flow cytometry. As shown in Figure 5.9B, whereas surface HLA class I expression is unaffected by CD74 depletion in wild-type THP-1 cells, CD74 depletion moderately increases surface HLA class I in THP-1-TAP-1-KO cells. These results suggest that in TAP-deficient THP-1 cells, HLA class I molecules transported to endocytic compartments in a CD74-dependent manner are degraded rather than productively assembled for further transport to the plasma membrane. The destination endocytic/lysosomal compartment following CD74-dependent transport could be unfavorable for assembly and likely distinct from $Rab11a^+$ recycling compartments.

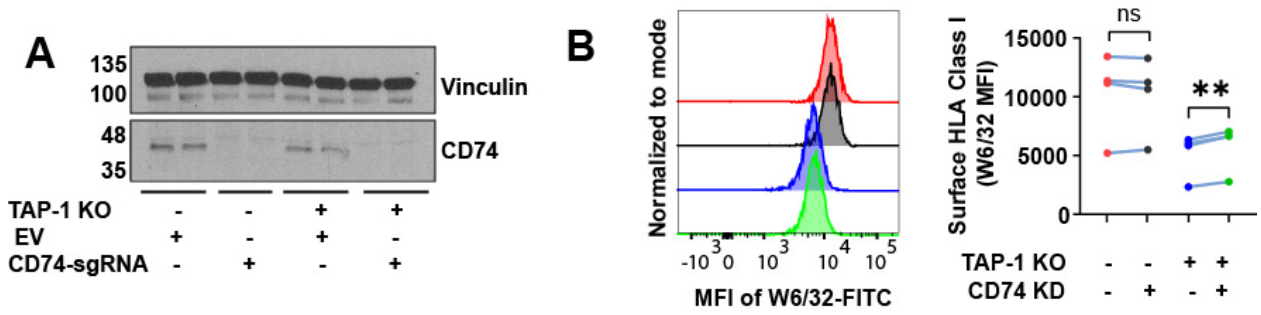

Figure 5.9: CD74 depletion increases surface HLA class I expression in TAP-deficient THP-1 cells. A) Immunoblot showing CD74 expression levels in THP-1 or THP-1-TAP-1-KO cells transduced with empty lentivirus CRISPR-Cas9 vector (EV) or CRISPR-Cas9 vector expressing CD74 single guide RNA (CD74-sgRNA). B) Surface HLA class I on THP-1 or THP-1-TAP-1-KO cells measured by flow cytometry after staining with W6/32-FITC. Representative histograms are shown on the left and compiled data from 3 experiments are on the right. Paired *t*-tests were used for pair-wise comparisons. ns = $p > 0.05$, ** = p value < 0.01.

5.4 Discussion

Peptide availability to HLA class I proteins in the ER relies on a TAP-dependent transport mechanism. Hence, in TAP dysfunctional conditions, HLA class I-peptide assembly is compromised, resulting in decreased surface expression and peptide presentation to effector cells. Although TAP deficiency downmodulates all HLA class I, the flow cytometric assessment of surface HLA class I alleles using specific antibodies (Figure 5.1B-D) revealed a differential dependence on TAP among the representative HLA-A, -B, and -C alleles, with HLA-B*15:11 most severely affected. This difference could have clinical consequences in the context of infections or diseases that impair TAP function. The relative dependence of HLA-B alleles upon TAP for their expression has been investigated previously (Geng et al., 2018). However, the extent to which TAP dysfunction affects various HLA-A and -C allotypes differently has not been investigated and hence remains an important area of further research.

The W6/32 immunoaffinity approach used in this study effectively precipitated HLA class I-peptide complex (Figures 4.2B and C). However, the number of peptides recovered through mass spectrometry is generally low, especially in the wild-type cells (with a functional TAP) in which more peptides were expected (Figure 5.3). This poor peptide recovery requires additional optimization of the protocol used for peptide isolation and mass spectrometric analysis. Nevertheless, the findings from this study are still valid and provide some novel insights into HLA class I assembly and antigen presentation in cells lacking TAP function. For instance, the flow cytometric assessment of surface HLA class I presented in Figures 4.1B-C, shows that some HLA class I are still expressed on the cell surface despite TAP deficiency, and corroborates the mass spectrometry results that a large fraction of peptides (up to 80%) is shared by THP-1 and THP-1-TAP-KO cells (Figure 5.3). Notably, the severe (~14-fold) downmodulation of HLA-B*15:11 in

TAP-deficient THP-1 cells (Figure 5.1C) translates to a severe reduction in the number of peptides (2 peptides) presented by the allele in THP-1-TAP-1-KO cells. Although HLA-C*03:03 is more dependent on TAP than HLA-A*02:01 (3.8- vs 2.3-fold reduction of surface expression in THP-1-TAP-1-KO cells) (Figures 4.2B and D), more TAP-independent or TAP-KO preferred peptides associate with HLA-C*03:03 (prediction of 19 peptides) than HLA-A*02:01 (13 peptides) (Figure 5.5A). This unexpected difference could be explained by the more restrictive anchor motifs of HLA-A*02:01 (Figure 5.5C), which may prevent the binding of some low-affinity peptides to the allotype under the suboptimal assembly conditions induced by TAP deficiency. This view is supported by the higher prevalence of peptides with predicted lower affinities that are presented by HLA-C*03:03 compared to HLA-A*02:01 (Figure 5.5C).

This study has identified novel TAP-independent peptides or peptides preferred by HLA class I alleles in TAP-deficient conditions, increasing the repertoire of peptides that could be explored for effective immunotherapies against infectious diseases or malignant conditions that disrupt the peptide transport function of TAP. The peptides unique to TAP1-KO cells are potential candidates for T-cell epitopes associated with impaired peptide processing (Marijt et al., 2018; Marijt et al., 2019) and should be further explored for $CD8^+$ T-cell activation. The study has also provided insights into HLA class I antigen presentation pathways and the nature of peptides presented in TAP-deficient cells. Notably, the extensive peptide sharing (> 80%) between wild-type and TAP-deficient cells suggests common pathways for peptide acquisition or select proteins under both conditions are favoured as peptide sources. One such pathway could involve Rab11a+ endocytic recycling compartments previously shown to be relevant to cross-presentation (Figure 5.10). Data in Chapter 3 support a Golgi-dependent trafficking pathway model for the cell surface expression of HLA class I in TAP-deficient cells. At least a subset of such HLA class I is expected to be

suboptimally loaded and peptide-receptive, following internalization through endocytosis. Subsequent assembly of the endocytosed HLA class I with peptides that are present or generated within early endosomes could allow for their enhanced recycling to the plasma membrane. This model (Figure 5.10) is consistent with both the bafilomycin (Figure 5.7A) and Rab11a (Figures 5.8B and D) sensitivity of HLA class I expression in wild-type and TAP-deficient cells. This model also supports the view that constitutive endosomal assembly can supplement ER assembly both under wild-type conditions (Olson et al., 2023) and when components of the antigen presentation machinery are impaired.

Overall, this study provides evidence for the involvement of endosomal pathways for HLA class I trafficking, which operates constitutively in both TAP-deficient and wild-type THP-1 cells. Although the small GTPase RAB11A promotes HLA class I recycling in TAP-deficient cells, the HLA class II invariant chain is associated with the degradation of HLA class I molecules. Thus, the endosomal assembly of HLA class I and class II is expected to involve distinct endocytic compartments.

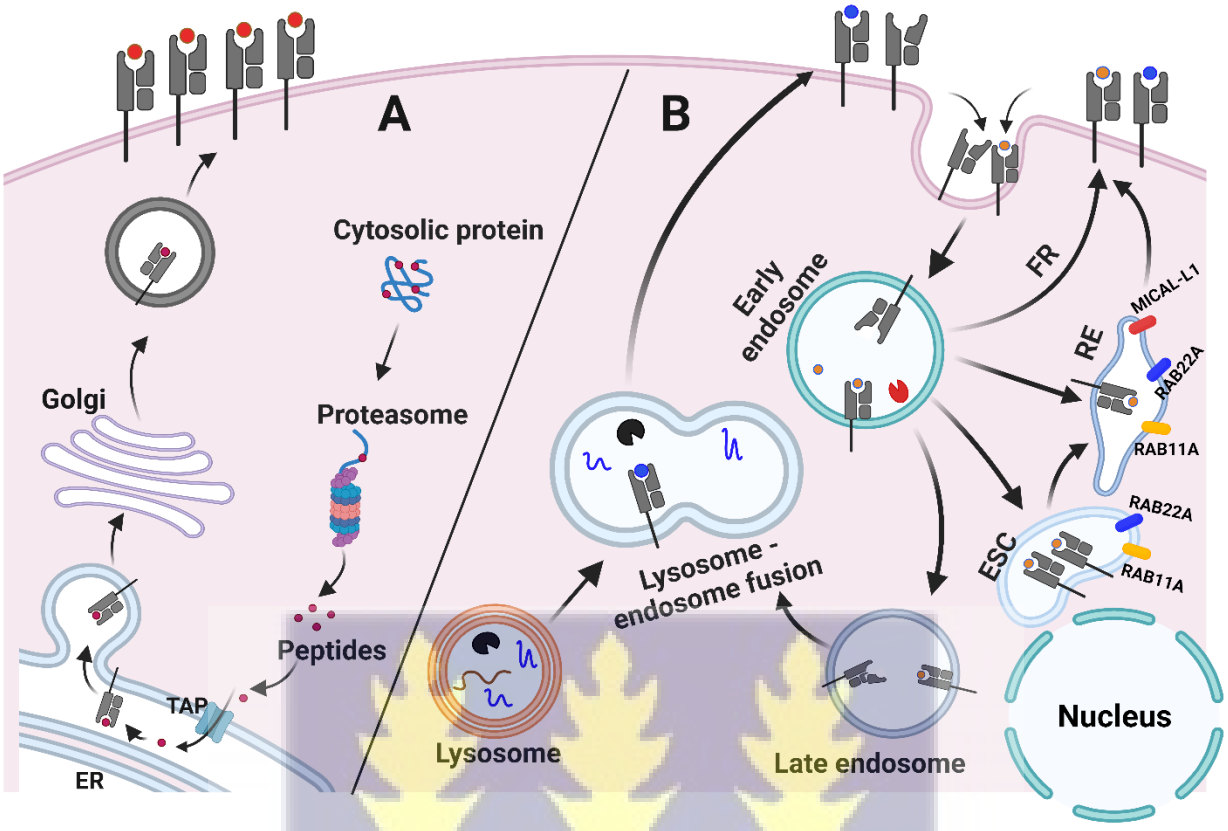

Figure 5.10: Suboptimally assembled HLA class I proteins undergo supplemental endosomal assembly in a pH- and Rab11a-dependent manner: A) Conventional HLA class I antigen presentation. Peptides generated in the proteasome are transported into the endoplasmic reticulum via TAP and are presented on the plasma membrane in a trans-Golgi-dependent pathway. B) Suboptimally assembled HLA class I proteins are internalized from the plasma membrane into an early endosome and proceed to a late endosome. The late endosome fuses with an antigen-bearing lysosome to form an endolysosomal compartment. Within this compartment, antigens are assembled with HLA class I and presented on the plasma membrane. This pathway is gradient pH-dependent and hence sensitive to brefeldin A. HLA class I in the early endosomes may quickly recycle to the plasma membrane through the fast-recycling route (FR) or are sorted into endocytic storage compartments (ESC, also known as endocytic recycling compartments, ERC) or recycling

endosomes and recycled to the plasma membrane in a Rab11a-dependent pathway. The recycling from endosomes may be influenced by other factors not investigated in this study, including Rab22a and molecules interacting with CasL-like protein 1 (MICAL-L1) (Blander, 2016; Grant & Donaldson, 2009; Montealegre & van Endert, 2018; van Endert, 2016). Image created in BioRender.com.

5.5 Conclusion

TAP-deficient THP-1 cells derive many peptides from non-canonical sources, but a large fraction of the peptides is shared with wild-type THP-1 cells. Endosomal assembly contributes to HLA class I assembly in TAP-deficient THP-1, as well as the wild-type cells. Although some HLA class I molecules are expressed on the cell surface via an endosomal pathway, CD74 mediates degradation of HLA class I under TAP deficiency.

GENERAL DISCUSSIONS

HLA class I proteins are transmembrane glycoproteins that play a crucial role in immunity by presenting antigens from intracellular (endogenous) or extracellular (exogenous) sources to CTLs. HLA class I proteins also moderate the activities of NK cells, ensuring a dynamic balance between NK cell activation and inhibition. The conventional pathway for HLA class I antigen presentation, which involves the transport of antigens from the ER to the plasma membrane through the Golgi, relies on TAP to translocate peptides from the cytosol into the ER (Blum et al., 2013; Deverson et al., 1990). Many viruses and cancers have evolved strategies to disrupt TAP function and antigen presentation, and evade immune surveillance (Mantel et al., 2022). However, HLA class proteins are highly polymorphic, and some allotypes exhibit less dependence on peptide transport by TAP (Geng et al., 2018). Such allotypes can present antigens for CTL activation even under TAP-deficient conditions.

The pathway for TAP-independent HLA class I antigen presentation and the nature and repertoire of peptides presented are poorly understood. Generic knowledge about N-glycan maturation during ER-Golgi glycoprotein trafficking (Aebi, 2013; Stanley et al., 2022), emerging concepts of ER stress-induced unconventional protein secretion (Ahat et al., 2022; Chiritoiu et al., 2019; Cleyrat et al., 2014; Gee et al., 2011; Kim et al., 2018; Nuchel et al., 2021), ER retention of misfolded HLA class I molecules in TAP deficient cells (de la Salle et al., 1999; Ljunggren et al., 1990; Raposo et al., 1995) and the discovery of Endo-H sensitive glycoforms on TAP-independent surface HLA class I molecules (Geng et al., 2018) offer valuable clues about HLA class I trafficking pathway under TAP deficiency. Briefly, secreted glycoproteins marked by Endo-H sensitive (immature) high mannose glycans are largely attributed to ER-stress-induced

unconventional (Golgi-bypass) trafficking; hence, it is likely also that TAP-independent HLA class I proteins utilize the unconventional secretory pathway.

Our survey of the unconventional pathway, depleting key factors implicated in unconventional trafficking, including GRASP55 (Ahat et al., 2019; Ahat et al., 2022; Gee et al., 2011; Rabouille, 2017), Sec22B (Barbet et al., 2021), and others (not reported in this thesis), yielded no evidence of unconventional HLA class I secretion specific to TAP deficiency (Figure 3.2). Rather, GRASP55 depletion decreases surface HLA class I expression in both wild-type and TAP-deficient cells, suggesting that a GRASP55-dependent pathway is operational in both conditions for HLA class I trafficking. GRASP55-mediated unconventional protein secretion is ER-stress and unfolded protein response-dependent (Ahat et al., 2019; Ahat et al., 2022; Chiritoiu et al., 2019; Nuchel et al., 2021). Since we did not observe any evidence, at least, of canonical unfolded protein response induction in either the TAP-deficient or the wild-type cells (Figure 3.2), it does appear that the influence of GRASP55 on HLA class I trafficking in these cells is not dependent on ER stress induction.

GRASP55 contributes to the structural integrity of the Golgi by participating in the Golgi stacking formation (Shorter et al., 1999). However, a significant functional redundancy of GRASP55 with its Golgi-resident homologue, GRASP65, has been reported, with only minimal or no Golgi stacking defects observed when either protein is depleted (Chiritoiu et al., 2019; Xiang & Wang, 2010; Zhang & Seemann, 2021). This suggests that the reduced HLA class I trafficking observed in our study is likely not induced by structural impairment of the Golgi, although we did not examine the Golgi structure. A study examining the function of GRASP55 and GRASP65 reported that the depletion of either or both proteins affects protein sorting, but this effect does not stem from structural impairment of the Golgi, unconventional protein secretion, or ER stress (Xiang et

al., 2013). The study found that upon depletion of GRASP55 or both GRASP55 and GRASP65, immature cathepsin D is missorted from the endosome/lysosome and instead secreted from the cell (Xiang et al., 2013). Although other endosomal/lysosomal proteins were not studied, this finding suggests a possible impaired endosomal/lysosomal function due to protein missorting under the GRASP55-impaired condition. A recent study (though yet to be peer-reviewed) indeed reported the missorting and secretion of lysosome-associated proteins, such as the beta-hexosaminidase subunit alpha, into extracellular compartments (Akaaboune et al., 2024) in GRASP55 knockout cells, hence confirming that GRASP55 alters the lysosomal proteome, and by extension, lysosomal functions.

Our findings in Chapter 5, that disruption of pH gradient-dependent endolysosomal functions (Figure 5.7) or recycling via Rab11a-marked endocytic compartments downmodulates surface HLA class I expression in both wild-type and TAP-deficient cells, could explain the observed effect of GRASP55 knockout on surface HLA class I expression. The assembly of endogenous peptides with HLA class I appears to be a constitutive event that contributes to antigen presentation more than appreciated in the past (our current data (Figures 5.7 and 5.8), Olson et al. (2023), and our unpublished data strongly support this position). Hence, it is plausible that GRASP55 depletion delocalizes from endolysosomes, proteins (enzymes) relevant to the constitutive HLA class I assembly in these compartments. GRASP55 knockout therefore reduces surface HLA class I expression. Further studies are required to confirm this unexpected but possible pathway through which GRASP55 regulates HLA class I trafficking.

Our data also revealed that TAP-independent HLA class I proteins utilize the ER-trans-Golgi (conventional) pathway (Figure 3.4), even though they retain their high mannose glycans on the plasma membrane (Figures 3.1D and E). We did not find evidence of a co-trafficking chaperone

under TAP deficiency that could prevent the high mannose glycans on HLA class I from being trimmed by glycan processing enzymes (Figures 3.6B and G). Additionally, significant changes in the expression of mannose-trimming enzymes were not observed, at least at the mRNA level (Figure 4.3). Moreover, although TAP deficiency specifically induces high mannose glycoform on HLA class I proteins (Figure 3.7), the high mannose induction is not specific to TAP deficiency, as other factors that compromise peptide assembly and increase misfolded HLA class I in the ER, for example, tapasin, also induce the high mannose glycoforms on surface HLA class I proteins (Figures 3.8C and D). Taken together, these findings suggest that when misfolded HLA class I proteins build up beyond the quality control capacity of the ER, HLA class I with high mannose glycans are exported to the plasma to maintain ER homeostasis. Hence, TAP deficiency does not induce ER stress (Figure 3.2) even though it increases misfolded HLA class I in the ER (de la Salle et al., 1999; Ljunggren et al., 1990; Raposo et al., 1995).

Our assessment of HLA class I trafficking regulation by ER and Golgi mannosidases revealed that EDEM1, EDEM3, MAN1A1, MAN1B1, or MAN1C1 depletion increases surface HLA class I expression. This suggests these proteins have degradative effects on HLA class I proteins and could be explored as immunotherapeutic targets.

GENERAL CONCLUSIONS

This study has made many important findings that could advance the understanding of HLA class I trafficking in normal cellular conditions and under impaired HLA class I assembly conditions, such as TAP or tapasin deficiency. TAP deficiency does not induce canonical ER stress. Under TAP-deficient conditions, HLA class I proteins traffic through the ER-trans-Golgi-dependent conventional secretory pathway despite expressing high mannose glycans on the cell surface. The

high mannose glycan expression is a homeostatic response to misfolded HLA class I accumulation in the ER, since tapasin deficiency, which induces misfolded HLA class I proteins, also triggers the high mannose expression on surface HLA class I. EDEM1, EDEM3, MAN1A1, MAN1B1, and MAN1C1 are negative regulators of surface HLA class I expression and could be explored as immunotherapeutic targets. Additionally, constitutive endolysosomal assembly of HLA class I contributes to endogenous antigen presentation in wild-type and TAP-deficient cells.

LIMITATIONS

1. We could not perform a structural analysis of the Golgi upon GRASP55 depletion. However, since previous studies have reported functional redundancy between GRASP55 and its homologue, GRASP65 (Chiritoiu et al., 2019; Xiang & Wang, 2010; Zhang & Seemann, 2021), we expect that the observed influence of GRASP55 depletion on HLA class I trafficking was not due to a structural impairment of the Golgi.

2. Among all the factors overexpressed in the surface proteome of TAP-deficient THP-1 cells, we only assessed calnexin for its possible co-trafficking with HLA class I. Although calnexin is a protein-folding chaperone, which justifies our choice of evaluating it, other factors overexpressed in the TAP-deficient cells' proteome should have been assessed.

3. Our proposed model of HLA class I trafficking under TAP deficiency indicates a defective mannose trimming resulting from the accumulation of misfolded HLA class I molecules. However, we could not pinpoint the glycan-processing step(s) and the HLA class I glycoform(s) accumulated in the trafficking pathway.

4. In the TCGA, we used bulk RNA sequence data to assess the expression levels of ER and Golgi mannosidases in cancer tumours. These bulk RNA sequence data may not reflect the cellular heterogeneity of the tumour microenvironment (Gondal et al., 2024); hence, some cell-specific gene expression differences may have been missed in our analysis.

5. Although our immunopeptidome analysis has increased the repertoire of TAP-independent peptides for HLA-A*02:01, B*15:11, and C*03:03, the total number of peptides used for the analysis (311) is relatively low. Hence, the protocol requires optimization.

RECOMMENDATIONS

1. Other factors overexpressed in TAP-deficient cells' surface proteome should be evaluated for their possible role in HLA class I glycan-processing impairment and trafficking.

2. Glycomic analysis should be performed on surface HLA class I proteins of wild-type and TAP-deficient cells to identify the glycan-processing step(s) compromised under TAP deficiency.

3. Single-cell RNA sequence data of malignant tumours should be used to compare the expression levels of the ER and Golgi mannosidases assessed in this study, as this could provide a more accurate assessment of their association with disease outcomes.

4. The TMT-mass spectrometry and sample preparation protocols for immunopeptidome analysis should be further optimized to increase the number of peptides recovered.

REFERENCES

Abele, R., & Tampe, R. (2004). The ABCs of immunology: structure and function of TAP, the transporter associated with antigen processing. *Physiology (Bethesda)*, *19*, 216-224. https://doi.org/10.1152/physiol.00002.2004

Adams, B. M., Canniff, N. P., Guay, K. P., & Hebert, D. N. (2021). The Role of Endoplasmic Reticulum Chaperones in Protein Folding and Quality Control. *Prog Mol Subcell Biol*, *59*, 27-50. https://doi.org/10.1007/978-3-030-67696-4_3

Adhikari, R., & Elliott, T. (2003). The Role of Calnexin and Calreticulin in MHC Class I Assembly. In P. Eggleton, Michalak, M. (Ed.), *Calreticulin* (pp. 85-93). Molecular Biology Intelligence Unit. Springer. https://doi.org/https://doi.org/10.1007/978-1-4419-9258-1_9

Adiko, A. C., Babdor, J., Gutierrez-Martinez, E., Guermonprez, P., & Saveanu, L. (2015). Intracellular Transport Routes for MHC I and Their Relevance for Antigen Cross-Presentation. *Front Immunol*, *6*, 335. https://doi.org/10.3389/fimmu.2015.00335

Aebi, M. (2013). N-linked protein glycosylation in the ER. *Biochim Biophys Acta*, *1833*(11), 2430-2437. https://doi.org/10.1016/j.bbamcr.2013.04.001

Ahat, E., Bui, S., Zhang, J., da Veiga Leprevost, F., Sharkey, L., Reid, W., Nesvizhskii, A. I., Paulson, H. L., & Wang, Y. (2022). GRASP55 regulates the unconventional secretion and aggregation of mutant huntingtin. *J Biol Chem*, *298*(8), 102219. https://doi.org/10.1016/j.jbc.2022.102219

Ahat, E., Li, J., & Wang, Y. (2019). New Insights Into the Golgi Stacking Proteins. *Front Cell Dev Biol*, *7*, 131. https://doi.org/10.3389/fcell.2019.00131

Akaaboune, S. R., Javed, A., Bui, S., Wierenga, A., & Wang, Y. (2024). GRASP55 Regulates Sorting and Maturation of the Lysosomal Enzyme beta-Hexosaminidase A. *bioRxiv*. https://doi.org/10.1101/2024.10.16.618769

Alimonti, J., Zhang, Q. J., Gabathuler, R., Reid, G., Chen, S. S., & Jefferies, W. A. (2000). TAP expression provides a general method for improving the recognition of malignant cells in vivo. *Nat Biotechnol*, *18*(5), 515-520. https://doi.org/10.1038/75373

Alloatti, A., Rookhuizen, D. C., Joannas, L., Carpier, J. M., Iborra, S., Magalhaes, J. G., Yatim, N., Kozik, P., Sancho, D., Albert, M. L., & Amigorena, S. (2017). Critical role for Sec22b-dependent antigen cross-presentation in antitumor immunity. *J Exp Med*, *214*(8), 2231-2241. https://doi.org/10.1084/jem.20170229

Almahayni, K., Spiekermann, M., Fiore, A., Yu, G., Pedram, K., & Mockl, L. (2022). Small molecule inhibitors of mammalian glycosylation. *Matrix Biol Plus*, *16*, 100108. https://doi.org/10.1016/j.mbplus.2022.100108

Almanza, A., Carlesso, A., Chintha, C., Creedican, S., Doultsinos, D., Leuzzi, B., Luis, A., McCarthy, N., Montibeller, L., More, S., Papaioannou, A., Puschel, F., Sassano, M. L., Skoko, J., Agostinis, P., de Belleroche, J., Eriksson, L. A., Fulda, S., Gorman, A. M., . . . Samali, A. (2019). Endoplasmic reticulum stress signalling - from basic mechanisms to clinical applications. *FEBS J*, *286*(2), 241-278. https://doi.org/10.1111/febs.14608

Anelli, T., & Sitia, R. (2008). Protein quality control in the early secretory pathway. *Embo Journal*, *27*(2), 315-327. https://doi.org/10.1038/sj.emboj.7601974

Bangia, N., Lehner, P. J., Hughes, E. A., Surman, M., & Cresswell, P. (1999). The N-terminal region of tapasin is required to stabilize the MHC class I loading complex. *Eur J Immunol*, *29*(6), 1858-1870. https://doi.org/10.1002/(SICI)1521-4141(199906)29:06<1858::AID-IMMU1858>3.0.CO;2-C

Barber, L. D., Patel, T. P., Percival, L., Gumperz, J. E., Lanier, L. L., Phillips, J. H., Bigge, J. C., Wormwald, M. R., Parekh, R. B., & Parham, P. (1996). Unusual uniformity of the N-linked oligosaccharides of HLA-A, -B, and -C glycoproteins. *J Immunol*, *156*(9), 3275-3284. https://www.ncbi.nlm.nih.gov/pubmed/8617950

Barbet, G., Nair-Gupta, P., Schotsaert, M., Yeung, S. T., Moretti, J., Seyffer, F., Metreveli, G., Gardner, T., Choi, A., Tortorella, D., Tampé, R., Khanna, K. M., García-Sastre, A., & Blander, J. M. (2021). TAP dysfunction in dendritic cells enables noncanonical cross-presentation for T cell priming. *Nature Immunology*, *22*(4), 497-509. https://doi.org/10.1038/s41590-021-00903-7

Barnstable, C. J., Bodmer, W. F., Brown, G., Galfre, G., Milstein, C., Williams, A. F., & Ziegler, A. (1978). Production of monoclonal antibodies to group A erythrocytes, HLA and other human cell surface antigens-new tools for genetic analysis. *Cell*, *14*(1), 9-20. https://doi.org/10.1016/0092-8674(78)90296-9

Basha, G., Omilusik, K., Chavez-Steenbock, A., Reinicke, A. T., Lack, N., Choi, K. B., & Jefferies, W. A. (2012). A CD74-dependent MHC class I endolysosomal cross-presentation pathway. *Nature Immunology*, *13*(3), 237-245. https://doi.org/10.1038/ni.2225

Bashirova, A. A., Viard, M., Naranbhai, V., Grifoni, A., Garcia-Beltran, W., Akdag, M., Yuki, Y., Gao, X., O'HUigin, C., Raghavan, M., Wolinsky, S., Bream, J. H., Duggal, P., Martinson, J., Michael, N. L., Kirk, G. D., Buchbinder, S. P., Haas, D., Goedert, J. J., . . . Carrington, M. (2020). HLA tapasin independence: broader peptide repertoire and HIV control. *Proc Natl Acad Sci U S A*, *117*(45), 28232-28238. https://doi.org/10.1073/pnas.2013554117

Bevan, M. J. (1976). Cross-Priming for a Secondary Cytotoxic Response to Minor H-Antigens with H-2 Congenic Cells Which Do Not Cross-React in Cytotoxic Assay. *Journal of Experimental Medicine*, *143*(5), 1283-1288. https://doi.org/DOI 10.1084/jem.143.5.1283

Bieberich, E. (2014). Synthesis, Processing, and Function of N-glycans in N-glycoproteins. *Adv Neurobiol*, *9*, 47-70. https://doi.org/10.1007/978-1-4939-1154-7_3

Biscari, L., Maza, M. C., Farre, C., Kaufman, C. D., Amigorena, S., Fresno, M., Girones, N., & Alloatti, A. (2023). Sec22b-dependent antigen cross-presentation is a significant contributor of T cell priming during infection with the parasite Trypanosoma cruzi. *Front Cell Dev Biol*, *11*, 1138571. https://doi.org/10.3389/fcell.2023.1138571

Bjorkman, P. J., Saper, M. A., Samraoui, B., Bennett, W. S., Strominger, J. L., & Wiley, D. C. (1987). Structure of the human class I histocompatibility antigen, HLA-A2. *Nature*, *329*(6139), 506-512. https://doi.org/10.1038/329506a0

Blander, J. M. (2016). The comings and goings of MHC class I molecules herald a new dawn in cross-presentation. *Immunol Rev*, *272*(1), 65-79. https://doi.org/10.1111/imr.12428

Blander, J. M. (2018). Regulation of the Cell Biology of Antigen Cross-Presentation. *Annu Rev Immunol*, *36*, 717-753. https://doi.org/10.1146/annurev-immunol-041015-055523

Blander, J. M. (2023). Different routes of MHC-I delivery to phagosomes and their consequences to CD8 T cell immunity. *Semin Immunol*, *66*, 101713. https://doi.org/10.1016/j.smim.2023.101713

Blander, J. M., Yee Mon, K. J., Jha, A., & Roycroft, D. (2023). The show and tell of cross-presentation. *Adv Immunol*, *159*, 33-114. https://doi.org/10.1016/bs.ai.2023.08.002

Blees, A., Januliene, D., Hofmann, T., Koller, N., Schmidt, C., Trowitzsch, S., Moeller, A., & Tampe, R. (2017). Structure of the human MHC-I peptide-loading complex. *Nature*, *551*(7681), 525-528. https://doi.org/10.1038/nature24627

Blum, J. S., Wearsch, P. A., & Cresswell, P. (2013). Pathways of antigen processing. *Annu Rev Immunol*, *31*, 443-473. https://doi.org/10.1146/annurev-immunol-032712-095910

Braakman, I., & Hebert, D. N. (2013). Protein folding in the endoplasmic reticulum. *Cold Spring Harb Perspect Biol*, *5*(5), a013201. https://doi.org/10.1101/cshperspect.a013201

Braud, V. M., Allan, D. S., Wilson, D., & McMichael, A. J. (1998). TAP- and tapasin-dependent HLA-E surface expression correlates with the binding of an MHC class I leader peptide. *Curr Biol*, *8*(1), 1-10. https://doi.org/10.1016/s0960-9822(98)70014-4

Burr, M. L., van den Boomen, D. J., Bye, H., Antrobus, R., Wiertz, E. J., & Lehner, P. J. (2013). MHC class I molecules are preferentially ubiquitinated on endoplasmic reticulum luminal residues during HRD1 ubiquitin E3 ligase-mediated dislocation. *Proc Natl Acad Sci U S A*, *110*(35), 14290-14295. https://doi.org/10.1073/pnas.1303380110

Cebrian, I., Visentin, G., Blanchard, N., Jouve, M., Bobard, A., Moita, C., Enninga, J., Moita, L. F., Amigorena, S., & Savina, A. (2011). Sec22b regulates phagosomal maturation and antigen crosspresentation by dendritic cells. *Cell*, *147*(6), 1355-1368. https://doi.org/10.1016/j.cell.2011.11.021

Chardin, P., & McCormick, F. (1999). Brefeldin A: the advantage of being uncompetitive. *Cell*, *97*(2), 153-155. https://doi.org/10.1016/s0092-8674(00)80724-2

Chatterjee, S., Ugonotti, J., Lee, L. Y., Everest-Dass, A., Kawahara, R., & Thaysen-Andersen, M. (2021). Trends in oligomannosylation and alpha1,2-mannosidase expression in human cancers. *Oncotarget*, *12*(21), 2188-2205. https://doi.org/10.18632/oncotarget.28064

Chen, M., & Bouvier, M. (2007). Analysis of interactions in a tapasin/class I complex provides a mechanism for peptide selection. *Embo Journal*, *26*(6), 1681-1690. https://doi.org/10.1038/sj.emboj.7601624

Chen, X., Shi, C., He, M., Xiong, S., & Xia, X. (2023). Endoplasmic reticulum stress: molecular mechanism and therapeutic targets. *Signal Transduct Target Ther*, *8*(1), 352. https://doi.org/10.1038/s41392-023-01570-w

Chiritoiu, M., Brouwers, N., Turacchio, G., Pirozzi, M., & Malhotra, V. (2019). GRASP55 and UPR Control Interleukin-1beta Aggregation and Secretion. *Dev Cell*, *49*(1), 145-155 e144. https://doi.org/10.1016/j.devcel.2019.02.011

Cleyrat, C., Darehshouri, A., Steinkamp, M. P., Vilaine, M., Boassa, D., Ellisman, M. H., Hermouet, S., & Wilson, B. S. (2014). Mpl traffics to the cell surface through conventional and unconventional routes. *Traffic*, *15*(9), 961-982. https://doi.org/10.1111/tra.12185

Cobb, B. A. (2020). The history of IgG glycosylation and where we are now. *Glycobiology*, *30*(4), 202-213. https://doi.org/10.1093/glycob/cwz065

Colbert, J. D., Cruz, F. M., & Rock, K. L. (2020). Cross-presentation of exogenous antigens on MHC I molecules. *Curr Opin Immunol*, *64*, 1-8. https://doi.org/10.1016/j.coi.2019.12.005

Cruz, F. M., Chan, A., & Rock, K. L. (2023). Pathways of MHC I cross-presentation of exogenous antigens. *Semin Immunol*, *66*, 101729. https://doi.org/10.1016/j.smim.2023.101729

Cummings, R. D., & Etzler, M. E. (2009). Antibodies and Lectins in Glycan Analysis. In A. Varki, R. D. Cummings, J. D. Esko, H. H. Freeze, P. Stanley, C. R. Bertozzi, G. W. Hart, & M. E. Etzler (Eds.), *Essentials of Glycobiology* (2nd ed.). https://www.ncbi.nlm.nih.gov/pubmed/20301245

de la Salle, H., Hanau, D., Fricker, D., Urlacher, A., Kelly, A., Salamero, J., Powis, S. H., Donato, L., Bausinger, H., Laforet, M., & et al. (1994). Homozygous human TAP peptide transporter mutation in HLA class I deficiency. *Science*, *265*(5169), 237-241. https://doi.org/10.1126/science.7517574

de la Salle, H., Saulquin, X., Mansour, I., Klayme, S., Fricker, D., Zimmer, J., Cazenave, J. P., Hanau, D., Bonneville, M., Houssaint, E., Lefranc, G., & Naman, R. (2002). Asymptomatic deficiency in the peptide transporter associated to antigen processing (TAP). *Clin Exp Immunol*, *128*(3), 525-531. https://doi.org/10.1046/j.1365-2249.2002.01862.x

de la Salle, H., Zimmer, J., Fricker, D., Angenieux, C., Cazenave, J. P., Okubo, M., Maeda, H., Plebani, A., Tongio, M. M., Dormoy, A., & Hanau, D. (1999). HLA class I deficiencies due to mutations in subunit 1 of the peptide transporter TAP1. *J Clin Invest*, *103*(5), R9-R13. https://doi.org/10.1172/JCI5687

de Waard, A. A., Verkerk, T., Hoefakker, K., van der Steen, D. M., Jongsma, M. L. M., Kadosh, D. M., Bliss, S., de Ru, A. H., Admon, A., van Veelen, P. A., Griffioen, M., Heemskerk, M. H. M., & Spaapen, R. M. (2021). Healthy cells functionally present TAP-independent SSR1 peptides: implications for selection of clinically relevant antigens. *Iscience*, *24*(2). https://doi.org/ARTN 10205110.1016/j.isci.2021.102051

Del Cid, N., Jeffery, E., Rizvi, S. M., Stamper, E., Peters, L. R., Brown, W. C., Provoda, C., & Raghavan, M. (2010). Modes of calreticulin recruitment to the major histocompatibility complex class I assembly pathway. *J Biol Chem*, *285*(7), 4520-4535. https://doi.org/10.1074/jbc.M109.085407

Della Chiesa, M., Sivori, S., Carlomagno, S., Moretta, L., & Moretta, A. (2015). Activating KIRs and NKG2C in Viral Infections: Toward NK Cell Memory? *Front Immunol*, *6*, 573. https://doi.org/10.3389/fimmu.2015.00573

Desikan, H., Kaur, A., Pogozheva, I. D., & Raghavan, M. (2023). Effects of calreticulin mutations on cell transformation and immunity. *J Cell Mol Med*, *27*(8), 1032-1044. https://doi.org/10.1111/jcmm.17713

Deverson, E. V., Gow, I. R., Coadwell, W. J., Monaco, J. J., Butcher, G. W., & Howard, J. C. (1990). MHC class II region encoding proteins related to the multidrug resistance family of transmembrane transporters. *Nature*, *348*(6303), 738-741. https://doi.org/10.1038/348738a0

Dick, T. P., Bangia, N., Peaper, D. R., & Cresswell, P. (2002). Disulfide bond isomerization and the assembly of MHC class I-peptide complexes. *Immunity*, *16*(1), 87-98. https://doi.org/10.1016/s1074-7613(02)00263-7

Diedrich, G., Bangia, N., Pan, M., & Cresswell, P. (2001). A role for calnexin in the assembly of the MHC class I loading complex in the endoplasmic reticulum. *J Immunol*, *166*(3), 1703-1709. https://doi.org/10.4049/jimmunol.166.3.1703

Dimou, S., Dionysopoulou, M., Sagia, G. M., & Diallinas, G. (2022). Golgi-Bypass Is a Major Unconventional Route for Translocation to the Plasma Membrane of Non-Apical Membrane Cargoes in Aspergillus nidulans. *Front Cell Dev Biol*, *10*, 852028. https://doi.org/10.3389/fcell.2022.852028

Domnick, A., Winter, C., Susac, L., Hennecke, L., Hensen, M., Zitzmann, N., Trowitzsch, S., Thomas, C., & Tampe, R. (2022). Molecular basis of MHC I quality control in the peptide loading complex. *Nat Commun*, *13*(1), 4701. https://doi.org/10.1038/s41467-022-32384-z

Dong, G., Wearsch, P. A., Peaper, D. R., Cresswell, P., & Reinisch, K. M. (2009). Insights into MHC class I peptide loading from the structure of the tapasin-ERp57 thiol oxidoreductase heterodimer. *Immunity*, *30*(1), 21-32. https://doi.org/10.1016/j.immuni.2008.10.018

Du, J. J., Klontz, E. H., Guerin, M. E., Trastoy, B., & Sundberg, E. J. (2020). Structural insights into the mechanisms and specificities of IgG-active endoglycosidases. *Glycobiology*, *30*(4), 268-279. https://doi.org/10.1093/glycob/cwz042

Dupont, N., Jiang, S., Pilli, M., Ornatowski, W., Bhattacharya, D., & Deretic, V. (2011). Autophagy-based unconventional secretory pathway for extracellular delivery of IL-1beta. *Embo Journal*, *30*(23), 4701-4711. https://doi.org/10.1038/emboj.2011.398

Elbein, A. D., Tropea, J. E., Mitchell, M., & Kaushal, G. P. (1990). Kifunensine, a potent inhibitor of the glycoprotein processing mannosidase I. *J Biol Chem*, *265*(26), 15599-15605. https://www.ncbi.nlm.nih.gov/pubmed/2144287

Embgenbroich, M., & Burgdorf, S. (2018). Current Concepts of Antigen Cross-Presentation. *Front Immunol*, *9*, 1643. https://doi.org/10.3389/fimmu.2018.01643

Falk, K., Rotzschke, O., Stevanovic, S., Jung, G., & Rammensee, H. G. (1991). Allele-specific motifs revealed by sequencing of self-peptides eluted from MHC molecules. *Nature*, *351*(6324), 290-296. https://doi.org/10.1038/351290a0

Ferris, S. P., Kodali, V. K., & Kaufman, R. J. (2014). Glycoprotein folding and quality-control mechanisms in protein-folding diseases. *Dis Model Mech*, *7*(3), 331-341. https://doi.org/10.1242/dmm.014589

Freeze, H. H., & Kranz, C. (2010). Endoglycosidase and glycoamidase release of N-linked glycans. *Curr Protoc Mol Biol*, *Chapter 17*, Unit 17 13A. https://doi.org/10.1002/0471142727.mb1713as89

Fruh, K., Ahn, K., Djaballah, H., Sempe, P., van Endert, P. M., Tampe, R., Peterson, P. A., & Yang, Y. (1995). A viral inhibitor of peptide transporters for antigen presentation. *Nature*, *375*(6530), 415-418. https://doi.org/10.1038/375415a0

Fujiwara, T., Oda, K., Yokota, S., Takatsuki, A., & Ikehara, Y. (1988). Brefeldin A causes disassembly of the Golgi complex and accumulation of secretory proteins in the endoplasmic reticulum. *J Biol Chem*, *263*(34), 18545-18552. https://www.ncbi.nlm.nih.gov/pubmed/3192548

Gaifem, J., Rodrigues, C. S., Petralia, F., Alves, I., Leite-Gomes, E., Cavadas, B., Dias, A. M., Moreira-Barbosa, C., Reves, J., Laird, R. M., Novokmet, M., Stambuk, J., Habazin, S., Turhan, B., Gumus, Z. H., Ungaro, R., Torres, J., Lauc, G., Colombel, J. F., . . . Pinho, S. S. (2024). A unique serum IgG glycosylation signature predicts development of Crohn's disease and is associated with pathogenic antibodies to mannose glycan. *Nature Immunology*. https://doi.org/10.1038/s41590-024-01916-8

Gao, B., Adhikari, R., Howarth, M., Nakamura, K., Gold, M. C., Hill, A. B., Knee, R., Michalak, M., & Elliott, T. (2002). Assembly and antigen-presenting function of MHC class I molecules in cells lacking the ER chaperone calreticulin. *Immunity*, *16*(1), 99-109. https://doi.org/10.1016/s1074-7613(01)00260-6

Garbi, N., Tan, P., Diehl, A. D., Chambers, B. J., Ljunggren, H. G., Momburg, F., & Hammerling, G. J. (2000). Impaired immune responses and altered peptide repertoire in tapasin-deficient mice. *Nature Immunology*, *1*(3), 234-238. https://doi.org/10.1038/79775

Gee, H. Y., Noh, S. H., Tang, B. L., Kim, K. H., & Lee, M. G. (2011). Rescue of DeltaF508-CFTR trafficking via a GRASP-dependent unconventional secretion pathway. *Cell*, *146*(5), 746-760. https://doi.org/10.1016/j.cell.2011.07.021

Geng, J., Zaitouna, A. J., & Raghavan, M. (2018). Selected HLA-B allotypes are resistant to inhibition or deficiency of the transporter associated with antigen processing (TAP). *PLoS Pathog*, *14*(7), e1007171. https://doi.org/10.1371/journal.ppat.1007171

George, G., Ninagawa, S., Yagi, H., Furukawa, J. I., Hashii, N., Ishii-Watabe, A., Deng, Y., Matsushita, K., Ishikawa, T., Mamahit, Y. P., Maki, Y., Kajihara, Y., Kato, K., Okada, T., & Mori, K. (2021). Purified EDEM3 or EDEM1 alone produces determinant oligosaccharide structures from M8B in mammalian glycoprotein ERAD. *Elife*, *10*. https://doi.org/10.7554/eLife.70357

George, G., Ninagawa, S., Yagi, H., Saito, T., Ishikawa, T., Sakuma, T., Yamamoto, T., Imami, K., Ishihama, Y., Kato, K., Okada, T., & Mori, K. (2020). EDEM2 stably disulfide-bonded to TXNDC11 catalyzes the first mannose trimming step in mammalian glycoprotein ERAD. *Elife*, *9*. https://doi.org/10.7554/eLife.53455

Gondal, M. N., Shah, S. U. R., Chinnaiyan, A. M., & Cieslik, M. (2024). A systematic overview of single-cell transcriptomics databases, their use cases, and limitations. *Front Bioinform*, *4*, 1417428. https://doi.org/10.3389/fbinf.2024.1417428

Graham, B. S., & Sullivan, N. J. (2018). Emerging viral diseases from a vaccinology perspective: preparing for the next pandemic. *Nature Immunology*, *19*(1), 20-28. https://doi.org/10.1038/s41590-017-0007-9

Grandea, A. G., 3rd, Golovina, T. N., Hamilton, S. E., Sriram, V., Spies, T., Brutkiewicz, R. R., Harty, J. T., Eisenlohr, L. C., & Van Kaer, L. (2000). Impaired assembly yet normal trafficking of MHC class I molecules in Tapasin mutant mice. *Immunity*, *13*(2), 213-222. https://doi.org/10.1016/s1074-7613(00)00021-2

Grant, B. D., & Donaldson, J. G. (2009). Pathways and mechanisms of endocytic recycling. *Nat Rev Mol Cell Biol*, *10*(9), 597-608. https://doi.org/10.1038/nrm2755

Gravel, N. H., Nelde, A., Bauer, J., Muhlenbruch, L., Schroeder, S. M., Neidert, M. C., Scheid, J., Lemke, S., Dubbelaar, M. L., Wacker, M., Dengler, A., Klein, R., Mauz, P. S., Lowenheim, H., Hauri-Hohl, M., Martin, R., Hennenlotter, J., Stenzl, A., Heitmann, J. S., . . . Walz, J. S. (2023). TOF(IMS) mass spectrometry-based immunopeptidomics refines tumor antigen identification. *Nat Commun*, *14*(1), 7472. https://doi.org/10.1038/s41467-023-42692-7

Greenwood, R., Shimizu, Y., Sekhon, G. S., & DeMars, R. (1994). Novel allele-specific, post-translational reduction in HLA class I surface expression in a mutant human B cell line. *J Immunol*, *153*(12), 5525-5536. https://www.ncbi.nlm.nih.gov/pubmed/7989754

Greppi, M., De Franco, F., Obino, V., Rebaudi, F., Goda, R., Frumento, D., Vita, G., Baronti, C., Melaiu, O., Bozzo, M., Candiani, S., Vellone, V. G., Papaccio, F., Pesce, S., & Marcenaro, E. (2024). NK cell receptors in anti-tumor and healthy tissue protection: Mechanisms and

therapeutic advances. *Immunol Lett*, *270*, 106932. https://doi.org/10.1016/j.imlet.2024.106932

Grieve, A. G., & Rabouille, C. (2011). Golgi bypass: skirting around the heart of classical secretion. *Cold Spring Harb Perspect Biol*, *3*(4). https://doi.org/10.1101/cshperspect.a005298

Gutierrez-Martinez, E., Planes, R., Anselmi, G., Reynolds, M., Menezes, S., Adiko, A. C., Saveanu, L., & Guermonprez, P. (2015). Cross-presentation of cell-associated antigens by MHC class I in dendritic cell subsets. *Front Immunol*, *6*, 363. https://doi.org/10.3389/fimmu.2015.00363

Haeri, M., & Knox, B. E. (2012). Endoplasmic reticulum stress and unfolded protein response pathways: potential for treating age-related retinal degeneration. *J Ophthalmic Vis Res*, *7*(1), 45-59. https://www.ncbi.nlm.nih.gov/pubmed/22737387

Hamester, F., Legler, K., Wichert, B., Kelle, N., Eylmann, K., Rossberg, M., Ding, Y., Kurti, S., Schmalfeldt, B., Milde-Langosch, K., & Oliveira-Ferrer, L. (2019). Prognostic relevance of the Golgi mannosidase MAN1A1 in ovarian cancer: impact of N-glycosylation on tumour cell aggregation. *Br J Cancer*, *121*(11), 944-953. https://doi.org/10.1038/s41416-019-0607-2

Harding, H. P., Novoa, I., Zhang, Y., Zeng, H., Wek, R., Schapira, M., & Ron, D. (2000). Regulated translation initiation controls stress-induced gene expression in mammalian cells. *Mol Cell*, *6*(5), 1099-1108. https://doi.org/10.1016/s1097-2765(00)00108-8

Haslund-Gourley, B. S., Woloszczuk, K., Hou, J., Connors, J., Cusimano, G., Bell, M., Taramangalam, B., Fourati, S., Mege, N., Bernui, M., Altman, M. C., Krammer, F., van Bakel, H., Network, I., Maecker, H. T., Rouphael, N., Diray-Arce, J., Wigdahl, B., Kutzler, M. A., . . . Comunale, M. A. (2024). IgM N-glycosylation correlates with COVID-19 severity and rate of complement deposition. *Nat Commun*, *15*(1), 404. https://doi.org/10.1038/s41467-023-44211-0

Hay, J. C., Chao, D. S., Kuo, C. S., & Scheller, R. H. (1997). Protein interactions regulating vesicle transport between the endoplasmic reticulum and Golgi apparatus in mammalian cells. *Cell*, *89*(1), 149-158. https://doi.org/10.1016/s0092-8674(00)80191-9

He, M., Zhou, X., & Wang, X. (2024). Glycosylation: mechanisms, biological functions and clinical implications. *Signal Transduct Target Ther*, *9*(1), 194. https://doi.org/10.1038/s41392-024-01886-1

Henderson, R. A., Michel, H., Sakaguchi, K., Shabanowitz, J., Appella, E., Hunt, D. F., & Engelhard, V. H. (1992). HLA-A2.1-associated peptides from a mutant cell line: a second pathway of antigen presentation. *Science*, *255*(5049), 1264-1266. https://doi.org/10.1126/science.1546329

Henle, A. M., Nassar, A., Puglisi-Knutson, D., Youssef, B., & Knutson, K. L. (2017). Downregulation of TAP1 and TAP2 in early stage breast cancer. *Plos One*, *12*(11). https://doi.org/ARTN e018732310.1371/journal.pone.0187323

Herr, W., Ranieri, E., Gambotto, A., Kierstead, L. S., Amoscato, A. A., Gesualdo, L., & Storkus, W. J. (1999). Identification of naturally processed and HLA-presented Epstein-Barr virus peptides recognized by CD4(+) or CD8(+) T lymphocytes from human blood. *Proc Natl Acad Sci U S A*, *96*(21), 12033-12038. https://doi.org/10.1073/pnas.96.21.12033

Hong, S., Hwang, I., Gim, E., Yang, J., Park, S., Yoon, S. H., Lee, W. W., & Yu, J. W. (2019). Brefeldin A-sensitive ER-Golgi vesicle trafficking contributes to NLRP3-dependent caspase-1 activation. *FASEB J*, *33*(3), 4547-4558. https://doi.org/10.1096/fj.201801585R

Howarth, M., Williams, A., Tolstrup, A. B., & Elliott, T. (2004). Tapasin enhances MHC class I peptide presentation according to peptide half-life. *Proc Natl Acad Sci U S A*, *101*(32), 11737-11742. https://doi.org/10.1073/pnas.0306294101

Howe, C., Garstka, M., Al-Balushi, M., Ghanem, E., Antoniou, A. N., Fritzsche, S., Jankevicius, G., Kontouli, N., Schneeweiss, C., Williams, A., Elliott, T., & Springer, S. (2009). Calreticulin-dependent recycling in the early secretory pathway mediates optimal peptide loading of MHC class I molecules. *Embo Journal*, *28*(23), 3730-3744. https://doi.org/10.1038/emboj.2009.296

Iannotti, M. J., Figard, L., Sokac, A. M., & Sifers, R. N. (2014). A Golgi-localized mannosidase (MAN1B1) plays a non-enzymatic gatekeeper role in protein biosynthetic quality control. *J Biol Chem*, *289*(17), 11844-11858. https://doi.org/10.1074/jbc.M114.552091

Istrail, S., Florea, L., Halldorsson, B. V., Kohlbacher, O., Schwartz, R. S., Yap, V. B., Yewdell, J. W., & Hoffman, S. L. (2004). Comparative immunopeptidomics of humans and their pathogens. *Proc Natl Acad Sci U S A*, *101*(36), 13268-13272. https://doi.org/10.1073/pnas.0404740101

Jahn, R., Cafiso, D. C., & Tamm, L. K. (2024). Mechanisms of SNARE proteins in membrane fusion. *Nat Rev Mol Cell Biol*, *25*(2), 101-118. https://doi.org/10.1038/s41580-023-00668-x

Jiang, J., Natarajan, K., Boyd, L. F., Morozov, G. I., Mage, M. G., & Margulies, D. H. (2017). Crystal structure of a TAPBPR-MHC I complex reveals the mechanism of peptide editing in antigen presentation. *Science*, *358*(6366), 1064-1068. https://doi.org/10.1126/science.aao5154

Jiang, J., Taylor, D. K., Kim, E. J., Boyd, L. F., Ahmad, J., Mage, M. G., Truong, H. V., Woodward, C. H., Sgourakis, N. G., Cresswell, P., Margulies, D. H., & Natarajan, K. (2022). Structural mechanism of tapasin-mediated MHC-I peptide loading in antigen presentation. *Nat Commun*, *13*(1), 5470. https://doi.org/10.1038/s41467-022-33153-8

Jin, Z. C., Kitajima, T., Dong, W., Huang, Y. F., Ren, W. W., Guan, F., Chiba, Y., Gao, X. D., & Fujita, M. (2018). Genetic disruption of multiple alpha1,2-mannosidases generates mammalian cells producing recombinant proteins with high-mannose-type N-glycans. *J Biol Chem*, *293*(15), 5572-5584. https://doi.org/10.1074/jbc.M117.813030

Johnson, L. S., Dunn, K. W., Pytowski, B., & McGraw, T. E. (1993). Endosome acidification and receptor trafficking: bafilomycin A1 slows receptor externalization by a mechanism involving the receptor's internalization motif. *Mol Biol Cell*, *4*(12), 1251-1266. https://doi.org/10.1091/mbc.4.12.1251

Jones, P. P., Murphy, D. B., Hewgill, D., & McDevitt, H. O. (1979). Detection of a common polypeptide chain in I--A and I--E sub-region immunoprecipitates. *Mol Immunol*, *16*(1), 51-60. https://doi.org/10.1016/0161-5890(79)90027-0

Jung, J., Kim, J., Roh, S. H., Jun, I., Sampson, R. D., Gee, H. Y., Choi, J. Y., & Lee, M. G. (2016). The HSP70 co-chaperone DNAJC14 targets misfolded pendrin for unconventional protein secretion. *Nat Commun*, *7*, 11386. https://doi.org/10.1038/ncomms11386

Kaur, A., Surnilla, A., Zaitouna, A. J., Mumphrey, M. B., Basrur, V., Grigorova, I., Cieslik, M., Carrington, M., Nesvizhskii, A. I., & Raghavan, M. (2023). Mass Spectrometric Profiling of HLA-B44 Peptidomes Provides Evidence for Tapasin-Mediated Tryptophan Editing. *J Immunol*, *211*(9), 1298-1307. https://doi.org/10.4049/jimmunol.2300232

Kim, J., Gee, H. Y., & Lee, M. G. (2018). Unconventional protein secretion - new insights into the pathogenesis and therapeutic targets of human diseases. *J Cell Sci*, *131*(12). https://doi.org/10.1242/jcs.213686

Kozutsumi, Y., Segal, M., Normington, K., Gething, M. J., & Sambrook, J. (1988). The presence of malfolded proteins in the endoplasmic reticulum signals the induction of glucose-regulated proteins. *Nature*, *332*(6163), 462-464. https://doi.org/10.1038/332462a0

Kulski, J. K., Suzuki, S., & Shiina, T. (2022). Human leukocyte antigen super-locus: nexus of genomic supergenes, SNPs, indels, transcripts, and haplotypes. *Hum Genome Var*, *9*(1), 49. https://doi.org/10.1038/s41439-022-00226-5

Lamoliatte, F., McManus, F. P., Maarifi, G., Chelbi-Alix, M. K., & Thibault, P. (2017). Uncovering the SUMOylation and ubiquitylation crosstalk in human cells using sequential peptide immunopurification. *Nat Commun*, *8*, 14109. https://doi.org/10.1038/ncomms14109

Lamoreaux, L., Roederer, M., & Koup, R. (2006). Intracellular cytokine optimization and standard operating procedure. *Nat Protoc*, *1*(3), 1507-1516. https://doi.org/10.1038/nprot.2006.268

Lampen, M. H., Verweij, M. C., Querido, B., van der Burg, S. H., Wiertz, E. J., & van Hall, T. (2010). CD8+ T cell responses against TAP-inhibited cells are readily detected in the human population. *J Immunol*, *185*(11), 6508-6517. https://doi.org/10.4049/jimmunol.1001774

Lee, J., Oldham, M. L., Manon, V., & Chen, J. (2024). Principles of peptide selection by the transporter associated with antigen processing. *Proc Natl Acad Sci U S A*, *121*(23), e2320879121. https://doi.org/10.1073/pnas.2320879121

Lee, J. M., Hammaren, H. M., Savitski, M. M., & Baek, S. H. (2023). Control of protein stability by post-translational modifications. *Nat Commun*, *14*(1), 201. https://doi.org/10.1038/s41467-023-35795-8

Lehnert, E., & Tampe, R. (2017). Structure and Dynamics of Antigenic Peptides in Complex with TAP. *Front Immunol*, *8*, 10. https://doi.org/10.3389/fimmu.2017.00010

Li, T., Fu, J., Zeng, Z., Cohen, D., Li, J., Chen, Q., Li, B., & Liu, X. S. (2020). TIMER2.0 for analysis of tumor-infiltrating immune cells. *Nucleic Acids Res*, *48*(W1), W509-W514. https://doi.org/10.1093/nar/gkaa407

Li, X., You, J., Hong, L., Liu, W., Guo, P., & Hao, X. (2023). Neoantigen cancer vaccines: a new star on the horizon. *Cancer Biol Med*, *21*(4), 274-311. https://doi.org/10.20892/j.issn.2095-3941.2023.0395

Lizee, G., Basha, G., Tiong, J., Julien, J. P., Tian, M., Biron, K. E., & Jefferies, W. A. (2003). Control of dendritic cell cross-presentation by the major histocompatibility complex class I cytoplasmic domain. *Nature Immunology*, *4*(11), 1065-1073. https://doi.org/10.1038/ni989

Ljunggren, H. G., Stam, N. J., Ohlen, C., Neefjes, J. J., Hoglund, P., Heemels, M. T., Bastin, J., Schumacher, T. N., Townsend, A., Karre, K., & et al. (1990). Empty MHC class I molecules come out in the cold. *Nature*, *346*(6283), 476-480. https://doi.org/10.1038/346476a0

Lorente, E., Infantes, S., Barnea, E., Beer, I., Barriga, A., Garcia-Medel, N., Lasala, F., Jimenez, M., Admon, A., & Lopez, D. (2013). Diversity of natural self-derived ligands presented by different HLA class I molecules in transporter antigen processing-deficient cells. *Plos One*, *8*(3), e59118. https://doi.org/10.1371/journal.pone.0059118

Luo, H., Jiao, Q., Shen, C., Shao, C., Xie, J., Chen, Y., Feng, X., & Zhang, X. (2023). Unraveling the roles of endoplasmic reticulum-associated degradation in metabolic disorders. *Front Endocrinol (Lausanne)*, *14*, 1123769. https://doi.org/10.3389/fendo.2023.1123769

Lutz, C. T., Smith, K. D., Greazel, N. S., Mace, B. E., Jensen, D. A., McCutcheon, J. A., & Goeken, N. E. (1994). Bw4-reactive and Bw6-reactive antibodies recognize multiple distinct HLA structures that partially overlap in the alpha-1 helix. *J Immunol*, *153*(9), 4099-4110. https://www.ncbi.nlm.nih.gov/pubmed/7523516

Madden, D. R., Garboczi, D. N., & Wiley, D. C. (1993). The antigenic identity of peptide-MHC complexes: a comparison of the conformations of five viral peptides presented by HLA-A2. *Cell*, *75*(4), 693-708. https://doi.org/10.1016/0092-8674(93)90490-h

Mamrosh, J. L., Sherman, D. J., Cohen, J. R., Johnston, J. A., Joubert, M. K., Li, J., Lipford, J. R., Lomenick, B., Moradian, A., Prabhu, S., Sweredoski, M. J., Vander Lugt, B., Verma, R., & Deshaies, R. J. (2023). Quantitative measurement of the requirement of diverse protein degradation pathways in MHC class I peptide presentation. *Sci Adv*, *9*(25), eade7890. https://doi.org/10.1126/sciadv.ade7890

Mantel, I., Sadiq, B. A., & Blander, J. M. (2022). Spotlight on TAP and its vital role in antigen presentation and cross-presentation. *Mol Immunol*, *142*, 105-119. https://doi.org/10.1016/j.molimm.2021.12.013

Maricchiolo, E., Panfili, E., Pompa, A., De Marchis, F., Bellucci, M., & Pallotta, M. T. (2022). Unconventional Pathways of Protein Secretion: Mammals vs. Plants. *Front Cell Dev Biol*, *10*, 895853. https://doi.org/10.3389/fcell.2022.895853

Marijt, K. A., Blijleven, L., Verdegaal, E. M. E., Kester, M. G., Kowalewski, D. J., Rammensee, H. G., Stevanovic, S., Heemskerk, M. H. M., van der Burg, S. H., & van Hall, T. (2018).

Identification of non-mutated neoantigens presented by TAP-deficient tumors. *J Exp Med*, *215*(9), 2325-2337. https://doi.org/10.1084/jem.20180577

Marijt, K. A., Doorduijn, E. M., & T., H. (2019). TEIPP antigens for T-cell based immunotherapy of immune-edited HLA class I low cancers. *Molecular Immunology 113* 43–49. https://doi.org/https://doi.org/10.1016/j.molimm.2018.03.029

Martin-Galiano, A. J., & Lopez, D. (2019). Computational characterization of the peptidome in transporter associated with antigen processing (TAP)-deficient cells. *Plos One*, *14*(1), e0210583. https://doi.org/10.1371/journal.pone.0210583

McAlister, G. C., Nusinow, D. P., Jedrychowski, M. P., Wuhr, M., Huttlin, E. L., Erickson, B. K., Rad, R., Haas, W., & Gygi, S. P. (2014). MultiNotch MS3 enables accurate, sensitive, and multiplexed detection of differential expression across cancer cell line proteomes. *Anal Chem*, *86*(14), 7150-7158. https://doi.org/10.1021/ac502040v

McMurtrey, C., Trolle, T., Sansom, T., Remesh, S. G., Kaever, T., Bardet, W., Jackson, K., McLeod, R., Sette, A., Nielsen, M., Zajonc, D. M., Blader, I. J., Peters, B., & Hildebrand, W. (2016). Toxoplasma gondii peptide ligands open the gate of the HLA class I binding groove. *Elife*, *5*. https://doi.org/10.7554/eLife.12556

Megger, D. A., Pott, L. L., Ahrens, M., Padden, J., Bracht, T., Kuhlmann, K., Eisenacher, M., Meyer, H. E., & Sitek, B. (2014). Comparison of label-free and label-based strategies for proteome analysis of hepatoma cell lines. *Biochim Biophys Acta*, *1844*(5), 967-976. https://doi.org/10.1016/j.bbapap.2013.07.017

Meyer, B. A., & Doroudgar, S. (2020). ER Stress-Induced Secretion of Proteins and Their Extracellular Functions in the Heart. *Cells*, *9*(9). https://doi.org/10.3390/cells9092066

Meyer, T. H., van Endert, P. M., Uebel, S., Ehring, B., & Tampe, R. (1994). Functional expression and purification of the ABC transporter complex associated with antigen processing (TAP) in insect cells. *FEBS Lett*, *351*(3), 443-447. https://doi.org/10.1016/0014-5793(94)00908-2

Montealegre, S., & van Endert, P. M. (2018). Endocytic Recycling of MHC Class I Molecules in Non-professional Antigen Presenting and Dendritic Cells. *Front Immunol*, *9*, 3098. https://doi.org/10.3389/fimmu.2018.03098

Muller, I. K., Winter, C., Thomas, C., Spaapen, R. M., Trowitzsch, S., & Tampe, R. (2022). Structure of an MHC I-tapasin-ERp57 editing complex defines chaperone promiscuity. *Nat Commun*, *13*(1), 5383. https://doi.org/10.1038/s41467-022-32841-9

Munz, C. (2018). Non-canonical Functions of Macroautophagy Proteins During Endocytosis by Myeloid Antigen Presenting Cells. *Front Immunol*, *9*, 2765. https://doi.org/10.3389/fimmu.2018.02765

Nair-Gupta, P., Baccarini, A., Tung, N., Seyffer, F., Florey, O., Huang, Y., Banerjee, M., Overholtzer, M., Roche, P. A., Tampe, R., Brown, B. D., Amsen, D., Whiteheart, S. W., & Blander, J. M. (2014). TLR signals induce phagosomal MHC-I delivery from the endosomal recycling compartment to allow cross-presentation. *Cell*, *158*(3), 506-521. https://doi.org/10.1016/j.cell.2014.04.054

Naslavsky, N., Weigert, R., & Donaldson, J. G. (2004). Characterization of a nonclathrin endocytic pathway: membrane cargo and lipid requirements. *Mol Biol Cell*, *15*(8), 3542-3552. https://doi.org/10.1091/mbc.e04-02-0151

Natsume, M., Niwa, M., Ichikawa, S., Okamoto, T., Tsutsui, H., Usukura, D., Murata, T., Abe, R., Shimonaka, M., Nishida, T., Shiina, I., & Obata, Y. (2024). Brefeldin A and M-COPA block the export of RTKs from the endoplasmic reticulum via simultaneous inactivation of ARF1, ARF4, and ARF5. *J Biol Chem*, *300*(6), 107327. https://doi.org/10.1016/j.jbc.2024.107327

Neefjes, J., Jongsma, M. L., Paul, P., & Bakke, O. (2011). Towards a systems understanding of MHC class I and MHC class II antigen presentation. *Nat Rev Immunol*, *11*(12), 823-836. https://doi.org/10.1038/nri3084

Nickel, W., & Seedorf, M. (2008). Unconventional mechanisms of protein transport to the cell surface of eukaryotic cells. *Annu Rev Cell Dev Biol*, *24*, 287-308. https://doi.org/10.1146/annurev.cellbio.24.110707.175320

Ninagawa, S., Okada, T., Sumitomo, Y., Kamiya, Y., Kato, K., Horimoto, S., Ishikawa, T., Takeda, S., Sakuma, T., Yamamoto, T., & Mori, K. (2014). EDEM2 initiates mammalian glycoprotein ERAD by catalyzing the first mannose trimming step. *J Cell Biol*, *206*(3), 347-356. https://doi.org/10.1083/jcb.201404075

Nuchel, J., Tauber, M., Nolte, J. L., Morgelin, M., Turk, C., Eckes, B., Demetriades, C., & Plomann, M. (2021). An mTORC1-GRASP55 signaling axis controls unconventional secretion to reshape the extracellular proteome upon stress. *Mol Cell*, *81*(16), 3275-3293 e3212. https://doi.org/10.1016/j.molcel.2021.06.017

Nyambura, L. W., Jarmalavicius, S., & Walden, P. (2018). Impact of Leishmania donovani infection on the HLA I self peptide repertoire of human macrophages. *Plos One*, *13*(7), e0200297. https://doi.org/10.1371/journal.pone.0200297

O'Connell, J. D., Paulo, J. A., O'Brien, J. J., & Gygi, S. P. (2018). Proteome-Wide Evaluation of Two Common Protein Quantification Methods. *J Proteome Res*, *17*(5), 1934-1942. https://doi.org/10.1021/acs.jproteome.8b00016

O'Connor, G. M., Vivian, J. P., Widjaja, J. M., Bridgeman, J. S., Gostick, E., Lafont, B. A., Anderson, S. K., Price, D. A., Brooks, A. G., Rossjohn, J., & McVicar, D. W. (2014). Mutational and structural analysis of KIR3DL1 reveals a lineage-defining allotypic dimorphism that impacts both HLA and peptide sensitivity. *J Immunol*, *192*(6), 2875-2884. https://doi.org/10.4049/jimmunol.1303142

Olivari, S., & Molinari, M. (2007). Glycoprotein folding and the role of EDEM1, EDEM2 and EDEM3 in degradation of folding-defective glycoproteins. *FEBS Lett*, *581*(19), 3658-3664. https://doi.org/10.1016/j.febslet.2007.04.070

Oliveira-Ferrer, L., Legler, K., & Milde-Langosch, K. (2017). Role of protein glycosylation in cancer metastasis. *Semin Cancer Biol*, *44*, 141-152. https://doi.org/10.1016/j.semcancer.2017.03.002

Olson, E., Ceccarelli, T., & Raghavan, M. (2023). Endo-lysosomal assembly variations among human leukocyte antigen class I (HLA class I) allotypes. *Elife*, *12*. https://doi.org/10.7554/eLife.79144

Olson, E., & Raghavan, M. (2023). Major histocompatibility complex class I assembly within endolysosomal pathways. *Curr Opin Immunol*, *84*, 102356. https://doi.org/10.1016/j.coi.2023.102356

Ortmann, B., Copeman, J., Lehner, P. J., Sadasivan, B., Herberg, J. A., Grandea, A. G., Riddell, S. R., Tampe, R., Spies, T., Trowsdale, J., & Cresswell, P. (1997). A critical role for tapasin in the assembly and function of multimeric MHC class I-TAP complexes. *Science*, *277*(5330), 1306-1309. https://doi.org/10.1126/science.277.5330.1306

Oslowski, C. M., & Urano, F. (2011). Measuring ER stress and the unfolded protein response using mammalian tissue culture system. *Methods Enzymol*, *490*, 71-92. https://doi.org/10.1016/B978-0-12-385114-7.00004-0

Pan, S., Cheng, X., & Sifers, R. N. (2013). Golgi-situated endoplasmic reticulum alpha-1, 2-mannosidase contributes to the retrieval of ERAD substrates through a direct interaction with gamma-COP. *Mol Biol Cell*, *24*(8), 1111-1121. https://doi.org/10.1091/mbc.E12-12-0886

Parham, P., & Brodsky, F. M. (1981). Partial purification and some properties of BB7.2. A cytotoxic monoclonal antibody with specificity for HLA-A2 and a variant of HLA-A28. *Hum Immunol*, *3*(4), 277-299. https://doi.org/10.1016/0198-8859(81)90065-3

Peaper, D. R., & Cresswell, P. (2008). The redox activity of ERp57 is not essential for its functions in MHC class I peptide loading. *Proc Natl Acad Sci U S A*, *105*(30), 10477-10482. https://doi.org/10.1073/pnas.0805044105

Peh, C. A., Burrows, S. R., Barnden, M., Khanna, R., Cresswell, P., Moss, D. J., & McCluskey, J. (1998). HLA-B27-restricted antigen presentation in the absence of tapasin reveals polymorphism in mechanisms of HLA class I peptide loading. *Immunity*, *8*(5), 531-542. https://doi.org/10.1016/s1074-7613(00)80558-0

Petersen, J. L., Morris, C. R., & Solheim, J. C. (2003). Virus evasion of MHC class I molecule presentation. *J Immunol*, *171*(9), 4473-4478. https://doi.org/10.4049/jimmunol.171.9.4473

Plomp, R., Ruhaak, L. R., Uh, H. W., Reiding, K. R., Selman, M., Houwing-Duistermaat, J. J., Slagboom, P. E., Beekman, M., & Wuhrer, M. (2017). Subclass-specific IgG glycosylation is associated with markers of inflammation and metabolic health. *Sci Rep*, *7*(1), 12325. https://doi.org/10.1038/s41598-017-12495-0

Praveen, P. V., Yaneva, R., Kalbacher, H., & Springer, S. (2010). Tapasin edits peptides on MHC class I molecules by accelerating peptide exchange. *Eur J Immunol*, *40*(1), 214-224. https://doi.org/10.1002/eji.200939342

Presley, J. F., Mayor, S., McGraw, T. E., Dunn, K. W., & Maxfield, F. R. (1997). Bafilomycin A1 treatment retards transferrin receptor recycling more than bulk membrane recycling. *J Biol Chem*, *272*(21), 13929-13936. https://doi.org/10.1074/jbc.272.21.13929

Pymm, P., Saunders, P. M., Anand, S., MacLachlan, B. J., Faoro, C., Hitchen, C., Rossjohn, J., Brooks, A. G., & Vivian, J. P. (2024). The Structural Basis for Recognition of Human Leukocyte Antigen Class I Molecules by the Pan-HLA Antibody W6/32. *J Immunol*. https://doi.org/10.4049/jimmunol.2400328

Rabouille, C. (2017). Pathways of Unconventional Protein Secretion. *Trends Cell Biol*, *27*(3), 230-240. https://doi.org/10.1016/j.tcb.2016.11.007

Raghavan, M., Del Cid, N., Rizvi, S. M., & Peters, L. R. (2008). MHC class I assembly: out and about. *Trends Immunol*, *29*(9), 436-443. https://doi.org/10.1016/j.it.2008.06.004

Raghavan, M., Wijeyesakere, S. J., Peters, L. R., & Del Cid, N. (2013). Calreticulin in the immune system: ins and outs. *Trends Immunol*, *34*(1), 13-21. https://doi.org/10.1016/j.it.2012.08.002

Raghuraman, G., Lapinski, P. E., & Raghavan, M. (2002). Tapasin interacts with the membrane-spanning domains of both TAP subunits and enhances the structural stability of TAP1 x TAP2 Complexes. *J Biol Chem*, *277*(44), 41786-41794. https://doi.org/10.1074/jbc.M207128200

Rajagopalan, S., & Brenner, M. B. (1994). Calnexin retains unassembled major histocompatibility complex class I free heavy chains in the endoplasmic reticulum. *J Exp Med*, *180*(1), 407-412. https://doi.org/10.1084/jem.180.1.407

Raposo, G., van Santen, H. M., Leijendekker, R., Geuze, H. J., & Ploegh, H. L. (1995). Misfolded major histocompatibility complex class I molecules accumulate in an expanded ER-Golgi intermediate compartment. *J Cell Biol*, *131*(6 Pt 1), 1403-1419. https://doi.org/10.1083/jcb.131.6.1403

Raskov, H., Orhan, A., Christensen, J. P., & Gögenur, I. (2021). Cytotoxic $CD8^+$ T cells in cancer and cancer immunotherapy. *British journal of cancer*, *124*(2), 359–367. https://doi.org/10.1038/s41416-020-01048-4

Reynisson, B., Alvarez, B., Paul, S., Peters, B., & Nielsen, M. (2020). NetMHCpan-4.1 and NetMHCIIpan-4.0: improved predictions of MHC antigen presentation by concurrent motif deconvolution and integration of MS MHC eluted ligand data. *Nucleic Acids Res*, *48*(W1), W449-W454. https://doi.org/10.1093/nar/gkaa379

Rizvi, S. M., Del Cid, N., Lybarger, L., & Raghavan, M. (2011). Distinct functions for the glycans of tapasin and heavy chains in the assembly of MHC class I molecules. *J Immunol*, *186*(4), 2309-2320. https://doi.org/10.4049/jimmunol.1002959

Rizvi, S. M., & Raghavan, M. (2006). Direct peptide-regulatable interactions between MHC class I molecules and tapasin. *Proc Natl Acad Sci U S A*, *103*(48), 18220-18225. https://doi.org/10.1073/pnas.0605131103

Rizvi, S. M., & Raghavan, M. (2010). Mechanisms of function of tapasin, a critical major histocompatibility complex class I assembly factor. *Traffic*, *11*(3), 332-347. https://doi.org/10.1111/j.1600-0854.2009.01025.x

Rizvi, S. M., Salam, N., Geng, J., Qi, Y., Bream, J. H., Duggal, P., Hussain, S. K., Martinson, J., Wolinsky, S. M., Carrington, M., & Raghavan, M. (2014). Distinct assembly profiles of HLA-B molecules. *J Immunol*, *192*(11), 4967-4976. https://doi.org/10.4049/jimmunol.1301670

Roche, P. A., & Furuta, K. (2015). The ins and outs of MHC class II-mediated antigen processing and presentation. *Nature Reviews Immunology*, *15*(4), 203–216. https://doi.org/10.1038/nri3818

Rock, K. L., Gramm, C., Rothstein, L., Clark, K., Stein, R., Dick, L., Hwang, D., & Goldberg, A. L. (1994). Inhibitors of the proteasome block the degradation of most cell proteins and the generation of peptides presented on MHC class I molecules. *Cell*, *78*(5), 761-771. https://doi.org/10.1016/s0092-8674(94)90462-6

Roeth, J. F., Williams, M., Kasper, M. R., Filzen, T. M., & Collins, K. L. (2004). HIV-1 Nef disrupts MHC-I trafficking by recruiting AP-1 to the MHC-I cytoplasmic tail. *J Cell Biol*, *167*(5), 903-913. https://doi.org/10.1083/jcb.200407031

Roth, J., & Zuber, C. (2017). Quality control of glycoprotein folding and ERAD: the role of N-glycan handling, EDEM1 and OS-9. *Histochem Cell Biol*, *147*(2), 269-284. https://doi.org/10.1007/s00418-016-1513-9

Ryan, S. O., & Cobb, B. A. (2012). Roles for major histocompatibility complex glycosylation in immune function. *Semin Immunopathol*, *34*(3), 425-441. https://doi.org/10.1007/s00281-012-0309-9

Rymen, D., Peanne, R., Millon, M. B., Race, V., Sturiale, L., Garozzo, D., Mills, P., Clayton, P., Asteggiano, C. G., Quelhas, D., Cansu, A., Martins, E., Nassogne, M. C., Goncalves-Rocha, M., Topaloglu, H., Jaeken, J., Foulquier, F., & Matthijs, G. (2013). MAN1B1 deficiency: an unexpected CDG-II. *PLoS Genet*, *9*(12), e1003989. https://doi.org/10.1371/journal.pgen.1003989

Sabapathy, K., & Nam, S. Y. (2008). Defective MHC class I antigen surface expression promotes cellular survival through elevated ER stress and modulation of p53 function. *Cell Death Differ*, *15*(9), 1364-1374. https://doi.org/10.1038/cdd.2008.55

Sadasivan, B., Lehner, P. J., Ortmann, B., Spies, T., & Cresswell, P. (1996). Roles for calreticulin and a novel glycoprotein, tapasin, in the interaction of MHC class I molecules with TAP. *Immunity*, *5*(2), 103-114. https://doi.org/10.1016/s1074-7613(00)80487-2

Sagert, L., Winter, C., Ruppert, I., Zehetmaier, M., Thomas, C., & Tampe, R. (2023). The ER folding sensor UGGT1 acts on TAPBPR-chaperoned peptide-free MHC I. *Elife*, *12*. https://doi.org/10.7554/eLife.85432

Sakhi, S., Cholet, S., Wehbi, S., Isidor, B., Cogne, B., Vuillaumier-Barrot, S., Dupre, T., Detleft, T., Schmitt, E., Leheup, B., Bonnet, C., Feillet, F., Muti, C., Fenaille, F., & Bruneel, A. (2021). MAN1B1-CDG: Three new individuals and associated biochemical profiles. *Mol Genet Metab Rep*, *28*, 100775. https://doi.org/10.1016/j.ymgmr.2021.100775

Sarkizova, S., Klaeger, S., Le, P. M., Li, L. W., Oliveira, G., Keshishian, H., Hartigan, C. R., Zhang, W., Braun, D. A., Ligon, K. L., Bachireddy, P., Zervantonakis, I. K., Rosenbluth, J. M., Ouspenskaia, T., Law, T., Justesen, S., Stevens, J., Lane, W. J., Eisenhaure, T., . . . Keskin, D. B. (2020). A large peptidome dataset improves HLA class I epitope prediction across most of the human population. *Nat Biotechnol*, *38*(2), 199-209. https://doi.org/10.1038/s41587-019-0322-9

Schroder, B. (2016). The multifaceted roles of the invariant chain CD74--More than just a chaperone. *Biochim Biophys Acta*, *1863*(6 Pt A), 1269-1281. https://doi.org/10.1016/j.bbamcr.2016.03.026

Sengupta, D., Galicia-Pereyra, R., Han, P., Graham, M., Liu, X., Arshad, N., & Cresswell, P. (2024). Cutting Edge: Phagosome-associated Autophagosomes Containing Antigens and

Proteasomes Drive TAP-Independent Cross-Presentation. *J Immunol*, *212*(7), 1063-1068. https://doi.org/10.4049/jimmunol.2200446

Sengupta, D., Graham, M., Liu, X., & Cresswell, P. (2019). Proteasomal degradation within endocytic organelles mediates antigen cross-presentation. *The EMBO Journal*, *38*(16), e99266. https://doi.org/10.15252/embj.201899266

Shalem, O., Sanjana, N. E., Hartenian, E., Shi, X., Scott, D. A., Mikkelson, T., Heckl, D., Ebert, B. L., Root, D. E., Doench, J. G., & Zhang, F. (2014). Genome-scale CRISPR-Cas9 knockout screening in human cells. *Science*, *343*(6166), 84-87. https://doi.org/10.1126/science.1247005

Shenkman, M., Ron, E., Yehuda, R., Benyair, R., Khalaila, I., & Lederkremer, G. Z. (2018). Mannosidase activity of EDEM1 and EDEM2 depends on an unfolded state of their glycoprotein substrates. *Commun Biol*, *1*, 172. https://doi.org/10.1038/s42003-018-0174-8

Shorter, J., Watson, R., Giannakou, M. E., Clarke, M., Warren, G., & Barr, F. A. (1999). GRASP55, a second mammalian GRASP protein involved in the stacking of Golgi cisternae in a cell-free system. The *EMBO Journal*, *18*(18), 4949-4960. https://doi.org/10.1093/emboj/18.18.4949

Sijts, E. J., & Kloetzel, P. M. (2011). The role of the proteasome in the generation of MHC class I ligands and immune responses. *Cell Mol Life Sci*, *68*(9), 1491-1502. https://doi.org/10.1007/s00018-011-0657-y

Siwecka, N., Rozpedek-Kaminska, W., Wawrzynkiewicz, A., Pytel, D., Diehl, J. A., & Majsterek, I. (2021). The Structure, Activation and Signaling of IRE1 and Its Role in Determining Cell Fate. *Biomedicines*, *9*(2). https://doi.org/10.3390/biomedicines9020156

Sokolowska, I., Pilka, E. S., Sandvig, K., Wegrzyn, G., & Slominska-Wojewodzka, M. (2015). Hydrophobicity of protein determinants influences the recognition of substrates by EDEM1 and EDEM2 in human cells. *BMC Cell Biol*, *16*, 1. https://doi.org/10.1186/s12860-015-0047-7

Sousa, M., & Parodi, A. J. (1995). The molecular basis for the recognition of misfolded glycoproteins by the UDP-Glc:glycoprotein glucosyltransferase. *Embo Journal*, *14*(17), 4196-4203. https://doi.org/10.1002/j.1460-2075.1995.tb00093.x

Stanley, P., Moremen, K. W., Lewis, N. E., Taniguchi, N., & Aebi, M. (2022). N-Glycans. In A. Varki, R. D. Cummings, J. D. Esko, P. Stanley, G. W. Hart, M. Aebi, D. Mohnen, T. Kinoshita, N. H. Packer, J. H. Prestegard, R. L. Schnaar, & P. H. Seeberger (Eds.), *Essentials of Glycobiology* (4th ed., pp. 103-116). https://doi.org/10.1101/glycobiology.4e.9

Sugawara, S., Abo, T., & Kumagai, K. (1987). A simple method to eliminate the antigenicity of surface class I MHC molecules from the membrane of viable cells by acid treatment at pH 3. *J Immunol Methods*, *100*(1-2), 83-90. https://doi.org/10.1016/0022-1759(87)90175-x

Sugita, M., & Brenner, M. B. (1995). Association of the invariant chain with major histocompatibility complex class I molecules directs trafficking to endocytic compartments. *J Biol Chem*, *270*(3), 1443-1448. https://doi.org/10.1074/jbc.270.3.1443

Sun, A. H., Collette, J. R., & Sifers, R. N. (2020). The cytoplasmic tail of human mannosidase Man1b1 contributes to catalysis-independent quality control of misfolded alpha1-antitrypsin. *Proc Natl Acad Sci U S A*, *117*(40), 24825-24836. https://doi.org/10.1073/pnas.1919013117

Sun, W., Tian, B. X., Wang, S. H., Liu, P. J., & Wang, Y. C. (2020). The function of SEC22B and its role in human diseases. *Cytoskeleton (Hoboken)*, *77*(8), 303-312. https://doi.org/10.1002/cm.21628

Sung, H., Ferlay, J., Siegel, R. L., Laversanne, M., Soerjomataram, I., Jemal, A., & Bray, F. (2021). Global Cancer Statistics 2020: GLOBOCAN Estimates of Incidence and Mortality Worldwide for 36 Cancers in 185 Countries. *CA Cancer J Clin*, *71*(3), 209-249. https://doi.org/10.3322/caac.21660

Tan, P., Kropshofer, H., Mandelboim, O., Bulbuc, N., Hammerling, G. J., & Momburg, F. (2002). Recruitment of MHC class I molecules by tapasin into the transporter associated with antigen processing-associated complex is essential for optimal peptide loading. *J Immunol*, *168*(4), 1950-1960. https://doi.org/10.4049/jimmunol.168.4.1950

Tang, H. Y., Huang, C. H., Zhuang, Y. H., Christianson, J. C., & Chen, X. (2014). EDEM2 and OS-9 are required for ER-associated degradation of non-glycosylated sonic hedgehog. *Plos One*, *9*(6), e92164. https://doi.org/10.1371/journal.pone.0092164

Taylor, B. C., & Balko, J. M. (2022). Mechanisms of MHC-I Downregulation and Role in Immunotherapy Response. *Front Immunol*, *13*, 844866. https://doi.org/10.3389/fimmu.2022.844866

Thastrup, O., Cullen, P. J., Drobak, B. K., Hanley, M. R., & Dawson, A. P. (1990). Thapsigargin, a tumor promoter, discharges intracellular Ca2+ stores by specific inhibition of the endoplasmic reticulum Ca2(+)-ATPase. *Proc Natl Acad Sci U S A*, *87*(7), 2466-2470. https://doi.org/10.1073/pnas.87.7.2466

Thomsen, M. C., & Nielsen, M. (2012). Seq2Logo: a method for construction and visualization of amino acid binding motifs and sequence profiles including sequence weighting, pseudo counts and two-sided representation of amino acid enrichment and depletion. *Nucleic Acids Res*, *40*(Web Server issue), W281-287. https://doi.org/10.1093/nar/gks469

Timms, R. T., Menzies, S. A., Tchasovnikarova, I. A., Christensen, L. C., Williamson, J. C., Antrobus, R., Dougan, G., Ellgaard, L., & Lehner, P. J. (2016). Genetic dissection of mammalian ERAD through comparative haploid and CRISPR forward genetic screens. *Nat Commun*, *7*, 11786. https://doi.org/10.1038/ncomms11786

Troegeler, A., Lastrucci, C., Duval, C., Tanne, A., Cougoule, C., Maridonneau-Parini, I., Neyrolles, O., & Lugo-Villarino, G. (2014). An efficient siRNA-mediated gene silencing in primary human monocytes, dendritic cells and macrophages. *Immunol Cell Biol*, *92*(8), 699-708. https://doi.org/10.1038/icb.2014.39

Trombetta, S. E., & Parodi, A. J. (1992). Purification to apparent homogeneity and partial characterization of rat liver UDP-glucose:glycoprotein glucosyltransferase. *J Biol Chem*, *267*(13), 9236-9240. https://www.ncbi.nlm.nih.gov/pubmed/1533626

Trzos, S., Link-Lenczowski, P., & Pochec, E. (2023). The role of N-glycosylation in B-cell biology and IgG activity. The aspects of autoimmunity and anti-inflammatory therapy. *Front Immunol*, *14*, 1188838. https://doi.org/10.3389/fimmu.2023.1188838

Tu, H. C., Hsiao, Y. C., Yang, W. Y., Tsai, S. L., Lin, H. K., Liao, C. Y., Lu, J. W., Chou, Y. T., Wang, H. D., & Yuh, C. H. (2017). Up-regulation of golgi alpha-mannosidase IA and down-regulation of golgi alpha-mannosidase IC activates unfolded protein response during hepatocarcinogenesis. *Hepatol Commun*, *1*(3), 230-247. https://doi.org/10.1002/hep4.1032

van Els, C. A., Herberts, C. A., van der Heeft, E., Poelen, M. C., van Gaans-van den Brink, J. A., van der Kooi, A., Hoogerhout, P., Jan ten Hove, G., Meiring, H. D., & de Jong, A. P. (2000). A single naturally processed measles virus peptide fully dominates the HLA-A*0201-associated peptide display and is mutated at its anchor position in persistent viral strains. *Eur J Immunol*, *30*(4), 1172-1181. https://doi.org/10.1002/(SICI)1521-4141(200004)30:4<1172::AID-IMMU1172>3.0.CO;2-J

van Endert, P. (2016). Intracellular recycling and cross-presentation by MHC class I molecules. *Immunol Rev*, *272*(1), 80-96. https://doi.org/10.1111/imr.12424

van Raam, B. J., Lacina, T., Lindemann, R. K., & Reiling, J. H. (2017). Secretory stressors induce intracellular death receptor accumulation to control apoptosis. *Cell Death Dis*, *8*(10), e3069. https://doi.org/10.1038/cddis.2017.466

Verweij, M. C., Horst, D., Griffin, B. D., Luteijn, R. D., Davison, A. J., Ressing, M. E., & Wiertz, E. J. (2015). Viral inhibition of the transporter associated with antigen processing (TAP): a striking example of functional convergent evolution. *PLoS Pathog*, *11*(4), e1004743. https://doi.org/10.1371/journal.ppat.1004743

Wang, X., Chen, B., Cao, Y., He, Y., & Chen, W. (2022). Identification of MAN1B1 as a Novel Marker for Bladder Cancer and Its Relationship with Immune Cell Infiltration. *J Oncol*, *2022*, 3387671. https://doi.org/10.1155/2022/3387671

Wang, X. Z., Lawson, B., Brewer, J. W., Zinszner, H., Sanjay, A., Mi, L. J., Boorstein, R., Kreibich, G., Hendershot, L. M., & Ron, D. (1996). Signals from the stressed endoplasmic reticulum induce C/EBP-homologous protein (CHOP/GADD153). *Mol Cell Biol*, *16*(8), 4273-4280. https://doi.org/10.1128/MCB.16.8.4273

Wassenaar, T. M., Harville, T., Chastain, J., Wanchai, V., & Ussery, D. W. (2024). DNA structural features and variability of complete MHC locus sequences. *Front Bioinform*, *4*, 1392613. https://doi.org/10.3389/fbinf.2024.1392613

Wearsch, P. A., & Cresswell, P. (2007). Selective loading of high-affinity peptides onto major histocompatibility complex class I molecules by the tapasin-ERp57 heterodimer. *Nature Immunology*, *8*(8), 873-881. https://doi.org/10.1038/ni1485

Wearsch, P. A., Peaper, D. R., & Cresswell, P. (2011). Essential glycan-dependent interactions optimize MHC class I peptide loading. *Proc Natl Acad Sci U S A*, *108*(12), 4950-4955. https://doi.org/10.1073/pnas.1102524108

Wei, M. L., & Cresswell, P. (1992). HLA-A2 molecules in an antigen-processing mutant cell contain signal sequence-derived peptides. *Nature*, *356*(6368), 443-446. https://doi.org/10.1038/356443a0

Wei, Y., Chen, Q., Chen, J., Zhou, C., Geng, S., Shi, D., Huang, S., Liang, Z., Chen, X., Ren, N., & Jiang, J. (2023). Loss of alpha-1,2-mannosidase MAN1C1 promotes tumorigenesis of intrahepatic cholangiocarcinoma through enhancing CD133-FIP200 interaction. *Cell Rep*, *42*(12), 113588. https://doi.org/10.1016/j.celrep.2023.113588

Weinzierl, A. O., Rudolf, D., Hillen, N., Tenzer, S., van Endert, P., Schild, H., Rammensee, H. G., & Stevanovic, S. (2008). Features of TAP-independent MHC class I ligands revealed by quantitative mass spectrometry. *Eur J Immunol*, *38*(6), 1503-1510. https://doi.org/10.1002/eji.200838136

Williams, A. P., Peh, C. A., Purcell, A. W., McCluskey, J., & Elliott, T. (2002). Optimization of the MHC class I peptide cargo is dependent on tapasin. *Immunity*, *16*(4), 509-520. https://doi.org/10.1016/s1074-7613(02)00304-7

Williams, S. E., Noel, M., Lehoux, S., Cetinbas, M., Xavier, R. J., Sadreyev, R. I., Scolnick, E. M., Smoller, J. W., Cummings, R. D., & Mealer, R. G. (2022). Mammalian brain glycoproteins exhibit diminished glycan complexity compared to other tissues. *Nat Commun*, *13*(1), 275. https://doi.org/10.1038/s41467-021-27781-9

Wu, S. J., Niknafs, Y. S., Kim, S. H., Oravecz-Wilson, K., Zajac, C., Toubai, T., Sun, Y., Prasad, J., Peltier, D., Fujiwara, H., Hedig, I., Mathewson, N. D., Khoriaty, R., Ginsburg, D., & Reddy, P. (2017). A Critical Analysis of the Role of SNARE Protein SEC22B in Antigen Cross-Presentation. *Cell Rep*, *19*(13), 2645-2656. https://doi.org/10.1016/j.celrep.2017.06.013

Xiang, Y., & Wang, Y. (2010). GRASP55 and GRASP65 play complementary and essential roles in Golgi cisternal stacking. *J Cell Biol*, *188*(2), 237-251. https://doi.org/10.1083/jcb.200907132

Xiang, Y., Zhang, X., Nix, D. B., Katoh, T., Aoki, K., Tiemeyer, M., & Wang, Y. (2013). Regulation of protein glycosylation and sorting by the Golgi matrix proteins GRASP55/65. *Nat Commun*, *4*, 1659. https://doi.org/10.1038/ncomms2669

Yabe, T., Kawamura, S., Sato, M., Kashiwase, K., Tanaka, H., Ishikawa, Y., Asao, Y., Oyama, J., Tsuruta, K., Tokunaga, K., Tadokoro, K., & Juji, T. (2002). A subject with a novel type I bare lymphocyte syndrome has tapasin deficiency due to deletion of 4 exons by Alu-mediated recombination. *Blood*, *100*(4), 1496-1498. https://doi.org/10.1182/blood-2001-12-0252

Yang, X., Gao, M., Chen, G., Pierce, B. G., Lu, J., Weng, N. P., & Mariuzza, R. A. (2015). Structural Basis for Clonal Diversity of the Public T Cell Response to a Dominant Human Cytomegalovirus Epitope. *J Biol Chem*, *290*(48), 29106-29119. https://doi.org/10.1074/jbc.M115.691311

Yarzabek, B., Zaitouna, A. J., Olson, E., Silva, G. N., Geng, J., Geretz, A., Thomas, R., Krishnakumar, S., Ramon, D. S., & Raghavan, M. (2018). Variations in HLA-B cell surface expression, half-life and extracellular antigen receptivity. *Elife*, *7*. https://doi.org/10.7554/eLife.34961

Yee Mon, K. J., & Blander, J. M. (2023). TAP-ing into the cross-presentation secrets of dendritic cells. *Curr Opin Immunol*, *83*, 102327. https://doi.org/10.1016/j.coi.2023.102327

Yewdell, J. W. (2022). MHC Class I Immunopeptidome: Past, Present, and Future. *Mol Cell Proteomics*, *21*(7), 100230. https://doi.org/10.1016/j.mcpro.2022.100230

Yewdell, J. W., Anton, L. C., & Bennink, J. R. (1996). Defective ribosomal products (DRiPs): a major source of antigenic peptides for MHC class I molecules? *J Immunol*, *157*(5), 1823-1826. https://www.ncbi.nlm.nih.gov/pubmed/8757297

Yewdell, J. W., & Nicchitta, C. V. (2006). The DRiP hypothesis decennial: support, controversy, refinement and extension. *Trends Immunol*, *27*(8), 368-373. https://doi.org/10.1016/j.it.2006.06.008

Yokoyama, W. M., Altfeld, M., & Hsu, K. C. (2010). Natural killer cells: tolerance to self and innate immunity to viral infection and malignancy. *Biol Blood Marrow Transplant*, *16*(1 Suppl), S97-S105. https://doi.org/10.1016/j.bbmt.2009.10.009

Yoneyama, M. S., Tobisawa, Y., Hatakeyama, S., Sato, M., Tone, K., Tatara, Y., Kakizaki, I., Funyu, T., Fukuda, M., Hoshi, S., Ohyama, C., & Tsuboi, S. (2017). A mechanism for evasion of CTL immunity by altered O-glycosylation of HLA class I. *J Biochem*, *161*(6), 479-492. https://doi.org/10.1093/jb/mvw096

Yoshida, H., Matsui, T., Yamamoto, A., Okada, T., & Mori, K. (2001). XBP1 mRNA is induced by ATF6 and spliced by IRE1 in response to ER stress to produce a highly active transcription factor. *Cell*, *107*(7), 881-891. https://doi.org/10.1016/s0092-8674(01)00611-0

Zaitoua, A. J., Kaur, A., & Raghavan, M. (2020). Variations in MHC class I antigen presentation and immunopeptidome selection pathways. *F1000Res*, *9*. https://doi.org/10.12688/f1000research.26935.1

Zhang, N., & Bevan, M. J. (2011). CD8(+) T cells: foot soldiers of the immune system. *Immunity*, *35*(2), 161-168. https://doi.org/10.1016/j.immuni.2011.07.010

Zhang, W., Wearsch, P. A., Zhu, Y., Leonhardt, R. M., & Cresswell, P. (2011). A role for UDP-glucose glycoprotein glucosyltransferase in expression and quality control of MHC class I molecules. *Proc Natl Acad Sci U S A*, *108*(12), 4956-4961. https://doi.org/10.1073/pnas.1102527108

Zhang, X., & Wang, Y. (2020). Nonredundant Roles of GRASP55 and GRASP65 in the Golgi Apparatus and Beyond. *Trends Biochem Sci*, *45*(12), 1065-1079. https://doi.org/10.1016/j.tibs.2020.08.001

Zhang, Y., & Seemann, J. (2021). Rapid degradation of GRASP55 and GRASP65 reveals their immediate impact on the Golgi structure. *J Cell Biol*, *220*(1). https://doi.org/10.1083/jcb.202007052

Zinkernagel, R. M., & Doherty, P. C. (1974). Restriction of in vitro T cell-mediated cytotoxicity in lymphocytic choriomeningitis within a syngeneic or semiallogeneic system. *Nature*, *248*(5450), 701-702. https://doi.org/10.1038/248701a0